The Expeditions ANTARKTIS XVIII/1-2 of the Research Vessel „Polarstern“ in 2000

Die Expeditionen ANTARKTIS XVIII/1-2 des Forschungsschiffes „Polarstern“ 2000

Edited by / Herausgegeben von
Victor Smetacek, Ulrich Bathmann, Saad El Naggar
with contributions of the participants /
unter Mitarbeit der Fahrtteilnehmer

Ber. Polarforsch. Meeresforsch. 400 (2001)
ISSN 1618 - 3193

ANTARKTIS XVIII/1 - 2

29. September 2000 – 3. Dezember 2000

KOORDINATOR/COORDINATOR
Heinrich Miller

ANT XVIII/1: Bremerhaven – Cape Town

FAHRTLEITER/CHIEF SCIENTIST

Saad El Naggar

ANT XVIII/2: Cape Town – Cape Town

FAHRTLEITER/CHIEF SCIENTIST

Victor Smetacek

INHALTSVERZEICHNIS / CONTENTS

FAHRTABSCHNITT ANT XVIII/1 BREMERHAVEN - KAPSTADT

FAHRTABSCHNITT ANT XVIII/2 KAPSTADT - KAPSTADT

FAHRTABSCHNITT ANT XVIII/1 BREMERHAVEN-KAPSTADT
REISEROUTE/ SHIP'S TRACK

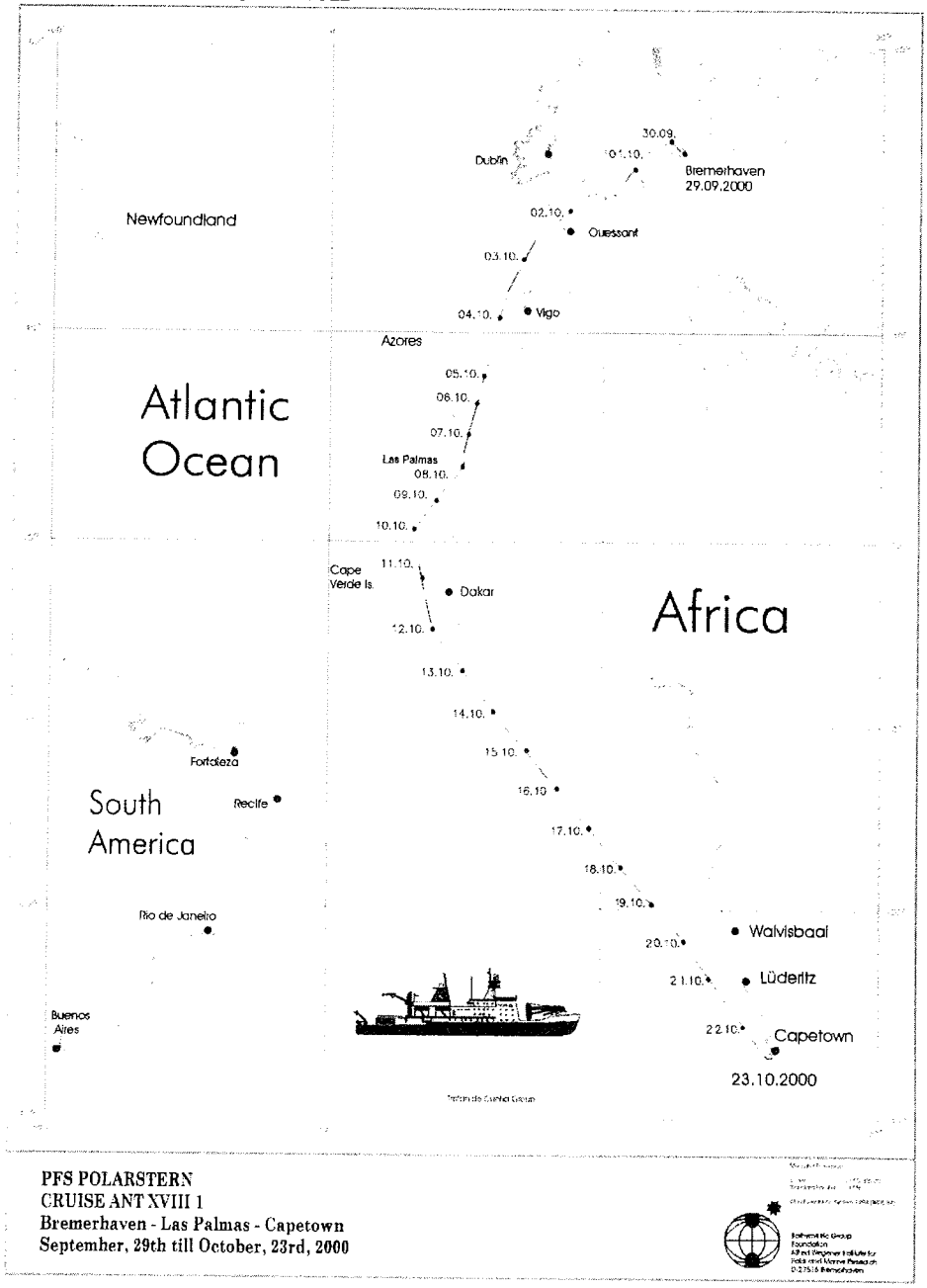

Abb.1: Reiseroute auf ANT XVIII/1 FS "Polarstern"
Fig. 1: Cruise route on ANT XVIII/1, RV "Polarstern"

A. ZUSAMMENFASSUNG

Saad El Naggar/ AWI-Logistik

Der erste Fahrtabschnitt der 18. Reise der FS "Polarstern" in die Antarktis wurde zur Erprobung von wissenschaftlichen Geräten und zur Durchführung von atmosphärischen Messungen genutzt.

Die Reise begann am 29.09.2000 in Bremerhaven und endete am 23.10.2000 in Kapstadt. Die "Polarstern" wurde auf kürzestem Wege nach Kapstadt geführt (Abb. 1), wobei und die Transferzeit ca. 24 Tage betrug. Zur Erprobung der Winden und der Maschinensteuerung wurden mehrere Stationen in der Biskaya für ca. 48 Stunden benötigt. Eine andere Station zur Aufnahme einer Verankerung in der Nähe von Cape Blanc (21°17 N; 20°43 W) wurde binnen von 6 Stunden erfolgreich abgeschlossen. Die wissenschaftlichen atmosphärischen, meereschemischen und luftchemischen Mes– sungen wurden bei voller Fahrt des Schiffes durchgeführt.

Ein Teil der Testmannschaft (AWI, INTER, RFL, ROCHEM, MTU, STNH, WERUM) wurde am 8.10.2000 in Gran Canaria (Las Palmas) ausgeschifft.

Im Rahmen der Generalreparatur der FS "Polarstern" wurde die gesamte Windensteuerung durch die Firma STN-Atlas-Elektronik, Hamburg, erneuert. Die Maschinensteurung wurde durch die Firma Motoren und Turbinen Union (MTU), Friedrichshafen, komplett modernisiert.

Beide Maßnahmen wurden auf See zwischen Bremerhaven und Las Palmas im realen Betrieb getestet und abgenommen.

Das alte Datenerfassungs- und Anzeigesystem der "Polarstern" (PODEV) wurde durch ein auf Echtzeit basierendes System (PODAS) durch die Firma WERUM ersetzt. Implementierung, Test, Abnahme und Inbetriebnahme des neuen Systems wurde auf diesem Fahrtabschnitt bis Kapstadt durchgeführt. Dabei wurden alle Sensoren angeschlossen, getestet und abgenommen. In diesem Rahmen wurden die alten VMS-Rechner (Digital Equipment) durch auf UNIX-basierende Rechner und Server (SUN Micro System) ausgetauscht. Mehr als 30 Anwender- und Anzeigerechner (COMPAQ, Windows 2000) wurden neu installiert und getestet und in Betrieb genommen.

Die UV-B-Gruppe des AWI hat während der Reise eine UV-B-Meßkampagne durchführen und die spektrale UV-Verteilungen (UV-B&UV-A) in Abhängigkeit von den Breitengraden ermittelt. Hierfür wurden kontinuierliche Spektralmessungen mit dem AWI-Spektrometer durchgeührt. Gleichzeitig wurden Dosismessungen mit vom AWI entwickelten Personen-UV-B-Dosimetern (ELUV-14) vorgenommen. Begleitend zu den UV-B-Messungen wurden täglich ECC-Ozon– sonden zur Sondierung der Atmosphäre und zur Ermittlung der Ozonverteilungen gestartet.

Eine Wissenschaftlergruppe der University of East Anglia, UK, führte verschiedene luft- und meereschemische Messungen durch. CO_2-Konzentrationen in Luft und Wasser wurden kontinuierlich registriert und analysiert. Aerosole wurden mit Saugpumpen und Filter sowie durch Regenwasser gesammelt und auf Eisengehalt untersucht. Biogen halogene Kohlenstoffe wurden ebenfalls kontinuierlich gemessen und analysiert.
Der Sonderfachbereich SFB 2612 der Universität Bremen (Geowissenschaften) untersucht durch Langzeitverankerung in der Nähe von Cape Blanc (21°17 N; 20°43 W) den Partikelfluss der Sahara. Eine Verankerung wurde dort geborgen und durch eine neue ersetzt.
Die Arbeitsgruppe Luftchemie am Institut für Umweltphysik, Universität Heidelberg, möchte dieses Jahr DOAS-Streulichtmessungen (differentielle optische Absorptions-Spektroskopie) wurden bis Kapstadt durchführen, bei denen atmosphärische Spurenstoffe anhand ihrer Lichtabsorption detektiert wurden.
Die Spurenmetallgruppe von NIOZ hat den Eisengehalt des Obflächenwassers während der Anreise bestimmt. Hierfür wurde das Seewasser mit einer Spezialeinrichtung angesaugt und analysiert. Ein Vergleich der Meßmethoden wurde durchgeführt.

A. SUMMARY

Saad El Naggar/ AWI-Logistics

The first leg of the 18th Antarctic cruise of RV "Polarstern" was started in Bremerhaven on 29.09.2000 and was completed in Cape Town on 23.10.2000. During this cruise different scientific instrumentations were tested and an atmospheric marine program was carried out. The ship was sailed on the shortest way to Cape Town (Fig. 1). The transfer time was about 24 days including 2 days for station works between Bremerahaven and Las Palmas for testing the winchs and the new machine control system. An other station of about 6 hours was carried out nearby Cape Blanc to recover one mooring at approx. 21°17 N; 20°43 W and redeploy it at the same position. A part of the testing crew (AWI, INTER, RFL, ROCHEM, MTU, STNH, WERUM) was disembark on 08.10.2000 in Gran Canaria (Las Palmas).
During the third step of the Midlife Conversion (MC) of RV "Polarstern" between 29.8.2000 - 29.09.2000 in Bremerhaven, the main machine control system was replaced by the company "Motoren und Turbinen Union, (MTU)", Friedrichshafen. The winch's power supply and control system was also replaced by the company "STN-Atlas-Elektronik", Hamburg and Bremerhaven. Sea trials of the mentioned systems were carried out during this cruise.

The old data acquisation and display system of RV "Polarstern" (PODEV) was replaced by a new (PODAS) on a real-time based data management system (RTDBMS). The company WERUM, Lüneburg has been developed this software package and did the sea trial during the cruise.
The on VMS-based computers (Digital Equipment) were replaced by SUN-Server (UNIX-based). More than 30 Compaq computers (Windows 2000) are installed for data display and acquisation. Installation and tests of the hardware has been carried out.
The UV-B-group of AWI has measured the UV-B-irradiance distributions (spectral and doses measure– ments) as a function of latitude. The AWI-spectrometer (UV-B & UV-A) and the electronic UV-B-personal dosimeter (ELUV-14) were used. Calibration of instruments was done. In addition, ozone profile soundings were carried out during the cruise.
A scientfic group from University of East Anglia, UK, has carried out different on-line measurements during the cruise:

- Aerosol and rain samples were collected using Graseby-Anderson high-volume samplers and collection funnels to determine the deposition of iron to Atlantic surface waters.
- Biogenic production of volatile organo-halogen and organo-nitrogen compounds in seawater were measured and analysed.
- Quantifying the air-sea exchange of carbon dioxide was the third programme of this group during this cruise.

The geoscience department of the University of Bremen, SFB 261, is monitoring the Sahara dust deposition to the Atlantic waters by using a mooring system located nearby Cape Blanc (21°17 N; 20°43 W). The mooring was recovered and a new one was deployed at the same location.
The institute of environmental Physics of the university of Heidelberg has carried out Differential Optical Absorption Spectroscopy (DOAS) measurements during the cruise to determine the distributions of different chemical tracers in the atmosphere.
The trace metal group from NIOZ made continuous underway measurements of dissolved iron using a towed fish and trace metal clean pumping system. Intercalibration of measuring systems was carried out.

B. ERPROBUNG UND ABNAHME DER NEUEN INSTALLATIONEN

Saad El Naggar/AWI-Logistik

Während der dritten Phase der Generalreparatur des FS „POLARSTERN" vom 29.08.2000 – 29.09.2000 wurden folgende Umbaumaßnahmen realisiert:

- Austausch des VAX-VMS-Rechners gegen 3 Sun-Enterprise 250-Server.
- Austausch der alten Anzeigerechner gegen neue COMPAQ-DESKPRO ENS 6600 (30 Stück).
- Austausch des alten Datenerfassungssystems PODEV gegen eine neue auf UNIX- und Real-Time-Datenbank basierende Software (PODAS).
- Abrüstung der wissenschaftlichen Navigationsanlage ANP 2000. Als Ersatz dafür wurde die Navigationsanlage NACOS–55-3 nach Anpassung der Sensorik eingesetzt.
- Abrüstung des Differential GPS-(DGPS)-Systems von RACAL SURVEY. Die Genauigkeit des GPS-Systems wurde durch die US-Regierung seit dem 01.05.2000 nicht mehr künstlich herabgesetzt und liegt nun bei ca. 18 m. Selective Availability (SA) ist abgeschaltet.
- Abrüstung des GPS-Rechners (VAX 4000).
- Modernisierung der Hauptmaschinensteuerung.
- Modernisierung der Versorgung und Steuerung der Winden.

Auf dem Teilabschnitt Bremerhaven – Las Palmas wurden die installierten Systeme im realen Betrieb getestet und zum Teil abgenommen. Die restlichen Arbeiten wurden bis Kapstadt durchgeführt.
Die Integration der neuen Erfassungssoftware PODAS wurde bis Kapstadt ergänzt aber nicht abgenommen.
Zur Abnahme von Maschinen- und Windensteuerungen wurden ca. 48 Stunden Schiffszeit benötigt.

B. SEA TRIAL OF THE NEW INSTALLATIONS

S. El Naggar/ AWI-Logistics

RV "POLARSTERN" was at the Lloyd Werft shipyard, Bremerhaven, from 29.08.2000 – 29.09.2000, where the third phase of the Midlife Conversion (MLC) was carried out. Following main installations were made:

- Replacement of all VAX-VMS-computers by three SUN-Enterprise-250-Servers.

- Replacement of all info terminals by COMPAQ-DESKPRO ENS 6600 computers with TFT-display (30 pieces).
- The old data acquisition system PODEV was replaced by the new PODAS, based on Real Time Data Based Management System (RTDBMS).
- The scientific navigation unit "ANP 2000" was dismantled. The new navigation system (NACOS-55-3) was modified to replace the "ANP 2000".
- Differential GPS (DGPS) of RACAL SURVEY was operationally stopped, due to the fact that the GPS system has now an accuracy of 18 m without DGPS. Selective availability (SA) was disabled since 01.05.2000.
- GPS-workstation was removed and replaced by different GPS-receivers and integrated navigation system (MINS).
- The main machine control system was replaced by a new one based on the newest technology.
- Supply and control system of the winch was dismantled and replaced by a state of the art system.

Between Bremerhaven and Las Palmas all newly installed equipments and systems were tested under real conditions. The used ship's time for the mentioned sea trials was about 48 hours.

Maschinensteuerung

S. El Naggar, R. Krause/AWI; E. Wagner, W. Manthei, V. Sculz, A. Pluder /RFL; H.-J. Thomas, H.-D. Längin, M. Müller /MTU; P. Drauschke/INTER

Die Maschinensteurung wurde durch die Firma Motoren und Turbinen Union (MTU), Friedrichshafen, unter Einsatz moderner Technologien konzipiert und realisiert. Dabei wurde die alte Steuerung komplett demontiert und durch neue Hard- und Software ersetzt. Die komplett neue Verkabelung wurde in der Werft vorgenommen und während der Überfahrt ergänzt. Die neue Software konnte nicht im Hafen getestet werden, da die Randbedingungen zur Regelung fehlten. Die Software wurde während der Reise angepaßt, getestet und kurz vor Las-Palmas erfolgreich abgenommen. Kleine Mängeln (Claims) wurden dann in Kapstadt beseitigt.
Es soll hier noch erwähnen werden, daß die Mitarbeiter der Firma MTU eine sehr gute Arbeit geleistet haben und eine sehr gute, effektive und ergonomische Steuerung geliefert haben.

Windensteuerung

S. El Naggar, R. Krause/AWI; E. Wagner, W. Manthei, V. Sculz, A. Pluder /RFL; G. Woike, D. Bade, C. Heckel/ STNH

Die Winden an Bord der Polarstern sind die Drehscheibe des Forschungsbetriebes und dementsprechend müssen sie technisch sicher und zuverlässig sein. Dadurch wurde ein neues Versorgungs- und Steuerungskonzept erarbeitet und realisiert. Zwei Jahre waren notwendig, um dieses Projekt zu planen und zu realisieren.
Die alte Windensteuerung wurde durch eine moderne auf SPS (Speicher Programmierbare Steuerung) basierende Steuerung durch die Firma STN-Atlas-Elektronik/ Hamburg (STNH) ersetzt. Dafür wurden neue Versorgungsmodule angeschafft, modular aufgebaut und in Betrieb genommen. Jede Winde hat dadurch ihre eigene Stromversorgung. Neue Fahrtpulte wurden angefertigt und aufgestellt. Alle Versorgungskabel wurden neu verlegt. Datenerfassung und –verteilung erfolgt über Windows-NT-Rechner.
Auf dem Teilabschnitt Bremerhaven-Laspalmas wurden alle Winden einzelnen eingestellt, getestet und unter realem Betrieb gefahren.
Das System hat sehr gut funktioniert und somit konnte die Steuerung komplett vor Las-Palmas abgenommen werden. Hier möchten wir ebenfalls erwähnen, daß die Mitarbeiter der Firma STNH sehr gute Arbeit geleistet und ein modernes System geliefert haben.

Biologische Kläranlage

S. El Naggar, R. Krause/AWI; E. Wagner, W. Manthei, V. Sculz, A. Pluder /RFL; U. Neuhäuser/ ROCHEM

Die biologische Kläranlage wurde während der Werftliegezeit durch eine moderne, ebenfalls auf Bioreaktor basierende Anlage ersetzt. Hierfür waren große Umbaumaßnahmen notwendig.
Das Ziel der Modernisierung war, eine gemeinsame Kläranlage für Schwarz- und Grauwasser zu installieren und somit die Effektivität zu erhöhen und als Vorbild beim Einsatz im Antarktischen Vertragsgebieten zu dienen . Die Anlage soll die Anforderungen an Kläranlagen auf Schiffen weitgehend übertreffen, so daß nur geklärtes reines Wasser über Bord geht.
Leider funktionierte das Vorfiltersystem an Bord nicht und es konnte die Anlage deshalb nicht mit voller Leistung gefahren werden. Modifikationen und Reparaturen an Bord haben den Betrieb aber sicher gestellt. Eine Ingenieurin der Firma ROCHEM nahm dann am folgenden Abschnitt teil, um neue Konzepte und Problemlösung für den sicheren Betrieb zu suchen.

Hydro-Sweep und Parasound

S. El Naggar, F. Niederjasper, R. Usbeck, S. Gauger /AWI; J.Hofmann /RFL

Das Hydrosweep wurde auf die volle Funktionalität nach Fehlerbeseitung in der Software durch die Firma STN-Atlas-Elektronik, Bremen, überprüft. Die neuen Datentelegramme , die nun durch die Navigationsanlage NACOS nach dem Abrüsten der ANP-anlage erzeugt werden, wurden auf Vollständigkeit, Kompatibilität und Integration überprüft.
Hydrosweep hat nun die volle Leistung und Funktionalität. Die Daten zeigten aber Ausfälle bei einigen Beam der Längswandler. Dies wurde auch an Hand der Einmessung in Bremerhaven bestätigt. Mehr als 50% der Längswandlerbasen sind elektrisch beschädigt und erfordern somit den Austausch des Wandlers.
Bei PARASOUND wurde das Datenerfassungsystem auf Windows-Rechner umgestellt. Dafür wurden zwei neue PC's mit Wechselplatten angeschaff, installiert und getestet.
Während der Fahrt bis Kapstadt wurde das System für den Dauereinsatz getestet.
Nach anfänglichen Schwierigkeiten lief dann das System problemlos durch. Die Daten zeigten, daß das System nun voll einsatzfähig ist.

Navigationsanlage NACOS-55-3

S. El Naggar, P. Gerchow /AWI, J. Hofmann /RFL

Die wissenschaftliche Navigationsanlage ANP 2000 STN-Atlas wurde während der Werftzeit abgerüstet. Sie diente als Datenerfassung für die Navigationssensorik und als Systemsteuerung. Als Ersatz dafür wurde die neue Navigationsanlage NACOS–55-3 nach Anpassung des Sensorikinterfaces eingesetzt.
Die Navigationssensoren wurden an die neue Datenerfassungsanlage (PODAS) direkt angeschlossen. Dafür waren viele Anpassungsarbeiten notwendig.
NACOS liefert nur die Systemparameter an PODAS und ersetzt aus nautischer Sicht die ANP2000 voll.
Der Datenaustausch zwischen NACOS und Hydrosweep konnte nicht realisiert werden. Hier müssen noch Grundsatzfragen der Zulassung bei der BSH geklärt werden.

GPS und DGPS

S. El Naggar, P. Gerchow /AWI, J. Hofmann /RFL

Die Genauigkeit des GPS-Systems wird auf Beschluß der US-Regierung seit dem 01.05.2000 nicht mehr künstlich herabgesetzt (Selective Availability (SA) wurde abgeschaltet). Die absolute Genauigkeit liegt nun bei ca. 18 m und kann mit

normalen GPS-Empfängern erreicht werden. Dadurch wurde der Einsatz des DGPS-Services von Racal Survey auf Polarstern überflüssig. Der Vertrag mit Racal Survey wurde zum 1.10.2000 gekündigt.
Das alte VAX-GPS-System wurde abgerüstet. Als Ersatz dafür wurde ein neues System geschaffen bestehend aus zwei hochwertigen Zweifrequenz-GPS-Empfängern (Trimble Typ MS750) und der Navigationsplattform MINS. MINS liefert die gefilterte Position und dient als Systemsensor für folgende Sensoren:
Position, Schiffsgeschwindigkeit über Grund, Heading und Course.
Diese Konstallation hat sich sehr gut bewährt und wird demnächst noch genauer auf Zuverlässigkeit und Genauigkeit untersucht.

Datenerfassungssystem PODAS

M. Reinke, P. Gerchow, , S. El Naggar /AWI; J. Hofmann/RFL, C. Sommer, T. Viergutz, U. Zenker, H. Schmidt /WERUM

Auf dem Fahrtabschnitt ANT XVIII/1 wurde das neue Schiffsinformationssystem PODAS als Nachfolge des PODEV Systems implementiert. Die Erneuerung erfolgte im Rahmen der Generalreparatur Polarstern. Das PODEV System war seit 1993 auf dem Schiff im Betrieb und ersetzte das INDAS System, das seit 1984 Schiffs- und Umweltdaten an Bord aufzeichnete. Vorrangig war der Ersatz durch die Bindung des alten Systems an die VAX Hardware und das VAX VMS Betriebssystem, die keine Konvertierung auf die neuen UNIX Rechner erlaubte, notwendig geworden. Weiterhin sollten bei dieser Gelegenheit auch die Datenqualität und die Verfügbarkeit an Bord und auch nach den Reisen verbessert werden.
Technisch beruht das PODAS System auf dem DAVIS (Data Audio Video Information) System der Fa. WERUM, Lüneburg). Über DAVIS werden die Meßdaten der schiffsseitigen Geräte, wie GPS, Lote, Meteorolgie aber auch die Winden, auf einem zentralen Server (Sun UNIX) gespeichert und parallel in (fast) Echtzeit auf die Anzeigegeräte (Info PC, Windows 200) verteilt. Die Anzeige auf den Info PC ist durch die Anwender für ihren jeweiligen Zweck frei konfigurierbar. Weiterhin werden Schnittstellen bereitgestellt, die diese Information auch über das Internet Protokoll (TCP/IP) für eigene Meßanwendungen zur Verfügung stellen. Neben den Standardgeräten können auch Geräte, die nur zeitweise im Rahmen von Projekten genutzt werden, in das System integriert werden. Über eine Schnittstelle des bordinteren Webservers können zu jeder Zeit beliebig verdichtete Zeitreihen ausgewählter Sensoren aus dem System heruntergeladen werden. Parallel werden in einer zentralen Datenbank auf 10 Minuten verdichete, ausgewählte Daten vorgehalten. Diese Datenbank ist über eine sogenannte „Open Database Connect Schnittstelle" (ODBC) auch aus Anwendungsprogrammen, wie Microsoft Excel, ESRI ArcView oder ArcInfo ansprechbar. Sie wird über alle Fahrten des Schiffes

weitergeführt, während die hochaufgelösten Daten nur auf dem jeweiligen Fahrtabschnitt an Bord verfügbar sind. Am Ende eines jeden Fahrtabschnittes werden die Daten auf Digital Versatil Disk (DVD) archiviert und eine Kopie nach Bremerhaven geschickt. Hier werden alle Daten über den zentralen Webserver in maximaler Auflösung verfügbar gemacht (Landsystem).
Die Verfügbarkeit des Systems wird dadurch optimiert, daß es parallel auf drei UNIX Rechnern (SUN) läuft. Es könnte aber leistungsmäßig und durch die Systemadministratoren konfigurierbar auch einem dieser Rechner arbeiten. Die von den Geräten einlaufenden Meßdaten werden direkt durch das System auf ihre Plausibilität geprüft. Bei Abweichungen werden ein elektronisches Protokoll angelegt und die Systemadministratoren alarmiert. Das Fehlerprotokoll kann zusammen mit den Daten ausgegeben werden.
Im Bremerhavener Landsystem werden neben den PODAS Daten, die seit ANT XVIII/1 gewonnen wurden, auch die alten PODEV Daten und –soweit möglich auch die INDAS Daten - mittelfristig verfügbar gemacht werden.
Auf dem Fahrtabschnitt ANT XVIII/8 wurden umfangreiche Tests an dem System durchgeführt. Geprüft wurde auf Grundlage des ausführlichen Pflichtenheftes, die korrekte Speicherung; Anzeige und Extraktion der Daten. Besonderen Wert wurde insbesondere auf die genaue zeitliche Zuordnung der Daten untereinander gelegt. Die Anbindung der ca. 20 Geräte mit ca. 100 Sensoren erwies sich als erheblich aufwendiger als angenommen, da die vorhandene Dokumentation der Meßgeräte in vielen Fällen lückenhaft war. Zur Sicherstellung der Funktionalität des Systems nahm deshalb ein Ingenieur der Lieferfirma auch noch am Fahrtabschnitt ANT XVIII/2 teil. Am Ende dieses Fahrtabschnittes wurde für das System eine Teilabnahme erteilt, da die alle kritischen Anforderungen erfüllt waren. Kleinere Nachbesserungen bis zur endgültigen Abnahme werden auf den nächsten Fahrtabschnitten vorgenommen werden.
Zusätzlich zu den bereits installierten Programmen werden an Bord im ersten Halbjahr 2001 eine elektronische Stationsplanung und ein elektronisches Stationsbuch als Bestandteil des PODAS Systems in Betrieb genommen.
Die elektronische Stationsplanung ermöglicht der wissenschaftlichen Fahrtleitung, die in den täglichen Planungssitzungen an Bord festgelegten Abläufe, in einfacher Weise über alle Info PC sichtbar zu machen. Da Änderungen in der Planung automatisch hervorgehoben werden, können sich die Fahrtteilnehmer an jedem Info PC schnell über den aktuellen Stand informieren.
Das elektronische Stationsbuch ersetzt das auf der Brücke geführte Stationsbuch. Die zum Zeitpunkt eines Geräteeinsatzes gemessenen Parameter, wie Position, Wassertiefe, Geschwindigkeit etc., werden automatisch in das Protokoll eingetragen. Das Stationsbuch kann, zu jedem Zeitpunkt, über den bordinternen Web Server abgefragt und die Daten herunter geladen werden. Es ist geplant, alle früheren

Polarstern Stationen in das elektronische Stationsbuch nachzutragen. Das Stationsbuch wird auch über das Landsystem im Intra- und Internet verfügbar sein. Mit PODAS verfügt Polarstern über das modernste Schiffsinformationssystem innerhalb der deutschen Forschungschiffflotte.

C. FORSCHUNGSPROGRAMME / SCIENTIFIC PROGRAMME

C.1 UV-B-Dosimetrie und Ozonverteilung von Bremerhaven bis Kapstadt

Saad El Naggar, Otto Schrems, Helmut Tüg, Christian Groß, Taddäus Bluszcz, AWI

Die solare UV-B-Strahlung in der Antarktis hat in den letzten 17 Jahren, bedingt durch den Ozonabbau, drastisch zugenommen. Die Auswirkung dieser Strahlenbelastung auf die Biosphäre ist heute ein Schwerpunkt vieler wissenschaftlicher Programme. Die Auswirkungen auf die Menschen, die sich in antarktischen Gebieten aufhalten, bedarf jedoch noch systematischer Studien. Zu diesem Projekt sollten Basisdaten gewonnen werden.
Bedingt durch die erhöhte Einstrahlung und das hohe Albedo des Schnees in der Antarktis (85% im UV-B-Bereich), ist die schädigende Wirkung der UV-B-Strahlung auf den Menschen sehr hoch. Mit Hilfe verschiedener Dosimetersysteme (Bio-, *Bacillus Subtilis,* Polysulphon- und elektronisches Dosimeter), sollte in einer Langzeitstudie die maximal vorkommende UV-B-Dosis auf der Neumayer-Station ermittelt werden, um Risikofaktoren abschätzen zu können. Dafür wurden UV-B-Personen-Dosimetrie-Messungen an Überwinterern und Expeditionsteilnehmern durchgeführt.
Für die Risikoabschätzung werden Vergleichsdaten benötigt. Diese sollen auf meridionalen Abschnitten zu verschiedenen Jahreszeiten ermittelt werden.
Dadurch gewinnt man die maximal zu erwartende Dosis auf Meeresniveau und deren Variationen.

Ziele des Forschungsvorhabens sind:

a) Bestimmung der globalen UV-B-Dosis auf dem meridionalen Abschnitt zwischen Bremerhaven und Kapstadt unter Verwendung des Biofilms, des Polysulphondosimeters und des elektronischen UV-B-Dosimeters ELUV-14
b) Bestimmung der maximalen Tagesdosis in Abhängigkeit von der Sonnenhöhe und Ozonkonzentration
c) Messung der meridionalen spektralen UV-B-Strahlungsverteilung
d) Messung der meridionalen Ozonverteilung

Arbeitsprogramm:

Das Arbeitsprogramm umfaßte:

- Exponieren der verschiedenen Dosimeter zur Bestimmung der globalen Tagesdosis
- Spektrale Messung der solaren Strahlung mit Hilfe des AWI-Spektrometers
- Bestimmung der Ozonkonzentrationen mit Radiosonden.

Durchführung:

a) Dosisbestimmung:

Die Dosismessungen wurden vom 01.10.2000 bis 25.10.2000 mit folgenden Dosimetern durchgeführt:

- Täglich wurden zwei elektronische Dosimeter (Eluv-14) exponiert, die zeitaufgelöst die gewichtete UV-B-Strahlungsleistung jede Minute aufgezeichnet haben. Sie wurden täglich ausgelesen und ausgewertet.
- Täglich wurden zwei Polysulphon-Dosimeter exponiert, die die gewichtete UV-B-Strahlungsleistung integrierend aufgezeichnet haben. Diese Dosimeter können nicht vor Ort ausgewertet werden. Sie liefern nur die Tagesdosis.
- Täglich wurden zwei biologische (Bacillus Subtilis) Dosimeter exponiert, die die gewichtete UV-B-Strahlungsleistung integrierend aufgezeichnet haben. Diese Dosimeter können ebenfalls nicht vor Ort ausgewertet werden.

UV-B-Messungen am Boden sind vom Bedeckungsgrad des Himmels durch Wolken stark abhängig. Um eine absolute Bestimmung der Strahlungsintensität zu garantieren, muß der Himmel Wolkenfrei sein. Die Tatsache, daß man während der Reise einige bewölkte Tage vorfinden wird, wurde bei der Planung der Reise berücksichtigt. Die Messergebnisse sind in der Tabelle Tab1-UVB zusammengefasst.

Während dieser Reise gab es aber nur wenige wolkenfreie Tage. Dadurch sind die gesteckten Ziele nicht erreicht worden. Die aufgezeichnete Dosisverteilung war von der starken Bewölkung ab dem Äquator eingeprägt und somit war eine Aussage über die absolute Verteilung nicht möglich (Abb. 1-UVB). Man kann aber die Daten von mehreren Expeditionen zusammenlegen und die absolute Verteilung interpolieren, indem man nur die wolkenfreien Tage zur Berechnung verwendet.

Die ermittelten Tagesdosen der ungewichteten UV-B-Strahlung lagen zwischen 2000 und 60000 J/m^2. Die erythem-gewichteten lagen dagegen zwischen 700 und 3700 J/m^2. Dies entspricht 3.3 bis 17.6 MED (Minimal Erythemal Dose = 210 J/m^2).

Die maximal von 290 bis 322 nm integrierte Strahlungsleistung lag bei 3.3 W/m^2 für die ungewichtete und bei 215 mW/m^2 für die Erythem-gewichtete Strahlung.

b) Spektrale Messung der UV-B-Strahlung:

Zur spektralen Messung der UV-B-Strahlungsintensitäten wurde das modifizierte AWI-Spektrometer Land 5 eingesetzt. Dabei wurden aller 5 Minuten Spektren zwischen 280 und 322 nm sowie im UV-A-Bereich zwischen 305 und 460 nm aufgezeichnet.

Die Daten wurden vor Ort auf ihre Qualität überprüft und bearbeitet. Dabei wurden Integrale zur Berechnung der UV-B-Dosis gebildet und mit den Ergebnissen anderer Dosimeter verglichen.

Die Spektraldaten dienen als Basis zur Erstellung von Langzeitmeßreihen und zur Berechnung aller abgeleiteten Größen sowie zur Kalibrierung der verwendeten Meßsystemen.

Das Spektrometer wurde technisch erneuert und kann nun auch die UV-A-Starhlung messen. Es wurde auch mit einer neuen Software ausgestattet. Der Erfassungsrechner ist leider vom 14.10.2000 bis 17.10.2000 ausgefallen. Dadurch entstand eine Datenlücke von drei Tagen, die durch Interpolation von anderen Meßsystemen (Eluv-14) ergänzt wurde. In Abb. 2-UVB ist ein Spektrum vom 18.10.2000 als Beispiel dargestellt. Dort ist erkennbar, daß praktisch unter 290 nm keine meßbare Intensität vorhanden ist.

C) Ozonmessungen:

Ozonprofile bis zu 35 Km Höhe wurden täglich seit dem 03.10.00 mit ECC-Ozonsonden ermittelt. Es wurden insgesamt 25 Ozonsonden gestartet jedoch nur 17 waren davon auswertbar. Es traten verschiedene Fehler auf, wie Signalverlust der Sonde, Ozonwertverlust und Programmabsturz. Große Variationen des Ozonorofils wurden im Norden beobachtet. Im Süden hingegen zeigten die Ozonprofile stabile Verhältnisse mit gut ausgeprägtem Maxima bei ca. 26 Km.

Totalozonkonzentrationen nahmen vom 50° N bis ca. 5° N stetig ab (300 bis 250 DU). Ab 5° N bis 30° S stieg das Gesamtozon stetig an und erreichte die 300 DU wieder. In Tabelle Tab.2-UVB sind die Ergebnisse der Ozonsondierungen zusammengefaßt.

Abbildung Abb.3-UVB zeigt den gewonnen Ozonveraluf.

Tab. 1-UVB (1 MED = 210 J/m2)

Date	Latitude [deg]	Longitude [deg]	UV-B-dose [J/m_]	Erythemal dose [J/m_]	Erythemal Dose [MED]	Ozone [DU]	Max.Sun Elevation [°]
01.10.00	52.1	2.9	18523.488	731.744	3.484		17.6
02.10.00	49.4	-4.0	17262.555	740.637	3.527		20.8
03.10.00	45.8	-9.1	20476.813	910.846	4.337	263.6	39.4
04.10.00	41.0	-11.5	27197.888	1295.680	6.170		44.9
05.10.00	36.2	-13.0	25426.494	1183.049	5.634	298.9	49

06.10.00	33.6	-13.7	29958.793	1398.929	6.662	310	51.3
07.10.00	31.1	-14.6	33206.185	1583.542	7.541		53.9
08.10.00	26.1	-16.7	38751.374	2379.748	11.332	293.4	57.4
09.10.00	22.3	-19.8	44482.802	2379.748	11.332	294.6	59.8
10.10.00	21.1	-20.6	45209.955	2514.362	11.973	242.9	62.1
11.10.00	16.2	-19.8	40567.101	2292.222	10.915	272.6	67.2
12.10.00	10.6	-18.6	42623.282	2497.313	11.892	278.3	72.3
13.10.00	6.1	-15.3	39560.198	2451.525	11.674	248.2	76.4
14.10.00	1.6	-11.7	55572.515	3443.800	16.410	264	80.9
15.10.00	-2.7	-8.2	60505.100	3749.470	17.800	264.5	84.5
16.10.00	-6.9	-4.8	36782.395	2279.386	10.850		88
17.10.00	-11.3	-1.3	26642.654	1535.814	7.313	288.9	87.7
18.10.00	-13.4	0.3	55345.610	3145.858	14.980	311.5	83.9
19.10.00	-17.1	3.4	52979.124	3037.950	14.466	316.5	80.2
20.10.00	-20.9	6.6	31700.221	1623.521	7.731	309.2	77.2
21.10.00	-23.1	8.5	44423.052	2397.212	11.415	305.2	74.7
22.10.00	-26.7	11.7	60393.286	3191.532	15.198	321.3	70.4
23.10.00	-32.9	17.4	33994.319	1737.587	8.274		
24.10.00	-33.9	18.4	54015.571	2678.706	12.756		
25.10.00	-33.9	18.4	59187.855	2932.583	13.965		

Tab. 2-UVB

Date	Start Time [UTC]	Latitude [deg]	Longitude [deg]	Max.Height [km]	Ozone Measured [DU]	Ozone Residual [DU]	Ozone Total [DU]	Max. Sun Elevation [°]
03.10.00	10:12	45.69	-9.28	34350	231.9	31.7	263.6	39.4
04.10.00	10:02	41.57	-11.75	34211				44.9
05.10.00	10:14	36.3	-13.01	30505	232.2	66.7	298.9	49
06.10.00	09:50	33.74	-13.7	33207	258.9	51.1	310	51.3
07.10.00	10:02	31.11	-14.55	30904				53.9
08.10.00	13:22	27.03	-15.31	32100	232	61.4	293.4	57.4
09.10.00	09:50	24.63	-17.77	32417	236.9	57.7	294.6	59.8
10.10.00	14:32	21.2	-20.7	27775	152.8	90.1	242.9	62.1
11.10.00	10:01	16.67	-19.09	30263	198.2	74.4	272.6	67.2
12.10.00	10:50	10.73	-18.71	29979	189	89.3	278.3	72.3
13.10.00	10:13	6.45	-15.63	34972	216.8	31.4	248.2	76.4
14.10.00	10:03	1.7	-12.05	32923	207	57	264	80.9
15.10.00	10:00	-2.34	-8.61	33031	217.6	46.9	264.5	84.5
16.10.00	10:01	-6.57	-5.21	32054				88
17.10.00	14:16	-11.65	-1.1	29007	194.5	94.4	288.9	87.7
18.10.00	09:52	-15.4	1.76	33136	254.7	56.8	311.5	83.9
19.10.00	09:59	-19.15	5.12	31505	241.4	75.1	316.5	80.2
20.10.00	10:29	-22.94	8.34	31205	254.8	54.4	309.2	77.2
21.10.00	13:20	-26.94	11.89	31841	245.7	59.5	305.2	74.7
22.10.00	10:38	-30.55	15.17	32402	264.7	56.6	321.3	70.4

Abb. 1

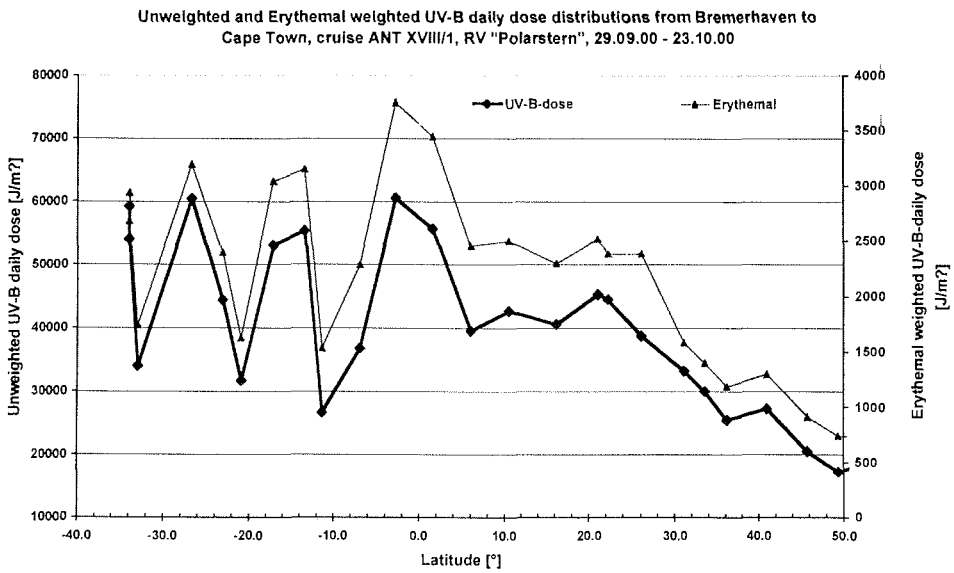
Unweighted and Erythemal weighted UV-B daily dose distributions from Bremerhaven to Cape Town, cruise ANT XVIII/1, RV "Polarstern", 29.09.00 - 23.10.00
UV-B-dose
Erythemal
Unweighted UV-B daily dose [J/m²]
Erythemal weighted UV-B-daily dose [J/m²]
Latitude [°]
80000
70000
60000
50000
40000
30000
20000
10000
4000
3500
3000
2500
2000
1500
1000
500
0
-40.0
-30.0
-20.0
-10.0
0.0
10.0
20.0
30.0
40.0
50.0

Abb. 2

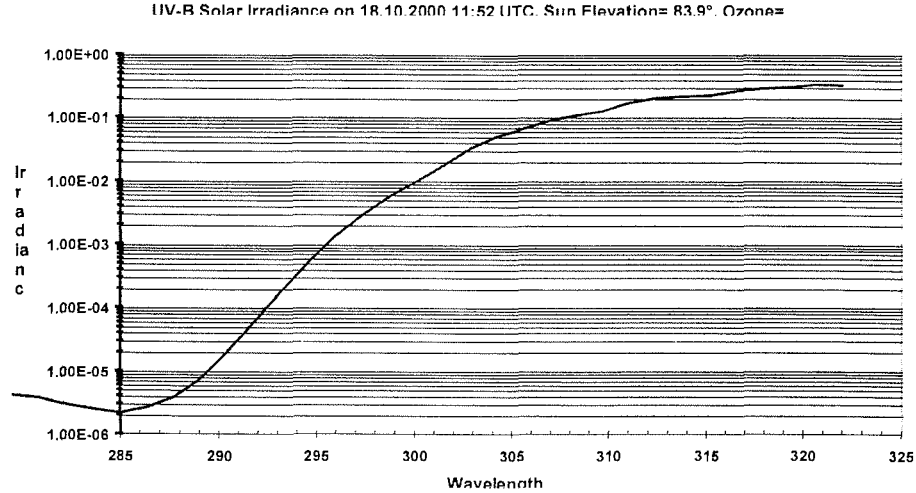
UV-B Solar Irradiance on 18.10.2000 11:52 UTC. Sun Elevation= 83.9°. Ozone=
Irradiance
Wavelength
1.00E+00
1.00E-01
1.00E-02
1.00E-03
1.00E-04
1.00E-05
1.00E-06
285
290
295
300
305
310
315
320
325

Abb. 3

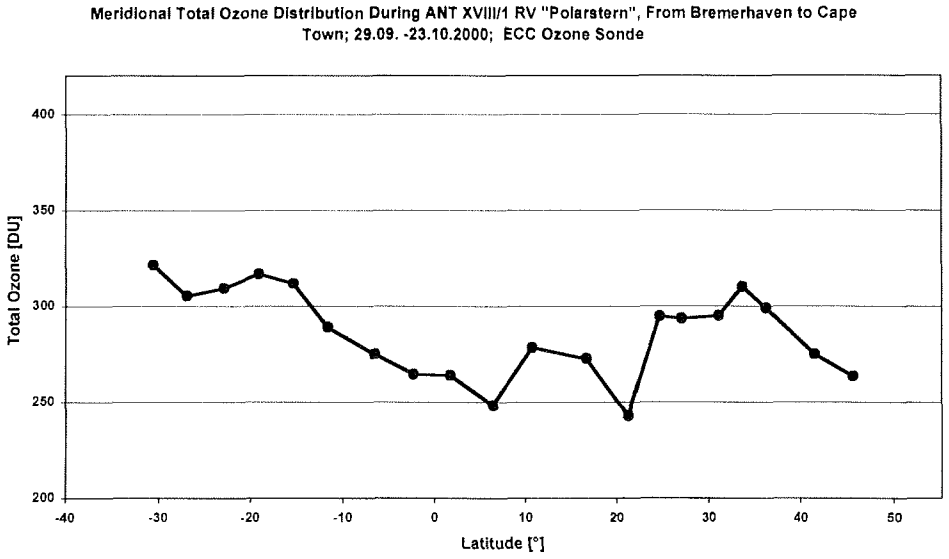

C.2 Long term particle flux studies in the upwelling system off Cape Blanc Water sampling from the ships sea-water system

Monika Segl and Raphael Schäfer /UB, Dept. of Geosciences, Univ. Bremen

Since 1988, long term particle flux studies by means of sediment-trap moorings, have been performed in the Cape Blanc region at 21°17N, 20°43W. Our mesotrophic site is located at the edge of the seasonally moving Cape Blanc filament, which travels several km offshore into the open eastern Atlantic.

On this cruise, mooring CB10 was recovered and CB11 was deployed. CB 10 has one sediment trap 500m above the sediment surface (ca. 3500m water depth) and another sediment trap at ca. 1000m water depth. 20m below the upper trap, a current meter was installed. In CB11 Traps and current meter were deployed at the same depths again.

CB10 was released in the early morning of the 10th. of october. 15 minutes later the top-buoy was floating at the surface and the whole equipment was recovered within two hours. Unfortuanately, the computer of the sediment-traps had the year2000

problem so it hasn't changed the sampling cup since december 1999 and we have only one sample per trap from january to october 2000.

In addition to the sediment trap deployment daily samples were taken from the ships seawater pumps. Those samples are for calibration of paleoceanographic proxis. 60 l of seawater were filtered every day for alkenone investigations. The uk-index of the alkenones, which is closely related to the sea surface temperature, will be meassured on the particulate matter on the filters. As we crossed several temperature zones from 17° to 28°, those samples will be very important for calibration.
Twice a day the seawater was pumped over a 20_m net for several hours. From those samples foraminifera were collected immediatly. On this foraminifera samples the assamblage of different species will be investigated, afterwards the stable carbon and oxygen isotopes of the shells will be meassured. Both is done as well to calibrate the parameters as paleoceanographic proxis.

Table UB-1 and Tab UB-2 show the locations for the alkenon and foraminifera sampling.

Tab. UB 1: Alkenon – Sampling

Sample-No..	Date	Time (UTC)	Position	Watertemp	Salinity
1	3.10.2000	9:18	46°01,6N, 008°48,0W	17,5	35,59
2	4.10.2000	8:14	41°28,5N, 011°24,1W	19,4	35,76
3	5.10.2000	8:12	36°39,1N, 012°55,6W	21,3	36,25
4	6.10.2000	17:55	33°33,4N, 013°50,9W	22,3	36,60
5	7.10.2000	8:08	31°14,4N, 014°30,8W	22,7	36,76
6	8.10.2000	18:33	27°00,3N, 016°00,7W	22,8	36,47
7	9.10.2000	13:00	24°02,2N, 018°27,2W	23,1	36,55
8	11.10.2000	8:12	16°57,1N, 019°56,2W	27,0	36,12
9	12.10.2000	9:34	11°07,5N, 018°45,4W	28,7	34,49
10	13.10.2000	9:10	06°32,2N, 015°42,2W	28,3	34,28
11	14.10.2000	9:19	02°00,0N, 012°04,2W	26,9	35,38
12	14.10.2000	22:10	00°20,0S, 010°12,3W	24,5	35,73
13	16.10.2000	8:24	06°23,8S, 005°21,0W	23,5	35,77
14	17.10.2000	9:15	10°54,1S, 001°42,6W	22,1	35,97
15	18.10.2000	9:16	15°08,3S, 001°45,9E	19,2	36,05
16	19.10.2000	9:10	19°08,2S, 005°06,4E	17,9	36,59
17	20.10.2000	8:34	22°43,4S, 008°10,5E	17,0	35,39

Tab. UB-2: Foraminifera Sampling

Sample Nr.	Date	Start Time [UTC]	Position	WaterTemp	Salinity	Stop Time [UTC]	Position	Water Temp	Salinity
F1	3.10.2000	9:18	46°01N, 008°48W	17.5	35,59	12:00	45°47N, 009°09W	17,4	35,59
F2	3.10.2000	15:06	45°18N, 009°48W	18,4	35,59	17:45	44°49N, 010°10W	17,9	35,58
F3	4.10.2000	8:14	41°28N, 011°24W	19,4	35,75	9:54	41°15N, 011°29W	20,2	35,87
F4	4.10.2000	15:00	40°25N, 011°45W	20,4	35,89	17:18	40°01N, 011°53W	20,7	35,91
F5	5.10.2000	8:13	36°39N, 012°56W	21,3	36,25	10:26	36°19N, 013°05W	21,6	36,42
F6	5.10.2000	16:16	36°05N, 013°05W	21,7	36,47	17:55	35°44N, 013°11W	22,2	36,67
F7	6.10.2000	17:55	33°33N, 013,51W	22,3	36,60	19:12	33°21N, 013°54W	22,3	36,62
F8	7.10.2000	9:11	31°07N, 014°33W	22,6	36,77	10:58	30°55N, 014°36W	22,9	36,79
F9	7.10.2000	13:38	30°36N, 014°41W	23,1	36,74	16:25	30°12N, 014°48W	23,2	36,75
F10	8.10.2000	15:17	27°34N, 015°35W	22,7	36,36	17:17	27°12N, 015°50W	23,1	36,60
F11	9.10.2000	8:23	24°46N, 017°53W	23,2	36,64	10:56	27°23N, 018°12W	23,4	36,57
F12	9.10.2000	12:57	24°04N, 018°27W	23,1	36,55	18:25	23°11N, 019°11W	23,5	36,49
F13	11.10.2000	8:12	16°57N, 019°56W	27,0	36,12	13:17	15°49N, 019°44W	27,5	35,86
F14	11.10.2000	13:17	15°49N, 019°44W	27,5	35,86	16:10	15°07N, 019°37W	28,2	35,50
F15	12.10.2000	9:34	11°07N, 018°45W	28,7	34,49	11:00	10°51N, 018°42W	28,8	34,58
F16	12.10.2000	11:00	10°51N, 018°42W	28,8	34,58	16:45	09°37N, 018°11W	29,1	34,18
F17	13.10.2000	9:10	06°32N, 015°42W	28,3	34,28	12:17	06°00N, 015°16W	28,0	34,11
F18	13.10.2000	12:17	06°00N, 015°16W	28,0	34,11	16:08	05°17N, 014°42W	28,0	33,91
F19	14.10.2000	9:19	02°00N, 012°04W	26,9	35,38	12:55	01°23N, 011°35W	27,1	35,19
F20	14.10.2000	12:55	01°23N, 011°35W	27,1	35,19	16:15	00°45N, 011°04W	26,7	35,55
F21	14.10.2000	22:10	00°20S, 010°12W	24,5	35,73	8:37	02°12S, 008°42W	24,2	35,85
F22	15.10.2000	8:37	02°12S, 008°42W	24,2	35,85	14:31	03°13S, 007°54W	24,6	35,62
F23	16.10.2000	8:24	06°24S, 005°21W	23,5	35,77	9:29	06°35S, 005°11W	23,4	35,64

F24	17.10.2000	9:15	10°54S, 001°42W	22,1	35,97	10:47	11°09S, 001°30W	22,1	35,99
F25	17.10.2000	12:51	11°32S, 001°12W	22,2	36,02	16:02	12°03S, 000°45W	21,9	36,06
F26	18.10.2000	9:16	15°08S, 001°46E	19,2	36,05	12:12	15°36S, 002°09E	19,3	35,99
F27	18.10.2000	12:12	15°36S, 002°09E	19,3	35,99	15:50	16°12S, 002°39E	19,0	35,90
F28	19.10.2000	9:10	19°08S, 005°06E	17,9	36,59	12:54	19°41S, 005°34E	17,8	35,57
F29	19.10.2000	12:54	19°41S, 005°34W	17,8	35,57	16:06	20°10S, 005°59E	17,8	35,53
F30	20.10.2000	8:34	22°43S, 008°10E	17,0	35,39	9:32	22°52S, 008°18E	17,8	35,53

C.3 Measurement of latitudinal distributions of tropospheric trace species by Off-Axis Scattered Light Differential Optical Absorption Spectroscopy (DOAS

Hans Leser /UH, Institute for Environmental Physics, University of Heidelberg

There have been observed events of sudden reduction of the ozone-concentration in the lower troposphere in polar regions and in mid-latitudes. It is not yet clear what the reasons for these events could be, but there might be a connection of higher halogen (bromine, iodine) concentrations in the atmosphere with this ozone reduction, e.g. there is the catalytic ozone reduction cycle

$$2\,Br + 2\,O3 \longrightarrow 2\,BrO + 2\,O2$$

$$BrO + BrO2 \longrightarrow Br + O2$$

$$2\,O3 \longrightarrow 3\,O2$$

which reduces ozone to oxygen molecules in the presence of Br/BrO.
To get an insight in the tropospheric chemistry with respect to bromine species Off-Axis DOAS-measurements were performed to observe tropospheric O3, NO2, IO and BrOconcentrations during the Polarstern cruise AntXVIII/1 from Bremerhaven to Capetown.

Off-Axis Scattered Light DOAS is a spectroscopical technique that looks for differential absorption by trace species in the scattered sunlight. There is a movable telescope used to collect scattered light from a certain direction of the sky, the light is led to a spectroscope (resolution 0.3 nm) via a quartz-fibre and then the spectrum is detected by a photo-diode array. A computer collects the data and controls the movement of the telescope. Since the light absorption is given by the exponential

Beer-Law, the difference of the measured log-spectra to a reference log-solar spectrum is given by the absorption and scattering of atmospheric compounds. So it is possible to find out about the (slant) column density of the absorbing trace species by the calculation of a non-linear least-squares-fit on this difference with their small-banded differential absorption cross-sections and the broad-banded absorption and Rayleigh- and Mie-scattering (all put into a polynom).
Those slant column densities basically depend on three factors: the (vertical) column density, the length of the lightpath (airmass factor, which can be calculated by a radiation transport model in consideration of scattering processes and mainly depends on the solar zenith angle), and the height distribution of the species (via the ratio of the lightpath sections in different heights of the atmosphere, e.g. stratosphere/troposphere, which depends on the elevation angle of the telescope above the horizon). So, by comparison of measurements with the same vertical column density and airmass factor (short time distance) but different ratios of stratospheric and tropospheric lightpath (different telescope-elevationangle) it is possible to separate tropospheric from stratospheric concentrations.
In this experimental set-up measurements were made between sunrise and sunset from 1st Oct till 20th Oct with different elevation angles (90°, 60°, 40°, 20°, 10°, 5°) in the spectral range 320...400 nm (for O3, NO2, and BrO) and in between from 1st till 15th Oct also 90°- and 5°-measurements in the spectral range 400...480 nm (NO2 and IO) which became impossible to proceed after a controller broke down in 15th Oct. Each measurement took about 5 to 10 minutes.

Up untill now, some of the data has been used to calculate the slant column densities of O3 and NO2. As an example (Fig. 1-UH) of the diurnal variation of those species on 1st Oct is , when the ship was in the northsea, with its comparatively high NO2-concentration in the troposphere because of proximity to Europe. It is clearly visible how this data can be used to distinguish tropospheric from stratospheric distributions because on the one hand there is the mainly stratospheric ozone, which is not sensitive to longer lightpaths in the troposphere as given by small elevation angles, and on the other hand there is NO2 which has much higher slant column densities at small elevation angles as at big ones because it is mainly located in the troposphere.
After the cruise, the collected data will be checked for BrO- and IO-absorption, airmass factors have to be calculated and the height distribution of the species have to be estimated.
With this new gained data, hopefully it will be possible to validate the understanding of halogenic chemistry in the lower atmosphere.

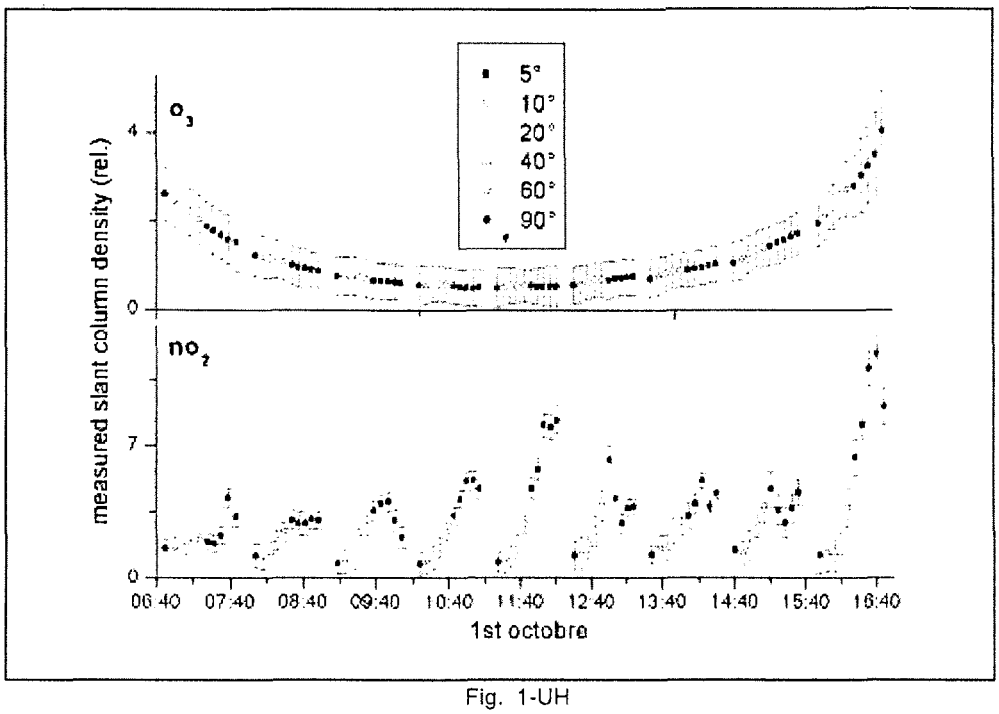

Fig. 1-UH

C.4 Atmospheric Deposition of Iron to the Atlantic and Surface Water Iodine Speciation

Dr. Alex Baker /UEA, University of East Anglia, Norwich, UK

Introduction:

The dry and wet deposition of iron from the atmosphere to the sea surface has been studied during ANT XVIII/1 as part of the EU-funded IRONAGES project. The passage passed the coast of West Africa was of particular interest as the Sahara is a major source of dust to the atmosphere. The deposition of this dust may represent an important source of nutrient iron to remote ocean regions. The chemical and physical properties of the dust play a large role in determining the solubility of iron once it is deposited into seawater and hence how much iron is available to phytoplankton. Iron solubility in atmospheric dust is probably around 0.1 - 1%. Rain-out of dust may enhance the input of iron for several reasons: deposition in rain is much more efficient than dry deposition of aerosol; the low pH of rainwater (<5.5) enhances iron solubility; there may be iron-binding ligands present in rain which further enhance its solubility.

Two High Volume aerosol collectors were situated at the front of the Peildeck and sampled at flow rates of ~ 1 m3 min-1 for periods of around 24 hours. One of the collectors was of the cascade impactor type, in which a number of filters are placed in series to collect particles of progressively smaller size. The size fractionation process provides information on particle source (very small particles tend to be products of atmospheric gas to particle conversion reactions, while very large particles are more commonly mechanically generated, e.g. terrestrial dust or seasalt particles) and also on particle fate, since large particles precipitate at faster rates than small ones. Samples collected using the cascade impactor will be analysed primarily for their iron content. The second collector contained a single filter only, hence no size fractionation took place, and these samples will be analysed for their major ion content (Na+, Ca2+, Mg2+, Cl-, NO3-, SO4-). These ions will provide further information on the air masses sampled and should also give some indication of the relative dry deposition rates of iron and nitrate.
Three rain collection funnels were deployed: 28 cm diameter funnels for major ion and total iron sampling and a 42 cm diameter funnel for iron-binding ligand sampling.

Samples Collected:
A summary of the aerosol samples collected during ANT XVIII/1 is shown in Table 1. The manoeuvres carried out in order to test the newly installed ship's engine control system during our passage to Las Palmas unfortunately may have caused some contamination of the sample with smoke from the stack. The collectors were often turned off during passage for this reason. After our departure from Las Palmas our course coincided with the wind direction so that smoke was continually blown over the collectors and sampling was not possible for two days. However, once the Universität Bremen mooring had been recovered on 10th October sampling resumed and continued until 19th October. The samples collected on 10th, 11th and 12th October all contained orange/red dust, presumably Saharan in origin. Sampling ceased on 19th October as the collectors were becoming soaked with spray from the bows and the samples were contaminated by this spray.
Sadly (for me), ANT XVIII/1 was a rather dry cruise. The only significant rain sample was collected at 02:00 UTC on 13th October as we passed, all too quickly, through the Inter-tropical Convergence Zone.

Table 1-UEA: Aerosol samples collected during ANT XVIII/1.

Start Date	No. of Impactor Stages	Comments
4/10/00	2	Stack smoke?
5/10/00	2	Stack smoke?
10/10/00	6	Orange dust on first 4 stages
11/10/00	2	First stage red
12/10/00	2	First stage orange
13/10/00	2	All stages grey
14/10/00	2	All stages grey
15/10/00	2	All stages grey
16/10/00	2	All stages grey
17/10/00	2	All stages grey
18/10/00	2	All stages grey
19/10/00	2	Gross contamination of first stage with seaspray

Iodine Speciation:

The thermodynamically stable form of iodine in seawater is iodate (IO3-), but in surface waters significant concentrations of the reduced form iodide (I-) are commonly found. The reduction process is biological and may be linked to the nitrogen reductase metabolism of bacteria or phytoplankton, however the mechanism is unclear. During ANT XVIII/1 a sample was collected daily from the Teflon pumped seawater supply and analysed for its iodide and total iodine content. Iodide was generally present in higher proportion in tropical waters along the transect (Figure 1). The low value at 2.3°S may be caused by equatorial upwelling, as deep waters normally contain very low concentrations of iodide.

Figure 1-UEA/: Variation in percentage of iodide-iodine between 33.8°N and 22.6°S during ANT XVIII/1

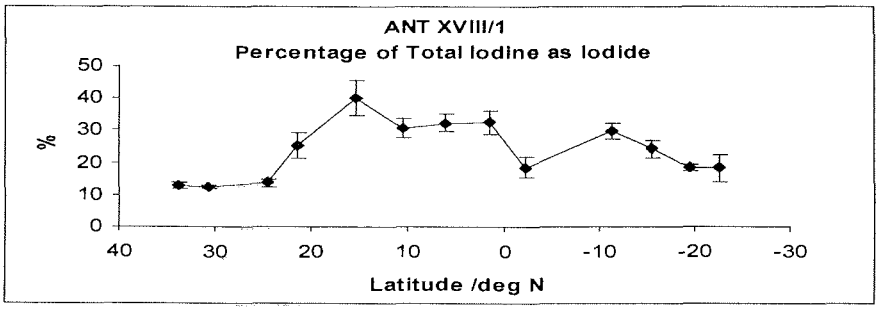

C.5 Preparations for CARUSO / EisenEx

Dorothee Bakker and Adèle Chuck /UEA, University of East Anglia, Norwich, U.K.

During Polarstern's southward transit preparations were made for the oncoming iron enrichment experiment in ANT XVIII-2. These included testing of the ARGOS emission of a lagrangian buoy and installation of a GPS connection for the continuous analysis of sulphur hexafluoride (SF6) in surface water. Furthermore Peter Gerchow (AWI) installed and tested the software VNC Viewer, which will allow the real-time display of the surface water distribution of SF6 on monitors around the ship during the release experiment. We are grateful for the support of Peter Gerchow, the ship's system manager and electronic officers.

C.6 The partial pressure of carbon dioxide in eastern Atlantic Ocean surface waters

Dorothee Bakker /UEA, University of East Anglia, Norwich, U.K.

Little is known about the seasonal and year-to-year variability of the air-sea transfer of the greenhouse gas carbon dioxide (CO2) in the equatorial and South Atlantic Ocean. In particular, variations in the strength of coastal and equatorial upwelling are likely to affect CO2 air-sea exchange in these waters.

Continuous measurements of the partial pressure of carbon dioxide (pCO2) in surface water and marine air were carried out from 30°N to 30°S in the eastern Atlantic Ocean in October 2000. The partial pressure difference across the sea surface will be combined with shipboard wind speed in order to calculate CO2 air-sea exchange along the ship's trajectory. The measurements of ANT XVIII/1 form a sequel to surface water pCO2 data, which were collected along similar cruise tracks in October-November 1993 (ANT XI/1) and in May-June 1994 (ANT XI/5). The annual increase of surface water pCO2 will be assessed from the three data sets. This annual increase in various oceanic regimes remains one of the major uncertainties in estimates of the net global oceanic CO2 uptake.

In ANT XVIII/1 the ship travelled south from early autumn in the northern hemisphere to early spring in the southern one. The distribution of surface water pCO2 reflected seasonal temperature changes, biological activity, equatorial and coastal upwelling and rainfall. Intriguing are the low surface water CO2 values in a low salinity region

north of the equator, which were observed during all three cruises. The CO2-regime of region strongly contrasts with high pCO2 values in the subtropical gyre and near the equator. Dilution of seawater by high rainfall only explains part of the low surface water CO2 values. One may speculate that biological uptake of CO2 has contributed to the low pCO2. It has even been suggested that iron input in rainwater is high and that nitrogen fixing species, such as Trichodesmium, reach high levels in this area. However, biological indicators, such as fluorescence, do not corroborate the presence of high biological activity.

On arrival in the equatorial region surface water pCO2 sharply increased by 50 µatm, whereas temperature decreased by 2.5°C. Such a strong upwelling signature in Mid-October 2000 was surprising, as the equatorial upwelling in the Atlantic has its maximum in June to August and soon diminishes afterwards.

The pCO2 data of the cruises will be collocated with satellite observations of sea surface temperature and ocean colour (the latter only for ANT XVIII/1). Satellite observations are powerful tools to study the evolution of processes, which affect pCO2 and which have a strong signature in the surface ocean, such as upwelling and algal blooms. With these techniques the variability of pCO2 and its causes will be studied at various space and time scales. Combination of the data with measurements by other researchers will provide case studies for future work on the interpolation of surface water pCO2 by using satellite observations and simple models.

C.7 Measurements of biogenic organohalogens and light alkyl nitrates in seawater and air

Adele Chuck /UEA, University of East Anglia, School of Environmental Sciences, Norwich, UK

Introduction:

The production of low molecular weight organohalogens in the open ocean, and subsequent fluxes of these compounds out of the ocean into the atmosphere is still associated with many uncertainties. What compounds are produced and in what concentrations; which species are responsible for the production and why are they producing them; what seasonal/temporal variations exist - are just some of the questions still requiring answers. Once in the atmosphere, the organohalogens are photochemically broken down into radical species which then play a part in the destruction of ozone.

Alkyl nitrates (RONO2) are important NOy reservoir species and play a role in a variety of atmospheric processes such as tropospheric and stratospheric ozone production and destruction. They are primarily formed by the photochemical oxidation of alkenes by NOx but atmospheric measurements taken over the equatorial Pacific Ocean (Atlas et al, 1993) have indicated that there may be a possible oceanic source.

The purpose of the measurements on ANTXVI/III was to build on a previously collected dataset in the Atlantic Ocean on the Atlantic Meridional Transect 9 cruise in which measurements of methyl iodide, methyl nitrate, ethyl nitrate, chloroiodomethane and bromoform were obtained. For the alkyl nitrates, these previous measurements showed the two compounds to be present in seawater although preliminary calculations of the percent saturation in the ocean indicated that only in a few areas were these compounds fluxing out of the ocean. The major aim for this cruise was to carry out paired seawater and air measurements in order to better parameterise the variation in strength of the sea-air flux and, with respect to the alkyl nitrates, determine the percentage saturation of methyl and ethyl nitrate in seawater in order to gain more evidence that the ocean is a potential source of these compounds.

Methodology:
The organohalogens and alkyl nitrates were measured by purge-and-trap gas chromatography with electron capture detection. Seawater samples were taken from the stainless steel underway supply in 100 ml glass syringes every three hours and kept in running seawater in the dark until analysed. Samples were stored for no longer than one hour. Air samples were pumped into an electropolished 3 litre aluminium flask. The samples were taken either from the peildeck (20.75m above sea level) when the wind was between +/- 90 degrees relative direction, or from the stern of the ship (2 m above sea level) when the wind was coming from behind the ship. Five hundred mls of seawater was filtered through GFF filters for chlorophyll determination and flash frozen in liquid nitrogen. These were stored in the -24_C freezer before being transported back to the lab for analysis. Figure 1 shows an example chromatogram with some of the peaks of interest marked. B shows the increase in methyl and ethyl nitrate peaks, when going through an area of upwelling.

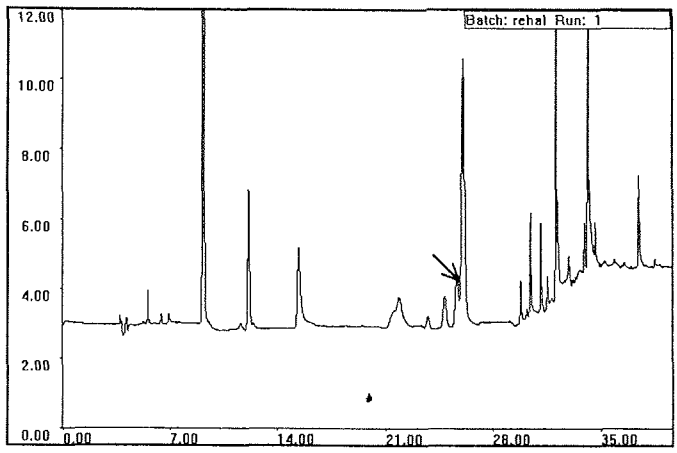

Fig. 1A-UEA-2:

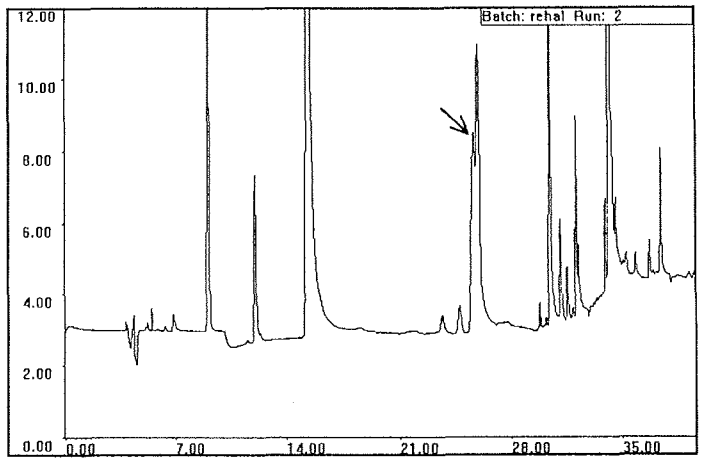

Fig. 1B-UEA-2:

Fig. 1A & 1B: Chromatograms of the analysis of 40 mls of seawater. A) from 22°45'89N, 19°31'32W and B) from 03°18'95S, 07°49'63W, an area of upwelling. Peak identification: 1=CH3I, 2=MeONO2, 3=EtONO2, 4=CHBr3. Plot shows response (mV) against time(mins).

Results:

The results presented are preliminary and are presented in units of peak area as calibration will be carried out back in the lab. An air standard was used as a working standard and was run at least once a day. Figure 2 shows the latitudinal distribution of methyl iodide and methyl nitrate and ethyl nitrate along the cruise track. Figure 3 shows the percentage saturation of these compounds in seawater with respect to the air concentration. These initial calculations do not take the water temperature.

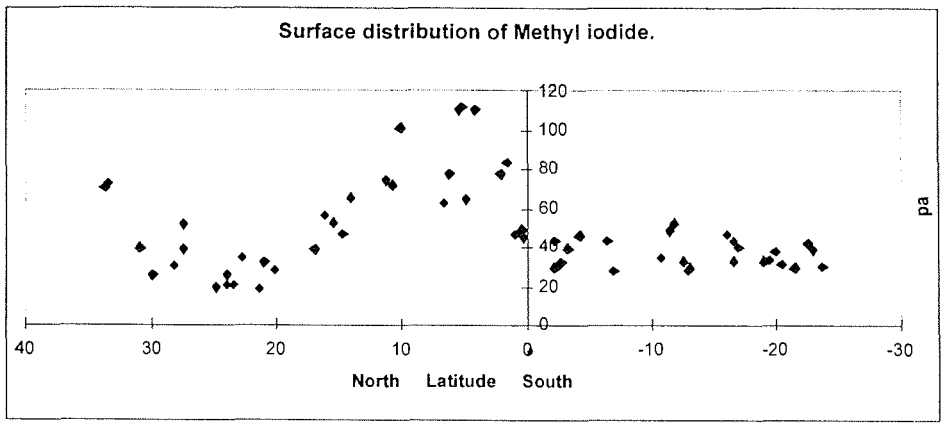
Surface distribution of Methyl iodide.
120
100
80
60
40
20
0
pa
40
30
20
10
0
-10
-20
-30
North Latitude South

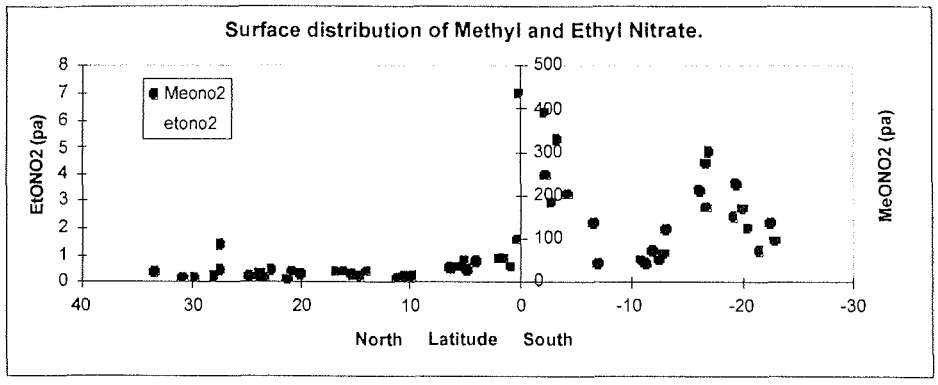
Surface distribution of Methyl and Ethyl Nitrate.
Meono2
etono2
EtONO2 (pa)
MeONO2 (pa)
8
7
6
5
4
3
2
1
0
500
400
300
200
100
0
40
30
20
10
0
-10
-20
-30
North Latitude South

Fig. 2-UEA-2

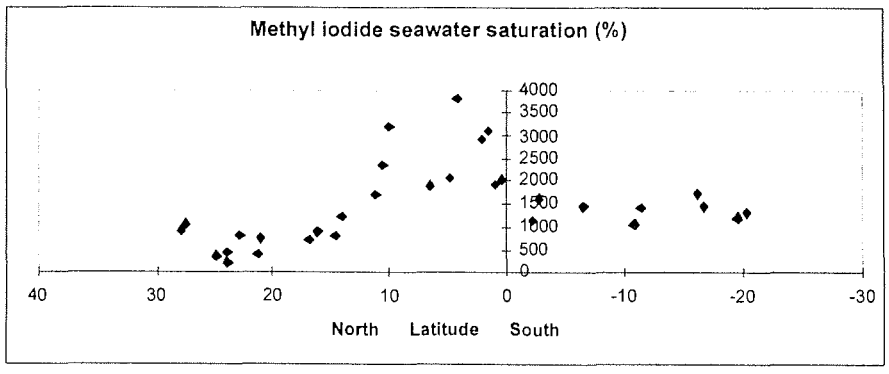
Methyl iodide seawater saturation (%)
4000
3500
3000
2500
2000
1500
1000
500
0
40
30
20
10
0
-10
-20
-30
North Latitude South

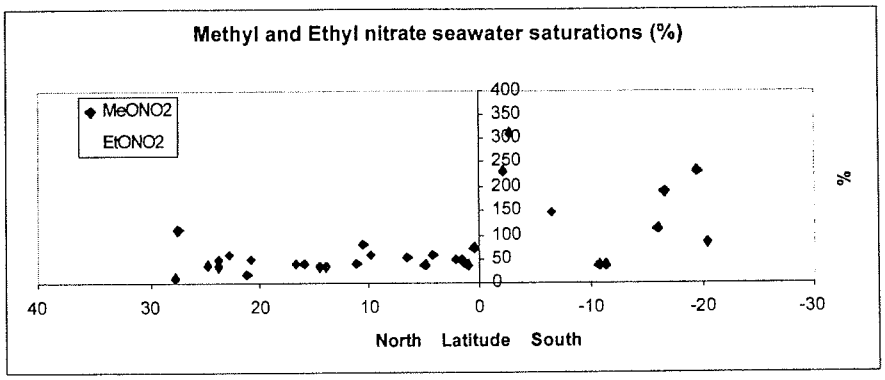

Fig. 3-UEA-2

Discussion:

The percent saturation of methyl and ethyl nitrate in seawater indicates that the ocean can be a potential source of these compounds. The different distributions of methyl iodide compared to the alkyl nitrates suggest that if these trace gases are produced biogenically by phytoplankton, production may be species specific. The reason for production of the alkyl nitrates is unclear and puzzling. Further work will be done with phytoplankton cultures back at UEA to attempt to find out which species are responsible. The data collected on this cruise, together with my dataset from AMT9, provide the first open ocean measurements of methyl and ethyl nitrate.

References:

Atlas, E., Pollock, W., Greenberg, J. and Heidt, L. 1993. Alkyl nitrates, nonmethane hydrocarbons and halocarbon gases over the equatorial Pacific Ocean during Saga 3. Journal of Geophysical Research, 98, 169333-16947.

C.8 Intercalibration for dissolved iron and distribution of surface Iron in the Atlantic Ocean

P.L. Croot, M. Boye, P. Laan /NIOZ; E. Achterberg, A. Bowie /UoP; A. Baker /UEA; S. Blain, G. Sarthou /UBO

Introduction and Overview

It is now well established that iron can play a role as a (co)limiting nutrient for phytoplankton in High Nutrient Low Chlorophyll (HNLC) regions of the world. However many questions remain about the biogeochemistry of iron and how well we are currently able to measure this element in open ocean seawater. As iron exists at extremely low levels in seawater, the potential for contamination on ships

constructed mostly of steel is large. During ANTXVIII-1, the trace metal group from NIOZ, along with groups from France and England made continuous underway measurements for dissolved iron using a towed fish and trace metal clean pumping system. The purpose of this work was to perform the first at sea intercalibration for iron, and also obtain a large volume, low iron concentration standard for distribution to other labs taking part in a joint SCOR/IUPAC iron intercalibration. . At the present time there are several different methods for the determination of iron at sub nano-molar levels (< 1 x 10-9 mol/L), but no comparison between these methods has been made until now. The chemistry of iron in seawater is very complex, and the different analytical methods used for measuring iron may not all be measuring the same concentrations for chemical reasons. For this reason it is important that the various methods are used on the same fresh samples so that we can fully understand the differences between the methods and what that tells us about the chemistry. This work is of extreme importance, as iron has been shown to be a major limiting factor for primary productivity in many open ocean regions, noticeably the Southern Ocean.

Methods

Spatial distribution of iron:

Samples were taken using a peristaltic pump connected to a polyurethane coated 'ironfish' (towed fish, torpedo style – 1m length and weighing 50kg in air), by acid cleaned polyethylene tubing. The 'ironfish' was towed alongside the ship at a distance of several meters from the hull at the ships maximum speed of 14.5 knots. A water sample was delivered to, and filtered inline (0.2 _m Sartorious filter), in the clean container every hour. The samples collected from the underway system were analyzed for dissolved iron onboard ship.

Measurement of iron :

To prevent sample contamination, trace metal clean techniques were applied. All samples for total metal analysis were acidified to pH < 2 with ultraclean quartz distilled concentrated hydrochloric acid. Total dissolved iron (0.2 _m) were measured on-board using a flow injection technique with in-line pre-concentration on a chelating resin followed by chemiluminescence detection (FIA-CL) ((de Jong et al., 1998; Landing et al., 1986; Obata et al., 1993). Iron from an acidified sample is buffered on line and preconcentrated onto a column of immobilizied 8-hydroxyquinoline. After a loading time of 4 minutes, the column is washed with deionised water and the iron is eluted with dilute hydrochloric acid. The iron mixes with luminol, hydrogen peroxide and ammonium hydroxide to produce chemiluminescence in the flow cell of a photomultiplier tube connected to a photon counter. The chemiluminescence occurs as a result of the iron catalyzed oxidation of luminol (3-aminophtalhydrazide) by hydrogen peroxide, producing blue light (424

nm). The accuracy of the method was checked and confirmed using NASS-4 reference sea water. Throughout the cruise, the blank and detection limit (3x standard deviation of blank) remained constant at 0.032 and 0.01 nM respectively. Reproducibility was typically 2% at the 0.3 nM concentration and better than 10% at the 0.06 nM level.

Preliminary results and discussion

During the anreise, only surface waters were sampled. Most of the transect was sampled at one hour intervals where possible, Table 1 lists the times at which the fish was recovered for maintenance or some other reason. In general the fish was able to cope adequately at 14.5 knots, but in high winds the stress on the line caused some failure of key components which need to be replaced periodically. A total of 219 samples were taken during the underway sampling exercise and analyzed onboard, covering roughly the ships transect from 20_ N to 20_ S in the Atlantic. Preliminary results indicate that there was extremely low iron concentrations away from the coastal regions (< 0.1 nM), a result which was somewhat surprising, as early work in this region had shown much higher levels of iron in these waters (Powell et al., 1995). Higher iron levels (0.4 – 1 nM) were found closer to the continent and may be due to atmospheric deposition of iron from the Sahara.

During the cruise, the large sample container was rinsed with seawater, acidified and flushed several times prior to the collection of the final sample. The final sample was then sub-sampled into over 200 1 L bottles for later distribution to other international laboratories. The concentration of iron in the effluent from the container was monitored during the filling process as a quality control.

Acknowledgments:

The authors would like to show their deep thanks and appreciation to the crew of the R.V. Polarstern, for all their efforts in helping us throughout ANTXVIII-1. Special thanks must go to the deck crew for their efforts with deploying the iron-fish and also to the engineers who helped resuscitate some overworked air-conditioners in the containers during our passage through the tropics. Thanks also to the Chief Scientist, Dr. Saad El Naggar and to the AWI for making this cruise possible.

References:

de Jong, J.T.M. et al., 1998. Dissolved iron at subnanomolar levels in the Southern Ocean as determined by ship-board analysis. Analytica Chimica Acta, 377: 113-124.

Landing, W.M., Haraldsson, C. and Paxeus, N., 1986. Vinyl Polymer Agglomerate Based Transition Metal Cation Chelating Ion-Exchange Resin Containing the 8-Hydroxyquinoline Functional Group. Analytical Chemistry, 58: 3031-3035.

Obata, H., Karatani, H. and Nakayama, E., 1993. Automated Determination of Iron in Seawater by Chelating Resin Concentration and Chemiluminescence Detection. Analytical Chemistry, 65: 1524-1528.
Powell, R.T., King, D.W. and Landing, W.M., 1995. Iron distributions in surface waters of the south Atlantic. Marine Chemistry, 50: 13-20.

Table 1- Croot et al.: Summary of underway sampling deployments during ANTXVIII/1. Samples numbers collected during each deployment of the 'Iron-Fish'. All times are UTC.

Sample #	Comment	Timespan (UTC)
003-018	Fish recovered as very low flow rate, discovered to be due to blocked tube	19:00 08/10 – 10:00 09/10
019-036	Fish recovered due to mooring work	13:20 09/10 – 6:00 10/10
037-056	Fish running close to ship, tube bent sideways leading to low flow.	15:00 10/10 – 10:00 11/10
057-077	No sample taken at 9:00 as work on clean container prevented sampling.	12:00 11/10 – 8:00 12/10
078-105	Fish porpoising in high winds at 14.5 knots, recovered as safety measure.	10:10 12/10 – 13:00 13/10
106-126	6mm steel cable frayed, replaced with new 8mm cable	11:00 14/10 – 7:00 15/10
127-219	**Sampling continued until completion of experiment at approximately 20° S.**	13:30 15/10 – 09:00 19/10

C. 9 Latitudinal distribution of dissolved Fe in surface seawater

Andrew R. Bowie and Eric P. Achterberg /UoP

During the voyage ANTXVIII/1, the Plymouth group had four main objectives listed below.

Latitudinal dissolved Fe surface transect
In collaboration with NIOZ (NL) and UBO (FR), samples of dissolved Fe were taken underway from a towed torpedo fish deployed at 1-2 m below the surface using a trace metal clean peristaltic pumping system. The sampling was initiated shortly after departure from Las Palmas on 8th October and completed on 19th October, covering a transect of approximately 20oN to 20oS. This exercise represented one of the first attempts to perform a shipboard intercomparison of analytical methods for measuring Fe.

The Plymouth team collected 219 samples over the 12 day period. Samples were collected in a 1 l PTFE bottle and immediately poured into a 250 ml LDPE bottle,

following clean protocols. In addition, unfiltered samples (total dissolvable Fe) were collected twice daily. All underway Fe analyses were performed using a flow injection - chemiluminescence (FI-CL) technique based on the luminol reaction using dissolved oxygen as the oxidant (Bowie et al., 1998). In-line matrix elimination and sample preconcentration was achieved using a 8-hydroxyquinoline micro-column. Dissolved Fe analyses, comprising Fe(II)+Fe(III), were carried out after an acidification (Q-HCl, quartz distilled; pH < 2) and reduction (Na2SO3; 100 µM) step for at least 4 h prior to analysis. Every other sample collected will taken back for reference and possible future laboratory-based analyses of Fe and other trace metals (Co, Zn, Al, Mn) in order to fingerprint input mechanisms. Preliminary data show levels ranging from 0.1 nM in the oligotrophic South Atlantic to 1.5 nM in waters to the west coast of Africa under the influence of the Saharan dust plume.

Collection of low Fe standard seawater sample

In collaboration with NIOZ (NL) and UBO (FR) a large volume dissolved seawater sample (700 l at ca. 1.5 l/min) was collected on 16th October 2000 in a 1000 litre polyethylene cubic vessel. Seawater was supplied using a towed fish and a peristaltic pump. On-line filtration was carried out using a Sartobran-P capsule unit (0.45 _m pre-filter, 0.2 _m final filter; cellulose acetate membrane, polypropylene housing; Sartorius UK). The sample was acidified (pH 2) using quartz distilled HCl and gently agitated. Dissolved Fe was analysed by the different groups, and deemed appropriate for a low Fe seawater standard. The sample was bottled on 19th and 20th October 2000. A total of 160 1 litre bottles were filled for UoP, and 40 1 litre bottles for NIOZ. Different bottle types and bottle cleaning procedures were used by these labs. Bottle filling was performed under a laminar flow hood in the NIOZ clean container by pumping the seawater through FEP tubing using a peristaltic pump. Bottles will be returned to the UK, and after stability trials shipped to approximately 25 worldwide laboratories participating in the certification exercise. This work is carried out under a joint IUPAC/SCOR programme examining the Fe biogeochemistry in seawater (working group 109). Funding was provided by the EU project IronAges.

On-line Fe(II) analyses

A novel FI-CL system, based on a modified version of Bowie et al. (1998), was used during four periods of the underway transect. The fully stand-alone system was directly fed with filtered seawater from the fish, providing a dissolved Fe(II) measurement every 3 minutes. The system was commenced at ca. 0300 h on three of the dates in order to investigate the night-day-night cycling of Fe(II) in seawater. Unfortunately, the fish deployment was prematurely aborted mid-morning prior to

completion of the 24 h cycle. On the fourth occasion, the system was used over 13 h from 11.00 to midnight.

Fe(II) analyses on deck incubations
In collaboration with NIOZ and IRI (NL), dissolved Fe(II) cycling in deck incubations was studied over a 18 h cycle from prior to sunrise until after sunset. For full details of the incubation experiments, refer to the cruise report by Micha Rijkenberg and Loes Gerringa. Samples were collected every 10 min, from different light conditions with respect to light intensity and wavelength. Samples were collected in dark bottles and immediately transferred into a cool box and analysed for Fe(II). Analysis of the samples was performed in duplicate. The method for the Fe(II) was a modification of the on-line system outlined above.

Reference
Bowie A.R., Achterberg E.P., Mantoura R.F.C. and Worsfold P.J., 1998. Determination of sub-nanomolar levels of iron in seawater using flow injection with chemiluminescence detection. Analytica Chimica Acta, 36, 189-200

C.10 Measurement of dissolved iron concentration using the Cathodic Stripping Voltammetry

Marie Boye, /NIOZ

A synopsis is presented here of underway measurement, by Cathodic Stripping Voltammetry (CSV), of low concentrations of Fe in filtered seawater. On the basis of comparison of two different procedures for measuring Fe by CSV and intercalibration results using CSV and FIA-chemiluminescence methods (see other partners), the feasibility of these methods will be evaluated.

Surface sampling was done by a peristaltic pump delivering seawater through a plastic tube that was attached to a tow fish. Analytical work was done in a container positive equipped with laminar flow hoods. For in-line filtration a Sartorius Sartobran (0.2 µm main filters) cartridges were used. Discrete samples were taken at about 4 hours interval time during the underway survey. By using the nominal 0.2 µm size cut-off we operationally separate 'dissolved' metal species (truly dissolved, but also colloidal, (in)organically complexed) from suspended particulate matter. About 50 samples were taken during the underway survey and measured on board using two different methods by CSV. Samples were also taken in the seawater tank used for

the elaboration of a certified seawater, in which dissolved Fe and the Fe-binding capacity were measured by CSV prior the acidification of the tank.

To describe the CSV method briefly, a synthetic ligand (2-(2-thiazolylazo)p-cresol, e.g. TAC) is added in large amount to the seawater sample to bind iron, after which voltammetric analysis is carried out [adapted from Croot and Johansson, 2000]. Previous methods recommend acidification and UV-digestion of the sample in order to destroy the dissolved complexing matter [Bruland et al., 1979; Landing and Bruland, 1987, Martin et al., 1991; Rue and Bruland, 1997; Gledhill and van den Berg, 1994; Wu and Luther, 1995, 1996]. However, these two steps firstly involve sample manipulations, which might introduce contamination and secondly, the pH has to be buffered to 6.7-7.8 [van den Berg et al., 1991] prior the measurement by CSV. This might also introduce contamination by buffer addition and sample manipulations. Buffering could also cause iron colloids to precipitate [Millero et al., 1995; Deng and Stumm, 1994], possibly decreasing the apparent iron concentration. For these reasons, two alternative methods have been adopted. In the first, the sample was UV-digested at the seawater pH. This UV-digestion of the sample for at least 90 min (without acidification) has been shown to efficiently destroy the iron-binding capacity of the dissolved organic ligands (Rue and Bruland, 1997; Aldrich and van den Berg, 1998). Secondly, a new method for total dissolved iron measurement has been developed, based on the out-competing of TAC to bind iron in the non-UV-irradiated and non-acidified sample (containing the Fe-complexes). In this method, a very high concentration of TAC is used with an equilibration period of ~7h in a voltammetric cell, which should, presumably, have caused most of or all (organic and inorganic) iron to be bound to TAC. The iron concentration analysed using this later method was called the "high-labile" fraction. Kinetics of the release of Fe from the dissolved organics were followed in discrete samples to check the reliability of the procedure.

The UV-digestion (using a 600 W high-pressure mercury-vapor lamp) was performed here on discrete samples (25 mL), with a conventional digestion time of 4 hours. Voltammetric measurement was carried out at pH 8.1 using borate buffer (final concentration 5 mM), with 10 µM of TAC for the UV-digested samples and with 50 µM of TAC for the "high-labile" fraction. No oxidant was added to the sample in order to decrease the analytical blank. Instead a long deposition time (500 sec) was used to increase the sensitivity of the measurement [Aldrich and van den Berg, 1998]. The voltammetric procedure was carried out using the fast linear sweep waveform (10.1 V.s-1, step potential 1.98 mV), with a deposition potential of –0.4 V.

The Fe-binding capacity in the seawater tank was estimated by titration of the free Fe-binding ligand against competition with TAC. TAC was used at a concentration of 10 µM (giving a detection window of 1011.4 to 1013.4), and the Fe-step additions

used to titrate the ligand were on the order of 0.5 nM to 1 nM Fe ranging from 0 to 8 nM Fe additions.

The data need to be treated in order to asses the reliability of two methods using CSV and to compare them with the data obtained in the same samples using FIA-chemiluminescence methods. Previous work has shown that the two protocols for dissolved Fe measurement using CSV (with 1-nitroso-2-naphtol as the added ligand) compared well encompassing ranges of dissolved-Fe of 0.56 to 1.9 nM (Boye, 2000), and that the CSV method using UV-digested samples at pH8 compared well with the FIA-chemiluminescence technique [de Jong et al., 1998] within the Fe concentrations range of 0.5 and 1.7 nM [de Jong et al., 2000].

References:

Aldrich and van den Berg (1998). Determination of Iron and its redox speciation in seawater using Cathodic Stripping Voltammetry. Electroanalysis, 10, No 6, 369-373.

Boye (2000). Organic complexation and biogeochemistry of iron in the marine system : field data and culture experiments. PhD, University of Liverpool, 240 p.

Bruland K.W., Franks R.P., Knauer G.A. and Martin J.H. (1979). Sampling and analytical methods for determination of copper, cadmium, zinc, and nickel in seawater. Analytic Chemica Acta, 105, 233-245.

Croot P.L. and Johansson M. (2000).Determination of iron speciation by cathodic stripping voltammetry in seawater using the competing ligand 2-(2-thiazolylazo)-p-cresol (TAC). Electroanalysis, 12, 565-576.

de Jong J.T.M., den Das J., Bathmann U., Stoll M.H.C., Kattner G., Nolting R.F., de Baar H.J.W. (1998). Dissolved iron at subnanomolar levels in the Southern Ocean as determined by ship-board analysis. Analytica Chimica Acta, 377, No.2-3, 113-124.

de Jong J.T.M., M. Boye, V.F. Schoemann, R.F. Nolting and H.J.W. de Baar (2000). Shipboard techniques based on flow injection analysis for measuring dissolved Fe, Mn and Al in seawater. Advanced article in Journal of Environmental Monitoring of the Royal Society of Chemistry, in press.

Deng Y.W. and Stumm W. (1994). Reactivity of aquatic iron(III) oxyhydroxides implications for redox cycling of iron in natural-waters. Applied Geochemistry, 9, No.1, 23-36.

Gledhill M. and van den Berg C.M.G. (1994). Determination of complexation of iron(III) with natural organic complexing ligands in sea water using cathodic stripping voltammetry. Marine Chemistry, 47, 41-54.

Landing W.M. and Bruland K.W. (1987): The contrasting biogeochemistry of iron and manganese in the Pacific-Ocean. Geochimica et Cosmochimica Acta, 51, no.1, pp.29-43.

Martin J.H., Gordon R.M. and Fitzwater S.E. (1991). The case for iron. Limnology and Oceanography, 36, 1793-1802.
Millero F.J., Yao W. and Aicher J. (1995). The speciation of Fe(II) and Fe(III) in natural waters: Facts and speculations. In "Trace Metals in Seawater" (C.S. WONG et al. Eds.) Plenum Press New York.
Rue E.L. and Bruland K.W. (1997). The role of organic complexation on ambient iron chemistry in the equatorial Pacific Ocean and the response of a mesoscale iron addition experiment. Limnology and Oceanography, 42, vol.5, 901-910.
van den Berg C.M.G., Nimmo M., Abollino O., and Mentasti E. (1991). The determination of trace levels of iron in seawater using adsorptive cathodic stripping voltammetry. Electroanalysis, 3, no.6, 477-484.
Wu J. and Luther III G.W. (1995). Complexation of Fe(III) by natural organic ligands in the Northwest Atlantic Ocean by competitive ligand equilibration method and a kinetic approach. Marine Chemistry, 50, 159-178.
Wu J. and Luther III G.W. (1996). Spatial and temporal distribution of iron in surface water of the northwestern Atlantic Ocean. Geochimimica et Cosmochimica Acta, 60, N°15, 2729-2741.

C.11 Dissolved iron determination in the surface waters of the Atlantic Ocean using flow injection with chemiluminescence detection

Geraldine Sarthou and Stephane Blain /UOB

Introduction

This work is a part of the intercalibration exercise for low dissolved iron concentrations measurements (Croot et al. this issue). We contributed first to the on board analysis of 219 samples, second to the sampling of a large volume of clean seawater and to the sub sampling into 200 1 liter bottles .

Methods and preliminary results

Dissolved iron concentrations were analysed by flow injection with chemiluminescence (CL) detection using a method adapted from Obata et al. (1993). The acidified sample is buffered at pH 3.5-4 with ammonia and ammonium acetate buffer. It is then passed through a resin of 8-quinolinol immobilised on hydrophilic vinyl polymer for 1-2 min at a flow rate of 2ml/min. Then, the eluent (0,4M hydrochloric acid) is passed trough the column at a flow rate of 1ml/min in the reverse direction of the sampling. The eluent is mixed with a 0.74M luminol solution, a 1M ammonia, and a 0.7M hydrogen peroxide solution. The mixture is introduced

into the CL cell. The iron concentration is determined by the measurement of CL intensity with a standard calibration (Fig. 1 and 2). All the reagents are of suprapur or ultrapur grade, except the luminol solution, which is purified through a resin. The blank is determined as the average of 5 measurements of a sample with only 5 s of preconcentration (Fig. 1). The detection limit is equal to three times the standard deviation of the blank and is equal to 30pmol/l. The blanks of hydrochloric acid, ammonia, and ammonium acetate buffer are

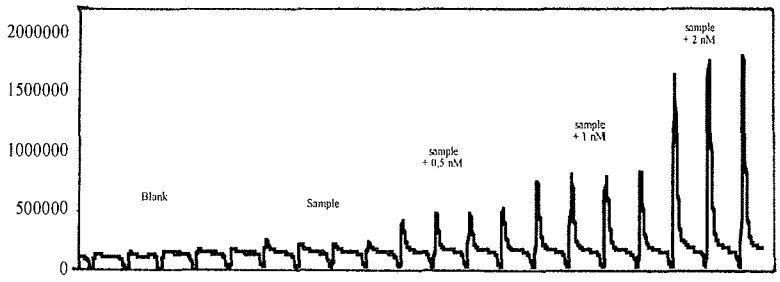

Figure 1

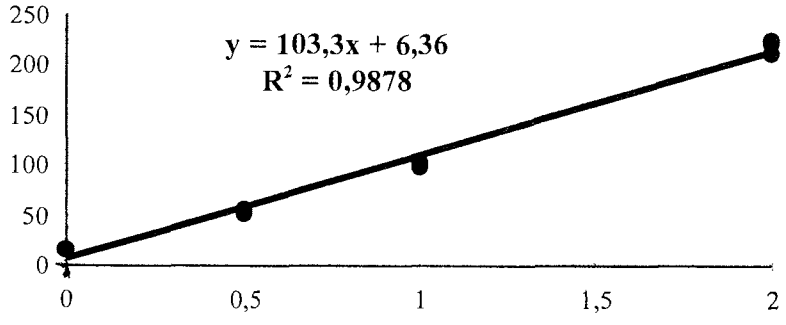

Figure 2

determined by addition of increasing amounts of these reagents in the sample and are found to be lower than our detection limit.

Samples were taken from the fish each hour. Details about sampling are reported in the NIOZ group cruise report. In total 219 samples were taken. An intercalibration exercise was carried out on these samples in collaboration with scientists from the NIOZ (Marie Boye, Peter Croot, Patrick Laan) and from the University of Plymouth (Eric Achterberg and Andrew Bowie) using different techniques. All the samples were analysed on board. Our dissolved iron concentrations varied between values lower than our detection limit to values as high as 1.11 nM. A preliminary examination of the data shows a good agreement between the different data sets. It is the first time that such low dissolved iron concentrations are reported in the South-Atlantic Ocean.

Acknowledgments
The authors would like to show their deep thanks and appreciation to the crew of the R.V. Polarstern, for all their efforts in helping us throughout ANTXVIII-1. Special thanks must go to the deck crew for their efforts with deploying the iron-fish and also to the engineers who helped resuscitate some overworked air-conditioners in the containers during our passage through the tropics. Thanks also to the Chief Scientist, Dr. Saad El Naggar and to the AWI for making this cruise possible.

Reference
Obata, H., Karatani, H. and Nakayama, E., 1993. Automated Determination of Iron in Seawater by Chelating Resin Concentration and Chemiluminescence Detection. Analytical Chemistry, 65: 1524-1528.

C.12 The influence of UV on Fe chemistry and peroxide formation in relation to Fe-availability for phytoplankton

L.J.A. Gerringa, K.R.Timmermans, P. Croot, B. van der Wagt, P. Laan, H.J.W. De Baar, /NIOZ; M.J.A. Rijkenberg, M. Boye, A.G.J. Buma, / University of Groningen, E. Achterberg, A. Bowie, /UoP; S. El Naggar / AWI, A.C.Fischer, J.J. Kroon, /IRI, Delft

Abstract
The chemistry of Fe in seawater is still poorly understood. The bio-availability of iron is crucial for life in seawater. It was assumed in this project that this availability was a function of the speciation of Fe, with the emphasis on the possibility that Fe(II) is the available fraction. Another interesting fraction, dissolved organic Fe(III) was also considered.
Here preliminary experiments, on the Fe chemistry, without considering phytoplankton, are discussed. As Fe(II) can only be produced by input of extra

energy, as by the UV part of the solar spectrum, the relation between light and Fe(II) concentration was investigated. To get an extra indication of the energy input by sunlight the oxygen radical H2O2 was measured as well.
The preliminary results show a positive relationship between intensity and H2O2 production on the one hand, and a very direct negative relationship with wavelength.

Introduction

It is accepted nowadays that Fe can be limiting to phytoplankton in seawater. This is partly due to the low solubility of iron oxides and hydroxides in the oxygenated seawater (Millero 1998 and many others). Organic ligands increase the solubility due to complex formation. Lately a lot of research is focussed on the availability of this organic fraction for phytoplankton, with sometimes contrasting and confusing results (Hutchins et al., 1999a, 1999b). Reduced iron, Fe(II), is found to have a positive relationship with algal growth and seems to be related to organic matter content of the seawater (Kuma et al. 1995). Since Fe(II) is not a stable species in oxygenated seawater the kinetics of formation and of oxidation are crucial for uptake rate of Fe(II) by the phytoplankton. The production of Fe(II) is largely generated by the energy of the sunlight, and especially the energy of the short wavelength region, the UV.
In this project we try to find a relationship between light and Fe(II) production as a function of algal growth. During ANT 18-1, the relationship between light, its intensity and wavelength spectrum, and Fe speciation, especially Fe(II) was investigated. Filtered seawater was incubated on deck in two liter bottles during 30 h (2 nights, 1 day). The sampling and incubation occurred near the equator (positions unknown at the moment).

Material and methods

A sample of 50 liters of seawater was taken on the 14 of October, at approximately 2° N and 12° W. The water was stored in the dark at seawater temperature (24 degrees) during the afternoon. After sunset the water was subsampled in 2 liter home made (University Groningen) polymethylmetacrylate (PMMA) bottles (Steeneken et al., 1995). This material is UV transparent (fig.1).Immediately after filling, the bottles

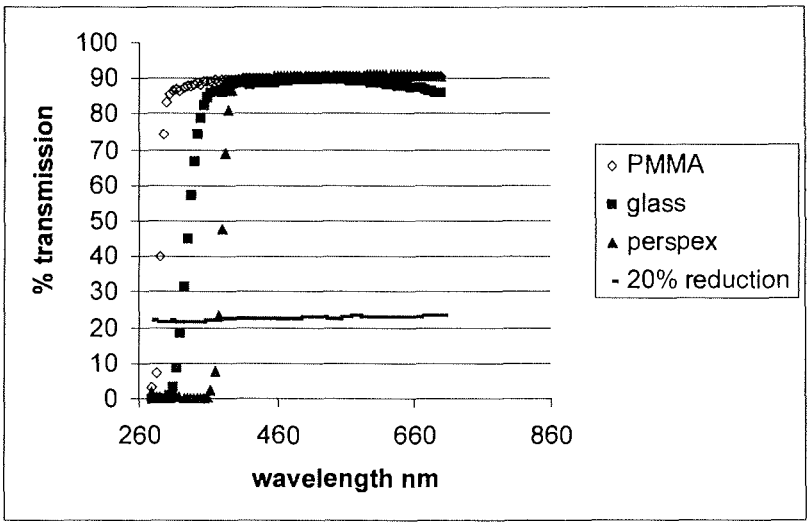

Figure 1: Transmission of light (%) as a function of wavelength (nm) of glass (UVB filter), perspex (UVA&B filter) PMMA (incubation bottles). As an example of the filters for reduction of the total intensity of the solar spectrum, the transmission through the 20% filter is shown.

were put in PMMA incubators on the 'peildeck' of the Polarstern. This deck was only shaded from the sun in early morning. The bottles were kept at a constant temperature of 26 _ C with flowing seawater from the ships underway pumping system. Two bottles packed in light tight black plastic functioned as blanks. Two bottles received the full solar spectrum (UVB&UVA&PAR), two bottles were screened by perspex (UVB filter in figure 1), receiving only UVA&PAR, two bottles were screened by glass thus only permeable for PAR (photo active radiation) (UVB&UVA filter in figure 1). Light intensity was varied by an aluminium gauze, painted black, causing a reduction of the full solar spectrum of 50%. 20% light reduction was obtained by wrapping two bottles in black plastic with tiny (1mm) holes (20% in figure 1).

Before use the incubator bottles were cleaned by soap solution (several days), a 3N HCl wash step (1 day) and a 1N HCl wash step, after which they were stored, containing seawater with a low iron content (<0.5 nM). All other material for Fe analysis was thoroughly acid cleaned in the home laboratory (NIOZ)

Peroxide was measured according to Miller and Kester (1988) by the demerization of (_-hydroxyphenyl)acetic acid and its subsequent fluorescence with a Waters fluorometer. The precision of the method was near 3%, its detection limit was smaller than 2 nM.

Sampling started at 5 h. in the morning of 15 October 2000 and continued till 23:00. Every 10 minutes one bottle was taken from deck, and was sampled in a laminar flow hood. Every bottle was thus sampled at least once per two hours, and every light condition was sampled at least every hour. The dark bottles were only sampled three times during the day. The sample for Fe(II) analysis, in a black Nalgene bottle, was brought immediately in a cool box to the clean container for analysis.
Fe(II) was measured by chemoluminescence (Bowie, in preparation).
Organic ligands were measured with differential pulse cathodic stripping voltammetry using TAC as the competing ligand (adapted after Croot and Johansson, 2000). The detection window used was 1011.4-1013.4.
Total dissolvable Fe was measured by flow injection chemoluminescence (de Jong et al, 1998).

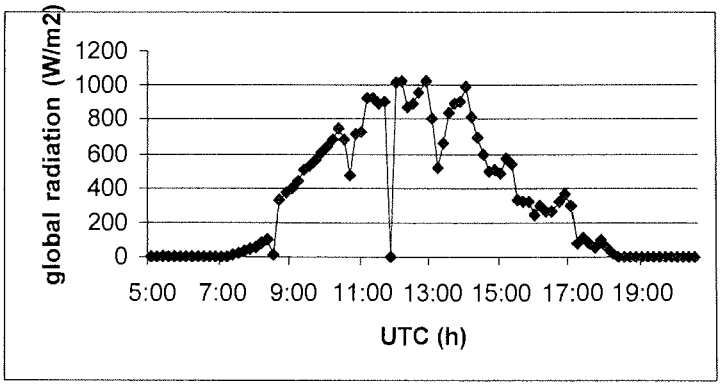

Figure 2: Global spectrum of the sunlight (from Polarstern's weatherstation) from 15 October 2000 against UTC time. The integrated values of measurements every ten minutes (W.m-2) are shown against UTC time.

Light measurement from the ship was used to obtain a rough estimate of the energy (Figure 2). UV dose was obtained by electrical dosimeters, ELUV-14 (El Naggar et al., 1995). Every minute 32 wavelength bands of 1.2 nm width were measured between 285 and 323 nm. The integrated values are shown in figure 3.

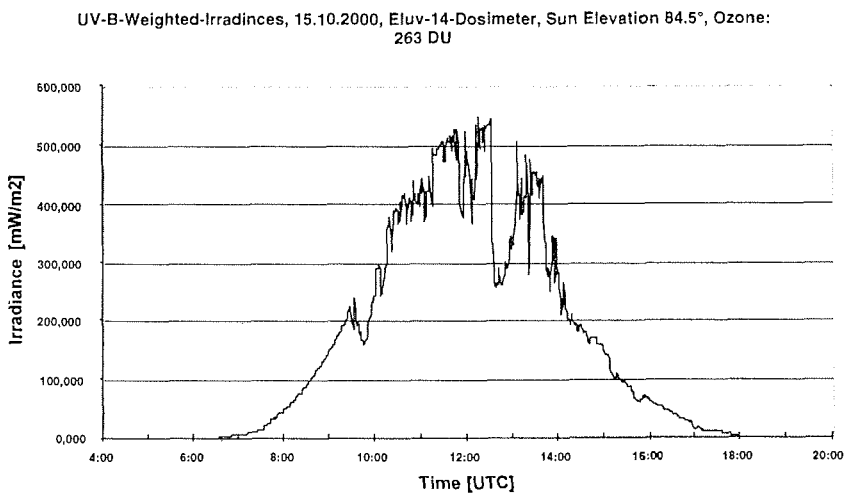

Figure 3:
Diurnal variation (15-10-2000) of UVB measurements with the ELUV-14 dosimeters (mW.m-2)

Preliminary results

The total dissolvable Fe concentration in the initial 50 liter sample was 0.40 nM. With the exception of the afternoon sampling (13:00) the concentrations in the bottles were for the majority close to this 0.4nM value (Table 1). The 13:00 sampling gave alarming results with concentrations up to 9 nM. Since the evening concentrations are low and close to 0.4 nM, contamination was probably during sampling in the sampling bottle and not in the incubator bottle. The only high concentration in the evening sampling was obtained in bottle 2 of UVA&PAR due to a tap that was left open after the previous sampling for peroxides and Fe(II). Another possible explanation for the variation in total dissolvable Fe concentrations could be contamination in the incubation bottles which is lost from solution due to adsorption on the bottle walls. However, the bottles were preconditioned with seawater. Research on this material in the Delft home laboratory with 55Fe has shown that adsorption on the walls is minimal and cannot explain a decrease in concentrations from 9 to 0.34 nM. Apart from the 13:00 sampling the Fe concentrations remained more or less

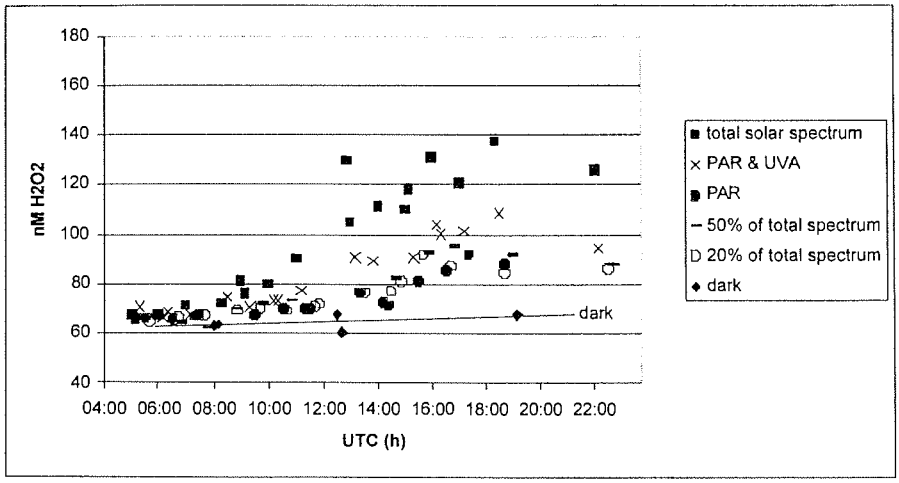

Fig. 4A

Fig. 4B

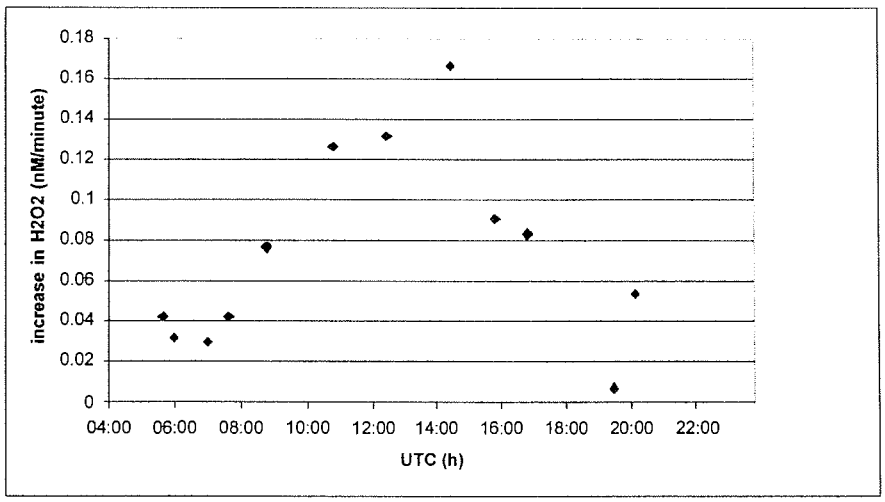

Figure 4:

A: Peroxide concentrations (nM) in the incubated bottles against time. The values of the dark bottles are accentuated with a line.

B: Production of peroxide per minute in the bottles that got the full solar spectrum.

constant, as was expected (hoped for !). Most likely the high concentrations are due to spot contamination on the sample bottle and not in the incubation bottles. In future experiments a better and safe sampling procedure must be used.

In figure 4A the clear relationship between peroxide concentration and light regime is shown. There is a clear relationship with wavelength. The lower the wavelength of the penetrating light, the more peroxide is produced. But even when only PAR is allowed to enter the bottles peroxide concentrations increase during the day, compared to the dark control bottles. The relationship to intensity is also straightforward, although the decrease in peroxide formation in the bottles with 50% reduction is larger than expected. To compare production more directly with light energy the slope of the concentrations with time in the bottles with the full solar spectrum was calculated representing the increase of peroxide in nM per minute (figure 4B). Comparing this figure with the light spectra of global radiation (Fig 2) and the UVB (Fig3) confirms the relationship with energy input by light and peroxide production. Regretfully the Fe(II) data and the data on the complexation characteristics of the seawater were not available at the end of the cruise.

In future experiments during ANTXVIII-2 we hope to repeat this experiment in the Southern Ocean,, using iron-enriched water as well as water from outside the enriched patch. In that experiment we want apply radio isotopes of Fe (55Fe and 59Fe). The radiotracer 55Fe has a high specific activity, so it can be added as a high pulse of radioactivity at a concentration of only 0.5 nM iron. This radiotracer will be added in the iron(III) inorganic form and the exchange kinetics with other Fe species will be measured.

Other experiments that will be performed are incubation of the natural population of the seawater and of single species cultures of diatoms. The objective here will be to study the relationship between Fe species and uptake by the algae. By means of the radio isotopes the kinetics of the uptake of Fe by the phytoplankton will be measured.

Table 1: Concentrations of total dissolvable Fe (nM) in the incubation bottles at three periods of the experiment. The 50 liter sample contained 0.40nM total dissolvable Fe:

	5:00		13:00		20:00	
	bottle1	bottle2	bottle 1	bottle2	bottle 1	bottle2
Total solar spectrum	1.29	0.45	9.03	0.76	0.34	0.72
PAR&UVA	1.05	0.46	0.83	5.85	0.24	1.56*
PAR	0.83	0.86	1.81	1.08	0.31	0.42
50%	0.55	0.44	5.01		0.33	0.36
20%	1.43	0.35	1.35		0.55	0.94
dark	0.92	0.55	3.29	2.24	0.25	0.23

* contamination because the tap of this bottle was left open at the previous sampling 1h before.

Acknowledgements
We are very grateful to captain Keil and his crew (it was never too much trouble, even a ship dripping at all sides of pouring seawater like the Niagara falls). We thank the Alfred Wegener Institute für Polar und Meeresforschung for their facilities and hospitality. Eddy Knuth und Herbert Köhler kindly provided fig. 2.

References

Croot, P.L., M. Johansson, 2000. Determination of iron speciation by cathodic stripping voltammetry in seawater using the competing ligand 2-(2-thiazolylazo)-_-cresol (TAC). Electoranalysis, 12, (8), 565-576.
De Jong, J.T.M., J. Den Das, U. Bathmann, M.H.C. Stoll, G. Kattner, R.F. Nolting, H.J.W. de Baar, 1998. Dissolved iron at subnanomolar levels in the Southern Ocean as determined by shipboard analysis. Anal. Chim., Acta, 377, 113-124.
El Naggar, S., H. Gustat, H. Magistr, R. Rochlintzer, 1995. An electronic personal UV-B dosimeter. J. Photochem. Photobiol., 31, 83-86.
Kuma ,K., S.Nakabayashi, K.Matsunaga, 1995. Photo-reduction of Fe(III)by hydroxycarboxilic acids in seawater. Water Research, 29, 1559-1569.
Miller, W.L., D. Kester, 1988. Hydrogen peroxide measurement in seawater by (_-hydroxyphenyl)acitic acid demerization. Anal. Chem. 60, 2711-2715.
Millero, F.J., 1998. Solubility of Fe(III) in seawater Earth Planet. Sci. Lett. 154, 323-329.
Hutchins, D.A., A.E. Witter, A. Butler, G.W. LutherIII 1999a. Competition among marine phytoplankton for different chelated iron species. Nature 40, 858-861
Hutchins, D.A., V.M. Franck, M.A. Brzezinski, K.W. Bruland, 1999b. Inducing phytoplankton iron limitation in iron replete coastal waters with a strong chelating ligand. Limnol. Oceanogr. 44, 1009-1018.
Steeneken, S.F., A.G.J.Buma, W.W.C. Gieskes. Changes in transmission characteristics of polymethylmethacrylate and cellulose (III) acetate during exposure to ultraviolet light. Photochem. Photobiol., 61, 276-280.

C.13 A new Geographic Information System (GIS)

Christopher Cogan (AWI)

Summary:
A new Geographic Information System (GIS) data reporting tool was implemented during the cruise. Using the GIS software ArcView, and the programing language Avenue, a near-real-time data access tool called "ShipMap" was developed. ShipMap reads data from the PODAS 10 minute database, displays a projected map

of the ships location with automatic updates as new data is generated by PODAS. The program is designed to access ancillary PODAS data via mouse click on the course map. Easy to use cartographic output for printed maps in several projections is also provided.

Goals

Previous track mapping software aboard Polarstern has evolved into a product that accurately depicted ships location and daily progress. The web based software also delivered summary data which could be retrieved from a map based spatial query. The goal for this cruise, has been to develop a new system that is compatible with the new PODAS information system, yet continues to deliver information in a familiar time-tested format. The new software is also intended to be flexible and expandable, ready to take advantage of more sophisticated database, data query, and cartographic standards. While building in more powerful options, a major design factor is to keep the program extremely simple to operate.

Product

The software package "ShipMap" was completed on board Polarstern, and demonstrated to ships personnel. A brief set of instructions and documentation was written to answer anticipated questions. The program is started by clicking on an icon, and selecting the appropriate options for start date, end date, desired background maps, and map projection. Once started, the program reads the selected portions of the PODAS 10 minute database via an ODBC connection, and draws a trackline of the ships locations. As a day marker, the ships position at 06:00 is depicted with a special symbol. The program can be stopped and restarted, or left to run unattended. As needed, the map will automatically pan and zoom as the ship moves to new areas.

Because the GIS map is actually a direct rendering of the PODAS database, clicking on any feature of the map causes a table to be displayed with ancillary data relating to that point, line, or area. The tabular data can then be queried, and if appropriate, the map redraws to display the results. Database queries (including spatial queries) can use any of the combined fields from external base maps as well as the PODAS data.

Future directions

- The delayed availability of the PODAS data did not allow full integration or testing of all the PODAS 10 minute data with ShipMap. Future upgrades should allow additional data to be delivered by graphical spatial query.
- Additional debugging will nodoubt be necessary as the program is tested with the PODAS data.
- User feedback may dictate changes to the graphical user interface.
- Additional background data will greatly improve the utility of the program. Availability of image processing software will allow imagery such as real-time SeaWiFS Chl.a data to be incorporated into the GIS map layer. Bathymetry data is also a logical product to incorporate.
- Future versions of the program may be more stable and upgradeable if it can run under ArcInfo, instead of ArcView. The possibility of soliciting an ArcInfo software donation from ESRI is under discussion.
- A web-based broadcast of the software to selected ships terminals is also under discussion.
- A mirror of the ships system could be run at the AWI, served out via the web. This system would use the same 10 minute database, as archived after every cruise

Conclusion:

The ShipMap software developed during this cruse is a working product, as well as a proof-of-concept tool that is designed to allow future upgrades. The software successfully met the immediate requirements, and offers many options for future expansion.

C.14 Ergänzung der Intranetseiten und Erstellung einer neuen Mail-Oberfäche

Michael Hofmann /AWI

In der Zeit vom 1. September bis 31. Oktober 2000 hatte ich am Alfred-Wegener-Institut eine Stelle als studentische Hiflskraft im Bereich Logistik zur Intranet-Verwaltung und -Programmierung. Meine Arbeit hat sich in zwei Teile gegliedert. In den ersten drei Wochen am AWI-Rechenzentrum in Bremerhaven habe ich mich um den Ausbau der bestehenden Seiten gekümmert. Insbesondere ging es dabei um die Übersetzung der vorhandenen deutschsprachigen Seiten in eine englische Fassung, damit auch Wissenschaftler aus dem nicht-deutschsprachigen Raum die angebotenen Informationen effizient nutzen können. Weiterhin fand eine Überarbeitung der vorhandenen Strukturen statt. Schwerpunkt wurde dabei auf eine verbesserte und logischere Benutzerführung gelegt.

Der zweite Teil der Arbeit fand im Wesentlichen direkt auf dem Forschungsschiff Polarstern während ANTXVIII/1 statt. Da das Mailsystem auf dem Schiff zur Zeit sehr umständlich realisiert wird, war eine Vereinfachung dringend notwendig geworden. Insbesondere die Abhängigkeit von Disketten zur Verwaltung der einzelnen Nutzer ist heute nicht mehr dem Stand der Software-Technik entsprechend. Als sehr einfach erschien deshalb die Programmierung einer Java-Lösung. Als Applet realisiert, ergeben sich die notwendigen Vorteile, wie Unabhängigkeit von den verwendeten Plattformen und eine universelle Einsetzbarkeit. Da das System nur an einen praktisch überall vorhandenen Java-tauglichen Webbrowser gebunden ist, kann es prinzipiell auf jedem Rechner ohne Probleme eingesetzt werden.
Im Laufe der Fahrt von Bremerhaven nach Kapstadt entstand dann ein Client, der mit den notwendigen Grundfunktionalitäten Senden und Empfangen von Mails, sowie mehreren Zusatzfunktionen für Drucken, Speichern und Verwaltung ausgestattet ist. Leider ist die Theorie immer einfacher als Praxis. Deshalb ist es bis zum Schluss der Fahrt nur gelungen, das System auf Internet Explorer und Netscape unter Windows lauffähig zu bekommen. Um den Benutzer in das System einzuführen, wurde am Ende der Fahrt eine auf das Intranet basierende Dokumentation entwickelt.
Zum Abschluss ist festzuhalten, dass das neue System noch nicht voll praxistauglich ist. Die wesentlichen Funktionen wurden entwickelt, aber eine ausgiebige Testphase fand aus Zeitgründen leider nicht statt. Somit bleiben als offene Punkte sicherlich noch die Lauffähigkeit auf allen Systemen. Außerdem können noch eine verbesserte Verwaltung für den Benutzer, sowie ein Adressbuch hinzugefügt werden. Dabei lohnt es sich Gedanken darüber zu machen, wie diese Daten – auch im generellen serverseitigen Verwaltungsprozess – gemanagt werden könnten. Ein Weg wäre dabei sicherlich die Strukturierung in XML.

C.15 Wetterbericht ANTXVIII/1

E. Knuth, H. Köhler /DWD

FS Polarstern verliess Bremerhaven am 29.09.00 gegen 14.30 Uhr zu seiner 18. Reise in die Antarktis mit kurzem Abstecher in die Nordsee westlich von Helgoland um die ersten Maschinentests, sowie die Abnahmen des BSH und GL durchzuführen. Diese Testfahrten dauerten bis zum 30.09. abends. Am Lotsenpunkt Elbe/Weser wurden 3 Techniker von Bord gegeben. Danach steuerte FS Polarstern Kurs Englischer Kanal.

FS Polarstern verliess Bremerhaven bei sonnigem Wetter mit leichten bis mässigen südöstlichen Winden. Ein Hoch lag mit 1027 hpa über Südrussland mit der Tendenz sich nordwärts zu verlagern. Ein Tief südlich von Irland zog langsam ostsüdost und füllte sich dabei auf.
Die Windrichtung änderte sich am Folgetag nur wenig, allerdings frischte der Wind zeitweise am vormittag auf 6 Bft auf, im weiteren Verlauf des Tages pendelte sich die Windstärke auf 2 bis 4 Bft ein. In der Nacht zum 1.10. drehte der Wind auf W bis NW und schwächte sich dabei weiter ab. Im Tagesverlauf drehte er weiter rück und frischte in den Abendstunden auf 5-6 Bft auf. In der Folgenacht zum 2.10. erreichten die Ausläufer eines Sturmtiefs über den Hebriden FS Polarstern im Westausgang des Englischen Kanals mit Wind der Sturmstärke von 9 Bft und in Böen 10 Bft. Seinen Höhepunkt erreichte der Sturm in den Morgenstunden des 2.10. , danach drehte der Wind auf westliche bis südwestliche Winde mit 4-5 Bft. In der Nacht zum 3.10. frischte der Wind noch einmal kurzfristig auf mit Böen bis 7 Bft und drehte im Verlauf des Tages auf nordwestliche bis nördliche Winde die leicht abnahmen, so daß die Überquerung der Biskaya unter moderaten Umständen erfolgte.
FS Polarstern dampfte im weiteren Reiseverlauf in den Bereich des umfangreichen nördlich der Azoren liegenden Hochs hinein und kam dabei in eine stabile nord- bis nordöstliche Luftströmung mit Windstärken um 3 bis 5 Bft. Eine schwache Kaltfront aus einem schwachen Tief östllich der Azoren brachte im Bereich der portugiesischen Küste nur starke Wolkenfelder. Diese Wolkenfelder begleiteten FS Polarstern weiterhin auch am 5.10. bei unveränderten Windverhältnissen.
Von nun an wurde der weitere Reiseverlauf vom Nordostpassat bestimmt, der überwiegend mit 4-5 Bft wehte, aber nördlich der Kanaren auf zeitweise 6 Bft auffrischte.

Am 8.10. morgens lief FS Polarstern im Vorhafen von Las Palmas ein um 24 Personen technischen Personals, Reederei- und AWI - Mitarbeitern auszubooten. Am Mittag desselben Tages setzte FS Polarstern die Reise fort und lief bei sonnigem Wetter und NE-Passat einen südwestlichen Kurs um am 10.10. morgens bei Kap Blanc (Mauretainen) eine mehrstündige Station durchzuführen. Hier wurde ein Verankerungssystem mit zwei Sinkstofffallen und einem Strömungsmesser aufgenommen und anschliessend wieder ausgesetzt.

Nach passieren der Kapverdischen Inseln liess die NE-Passatströmung weiter nach und mündete schliesslich am 12.10. bei etwa 9° nördlicher Breite in die Innertropische Konvergenz. Ab Mitternacht des 13.10. traten für die nächsten Stunden grössere Windsprünge auf von NW- bis SE-lichen Richtungen, die aber im Bereich von 3 Bft blieben. Die grösste Niederschlagsmenge gab es zwischen 3 und

4 Uhr UTC, in dieser Zeit waren die Schauer und Gewitter am intensivsten. Bis zum späten Vormittag trafen FS Polarstern dann nur noch vereinzelte leichte Schauer bei nun südlichen Winden von 3-4 Bft. Die dichte Wolkendecke lockerte sich im Tagesverlauf zunehmend auf und diese Bewölkungsverhältnisse blieben uns auch am 14.10. und am 15.10. erhalten.
Nach dem Überschreiten des Äquators am 14.10 gegen 20.25 Uhr UTC drehte der Wind in der darauffolgenden Nacht langsam auf SE mit 2 Bft. Auch am 15.10. blieb uns dieser schwache SE-Passat erhalten.
Die seit dem 16.10. stark bewölkten Verhältnisse änderten sich nur kurzfrisrtig für einen Tag am 18.10. Ab einer Breite von 15° Süd und ca. 1° östlicher Länge kam FS Polarstern in den Bereich des auffrischenden SE-Passates mit seinen üblichen 5-6 Windstärken die kurzfristig auch 7 Bft erreichten. Ebenso wuchs die Dünung auf 3 m bis 3,5 m seit dem 16.10. an.
Die für diese Region typischen, ausgedehnten, zählebigen und von nur wenigen Lücken durchsetzen Felder mit Schicht-Quellbewölkung minderten an vielen Tagen die Sonnen- einstrahlung, so dass die astronomisch möglichen Spitzenwerte der Global- und UV-Strahlung nur selten gemessen werden konnten. Der gesamte Eindruck trug nicht dazu bei, dass sich FS Polarstern in „tropischen Gewässern" aufhielt.
Diese Wetterlage wurde durch ein Subtropenhoch (festliegend) von 1033 hpa auf 38S/03W und einem Tief (SE-wandernd) von 1009 hpa an der Westküste Südafrikas noch etwas verschärft, so dass die zu erwartende ruhigere Wetterzone unter der Küste Südafrikas ausblieb. Erst kurz vor Kapstadt ging der starke SE Wind von 6-7 Bft und einem Seegang von 4 m auf S-SE 4-5 Bft zurück.
Am Morgen des 23.10.2000 lief FS Polarstern in Kapstadt ein.

D. BETEILIGTE INSTITUTIONEN/ PARTICIPATING INSTITUTIONS
ANT XVIII/1

Adresse/Address		Teilnehmer/Participants
AWI	Alfred-Wegener-Institut für Polar- und Meeresforschung Postfach 12 01 61 27515 Bremerhaven, Germany	9
DWD	Deutscher Wetterdienst Seewetteramt Bernhard-Nocht-Straße 20359 Hamburg, Germany	2
INTER	Interschalt Oberbrooksweg 42 22869 Schenefeld /Hamburg	1
IRI/ Delft	Interfacultair Reactor Instituut Technische Universiteit Delft Melkweg 15 2629 JB Delft, The Netherlands	2
MTU	Motoren und Turbinen Union Werk 3 88040 Friedrichshafen, Germany	3
NIOZ	Netherlands Institute for Sea Research Postbus 59, 1790 AB Den Burg – Texel, The Netherlands	5
RFL	Reederei F. Laeisz, Bremerhaven Barkhausen-Str.37 27568 Bremerhaven, Germany	3

Adresse/Address		Teilnehmer/Participants
ROCHEM	Rochem UF-Systeme GmbH Stadthausbrücke 1-2, Fleethof D–20355 Hamburg, Germany	1
STNH	STN-Atlas-Elektronik GmbH Behringer-Str. 120 22763 Hamburg, Germany	4
UB	Universität Bremen Fachbereich Geowissenschaften, SFB 261 Klagenfurter Strasse 28359 Bremen, Germany	2
UBO	Université de Bretagne Occidentale (University of Brest, UMR CNRS 6539) nstitut Universitaire Europeen de la mer Place Nicolas Copernic 29 280 PLOUZANE, FRANCE	2
UEA	University of East Anglia School of Environmental Sciences Norwich NR4 7TJ, United Kingdom	3
UH	Universität Heidelberg Institut für Umweltphysik Im Neuenheimer Feld 229 69120 Heidelberg, Germany	1
UoP	University of Plymouth Dept. of Environmental Sciences Plymouth PL4 8AA, United Kingdom	2
WERUM	Werum GmbH Erbstorfer LandStr. 14 21337 Lüneburg	4

E. FAHRTTEILNEHMER/PARTICIPANTS
ANT XVIII/1

Name/Name	Institut/Institute	Nationalität/Nationality
Bluszcz, Taddäus	AWI/Chemie	D
El Naggar, Dr. Saad (Chief Scientist)	AWI/Logistik	D
Gerchow, Peter	AWI/Infozentrum	D
Gauger, Steffen	AWI/Bathymetrie	D
Hofmann, Michael	AWI/Logistik	D
Krause, Dr. Reinhard	AWI/Logistik (Las Palmas)	D
Reinke, Dr. Manfred	AWI/ Infozentrum	D
Niederjasper, Fred	AWI/Bathymetrie (Las-Palmas)	D
Usbeck, Rigina	AWI/Geologie	D
Knuth, Edmund	DWD	D
Köhler, Herbert	DWD	D
Drauschke, Peter	INTER	D
Thomas, Dr. Hans-Jürgen	MTU (Las Palmas)	D
Längin, Hans-Dieter	MTU (Las Palmas)	D
Müller, Markos	MTU (Las Palmas)	D
Boye, Marie	NIOZ I + II	F
Croot, Dr. Peter	NIOZ I + II	NZL
Gerringa, Dr. Loes	NIOZ	NL
Laan, Patrick	NIOZ I + II	NL
Rijkenberg, Micha	NIOZ I + II	NL
Fischer, Astrid	NIOZ/(IRI, Delft) I + II	NL
Kroon, Koos	NIOZ/(IRI, Delft) I + II	NL
Wagner, Eberhard	RFL (Las Palmas)	D
Manthei, Wolfgang	RFL (Las Palmas)	D
Hofmann, Dr. Jörg	RFL D	
Neuhäuser, Uwe	ROCHEM (Las Palmas)	D
Bade, Dirk	STNH (Las Palmas)	D
Heckel, Christian	STNH (Las Palmas)	D
Woike, Günther	STNH (Las Palmas)	D
Schäfer, Raphael	UB	D
Segl, Dr. Monika	UB	D
Blain, DR. Stephane	UBO	F
Sarthou, DR. Geraldine	UBO	F
Baker, Dr. Alex	UEA	UK
Bakker, Dr. Dorothee	UEA	NL
Chuck, Adele	UEA	UK
Leser, Hans	UH	D
Achterberg, DR. Eric	UoP	UK
Bowie, Dr. Andy	UoP	UK
Schmidt, Horst	WERUM (Las Palmas)	D
Sommer, Christian	WERUM (Las Palmas)	D
Viergutz, Thomas	WERUM	D
Zenker, Uwe	WERUM	D

F. SHIP'S CREW/SCHIFFSBESATZUNG ANT XVIII/1

Master	Keil, Jürgen	
1. Offc.	Grundmann, Uwe	
2. Offc.	Spielke, Steffen	
Ch.Eng.	Schulz, Volker	
Ch.Eng.	Pluder, Andreas	(Las Palmas)
Doctor	Burat, Werner	
2. Offc.	Fallei, Holger	
R. Offc.	Hecht, Andreas	
1. Eng.	Delff, Wolfgang	
2. Eng.	Ziemann, Olaf	(Las Palmas)
2. Eng.	Folta, Henryk	
2. Eng.	Simon, Wofgang	
Electron.	Piskorzynski, Andreas	
Electron.	Roschinsky, Jörg	(Las Palmas)
Electron.	Fröb, Martin	
Electron.	Greitemann-Hackel, Andreas	(Las Palmas)
Electron.	Baier, Ulrich	
Electron.	Muhle, Helmut	(Las Palmas)
Electron.	Bretfeld, Holger	
Electron.	Dimmler, Werner	
Electr.	Holtz, Hartmut	
Electr.	Muhle, Heiko	(Las Palmas)
Boatsw.	Loidl, Reiner	
Carpenter	Neisner, Winfried	
A.B.	Bäcker, Andreas and Schmidt, Uwe	
A.B.	Winkler, Michael and Moser, Siegfried	
A.B.	Bindernagel, Knuth and Bastigkeit, Kai	
Storekeep.	Beth, Detlef	
Mot-man	Arias Iglesias, Bnr.	
Mot-man	Schubert, Holger	
Mot-man	Fritz, Günter	
Mot-man	Krösche, Eckard	
Mot-man	Dinse, Horst	
Cook	Fischer, Matthias	
Cooksmate	Tupy, Mario and Martens, Michael	
1. Stwdess	Dinse, Petra	
Stwdss/Nurse	Brendel, Christina	
2. Stwdess	Streit, Christina	
2. Stwdess	Schmidt, Maria	
2. Stwdess	Deuß, Stefanie	
2. Stwdess	Tu, Jlan Min	
2. Stwdess	Wu, Chi Lung	
Laundrym.	Yu, Chung Leung	
Trainee	Buchner, Bernd	

FAHRTABSCHNITT ANT XVIII/2 KAPSTADT - KAPSTADT
(24.10.01 - 03.12.01)

1. CRUISE SUMMARY

U. Bathmann and V. Smetacek

The in situ iron fertilization experiment EisenEx (Eisen-Experiment, ANT XVIII/2) was carried out from RV Polarstern in the Polar Frontal Zone (PFZ) due south of Africa (48° S; 21° E), between 25th Oct. and 5th Dec. 2000. The aim of the cruise was to fertilize, with iron-sulphate solution marked with an inert tracer, a patch of water in an eddy of the Antarctic Circumpolar Current and follow the physical, chemical and biological processes in the fertilized water till the end of the cruise. The 54 scientific personnel on board, representing a total of 15 nationalities, had been selected on the basis of expertise necessary to carry out the tasks required by the experiment. About half the scientists were biologists with physical and chemical oceanographers contributing about equal proportions to the other half.

Funding for EisenEx was provided primarily by the German Bundesministerium für Bildung und Forschung with additional support from the European Union (CARUSO), the Netherlands-Bremen-Oceanography programme (NEBROC), the National Environmental Research Council (United Kingdom) and various other funding sources.

Scientific background

Ice-core data show that changes in global temperature are closely linked to atmospheric CO_2 concentrations. However, the sources and sinks of atmospheric CO_2 between glacial and interglacial periods are not known as also the factors regulating its concentration during these periods. Since the oceans contain far more CO_2 than the atmosphere, the balance of carbon at the ocean surface has a critical effect on atmospheric concentrations. This balance is influenced by phytoplankton, the single celled algae that grow in the surface, sunlit layer. By taking up and converting dissolved CO_2 into biomass, the algae create a deficit in the surface layer that is compensated by CO_2 drawdown from the atmosphere. Phytoplankton growth is dependent on light supply and the availability of dissolved nutrients, of which nitrate is the most important. However in three vast regions of the ocean, the so-called high-nitrate, low-chlorophyll (HNLC) regions (Equatorial and Subarctic Pacific and the entire Southern Ocean), phytoplankton production is low, despite favourable light conditions and high nitrate concentrations. A solution to this enigma is emerging

from studies over the past decade. Iron appears to be the major limiting nutrient in these regions. It has been shown that the retention ability of sea water for iron is much less than that of nitrate and phosphate in terms of Redfield stoichiometry. In other words, iron is selectively lost to sinking processes relative to N and P. The iron retained in deeper water is sufficient to enhance phytoplankton biomass by a factor of 2 – 4 relative to surrounding water. Were all available nitrate utilised, the resulting biomass would be 2 orders of magnitude higher than the normal HNLC biomass.

The most convincing evidence for iron limitation of HNLC water has come from three in situ iron fertilization experiments, two carried out in the Equatorial Pacific (IRONEX I and II) and one in the Southern Ocean (SOIREE) showing that phytoplankton blooms could be induced by fertilising a patch of water a few km2 in extent with a few tonnes of dissolved iron. These experiments showed that it is essential to choose a suitable hydrographically calm region in order to follow and monitor the fertilized patch for several weeks. The Southern Ocean Iron Release Experiment (SOIREE), carried out in waters south of Australia, resulted in a phytoplankton bloom of over a 100 square kilometres in size. Because of a shortage of ship time, the fate of the SOIREE bloom could not be ascertained during the experiment. This is crucial for the CO_2 budget. If the biomass is broken down in the surface layer by bacteria and zooplankton, no net removal of CO_2 occurs. If the organic matter sinks out of the surface layer, however, the equivalent amount of CO_2 is removed from the atmosphere for tens to hundreds of years.

The source of the high nutrients in HNLC regions is upwelling and admixture of sub-pycnocline water to the surface mixed layer. In the North and Equatorial Pacific this upwelled water remains in the surface so the nutrients are eventually converted into organic matter, the bulk of which is transferred to depth via the normal pathway of the biological pump. Because of its hydrography, the situation in the Southern Ocean is very different. Most of the Southern Ocean consists of a broad eastward flowing ring of water, the Antarctic Circumpolar Current (ACC), divided by the Antarctic Polar Front (APF) into the northern Polar Frontal Zone (PFZ) and the southern Antarctic Zone. Along stretches of the northern border of the PFZ, i.e. along the Subantarctic Front, surface water tends to subduct under the neighbouring subantarctic zone leading to formation of Antarctic Intermediate Water. Since these are HNLC waters, the process of downwelling results in the transfer of substantial amounts of unutilized nitrate and phosphate from the surface into the ocean interior. Were enough iron available, the algae would grow faster, take up more nutrients and fix more carbon, which would either sink out as a rain of particles or be carried down to the deep sea with the subducting PFZ water.

John Martin (1990) proposed the hypothesis that iron, transported in airborne dust from the continents and deposited on the Southern Ocean, enhanced productivity during glacial periods and contributed to the lower concentrations of CO_2 in the atmosphere that characterized these colder periods in the Earth's history. Simple calculations indicate that about a third of the difference between glacial and interglacial CO_2 levels (ca. 30 Gigatonnes) could be accounted for by this iron-fertilization mechanism, i.e. complete incorporation of N and P into organic matter.

Prior to EisenEx a series of cruises dedicated to elucidating the relationship between mesoscale physics and plankton biology in the Antarctic Circumpolar Current (ACC) had been carried out from RV POLARSTERN. During cruise ANT X/6 performed in austral spring of 1992 high iron concentrations found north of the Polar Front (APF) led to build-up of a series of phytoplankton blooms there, whereas south of the Front, iron concentrations were lower and phytoplankton biomass remained an order of magnitude lower. An exceptional feature of this period was the large number of icebergs throughout the ACC (5 – 10 bergs in a radius of 10 nm around the ship) systematically recorded during all three transects carried out from end-October to mid-December (Smetacek et al. 1997). Although their role was discounted at the time (de Baar et al. 1995), we now suspect that the source of the high iron concentrations (>2 nmol/l^{-1}) was more rapid melting of the bergs in the warmer water of the PFZ (2° C) as compared to AZ water (-1.5°C). During subsequent cruises in austral summer and autumn (ANT XIII/2 and ANT XVI/2) iron concentrations were low throughout and not a single berg was recorded. Higher biomass of phytoplankton (the maximum values were factor-of-four higher than in the surroundings) was restricted to the vicinity of the APF where some iron could have been supplied by local upwelling of deeper water in connection with meandering of the APF. Species composition and biomass of phytoplankton was clearly related to mesoscale water masses, indicating differences in pre-conditioning of the respective stocks in adjacent water masses. Apparently, iron availability played a key role in determining productivity and species composition of the ACC plankton.

Although we were aware that ship-time allotted for EisenEx would not suffice to follow the eventual fate of the fertilized biomass, it was still worthwhile to carry out a short experiment to answer the following questions:

1. Is phytoplankton of the ACC iron-limited also in spring, at the start of the growing season and in the presence of heavy grazing pressure? SOIREE was carried out south of the APF in late austral summer, a period when grazing pressure is low and the phytoplankton is most likely to be iron-limited.

2. In what way would the spring pelagic ecosystem react differently to fertilization as compared to the experimental conditions tested during SOIREE.
3. Would it be possible to fertilise a patch and follow it over time during stormy spring conditions and in the strong flow field the ACC in the Atlantic sector of the Southern Ocean? Earlier studies had shown that meandering of the APF resulted in formation of mesoscale eddies. We reasoned that the low current speeds recorded in the centre of such an eddy would provide a stable water mass that maintained its integrity over the course of the experiment.

Description of cruise

The first week of the cruise was dedicated to selection of a suitable site for the experiment: the centre of a large eddy with low iron concentrations and phytoplankton biomass. In order to gain an overview of the position of Southern Ocean fronts we first carried out a meridional transect with the towed, undulating instrument package ScanFish that records temperature, salinity and chlorophyll fluorescence in the upper 250 metres. The 750 km transect along the 20E meridian commenced at the Subantarctic Front at 45S, covered the PFZ, crossed the APF and ended in the Antarctic Zone at 52S. Temperatures were lower, diatom stocks larger and silicate concentrations, used by diatoms to construct their shells, higher across a stretch of water around 48S. We identified this band of water as an eddy originating from the APF that had drifted 400 km northward. It exhibited similar current speeds as the water around it but in the opposite direction, i.e. towards the west. Where the currents shifted directions, speeds were at their lowest. Further support came from altimeter images indicating the core of an eddy.

The second week of the cruise was devoted to a fine scale hydrographical survey of the region. The preconditions were good: very low iron concentrations throughout and a sparse but species rich plankton community combined with fairly shallow mixed layers. Measurements of the photosynthetic performance of individual cells showed that the algae were growing at only 30% of their potential rates. A cause for concern was the large numbers of copepods (millimetre sized zooplankton) in the area. Their grazing pressure could nip the bloom in the bud.

Fertilization began on Nov. 7 in the centre of the eddy which we marked with a drifting buoy at approximately 48S, 21E. Four tonnes of iron sulphate dissolved in 30 cubic metres of acidified sea water was released through a hose around a spiral about 70 km in length and 7 km in diameter relative to the buoy trajectory.

The previous iron enrichment experiments had shown that the iron added to the patch vanishes within a few days. Thus an inert tracer, sulphur hexafluoride (SF_6), is added to the enriched water to identify the patch. Because SF_6 is volatile and escapes into the atmosphere, the iron and tracer mixture was released at a depth of 15 metres in the wake of the ship's propeller. About 40 gramms of SF_6 were added to the initial fertilizer. Subsequent fertilizations were not marked with SF_6.

The first signs of a response in the phytoplankton was found two days after fertilization, a day or two earlier than expected. Data from a fast repetition rate fluorometer, which measures the photosynthetic efficiency of algal cells, showed that the algae in the patch had increased their efficiency, hence growth rate, significantly. Despite the favourable light climate for the phytoplankton during the first half of the cruise, chlorophyll levels throughout the region stayed more or less constant. Within the patch, they more than doubled over the first five days. The bloom had begun.

The first severe storm of the cruise occurred five days after fertilization. The water column was mixed down to 60 m. A few long transects after the storm showed strong signals of SF_6 to the west of the buoy. The patch had stayed in the eddy's eye and was now moving west after describing a semicircle. After carrying out a series of long stations within and outside the patch, another few tonnes of iron in solution was added in its centre. Although iron concentrations were still high, they had dropped in the week since the first fertilization. Another complete spiral was fertilised on Nov. 16. By Nov. 18, the highest chlorophyll levels within the patch had increased to bloom proportions, with values roughly four times those found in the surrounding waters.

Preliminary results suggested that although the iron enriched plankton were growing at least twice as fast as those in the surrounding water, the accumulation of biomass was kept in check by the poor light conditions associated with intermittent stormy weather in combination with heavy grazing pressure exerted by the various organisms, ranging from protozoa to crustacean zooplankton, that feed on phytoplankton. The latter migrate vertically during dawn and dusk and feed in the surface layer during the night.

Since the patch was being diluted on its way around the eye of the eddy and iron concentrations were very low throughout, its centre, where SF_6 concentrations were highest, was fertilised for the third time on Nov. 22. Results from mapping transects showed close correlation between chlorophyll and SF_6 concentrations in an elongated coherent patch at least 15 km long and 10 km across, demonstrating beyond doubt that the bloom was a result of iron fertilization. The eddy maintained its integrity and remained more or less stationary for 4 weeks vindicating our reasoning

to carry out the experiment in the centre of a suitable eddy. The iron induced bloom circled its centre, steadily increasing in size as it mixed with the surrounding water.

A final grid with short CTD stations revealed that fertilized water now covered an area of 500 km^2, which extended over the entire eye of the eddy. The highest chlorophyll concentration we measured was 2.84 mg Chl m^{-3}, with a standing stock of more than 200 mg m^{-2}, which is a large algal biomass by any standard. Yet these values are a very rough measure of the total biomass built up by iron fertilization because they have to be corrected for dilution with surrounding water. A correct estimate of the carbon actually taken up as a result of iron fertilization will require a calculation of the total area covered by the bloom, estimated by means of the SF_6 and another tracer, ^{3}Helium, that was added to the water. The final estimate will be conservative, because we had to leave the eddy well before the bloom peaked. The budgets will incorporate a number of measurements carried out during EisenEx, including CO_2 deficits and nitrate, phosphate and silicate concentrations, as well as increases in biomass of bacteria, zooplankton and their waste products. In the water with the highest chlorophyll concentrations, nitrate and phosphate declined by only 10%, whereas silicate decreased by 30%. The lowest concentration of CO_2 found was equivalent to an uptake of about 7 gC m^{-2}.

If all the nitrate were converted into algal biomass, the equivalent chlorophyll concentration would be around 50 mg Chl m^{-3}, and the total amount of CO_2 converted to organic carbon in a water column 60 metres deep would be over 80 g C m^{-2}. These figures suggest the enormous potential of these waters for building up biomass and removing CO_2 from the atmosphere.

It was not clear at first which of the many groups of phytoplankton represented in the eddy were primarily responsible for the increase in chlorophyll within the patch. Plankton diversity was unusually high because the eddy had spun off from the APF in the south and carried with it large diatoms and presumably also the colonial flagellate *Phaeocystis*, which are typical of the Antarctic zone. Lighter surface water encroaching from the north carried species typical of the subantarctic: dinoflagellates, coccolithophorids and minute cyanobacteria that were mixed into the surface layer with the southern plankton. The smallest cells in our patch belonged to the cyanobacteria, which are about 1 µm in diameter, and the largest was a rod shaped diatom that is more than 2 mm long.

Growth rates, ecological preferences and life cycles of these species differ widely. Since the fate of the carbon fixed by the fertilised community depends largely on which size class and group accumulates most biomass, we closely followed changes

in community composition. Initially it appeared as though cells in the intermediate size class, between 10 and 20 µm, had increased in number the most, but during the third week of the experiment species of the cosmopolitan diatom genus *Pseudonitzschia* clearly attained dominant status. The heavily silicified, chain-forming pennate diatom *Fragilariopsis kerguelensis*, reported to have dominated the biomass of the SOIREE bloom, also contributed substantially. Many other algal species contributed to the EisenEx bloom, but in smaller numbers.

Preliminary results indicate that bacterial growth was also strongly stimulated by iron addition, but the extent to which the protozoa and zooplankton responded to the increase in food supply still needs to be analysed. Thorium isotope measurements indicated that there was little difference in loss rates between water inside the patch and outside. We assume that this changed significantly after we had to leave the study area. Heavy cloud cover throughout and following the experiment precluded use of satellite imagery to trace the fate of the bloom.

Conclusions

Although the cruise was too short to assess the eventual magnitude and fate of the bloom created, EisenEx was a great success. It was shown that plankton growth in the PFZ is limited by iron availability and that addition of this element can lead to a fivefold increase in biomass within a period of three weeks, despite heavy grazing and poor light conditions characteristic of the austral spring.

Amongst the many other results of this cruise, presented in the chapters of this report, one major success was the application of the method employed: Selecting a large eddy and fertilizing the zone of low current speeds in its centre. Despite mixing of the patch with the surrounding water, caused by lateral intrusions of adjacent water layers as well as strong storms, identity of the patch within the eddy´s centre was maintained over a period of 3 weeks and is likely to have been maintained for much longer. Weekly fertilization of the region of highest chlorophyll kept the plankton iron-replete and enabled continuous tracking of bloom development till the onset of self-shading. These results show that this technique can successfully be employed to carry out simultaneous, multi-patch experiments in different zonal regimes of the Southern Ocean.

Another striking result was the dominance of bloom biomass by a few genera. Whether continued fertilization and resultant aggravation of self-shading would have resulted in demise of one population and its replacement by another dominant species is an open question. Data from the STERNA cruises in the Bellingshausen

Sea indicate that phytoplankton populations of >5 mg Chlorophyll m^{-3} can survive for periods of weeks. The fate of the STERNA biomass could not be ascertained.

Clearly, further, longer-term iron fertilization experiments are urgently needed to test the iron hypothesis that the Southern Ocean can be a significant global CO_2 sink. In situ experiments represent a powerful tool to study the structure and functioning of pelagic ecosystems in relation to physico-chemical forcing and selective grazing pressure. For instance, the weakly silicified *Pseudonitzschia* will have a very different effect on silica and carbon budgets of the ACC than its heavily silicified counterparts *Fragilariopsis kerguelensis* and others. The data from ANT X/6 show that iron fertilization also occurs when large portions of dislodged shelf ice disintegrate into numerous bergs that eventually melt in the PFZ. Hence, patch fertilization simulates a natural process occurring on average several times per century. Insights provided by such experiments will greatly help in elucidating the biology of key species that contribute to the underlying sediments. This information can also contribute to improving interpretation of the sediment record and help in testing Martin´s iron hypothesis.

Last but not least, some commercial organisations intend carrying out large-scale fertilization of the Southern Ocean as a means of sequestering anthropogenic carbon. It is hence imperative that the scientific community carry out the necessary research to thoroughly study the effects of large-scale fertilization in terms of removal of carbon from the surface layer, the time-scales of such a sequestration (depth to which the organic matter is transported) and its effects on the perturbed ecosystems.

Acknowledgements

It is a pleasure to acknowledge the enthusiastic support and professional support we received throughout the cruise from the captain and crew of RV Polarstern. The experiment could not have been carried out without their skilled help.

References

Boyd et al., 2000, A mesoscale phytoplankton bloom in the polar Southern Ocean stimulated by iron fertilization, Nature, 407, 695-702

Martin, J. H., 1990, Glacial-interglacial CO_2 change : The iron hypothesis., Palaeoceanography, 5, 1-13

Baar H. J. W. de, J. T. M. de Jong, D. C. E. Bakker, B. M. Loescher, U. V. Bathmann and V. Smetacek (1995) Importance of iron for plankton blooms and carbon dioxide drawdown in the Southern Ocean. Nature 373: 412-415.

Smetacek, V., H. J. W. de Baar, ; U.V. Bathmann, K. Lochte, M. M. Rutgers van der Loeff (1997) Ecology and biogeochemistry of the Antarctic Circumpolar Current during austral spring: a summary of Southern Ocean JGOFS cruise ANT X/6 of R.V. *Polarstern*. Deep-Sea Res. II 44, 1-2: 1-21

Turner, D. and N.J.P. Owens (1995) A biogeochemical study in the Bellingshausen Sea: Overview of the STERNA 1992 expedition. Deep-Sea Res. II 42, 907 – 932

2. METEOROLOGISCHE BEDINGUNGEN

F.-U. Dentler (DWD)

Nach dem Auslaufen in Kapstadt am Abend des 25.10.2000 durchquerte POLARSTERN innerhalb weniger Tage mehrere Klimazonen vom subtropischen Hochdruckgürtel südlich Afrikas bis hin zur subpolaren Tiefdruckrinne südlich von etwa 50° Süd. Hoher Luftdruck über dem subtropischen Atlantik erzeugte westlich der Kapprovinz einen starken Südostwind mit Windgeschwindigkeiten bis zu 15 m/s im 10-minütigen Mittel. Nach Passage des „Kap der Guten Hoffnung" ließ der Wind nach und drehte auf nördliche Richtungen. Bis zum 27.10. herrschte überwiegend Strahlungswetter, wobei sich die Lufttemperatur ziemlich konstant bei 14 bis 15°C bewegte (Abb. 2.1).

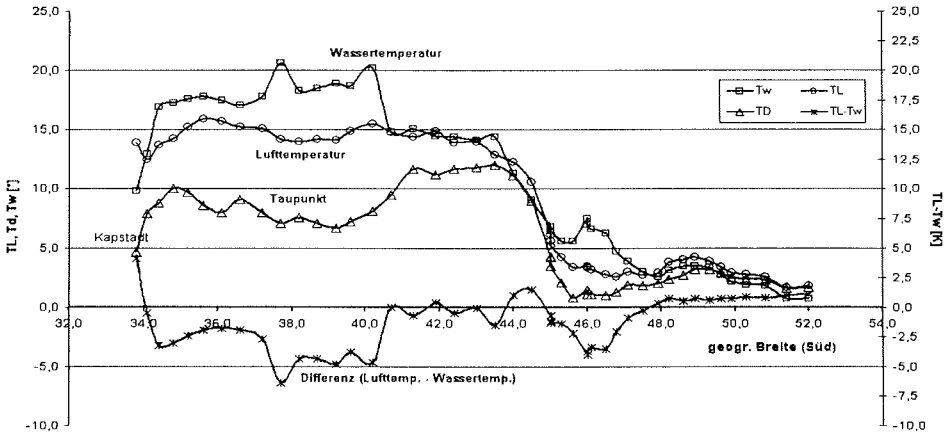

Abb. 2.1: Verlauf von Luft-, Wassertemperatur und Taupunkt während des Transects.

Die Wassertemperatur, die nach dem Auslaufen in Küstennähe von 12 auf 17°C gestiegen war, erreichte am 27.10. bei der Durchquerung des Agulhas-Stromes zeitweise 20°C. Seine südliche Begrenzung war sehr scharf, innerhalb einer Stunde ging die Temperatur von 20°C auf 14°C zurück (Abb. 2.1).
Am 28.10. durchquerten wir bei 45°Süd ein erstes – relativ kleines –Polarfront-Tief. Sowohl vorderseitig mit nördlichen Winden als auch auf seiner Rückseite mit Südwestwinden wurden kurzzeitig 16 m/s (entsprechend 7 Bft.) erreicht. Mit der Winddrehung auf südliche Richtungen setzte starke Kaltluftadvektion ein, sodass die Lufttemperatur rasch zurückging. Auch die Wassertemperatur sank – bedingt durch

den südlichen Kurs – an diesem Tag weitere in Richtung 0 °C (Abb. 1). Die Tagessumme der Globalstrahlung ging von 7,7 [kWh/m^2_] am 27.10. auf unter 3,45 [kWh/m^2_] zurück.
Mit Annäherung einer blockierenden Hochdruckzelle von Nordwesten her erholte sich der Luftdruck rasch wieder und ereichte am 29.10. mit 1034,0 hPa (reduziert auf NN) den höchsten Wert des gesamten Fahrtabschnitts. Diese „Blocking Situation" hielt bis zum Ende des Transects an und ließ einen ziemlich beständigen Wind aus nordwestlichen Richtungen mit 10 bis 12 m/s (Stärke Bft. 6) wehen. Diese antizyklonale Lage erzeugte ein kräftiges Absinken mit Erwärmung und starker Abtrocknung in der mittleren Troposphäre. Es zeigt sich markant im vertikalen Temperatur- und Feuchteprofil vom 31.10. (Abb. 2.2)

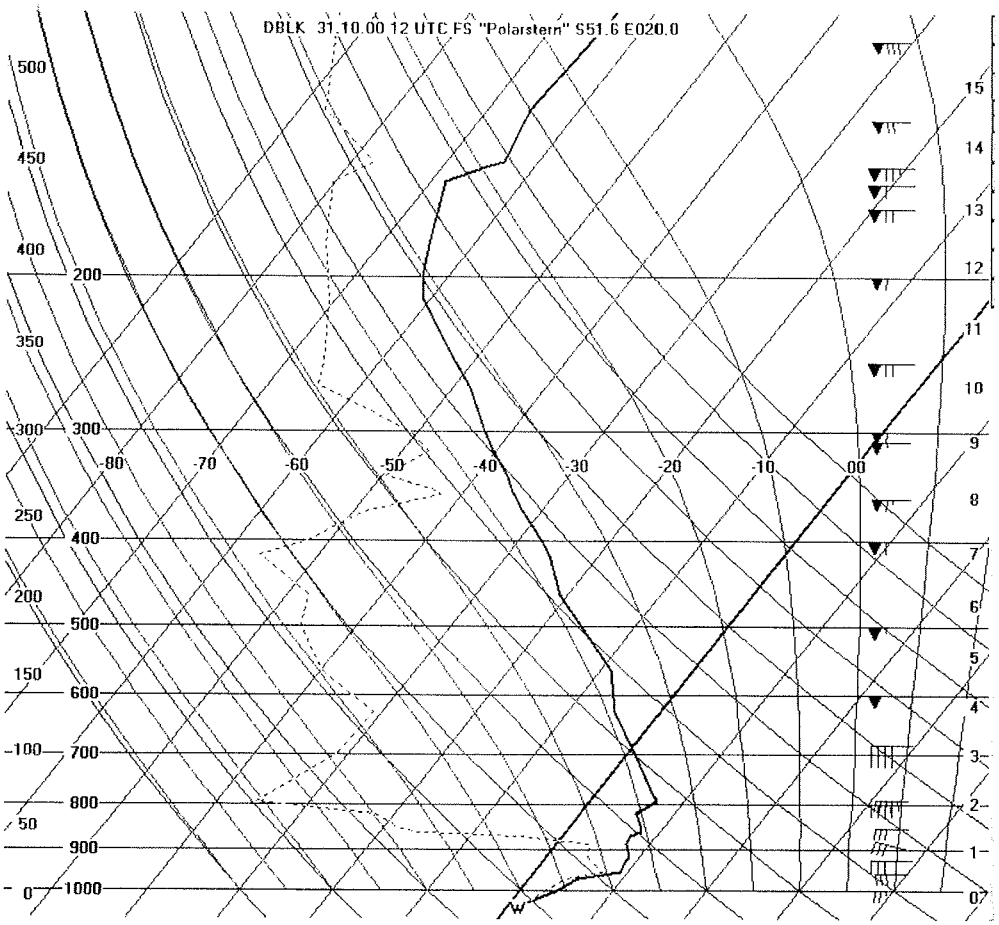

Abb. 2.2: Vertikales Temperatur-, Feuchte- und Windprofil am 31.10. um 12 UTC

Die niedrige Wassertemperatur von 2 bis 3°C hingegen verursachte innerhalb der atmosphärischen Grenzschicht eine starke Inversion, deren Untergrenze trotz starker Winde kaum von der Wasseroberfläche abgehoben wurde. Gleichzeitig wurde innerhalb der stark stabil geschichteten Grundschicht mit den vorherrschend nordwestlichen Winden ständig Feuchte aus niedrigeren Breiten herangeführt. Die Folge dieser Schichtungsverhältnisse war für die subpolare Seegebiete typisch: Hoher Feuchtegehalt der wassernahen Luftschichten mit schlechter Sicht und / oder tiefer Stratus. Da die Bewölkung jedoch relativ dünn war, ließ sie immerhin soviel an Sonneneinstrahlung durch, dass noch Tagessummen von etwa 4 [kWh/m^2_] gemessenen wurden.

Die Hochdruckrandlage setzte sich in den ersten Tagen der eigentlichen Experimentierphase sich zwar fort, es bahnte sich dennoch eine Umstellung in der Atmosphäre an. Die subtropische Hochdruckzone im südlichen Atlantik und Indik zerfiel allmählich in zwei Zellen, südlich Afrikas bildete sich ein Sattelpunkt im Druckfeld. Der Luftdruck fiel langsam aber steig von 1030 auf 1010 hPa. Damit wurde der Weg allmählich frei wurde für Randtiefs, die sich an der fast zonal verlaufenden Polarfront bildeten.

Druckfallgebiete, die in fast regelmäßigen Abständen an der Polarfront entlang zogen, erzeugten einen wellenförmigen Verlauf der Luftdruckkurve. Mehrfach pendelte der Luftdruck zwischen 1000 hPa und 1010 hPa. Verbunden waren die Randtiefs mehrfach mit einer Windzunahme auf 7 Bft., am 5. und 7. auf 8 Windstärken. Die Windrichtung pendelte meistens zwischen Nord und West. Da keine frische polare Kaltluft angezapft wurde, war es auch auf den Rückseiten der Randtiefs meist stark bewölkt, vorderseitig auch häufig neblig. Die Globalstrahlung lag mit 2 bis 4 kWh/m^2_ unter dem Durchschnitt (Abb. 2.3).

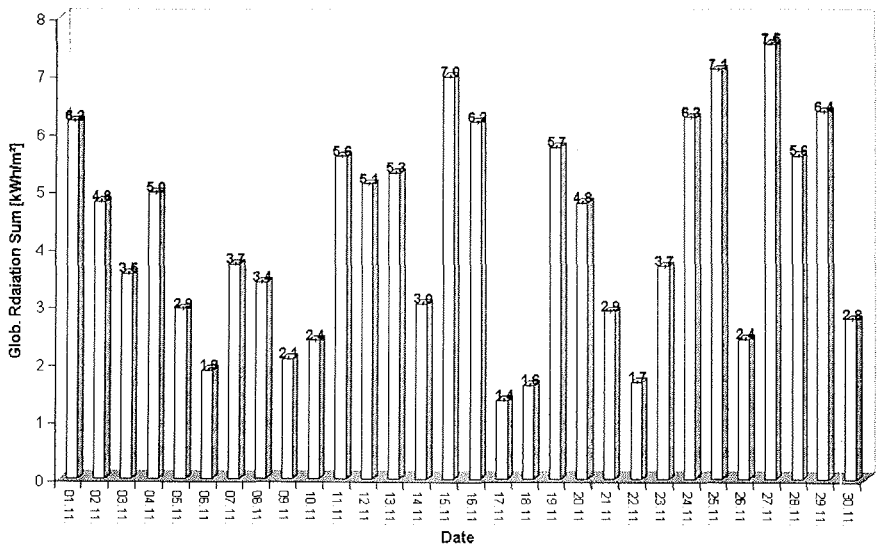

Abb. 2.3: Tägliche Summe der Globalstrahlung v. 01.11. bis 30.11.2000

Angeregt durch eine Sturmtiefentwicklung stromauf bei Gough-Island vertiefte sich am 12.11. eine bereits am Vortage bei Bouvet-Island entstandene Zyklone. Trotz nur mäßigen Druckfalls baute sich ein starker Luftdruckgradient zwischen der Schiffsposition und dem Kern, der zur Zeit des stärksten Sturmes etwa 600 NM südlich unserer Position lag, auf. Im Laufe der Nacht (12./13.11.) erreichte die Windgeschwindigkeiten im 10-Minuten-Mittel Windstärke 10 Bft (25m/s). Die hohen Windgeschwindigkeiten führten zu einem starken Anwachsen der bis dahin nur vorhandenen Deckschicht im Ozean.
In der darauffolgenden Nacht (13./14.11.) zog das bereits erwähnte Sturmtief von Gough-Island heran und ließ erneut die Windgeschwindigkeit auf Sturmstärke anwachsen; allerdings blieb die Maximalgeschwindigkeit um 5 m/s unter der des Vortages.
Auf der Rückseite dieser mittlerweile zum Orkanwirbel vertieften Zyklone stieg der Luftdruck in unserem Fahrtgebiet an und erreichte am 15.11. um 21 Uhr abends wieder die 1030-hPa-Marke. Allerdings fiel der Luftdruck danach genauso rasch wie er angestiegen war. 24 Stunden später betrug er nur noch etwa 1000 hPa. Dennoch gehören der 15. und der 16.11. zu den sonnscheinreichsten Tagen der Reise mit einer Globalstrahlungssumme von 7,0 kWh/m^2, bzw. 6,2 kWh/m^2 (Abb. 2.3).

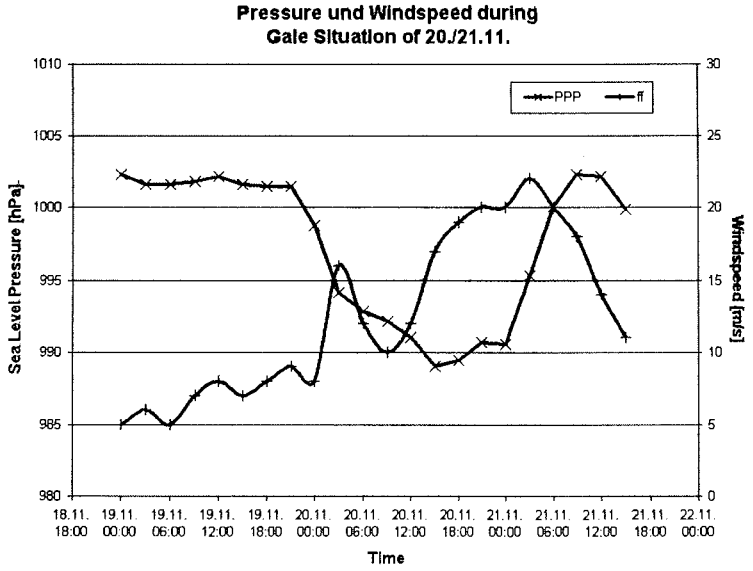

Abb. 2.4: Sturmwetterlage vom 20./21.11.2000

In der 5. Fahrtwoche (20. – 26.11.) häuften sich die Sturmereignisse. Mehrmals lag das Fahrtgebiet im Entstehungsgebiet kleiner sich explosionsartig vertiefenden Randtiefs, deren Kerne in der Regel knapp südlich vorbeizogen und dabei stürmische Winde zwischen Nordwest und Südwest erzeugten (Abb. 2.4). Da auf der Rückseite dieser Zyklonen Kaltluft nordostwärts vordrang, stellte sich ein Wechsel zwischen aufgelockerter und stärkerer Bewölkung ein. Dadurch nahm die Globalstrahlung zu. Sie erreichte am 27.11. mit 7,5 kWh/m_ den höchsten Wert der Reise. Einbrüche bei der Sichtweite gab es nur noch stundenweise auf der Vorderseite von Kaltfronten.
Die Rückreise führte uns noch einmal durch die Frontalzone. Starke, am 1.12. sogar stürmische westliche Winde und schlechte Sicht begleiteten den langsamen aber stetigen Temperaturanstieg von 3°C in der subantarktischen Kaltluft auf 15 °C bei 40°Süd. Erst südlich von 40°Süd flaute der Westwind ab.

Zusammenfassung
Während der Zeit vom 01.11.bis 30.11.2000 betrug die mittlere Windgeschwindigkeit 9,9 m/s, die Standardabweichung 4.9 m/s. An 55 von 696 stündlichen Wetterbeobachtungsterminen wurde eine mittlere Windgeschwindigkeit von mindestens 17 m/s (8 Bft. und mehr) gemessen. Dies entspricht etwa 8%. Die im „Marine Climatic Atlas of The World" (MCAW) der US-Navy publizierte

Überschreitungshäufigkeit Wert für 16 m/s liegt dagegen bei etwa 27%. Die Summenhäufigkeitsverteilung der Windgeschwindigkeit im Untersuchungsgebiet zeigt Abb. 2.5.
Die mittlere Luft- und Wassertemperatur betrug im Monat November 3,7°C bei einer Standardabweichung von nur 1,2 K (Luft), bzw. 0,5 K (Wasser), der mittlere Luftdruck 1007,3 hPa bei einer Standard-Abweichung von 10,7 hPa.

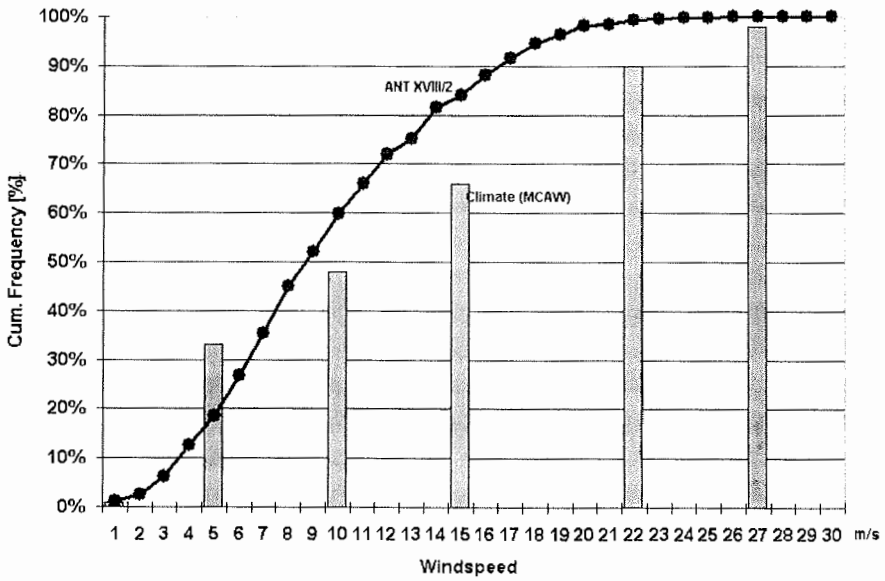

Abb. 2.5: Häufigkeitsverteilung der Windgeschwindigkeit v. 28.10. – 29.11.2000

3. SEAWIFS – DATA

A.Davidov (IfM,Kiel)

The method of ocean colour satellite remote sensing easily enables simultaneous observation of phytoplankton distribution over wide areas. It is very convenient for investigating the hypothesis of iron limitation in the "high nutrients, low chlorophyll" zone of the Southern Ocean and hence for comparing dynamics of phytoplankton growth within and outside the "Fe-fertilised" patch. The SeaSpace satellite receiving station on board the RV "Polarstern" was used for continuous recording of high

resolution, directly transmitted images from SeaWiFS (Sea-viewing Wide Field-of-view Sensor) placed on the Orbview-2 satellite. The decryption of the data requires a decryption device (SeaStar Ground Processor from NASA) and a SeaWiFS real-time license (with the encryption key changed every 14 days). This license was obtained by Dr. Gerhard Dieckmann, AWI for the duration of the Eisenex I experiment.
During the first week of the cruise there were difficulties with the alignment of the satellite dish. After the problems were resolved with the help of W. Dimmler, between 1 and 3 "good" (with respect to satellite elevation and the ship position and orientation) scans of the investigation area were received every day (Table 3.1).
The main limitation of the method is due to the fact, that optical "passive" sensors cannot "see" through clouds. Unfortunately the weather conditions for the duration of the cruise were unfavourable especially with respect to cloud-cover. This made regular monitoring of phytoplankton from satellite almost impossible. The problem was enhanced as the satellite passed over the investigation area for a few seconds only in the mornings within a period of 2 hours, further restricting the probability of obtaining reasonable data.
Most images were processed onboard the research vessel and chlorophyll concentration of the surface layer was calculated. Another difficulty arose due to the lack of sufficient *in situ* biochemical data for this part of the Southern Ocean. As a result of this, the validity of bio-optical algorithms in the investigation area had not been tested up to the time of the experiment. The comparison of 3 different algorithms (OC2, OC4 and NDPI) implemented in SeaDAS (SeaWiFS Data Analysis Software) showed no significant differences in the values of chlorophyll (Figure 3.1), therefore OC2 only (O'Reilly et al. 2000) was used for the onboard calculation. The processing of the SeaWiFS images included importing the data into SeaDAS-HDF file format, applying radiometric and atmospheric correction to the raw data as well as calculating the surface chlorophyll concentration with a bio-optical algorithm. The Level 1A, Level 2 and Level 3 (Figure 3.2) SeaWiFS products were generated as well and the data were visualised and analysed under SeaDAS. Additionally, the raw passes, Level 0 and Level 1A files were stored on DAT tapes for future re-processing in AWI (A. Belem) and re-calculation of chlorophyll in the surface layer using bio-optical algorithms including real-time climatological data and *in situ* chlorophyll measurements taken during the cruise.
Data from NOAA (Polar Orbiting Environmental Satellite) weather satellites were recorded with the TeraScan receiving station. The images from AVHRR (Advanced Very High Resolution Radiometer, obtaining measurements of visible, near infrared, and infrared spectrum) were extracted and stored on tapes.
Another instrument carried onboard of the NOAA satellites, ARGOS–DCS (Data Collection System), was used to get the GPS position of buoys drifting with the iron-enriched patch.

No	Julian Day	Date	Time GMT	Scan-lines
1.	293	19. Oct 00	11:14:02	
2.	294	20. Oct 00	11:59:15	
3.	295	21. Oct 00	11:02:01	
4.	296	22. Oct 00	10:09:29	
5.	296	22. Oct 00	11:45:59	
6.	297	23. Oct 00	10:50:19	3778
7.	298	24. Oct 00	11:36:56	1124
8.	299	25. Oct 00	10:42:29	1376
9.	301	27. Oct 00	10:34:43	1635
10.	303	29. Oct 00	10:20:39	3058
11.	304	30. Oct 00	09:29:45	2186
12.	305	31. Oct 00	08:37:37	Bad
13.	305	31. Oct 00	10:13:46	Bad
14.	306	1. Nov 00	09:12:45	Bad
15.	306	1. Nov 00	10:56:37	1788
16.	307	2. Nov 00	11:38:24	Bad
17.	308	3. Nov 00	09:00:34	3781
18.	308	3. Nov 00	10:42:25	2348
19.	309	4. Nov 00	09:42:39	4156
20.	309	4. Nov 00	11:22:17	3276
21.	310	5. Nov 00	08:48:39	3616
22.	310	5. Nov 00	10:25:33	2909
23.	311	6. Nov 00	09:30:59	4056
24.	311	6. Nov 00	11:09:32	3026
25.	312	7. Nov 00	08:37:20	2873
26.	312	7. Nov 00	10:13:29	3947
27.	313	8. Nov 00	09:20:59	3030
28.	313	8. Nov 00	10:57:07	3822
29.	314	9. Nov 00	08:26:38	2888
30.	314	9. Nov 00	10:01:21	3612
31.	315	10. Nov 00	09:07:10	4003
32.	315	10. Nov 00	10:45:01	3262
33.	316	11. Nov 00	08:14:14	2943
34.	316	11. Nov 00	09:49:15	3926
35.	316	11. Nov 00	11:29:24	2482
36.	317	12. Nov 00	08:55:34	3678
37.	317	12. Nov 00	10:32:24	4157
38.	318	13. Nov 00	08:03:04	2025
39.	318	13. Nov 00	09:37:25	3690
40.	318	13. Nov 00	11:16:55	3176
41.	319	14. Nov 00	08:43:54	3526
42.	319	14. Nov 00	10:20:24	4049
43.	320	15. Nov 00	11:04:24	3383
44.	321	16. Nov 00	08:32:05	2504
45.	321	16. Nov 00	10:08:24	2932
46.	324	19. Nov 00	09:01:54	3436
47.	324	19. Nov 00	10:39:24	3840
48.	325	20. Nov 00	08:09:25	2019
49.	325	20. Nov 00	09:44:25	3914
50.	325	20. Nov 00	11:24:04	2774
51.	326	21. Nov 00	08:50:25	2906
52.	326	21. Nov 00	10:27:25	4277
53.	327	22. Nov 00	09:32:15	4210
54.	327	22. Nov 00	11:11:15	2880
55.	328	23. Nov 00	08:38:44	2752
56.	328	23. Nov 00	10:15:05	4130
57.	329	24. Nov 00	09:20:34	3924
58.	329	24. Nov 00	10:58:54	3782
59.	330	25. Nov 00	08:27:15	3226
60.	330	25. Nov 00	10:03:04	3618
61.	331	26. Nov 00	09:08:45	2913
62.	331	26. Nov 00	10:46:25	2897
63.	332	27. Nov 00	08:15:34	2324
64.	332	27. Nov 00	09:50:54	4254
65.	332	27. Nov 00	11:31:14	2866

Table 3.1. The SeaWiFS images recorded onboard the RV "Polarstern" during the ANTXVIII-2 expedition (25.10 - 3.12.2000)

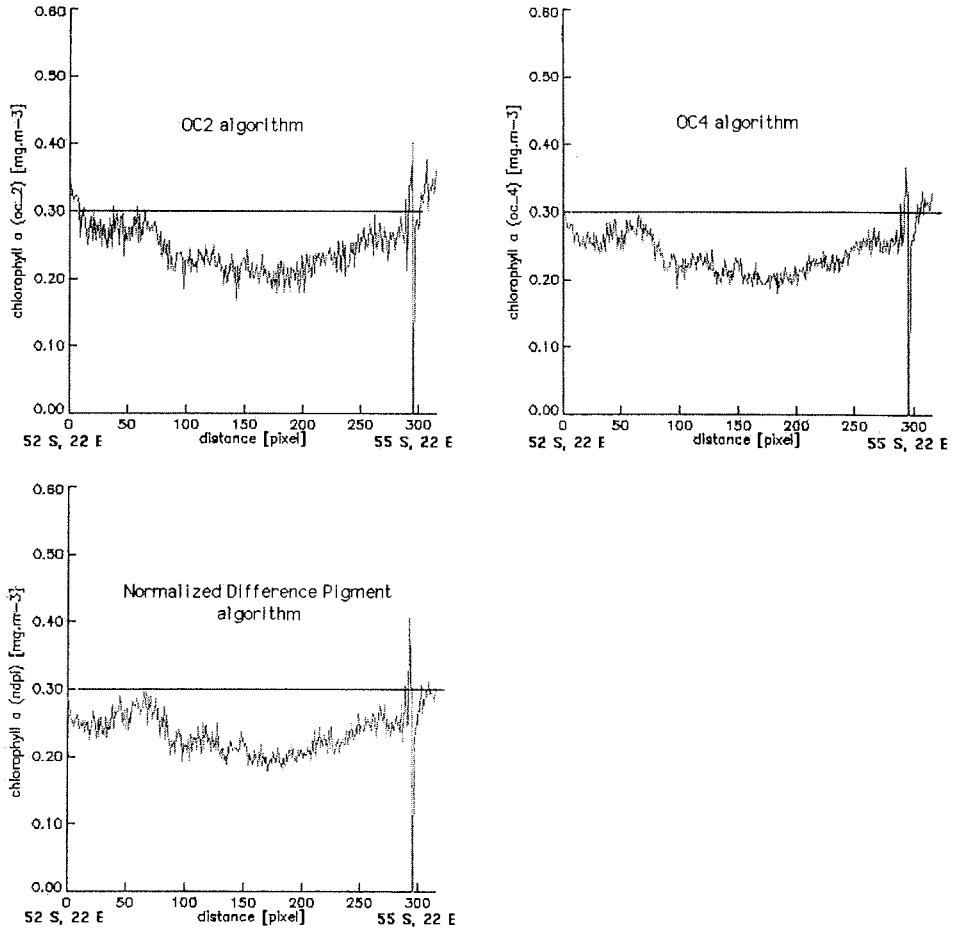

Figure 3.1. Chlorophyll values of the surface layer of the test area in the Southern Ocean calculated from 3 different bio-optical algorithms.

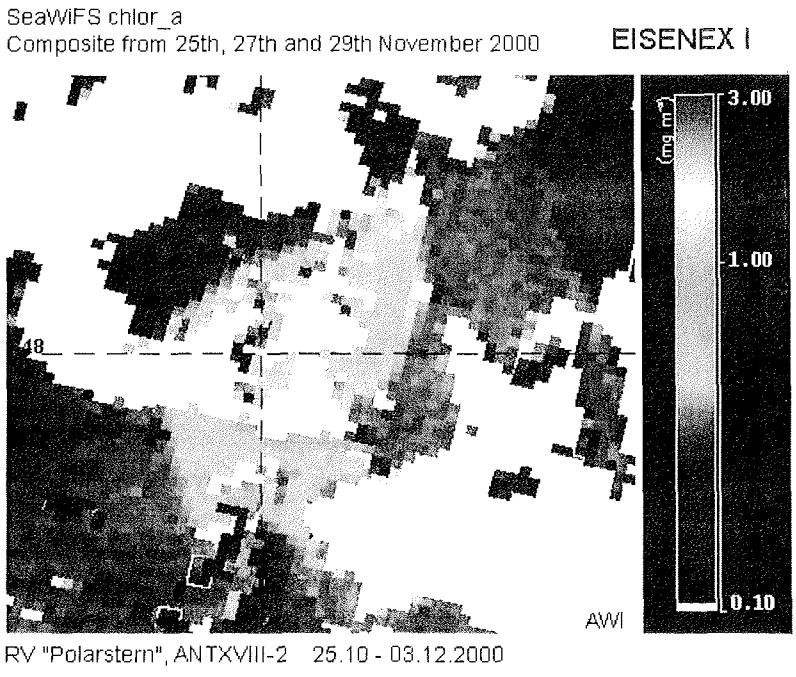

Figure 3.2. The iron "fertilised" patch at the end of the experiment viewed from SeaWiFS.

4. SF_6 MEASUREMENTS ON EISENEX

A. Watson, M.-J. Messias, L. Goldson (UEA), I. Skjelvan (UIB),
P. Nightingale, M. Liddicoat (PML)

Objectives

The aims of the SF_6 measurement effort during Eisenex were:

1) To provide a framework for the iron release experiment by the release of SF_6 tracer simultaneous with the initial iron release. The tracer could then be used to re-locate the region of water that was influenced by added iron.
2) To enable us to quantify the rates of dilution and spreading affecting the mixed layer water in both the horizontal and the vertical directions. It is hoped to be able to quantify rates of horizontal dispersion in the eddy, and mixing into the top of the seasonal thermocline. These measurements should be able to be related tothe physical processes forcing vertical mixing.

3) To perform a "dual tracer" air-sea gas exchange experiment, in llaboration with Oliver Huhn (U. Bremen) who was responsible for addition of 3-He to the initial release, and subsequent sampling for this isotope. This was the first dual tracer measurement to be carried out in Antarctic waters, and the most comprehensively sampled open-ocean experiment.

Methods:

Release: Prior to the first iron release, two tanks of seawater each containing approximately 2 m^3 of water were saturated with gaseous SF_6. The procedure was similar to that described in Upstill-Goddard et al., 1991. The tracer-saturated water was then mixed into the iron-containing water in a constant ratio during the release period. Aprroximately 60g of SF_6 was released during the ~15 hours of the initial release period. In the event, only one of the saturated tanks was used.

Measurements: Discrete SF_6 samples were sub-sampled into 500ml glass stoppered bottles from the sampling rosette. These were analysed for SF_6 using gas chrmotography with an electron capture detector, by the method of Law et al., 1994. A typical detection limit for the method is 5×10^{-17} M In practice, the background due to industrial release of SF_6 into the atmosphere, followed by dilution into surface waters, is readily detectable in surface water at about 1.5 fM ($1fM=10^{-15}M$) and variations on this background set a practical detection limit somewhat above the instrumental limit. Precisions for the analysis are typically better than 1% or 0.03 fMol, whichever is greater. Measurements were calibrated against gaseous standards prepared by Plymouth Marine Laboratory and calibrated against other groups doing SF_6 analysis; we believe the accuracy to be better than 5%.

Measurements of the concentration in pumped surface water were also made "underway", that is semi-continuously with measurements being reported each three minutes. These data are of lower absolute accuracy and precision than the discrete measurements from hydrocasts, but are of great value in navigating the ship into the patch of released iron and tracer, and in obtaining horizontal dispersion. The method also uses an electron-capture GC technique, and is described in Upstill-Goddard (1991).

Results

About 2000 samples were run on the discrete systems, and more than a hundred hours of continuous underway results were recorded. Here we give some initial and preliminary features of the data.

Figure 4.1 shows all the discrete samples up to cast 90, on a logarithmic scale. THe background shows up as the region near 1-2 fM that is well-populated with samples. The upper envelope gives a broad idea of the dilution of the patch maximum values. A notable feature is the amount of the dilution over the three weeks of the experiment shown here, which exceeds two orders of magnitude. This is mostly due to the very rapid horizontal spread of the tracer, consequent on the many storms we experieinced, especially in conjunction with the poorly mixed upper layer that we observed in the first part of the experiment. Gas exchange with the atmosphere may have contributed a factor of up to three decrease, while deepening of the mixed layer may have contributed another 50%. Horizontal dispersion seems to have been occuring at a rate sufficient to double the size of the patch every four or 5 days on average. This should be compared with the "SOIREE" experiment, where the patch doubled only once in a period of about 13 days.

Figure 4.2 shows approximate shapes and sizes of the patch, derived from the continuous measurements, on five surveys. The outlines of these patches are superimposed in lat, long co-ordinates in figure 3. During the initial phase of comparatively calm weather, the patch was ~5nmi in linear dimension. It increased explosively during the period 12-15 November, and again by the 21 November. There is evidence that the patch by that time had increased to occupy a sizeable proportion of the eddy that it was embedded in, and was being distorted and rotated by the non-uniform velocities in the eddy during the latter part of the experiment.

Work is now ongoing to derived quantitative mixing and dispersion from the very large data set collected during the experiment.

References

Law, C. S., Watson, A. J. & Liddicoat, M. I. Automated Vacuum Analysis Of Sulfur-Hexafluoride In Seawater - Derivation Of the Atmospheric Trend (1970-1993) and Potential As a Transient Tracer. *Marine Chemistry* **48**, 57-69 (1994).

Upstill-Goddard, R. C., Watson, A. J., Wood, J. & Liddicoat, M. I. Sulfur-Hexafluoride and He-3 As Sea-Water Tracers - Deployment Techniques and Continuous Underway Analysis For Sulfur-Hexafluoride. *Analytica Chimica Acta* **249**, 555-562 (1991).

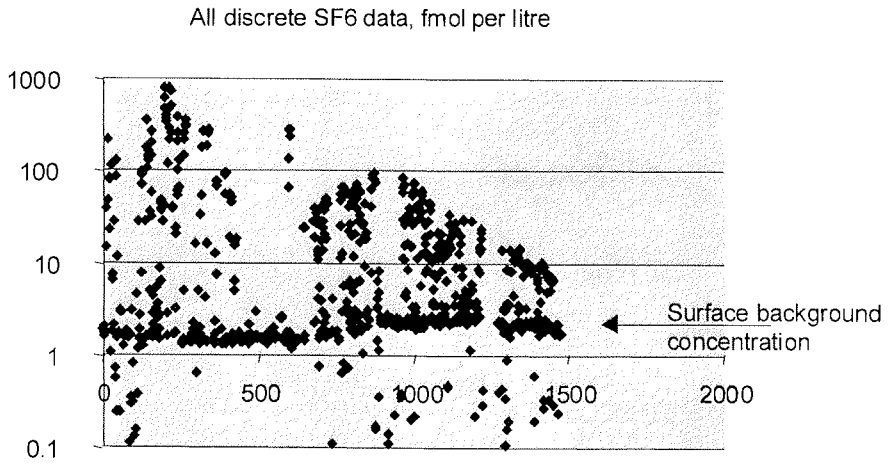

Figure 4.1: All SF_6 discrete data. The x-axis is the analysis number sequentially with time. The y axis is fmol per litre -- note the logarithmic scale. TH eupper envelope shows the decline with time of the maximum concentrations in the patch.

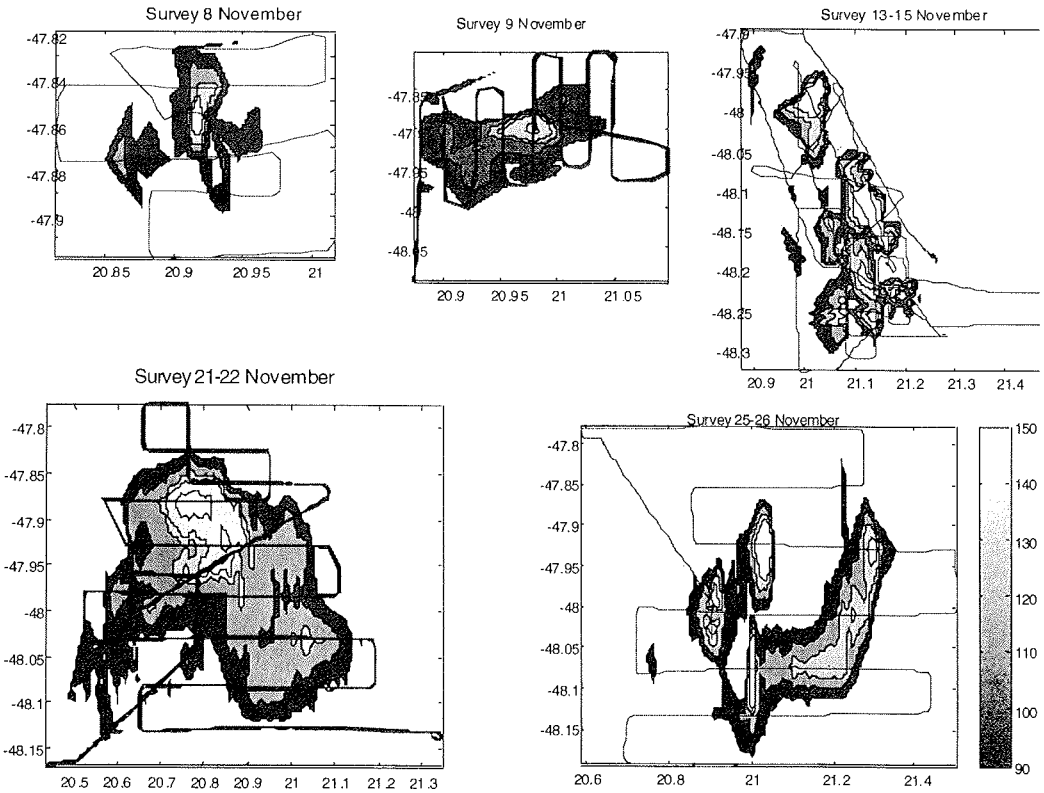

Figure 4.2: The SF_6 patch, from repeated surveys of the patch. SF_6 units are arbritrary.

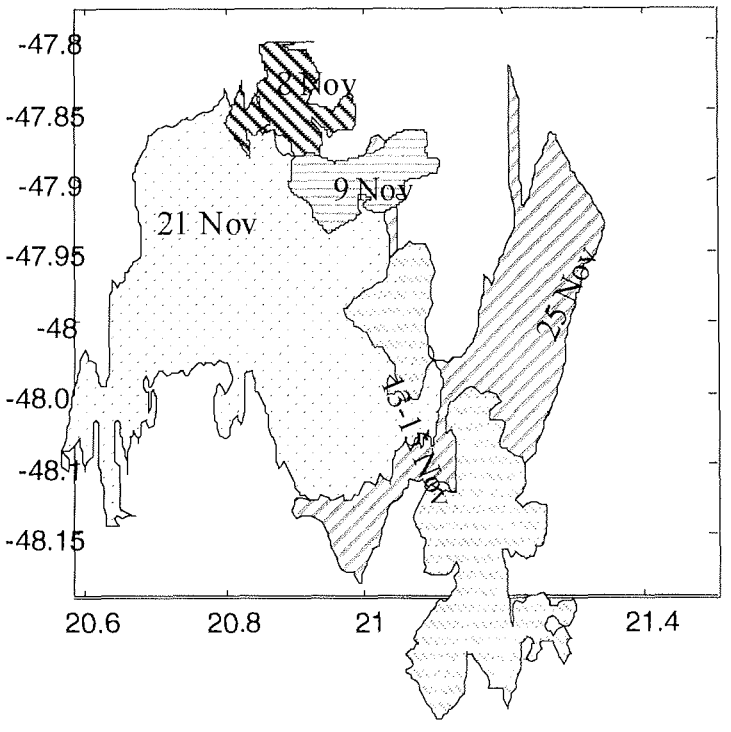

Figure 4.3: Outlines of the patches shown in Fig 2, superimposed and shown in actual latitude and longitude..

5 .HELIUM (3HE) MESSUNG

O. Huhn, Universität Bremen, Institut für Umweltphysik (IUP) - Ozeanographie

Zusätzlich zu Eisen und SF6 wurden bei der ersten Düngung ca. 4 Liter Helium (reines 3He) mit in die Deckschicht eingebracht. Helium ist leichter flüchtig als SF6, und beide Spurengase zusammen liefern Informationen über die Gasaustausch-Raten zwischen Ozean und Atmosphäre unter realen Bedingungen (realistische Windgeschwindigkeiten bis Sturm, Wellen, Blaseneinschlag) sowie eine obere Randbedingung für die Patches. Insgesamt wurden 415 Helium-Proben auf 52 Stationen zwischen Oberfläche und 100 Meter genommen, 144 Proben in Kupferrohren, an beiden Enden luftdicht zusammen-gequetscht, und 271 Proben in vorher evakuierten und nach dem Befüllen zugeschmolzenen Glasampullen. Alle Proben werden nach Bremen transportiert und dort mit dem Massenspektrometer gemessen.

Helium (3He) Measurment

O. Huhn, University of Bremen, Institute of Environmental Physics (IUP) - Oceanography

Additional to iron and SF6, a volume of approx. 4 litres of Helium (pure 3He) was released into the surface layer with the first fertilisation. Helium is a more volatile gas than SF6, thus both trace gases provide information concerning the gas exchange between ocean and atmosphere under field conditions (different wind speeds up to storm, waves, bubbles) and a surface constrain for the fertilised patch.

All together there were taken 415 Helium samples on 52 stations between the surface and 100 meters, 144 samples in copper tubes, both ends squeezed to avoid air contamination, and 271 samples in previously evacuated glass ampulles, flame sealed after sampling. All samples are taken to Bremen to be analysed with the mass spectrometer.

6. THE CO_2 SYSTEM AND DISSOLVED O2 IN CONTEXT OF RKR PROPORTIONS

H. de Baar, Y. Bozec (NIOZ), D. Bakker (UEA)

6.1 Total carbon dioxide (TCO2)

Y. Bozec, D. Bakker

Carbon dioxide (CO_2) behaves differently from other atmospheric gasses, such as O_2 and N_2. The dissolution of CO_2 in water results at first instance in dissolved CO_2 ($CO_{2,aqueous.}$), of which hydrolysis generates the unstable carbonic acid (H_2CO_3) as intermediate. This in turn dissociates further into bicarbonate (HCO_3^-) and a proton (H^+) and finally to carbonate (CO_3^{2-}) and another proton (H^+). The dissociation constants are functions of temperature, salinity and pressure but are now known very accurately. The summation of the concentrations of carbonate, bicarbonate, dissolved CO_2 (and the very small amount of carbonic acid) is called dissolved inorganic carbon (DIC):

$$DIC = [CO_{2,aqueous}] + [HCO_3^-] + [CO_3^{2-}] \quad (0)$$

whereof $[CO_{2,aqueous}]$ per definition includes the contribution of the unstable $[H_2CO_3]$.

DIC has been determined by the coulometric method of Johnson et al. (1993). The principle of coulometry relies on Faraday's law according to which 96485 Coulombs (C) correspond to 1mol of a chemical substance which electrical charge will be change by one unit. The corresponding *Faraday's constant* is the natural constant, *F*=96485C/mol. With other words, the amount of electricity (Coulombs) needed to change the electrical state of 1mol of a chemical species by one charge unit is 96485C. Thus, during a known electrochemical reaction the measurement of Coulombs during the reaction enable the determination of the concentration of the reacting chemical substance.

Material and Methods

An automated extraction line takes volumetrically a very accurate subsample which is acidified with 8.5% phosphoric acid (H_3PO_4). Due to this decrease in pH all HCO_3^-- and CO_3^{2-}- ions will be converted to $CO_{2,aqueous}$. The sample is stripped using ultra-pure nitrogen gas and the carrier gas is led into the titration cell. This cell contains a solution of Dimethylsulfoxide (DMSO), ethanolamine and a colourimetric indicator thymolphtalein. The irreversible reaction of the CO_2 gas with the ethanolamine generates the hydroxyethylcarbamic acid (1) which in turn gives a colour change of the (dark blue) indicator. The fading of the colour is detected photometrically. During the electrochemical tritation the hydroxyethylcarbamic acid is neutralised by OH^- ions (2-4). From start to end of the titration the current (*I*) is integrated over the time - that is the Coulombs required to destroy the acid - will be measured. The application of Faraday's law (Coulombs = Ampère*s = $6.0 * 10^{23}$ electrons) gives us the number of CO_2 molecules titrated, i.e. the concentration of DIC.

In equations:

$$CO_2 + HO(CH_2)_2NH_2 \rightarrow HO(CH_2)_2NHCOOH \quad (1)$$

$$2Ag^0 \rightarrow 2Ag^+ + 2e^- \quad (2)$$

$$2H_2O + 2e^- \rightarrow H_2(\uparrow) + 2OH^- \quad (3)$$

$$OH^- + HO(CH_2)_2NHCOOH \rightarrow H_2O + HO(CH_2)_2NHCOO^- \quad (4)$$

The coulometer exists of the following parts:
Extractor unit
Coulometer
PC + interface boards for data acquisition and processing
A high precision NTC thermistor measures the temperature of the sample in the pipette. Thus correction for thermal expansion of the boro-silicate pipette could be applied.

Samples were collected form the CTD Rosette bottle casts as well as in an underway mode from the ships pumping seawater lines. As a reulst two datasets were obtained, one for discrete samples along vertical profiles at the IN and oUT stations, and another semi-continuously throughou the cruise collected from the ships inlet at about 10 metres depth in the water column. The discrete samples were largely coordinated with sampling by the UEA group (Dorothee Bakker) for pCO2. Similar coordination was also done for the semi-continuous underway sampling where moreover comparison with the underway pH observations (Univ.Bergen) is intended.

Johnson, K.M., Wills, K.D., Butler, D.B., Johnson, W.K., and Wong, C.S., 1993. Coulometric total carbon dioxide analysis for marine studies: maximizing the performance of an automated gas extraction system and coulometric detector. *Marine Chemistry*, **44**, 167-187.

Results.
- For the first four or five IN patch stations after the release, it is difficult to observe a decrease in the TCO_2 concentrations. In fact, several storms had mixed the surface layer during this time. As a consequence the values stayed arround 2130 umol/kg inside and outside the patch during this 5 first days of the experiment. However it seems that the first decrease we can observe, happened at station 46: compared to the Out station 42, some 3 umol/kg had been lost within the upper 20 meters of the water column. The chlorophyll were also at maximum in this first 20 meters at this station.
- On the station 46 INside the patch, we saw a decrease of 7umol/kg compare to the OUT station 48 and the mixed layer was roughly 50 meters.
- On the other hand during the two grids we made, we observed that the OUT station also showed a decrease compared to the first three OUT station we did before. Maybe, those OUT stations during the grid were not really "out" of the patch but rather "on the edge", . On the other hand this can be due to a "normal spring bloom" outside of the patch.

- After the grid 2, we made the IN station 88 and the OUT station 90. Both these stations were after a big storm and we observed a decrease of 8 umol/kg in the 80 meters of the mixed layer. This means that the decrease could be bigger if the mixed layer were still 30 meters.

- The last IN patch station 103 was the station with the highest chloropyll values of the cruise. For TCO_2, we observed a decrease of 12-13 umol/kg in the first 80 meters with a minimum value of 2115 umol/kg at 40 meters for this atation.
- The results from the two final stations (107 IN et 108 OUT) will be process later.
However, to summarize, we can say that at the begining of the experiment, the values inside and outside the patch were roughly the same that is to say 2130 umol/kg (a little bit lower in the patch even before the release). On the other hand at the end of the experiment we found the lowest value of 2114,8 umol/kg in the patch and a value of 2127,6 umol/kg outside of the patch. That means a decrease of 12-13 umol/kg almost at the end of the experiment.

6.2 Dissolved oxygen

H. de Baar

The observed decreases of dissolved TCO_2 and nutrients within the iron-enriched patch should be accompanied by similar increases of dissolved O2 in accordance with the overall stoichiometry of net growth of phytoplankton:

$106\ CO_2 + 122\ H_2O + 16\ NO_3^- + H_2PO^{4-} + 3H^+ = [(CH_2O)_{106}(NH_3)_{16}H3PO_4]_{organic} + 138\ O_2$

in accordance with Redfield, Ketchum and Richards (1963). However large deivations form the RKR proportions have been observed ans were expected for Antarctic diatoms growing under suboptimal conditions of Fe supply (de Baar et al., 1997).

Methods.
Dissolved oxygen was determined with the direct spectrophotometric technique of Pai et al. (1993) with various modifications after G. Kraay (NIOZ). Discrete samples were collected in triplicate from the CTD / Rosette hydrocasts into 100 ml nominal volume glass stoppered bottles, ensuring replacement of about three bottle volumes with slowly inflowing seawater while avoiding bubble formation. Directly upon collection these bottles were

closed with their respective stoppers. Then in the laboratory the reagents manganese chloride and alkaline iodide were added in that order by means of dispensers, ensruningd elivery of the reagnet sin the lower part of the filled bottle. Upon firmly closing the bottles wer shaken as to ensure adequate reaction contact for the formation of the precipitate. Once having processed all sample bottles from one hydrocast, each bottle was genty shaken once again and then immersed in a bath of fresh water at room temperature, ensuring that the whole stoppered bottle was well submerged. Upon 6 to 18 hours of such storage the sample bottles were at room temperature thus avoiding bubble formation and outgassing during further handling. Bottles were taken out the bath and rinsed dry at the outside. Next for each bottle the third reagent sulphuric acid was added, as well as a magnetic stir bar. Upon gentle stirring for about 2 minutes the precipitate had been fully dissolved and the absorbance of the tri-iodide complex (I_3-) detected at wavelength 456 nm in a 1.0 cm flow through cuvette mounted in the light beam of a spectrophotometer. Reproducibility between triplicate samples was excellent at about 0.1-0.2 micromoles per liter.

Calibration was done by first producing a suite of blanco bottles. Filled 100 ml bottles were treated with the reagents in the reverse order. First only the sulphuric acid and the iodate reagent were added and the bottle closed and shaken vigourously. Next the mangensium chloride reagnet was added as well and the bottle closed again. A series of 6-8 bottles was then stored under water until use for the calibration. The potassium iodate standard solution was made up from Titrosol ampoule with cocnetrated potassium iodate being diluted into a 1000 ml volumetric flask. The stock solution was then transferred into two 500 ml galss stopperd gas tight water bottles, one for the calibrations done on shipboard, another one for control calibrations afterwards in the home laboratory. For each calibration line aliquots of 500, 1000, 1500, 2000 and 2500 microliters were transfeered into a balnco sewater bottle by using two gravimetrically calibrated Eppendorf pipettes. The ensuing calibration lines of voltage readout versus oxygen equivalents always had a goodness of linear fitting of r^2=1.000 for 6-8 datapoints along the line. Throughout the cruise some 10 calibration lines were performed. Due to an accidental shock to the spectrophotometer at the begin of the cruise this many calibrations had to be performed on shipboard, while further calibrations in the home laboratory will have to be performed afterwards as to ensure stable performance of the spectrophotometer. Therefore the data thus far is only preliminary.

Results.
The above chemical analyses were intended to serve mostly towards calibration of the oxygen electrode sensors on both the CTD/Rosette and the Sanfish towed instrument. Unfortunately it was not until after several weeks in the cruise that it was possible to mount these sensors which subsequently both broke down in irrepareable manner. By doing many chemical analyses this loss was only partly compensated. Hence the overall data coverage is still modest affecting significance of the intended derivation of deviations from the above RKR stoichiometry.

At the various IN stations there was a gradual increase observed of dissolved O_2 as compared to the OUT stations. At the end of the cruise this increase amounted to about 10 micromoles/kg seawater and this appears to be a nice mirro image of the above reported decreases of total dissolved CO_2, in keeping with RKR stoichiometry. Comparision with similar trends for the dissolved nutrients, notably nitrate and phosphate will be done afterwards in collaboration with the colleagues of the AWI nutrients team (for nutrients see elsewhere in this cruise report).

Pai, Su-Cheng, Gong, Gwo-Ching and Liu, Kon-Kee (1993) Determination of dissolved oxygen in seawater by direct spectrophotometry of total iodine. Marine Chemistry, 41, 343-351.

7. UNDERWAY SEAWATER PH AND *IN SITU* PCO2 MEASUREMENTS

Richard Bellerby and Solveig Kringstad (University of Bergen)

1. Objectives

The objectives of the study were 1) to determine the CO_2-system characteristics of the surface waters during the iron addition experiment through in situ pCO_2 measurements from a drifting buoy and on-line, continuous seawater pH measurements from the ship's seawater supply and 2) to provide real time in-situ measurements of pCO_2 in a diatom culture.

2. Work at Sea

Seawater pH

The pH of seawater was measured from samples automatically drawn from the ship's continuous laboratory supply through a flow injection manifold coupled to a fibre optic array. The method of determination was the dual spectrophotometric analysis of the seawater after the addition of a sulfonephthalein indicator. The background absorption spectrum of natural seawater was taken and an aliquot of thymol blue was injected into a seawater sample enclosed in a flowcell. After the solution was fully mixed, spectral scans were taken along with solution temperature. The pH (on the total hydrogen ion scale) was estimated from the change in absorption between blank and sample runs. The frequency of determination was 25 samples per hour which resulted in excess of 15,000 measurements throughout the cruise. The pH perturbation of the seawater sample through addition of the indicator will be determined at a later date although it rarely exceeds 0.01 pH units. Daily during the expedition, standard addition experiments were performed to ascertain the pH perturbation.

In situ pCO2

Seawater pCO_2 was measured *in situ* both in the surface ocean and within shipboard diatom culture experiments. The SAMI-CO_2 method was employed which measured the absorption spectrum of a bromothymol blue after CO_2 equilibration across a silicon membrane. The accuracy and precision of the instruments is 1 _atm and the measurement frequency was set to $48.d^{-1}$ and $96.d^{-1}$ for the ocean and culture instruments, respectively.

3. Preliminary results

Seawater pH

Surface pH between JD 300 and 311 are shown in Figure 1. The pH has been estimated from a salinity of 34 and normalized to a sea surface temperature of 10°C. Whilst no detailed examination of the data can be performed before the underway hydrographic data has been corrected, it can still be seen from Figure 1 that the underway precision of the pH method is better than 0.001 pH units. At constant alkalinity this precision equates to less than 1 _atm fCO_2 under *in situ* conditions.

The data will be used to over-determine the CO_2-system in conjunction with the measurements of fCO_2 and TCO_2 during the expedition and thus assuring the internal consistency and accuracy of the measurements. Of the

The data will be used to over-determine the CO_2-system in conjunction with the measurements of fCO_2 and TCO_2 during the expedition and thus assuring the internal consistency and accuracy of the measurements. Of the CO_2 parameters measured, seawater pH is the most precise and also has the highest measurements frequency and thus can be used as a proxy to interpolate for fCO_2 where fCO_2 measurements are not available. This is important due the highly variable nature of the patch with time through rapid planktonic carbon uptake and through space as the ship cannot maintain position over the same water mass.

These results form the most precise and detailed pH data set from the Polar Frontal Region of the Southern Ocean gathered to date. Together with the data collected in 1999 during the ANTXVI/3 expedition they establish the baseline to which future pH measurements should be compared in assessing the oceans pH response to anticipated increases in atmospheric carbon dioxide concentrations.

The pH data are also the first direct pH measurements during an iron release experiment in the Southern Ocean. In addition to the increased confidence in our understanding of the CO_2-system, the measurements should provide insight into the natural iron speciation in the surface waters during the study.

In situ pCO2

Unfortunately, the loss of the drifter during the cruise was accompanied by the loss of a SAMI-CO_2 instrument and due to time constraints it was deemed that the second SAMI-CO_2 should not be deployed in it's place. No data is currently available from the culture experiment.

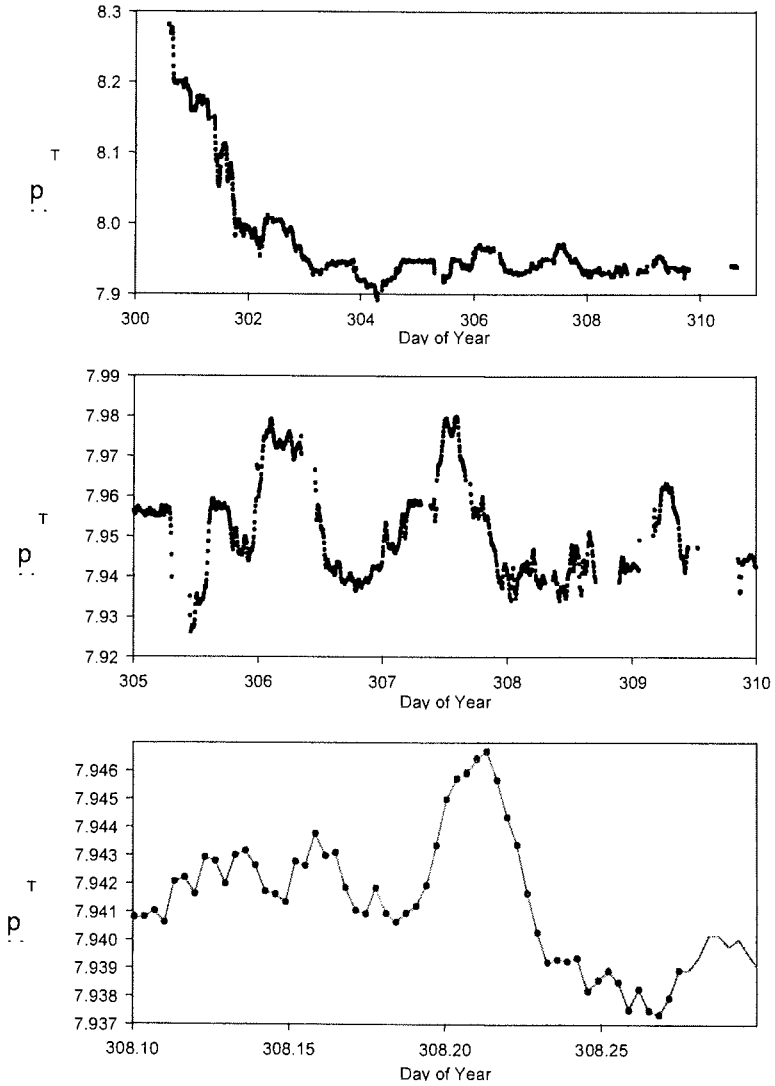

Figure 7.1 Surface pH_T measurements during the ANT XVIII/2 EISENEX study.

8. COMPLEX DRAWDOWN OF CARBON DIOXIDE UPON IRON ENRICHMENT

D. Bakker, A. Watson (UEA)

Introduction and Objectives

Low iron concentrations limit algal growth in large parts of the oceans. In the EisenEx/CARUSO experiment the effect of iron addition on algal growth and related biogeochemical parameters was studied in austral spring in the Antarctic Circumpolar Current. The centre of an eddy at roughly 47°S 21°E, between the Subantarctic Front and the Polar Front, was selected for the release, as the eddy provided moderately stable hydrographic conditions in a highly dynamic environment. Iron and the tracer sulphur hexafluoride (SF_6) were released on 7 to 8 November 2000. Additional iron was added 8 and 16 days after the first release.

Biological processes, such as algal growth, respiration and remineralisation directly affect the fugacity of carbon dioxide (fCO_2) in seawater. Our objective was to assess the effect of the iron enrichment and its ensuing biological changes on dissolved CO_2 and CO_2 air-sea exchange. Changes in fCO_2 will be compared to those during the Southern Ocean Iron Release Experiment (SOIREE), which was carried out south of the Polar Front at 61°S 141°E in February 1999. The comparison will give an indication of the variability of iron related CO_2 drawdown in the Southern Ocean.

Work at sea

Continuous measurements of surface water fCO_2 were made during the pre-site survey between 45° and 52°S along 20°E and during the 22 days of the experiment. The atmospheric CO_2 content was analysed in parallel, which will allow assessment of the CO_2 air-sea flux. Frequent CTD casts inside and outside the patch were sampled in order to obtain vertical profiles of fCO_2. For the measurement of fCO_2 in water samples, a headspace was equilibrated with the gas content of the seawater. The CO_2-content of the headspace was determined by non-dispersive infrared analysis.

Preliminary results

The iron addition promoted algal growth and algal carbon uptake in these dynamic Southern Ocean waters. Significant drawdown of surface water fCO_2 was observed in the iron enriched patch from roughly 4 days since the first release (eg. station 41) onwards. The maximum fCO_2 drawdown was close to 20 µatm, after

respectively 12, 18 and 20-22 days. The iron enriched waters became a sink for atmospheric CO_2 with high CO_2 uptake during the frequent gale force winds.

Algal carbon uptake, as seen from the corresponding fCO_2 changes, was a complex function of iron availability and of meteorological and hydrographic forcings. Without further data analysis it is difficult to know what caused the sudden increase in fCO_2 drawdown from 5 µatm after 8 days, to 12 µatm after 9 days and 20 µatm after 12 days. A storm after 5-6 days may have improved iron availability for algae in the initially shallow surface mixed layer. An algal bloom may have developed in the subsequent calm and sunny conditions. It seems unlikely that the second iron release after 8 days resulted in such a sudden strong uptake of CO_2.

Surface water fCO_2 drawdown in the patch centre decreased from 20 to 10 µatm during a heavy storm after 13 days, by mixing in of water with higher fCO_2 from below or from the edges of the patch. Another reduction in surface water fCO_2 drawdown from 20 to 17 µatm may also be related to a high wind speed event after 19 days.

The variable fCO_2 drawdown in this dynamic environment differs from the almost linear fCO_2 decrease during SOIREE. Total fCO_2 drawdown in SOIREE was as high as 35 µatm after 13 days relative to waters outside the patch. The different algal carbon uptake in these two Southern Ocean experiments was at least partly related to contrasting meteorological conditions with stable, grey weather during SOIREE and a rapid succession of calm, often sunny spells and gale force winds in November 2000.

Future work

Surface water fCO_2 showed a highly complex picture throughout the iron enrichment experiment. Future analysis of fCO_2 data will address the role of vertical and horizontal mixing, iron availability and of other factors in the surface water CO_2 signal and, hence, in algal carbon uptake. The interpolation of the surface water fCO_2 values and their collocation with SF_6 concentrations will demonstrate the spreading and shape of the CO_2-patch. Vertical fCO_2 profiles at IN and OUT stations will be studied along with mixed layer depth and the vertical distribution of SF_6, iron and biological activity. Combination of the fCO_2 data with dissolved inorganic carbon (DIC) (Yann Bozec, Hein de Baar - Netherlands Institute for Sea Research) and pH (Solveig Kringsted, Richard Bellerby - University of Bergen) will allow study of the evolution of the marine carbonate

system over the 22-day period. Total DIC drawdown across the patch will calculated by correcting the net DIC drawdown, for vertical diffusion, CO_2 air-sea exchange and lateral dispersion. In a carbon budget we will compare total DIC drawdown with algal carbon uptake, grazing rates and plankton carbon stocks.

9. BIOGENIC TRACE GASES

S. Turner and A. Chuck (UEA)

A large suite of trace gas measurements was made during the cruise, providing a description of surface water distributions at the mesoscale level as well as detailed vertical profiles within and outside the experimental iron-enriched patch.

For biogenic halocarbons such as methyl iodide and bromoform, there is only limited knowledge of oceanic distributions and this cruise was the first opportunity to determine the effects of *in situ* iron enrichment on their production. During an Eq Pac cruise in 1992, the results of shipboard incubation studies had suggested that the production of some species was enhanced by iron-enrichment. Very little is known about the alkyl nitrates and this cruise not only provided the 3rd dataset of distributions in seawater but also insights into production mechanisms. Initial examination of the data suggests that there was an overall increase in the concentrations of several compounds but this trend seemed to be the same for waters inside and outside of the patch. However, more detailed analysis of the data in the context of the physical structure of the water column and the distribution of SF_6 is required which may reveal some differences. Participation in ANTXIII/I and II provided the opportunity to characterise the concentrations over several biomes. For the iodinated halocarbons, levels were much higher in the tropical regions compared to the higher latitudes, indicating that light may be the controlling factor in the distribution of these compounds. Incubation studies were performed in collaboration with Klaas Timmermans and Peter Croot (NIOZ) to investigate the production of these trace gases in an unialgal culture as well as the natural assemblage from within the patch.

A large number of samples were analysed for dimethylsulphide (DMS) and its precursor dimethylsulphoniopropionate (DMSP), both particulate and dissolved. The results from the previous three iron enrichment experiments

showed that DMSP levels increased immediately after the addition of iron with a greater than 3-fold increase in DMS some days later. This response was not observed during this experiment. Ambient levels of DMS and DMSP were already quite high in the region where the experiment was conducted and there were only small changes over space and time.

The figure below shows the spatial distribution of DMS concentrations two weeks after the first iron infusion. The highest levels are coincident with the highest SF_6 concentrations. The higher DMS in the south is reasonably well correlated with elevated Fv/Fm.

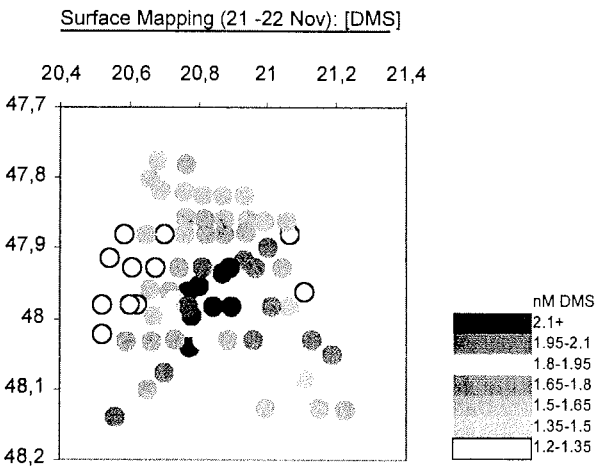

Figure 9.1

As for the other trace gases, the complex and changing structure of the water column together with high variability in the sea to air gas exchange rate due to a series of high wind events necessitates detailed analysis to reveal the extent to which DMS production was enhanced by the addition of iron.

Two novel experiments were conducted in collaboration with Peter Verity (Skidaway) to determine the effects of microzooplankton grazing on DMS production. Ciliates were concentrated from a sample of 'in-patch' water and added in 3 different amounts to ambient seawater. The results are ambiguous, for although increases in DMS were observed, they did not appear to be related to the number of grazers added.

A suite of samples was taken for analysis back in the home lab. These include water samples for iodine species, organic nutrients and DMSP lyase activity.

This was a successful cruise and we thank the ship's crew and officers for their support and the galley staff and stewardesses for looking after us so well. Many thanks to the physical oceanographers for doing all the CTD casts and providing us with samples (many!) and to all our fellow scientists.

10. THE PHYSICAL SETTING OF THE SOUTHERN OCEAN IRON FERTILISATION EXPERIMENT

V. Strass (AWI), H. Leach (Univ. Liverpool), B. Cisewski (AWI), S. Gonzalez (NIOZ), J. Post (Hydromod), V. da Silva Duarte (FURG) and F. Trumm (IfMH)

The Antarctic Circumpolar Ocean is considered as an ocean region of potential influence on global climate. This view in part is based on the observation of excess macro-nutrients which, after being upwelled in the Antarctic Divergence, are not completely utilised by phytoplankton primary production fuelling the biologically- mediated carbon draw-down but instead are subducted again at fronts within the Circumpolar Current. Possible reasons of the limitation of primary production include insufficient availability of light for the phytoplankton growing in the mixed layer when the mixing is deep due to wind stirring and convection, zooplankton grazing, and lack of trace nutrients such as iron.

Testing the iron hypothesis was the overarching goal of 'EISENEX'. That test was planned to be performed as an open ocean *in situ* experiment consisting of fertilising a patch of water with dissolved iron pumped from the ship into the

sea and of monitoring the biological response to fertilisation for as long as possible, and to compare the response with that in the surrounding waters unaffected by iron addition.

Prerequisite for conducting an open ocean *in situ* experiment is information about the physical setting. For that purpose, a suite of oceanographic measurements had to be carried out during Polarstern cruise ANT-XVIII/2 'EISENEX'. These measurements were aimed at three particular objectives.

Objective 1: To identify a suitable site for the iron fertilisation experiment. That site had to satisfy three differing conditions. Firstly, and ideally, it should be close to the Antarctic Polar Front where the silica-rich Antarctic Surface Water subducts, i.e. as close as possible to the region of potentially strongest impact on carbon draw-down. Secondly, on the other hand, the site had to be far enough away from vigorous frontal jets or edges of eddies to avoid the injected dissolved iron dispersing too rapidly. And thirdly, we had to identify a region not dominated by light limitation, i.e. a region where the mixed layer was not too deep.

The measurements aiming at Objective 1 were made by use of an instrument package combining a towed undulator (Scanfish) and the vessel-mounted acoustic Doppler current profiler (VM-ADCP). The Scanfish+ADCP package allowed the mesoscale density and velocity fields being mapped simultaneously with other physical and biological variables down to 200 - 300 m depth at high horizontal resolution in quasi-synoptic manner.

Using this instrument package and additional information on sea surface height variability obtained from satellilte altimetry just prior to the cruise, we succeeded after 14 days of surveying since departure from Cape Town to identify a hydrographic structure which appeared ideal for conducting the experiment. That structure consisted of a cyclonic eddy of approximately 150 km diameter which obviously was shed by the Antarctic Polar Front (APF) by detachment of a northward protruding meander. Due to its origin, the eddy contained in its centre the reasonably high concentrations of macro-nutrients typical of the southern APF side. And the eddy was topped with a mixed layer initially less than 50 m deep, considered shallow enough for providing a suilable light environment.

Objective 2: To monitor the displacement and spreading of the fertilised water body under the action of advection and diffusion.

For that purpose, different measuring techniques were used in combination.

(a) A surface buoy drogued at 10 – 15 m depth, equipped with GPS (Global Positioning System) receiver and radio as well as ARGOS satellite transmitters, was deployed in the centre of the identified eddy to aid the ship navigating in a Lagrangian manner while pumping the iron solution into the sea along a spiral-shaped track around the buoy in order to produce a fertilised patch as homogeneous as possible. After iron injection, the drift of the buoy as monitored via radio and ARGOS provided the primary source of information about the movement of the fertilised patch of water.

(b) Numerous casts of a CTD (Conductivity Temperature Depth) sonde, attached to a rosette water sampler, were done for hydrographic profiling from the surface to intermediate depths. Samples from the bottles were used to measure the concentration of SF_6, the tracer released together with the iron solution in order to mark the fertilised water. The CTD rosette sampler also was the major tool for supplying the various scientific disciplines on board with water samples. By performing repeated CTD surveys in the area at fine horizontal resolution of a few kilometres it was possible to map the three-dimensional distribution of the SF_6 and other constituents and thus to monitor the development of the fertilised patch in time.

(c) Measurements of currents by the vessel-mounted acoustic Doppler current profiler (VM-ADCP) were continously made throughout the cruise and processed aboard to monitor the mesoscale circulation.

(d) A tethered free-falling microstructure probe (MST profiler) equipped with two shear sensors (one for shear measurement, the other as a reference to flag noise caused by unexpected device vibrations and external disturbances), two temperature sensors (a fast for microstructure and a slow one for high precision measurements) and one pressure sensor was used for profiling small-scale turbulent motions down to 200 m depth. From these data the vertical distributions of turbulence parameters like the Ozmidov-, Kolmogorov- and Thorpe-scales can be estimated.

By using the combined information from measurements (a) through (c) and from continuous mapping of the SF_6 surface distribution (contribution of A. Watson and co-workers) we were able to follow the fertilised patch until we had to depart from our experimental site at the end of the cruise.

Objective 3: To provide a detailed description of the physical environment of the phytoplankton and zooplankton at the experimental site, and to provide the basic measurements needed for estimating fluxes of particulate and dissolved matter.

A detailed description of the physical environment can be obtained from combined analysis of the various measurements made. That description consists of the three dimensional distributions of temperature, salinity, density, currents and turbulence parameters as well as of the horizontal distribution of integral or bulk characteristics like the mixed layer depth, including a discrimination between just homogeneously mixed and actively mixing turbulent layers, and their variation in time. Further, by combining vertical profiles of the turbulent kinetic energy derived from the ADCP current measurements with the vertical distribution of the dissipation rate determined from the free-falling shear probe data, vertical eddy diffusivity profiles can be estimated. Comparison with the temporal change of the three-dimensional SF_6 distribution will add to our understanding of the physical processes acting to spread tracers. However, providing a detailed description of the physical environment is to large extent left to post-cruise work.

In five sections following below the made measurements are discribed in more detail.

10.1 Underway Measurements of Currents with the Vessel-Mounted Acoustic Doppler Current Profiler

B. Cisewski and V.Strass (AWI)

Vertical profiles of ocean currents down to roughly 300 m depth were measured with a Vessel Mounted Acoustic Doppler Current Profiler (VM-ADCP; manufacture of RDI, 150 kHz nominal frequency), installed at the ship's hull behind an acoustically transparent plastic window for ice protection. The ADCP has four transducer heads, arranged in a square formation, which point diagonally outwards at an angle of 30° relative to the vertical. The transducer heads simultaneously emit a sound pulse approximately every second, and record echoes returned from particles in suspension in the water. The echoes are range-gated into a series of vertical bins and analysed for their Doppler frequency shift which is related to the water velocity. Determination of the velocity components in geographical coordinates, however, requires that the attitude of the ADCP transducer head, its tilt,

heading, motion and geographic position is also known. Attitude variables of the VM-ADCP were taken from the ship's navigation system. In addition, the ADCP can be used as a detector for zooplankton abundance by evaluating the echo amplitude.

The instrument settings were chosen to give a vertical resolution of current measurements of 4 m in 80 depth bins, and a temporal resolution of 2 min after ensemble averaging over individual profiles taken at a rate of roughly 1 Hz. Calibration data for the ADCP velocity measurements were obtained during the cruise, during approach to and departure from stations. Processing of the VM-ADCP data was done using the CODAS software package (developed by E. Firing and colleagues, SOEST, Hawaii).

The VM-ADCP data were collected continously during the cruise except of two interruptions (Oct. 10, 11:59 – 19:22 and Nov. 4, 19:38 – Nov. 5, 11:36) caused by electrical problems.

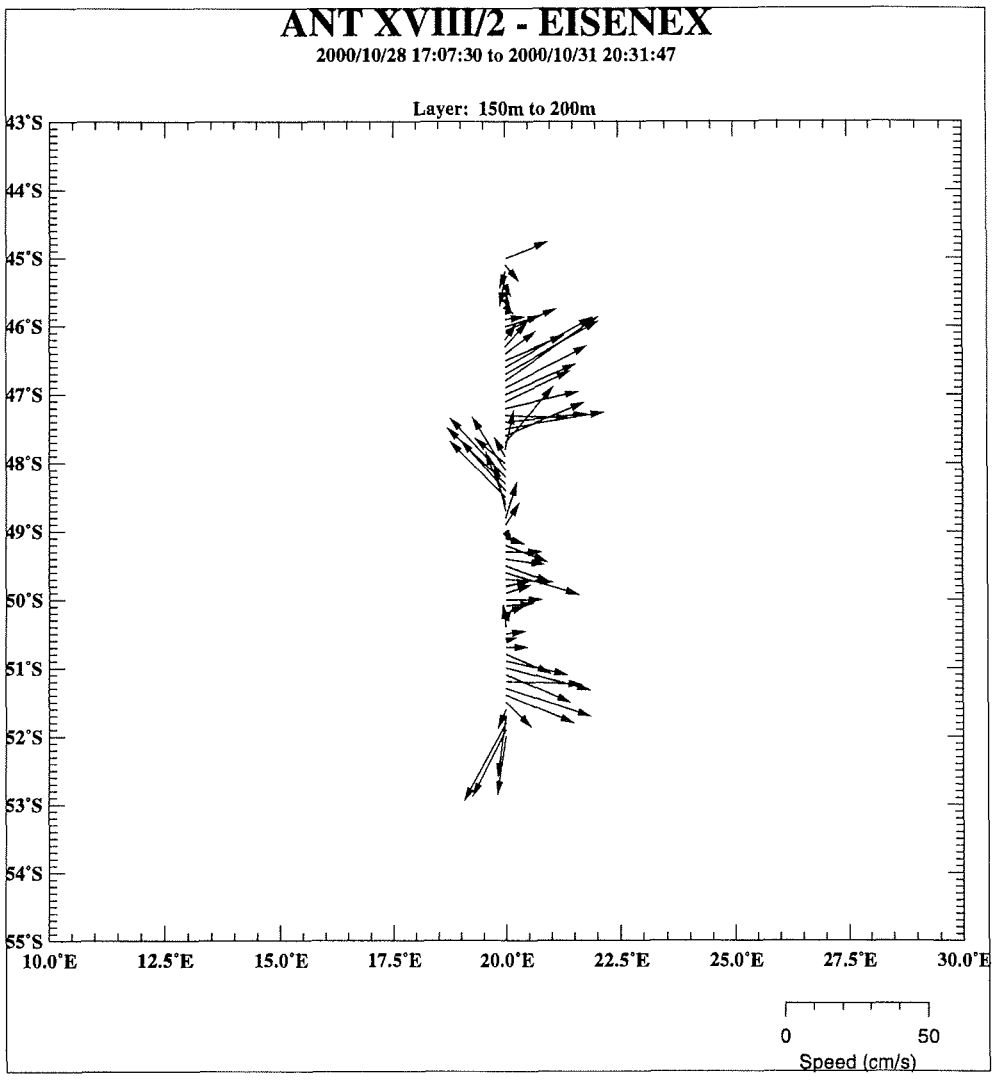

Fig. 10.1.1: Horizontal currents in the depth range 150 - 200 m measured with the VM-ADCP along 20 °E between latitudes 45 °S and 52 °S. The 20 °E section was the first performed during the survey to identify a suitable site for the fertilisation experiment. The shown pattern of currents can be interpreted as follows: The band of strong eastward currents in the latitude range 46 °S to 47 °S relates to the Subantarctic Front (SAF), the band of enhanced eastward currents between 49 °S and 50 °S marks the Antarctic Polar Front (APF), and the strong eastward currents between 51 and 51.5 °S are associated with the Southerly Polar Front (SPF). The westward currents crossed at around 48 °S gave first evidence of an eddy-like circulation.

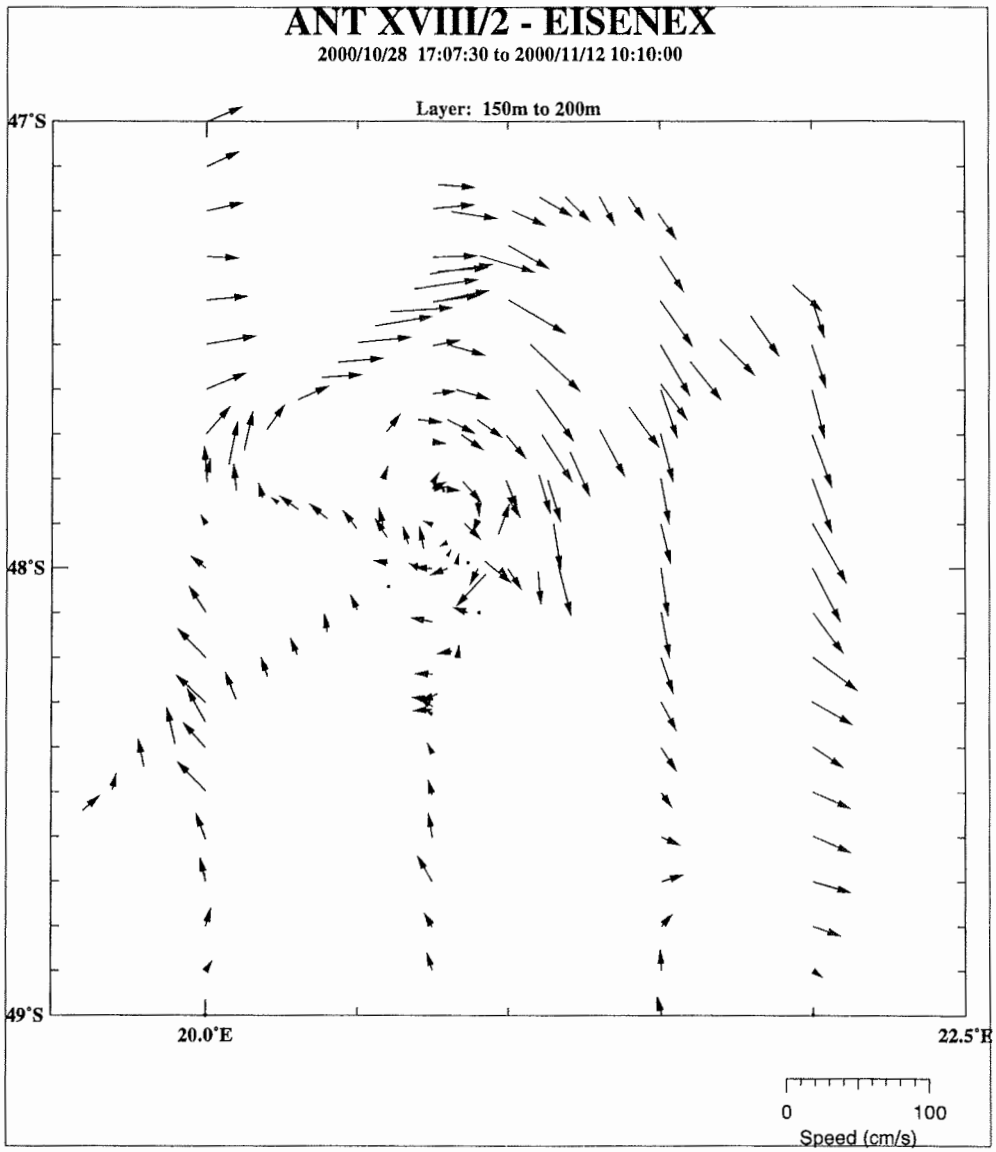

Fig. 10.1.2: Horizontal VM-ADCP currents in the depth range 150 – 200 m, obtained from a more detailed two-dimensional survey performed around the latitude of 48 °S where hints of an eddy where found during the first 20 °E section. The current pattern shown indeed reveals a closed cyclonic circulation centered at 47.85 °S, 20.75 °E which extends over roughly 100 - 150 km diameter. The centre of the closed circulation was chosen as the site to conduct the fertilisation experiment. Smaller scale mappings of the horizontal current structure, repeated at later times during the experiment, revealed that the eddy remained in its position apart from meridional shifts of the eddy centre between 47.85 °S and 48.2 °S.

10.2 Underway Measurements of Hydrographic and Biological Variables with the Towed Undulating Vehicle 'Scanfish'

V. Strass (AWI), S. Gonzalez (NIOZ), H. Leach (Univ.Liverpool),
J. Post (Hydromod), V. da Silva Duarte (FURG), F. Trumm (IfMH) and
H. de Baar (NIOZ)

The Scanfish (GMI Scanfish MK II) is a streamlined, wing-shaped body towed behind the steaming ship. By electrically turnable flaps at its rear end the Scanfish can be made to undulate vertically throught the upper water column according to the parameter settings entered at the control unit on deck. The depth range is usually enhanced by use of an active winch (Type Cormac 1500 assembled by Svendborg Skibshydraulik A/S) holding 2500 metres of 8.3 mm thick unfaired COAX towing cable, cable which is paid out during dive of the Scanfish and retrieved during climb. Due to technical problems with the winch control, however, the Scanfish mostly was towed at fixed cable length, and the depth range was limited to roughly 5 to 200 m at optimal towing speeds which varied between 6 and 7.5 knots. Those towing speeds, combined with a dive/climb rate of 0.4 m/s of the fish, resulted in a nominal horizontal resolution (half wavelength) of 2.6 to 3.6 km along-track. Scanfish attitude while being towed, as well as the scientific data, were monitored and recorded in real-time on deck.

The scientific payload of the Scanfish consisted of a CTD (Sea-Bird Electronics SBE 911*plus*), an oxygen sensor (AMT), a light meter for PAR (phosynthetic active radiation) and a fluorometer (Chelsea Instruments). From the CTD measurements the hydrographic variables of state, pressure (depth), temperature, salinity and density were determined, while the fluorometer readings were used to derive chlorophyll concentration as an indicator of phytoplankton biomass. The CTD temperature measurements are assumed accurate to 0.001 °C according to the manufacturers specifications. Salinity was calibrated by relating the data from the upper Scanfish turning points to concurrent readings from the hull-mounted thermosalinograph (POLDAS-TSK), which themselves were calibrated against salinity samples analysed using a salinometer (Guildline Autosal 8400A) in reference to I.A.P.S.O. Standard Seawater. The accuracy of the calibrated Scanfish salinities was estimated to about 0.01 (salinity units according to the Practical Salinity Scale PSS-78). The Scanfish fluorometer readings (Fl) were converted into concentrations of chlorophyll *a* (Chl) using a model in which the yield (Y = Fl/Chl) changes with ambient light as measured by the PAR sensor. This

enabled to reasonably remove the light-dependent quenching effect. Horizontal changes of yield were taken into account by comparison with Chl determined from underway surface samples by U. Riebesell and co-workers.

Measurements with the Scanfish were made at the begin of the cruise, prior to fertilisation, during two meridional sections along 20° E (Transects 1 and 2) and during a mesoscale survey (Grid 1) designed to cover the anticipated eddy centre. Details of these Scafish tows are listed in Table10i.2.1 below.

Tab. 10.2.1: ANTXVIII/2 Scanfish Tows

		Date	Time UTC	jday dayofyr	Lat degS	Lat minS	Lat deg	Lon degE	Lon minE	Lon deg
Transect 1	start	29.10.2000	0:00	303,00	45	0	-45,000	20	0	-20,000
	end	31.10.2000	4:00	305,17	49	51,55	-49,859	20	0	-20,000
Transect 2	start	31.10.2000	19:45	305,82	52	0	-52,000	20	0	-20,000
	end	01.11.2000	18:50	306,78	49	17,87	-49,298	20	0,61	-20,010
Grid 1	start	03.11.2000	1:55	308,08	47	22	-47,367	22	0	-22,000
	end	06.11.2000	6:00	311,25	47	10	-47,167	20	45	-20,750
date origin	31.12.1999									

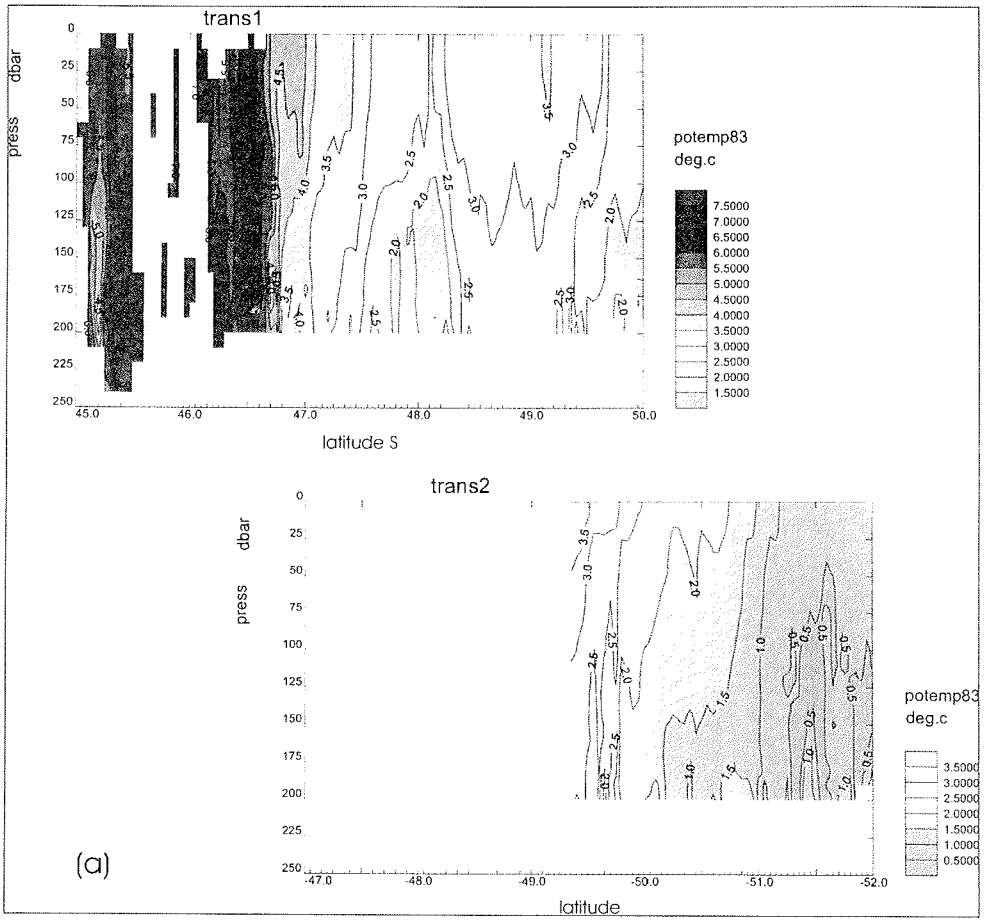
trans1
press dbar
latitude S
potemp83
deg.c
7.5000
7.0000
6.5000
6.0000
5.5000
5.0000
4.5000
4.0000
3.5000
3.0000
2.5000
2.0000
1.5000
trans2
press dbar
latitude
potemp83
deg.c
3.5000
3.0000
2.5000
2.0000
1.5000
1.0000
0.5000
(a)

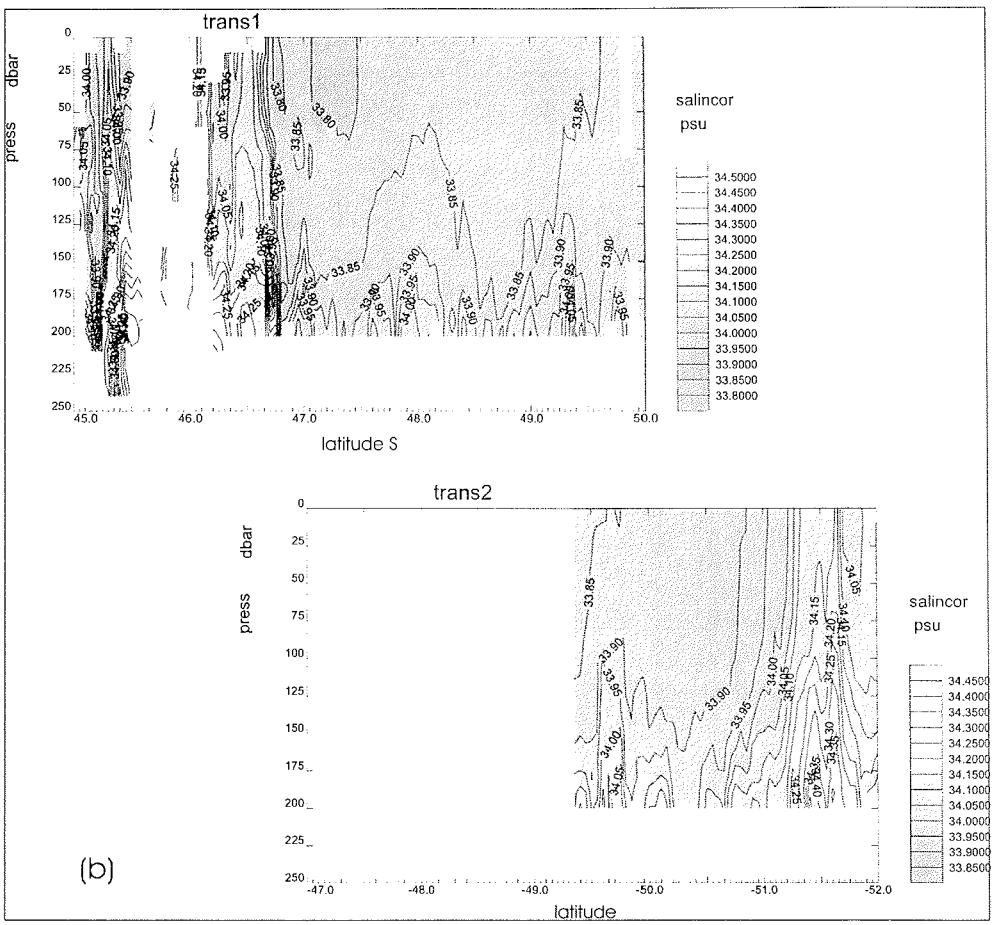
trans1
press dbar
latitude S
salincor
psu
34.5000
34.4500
34.4000
34.3500
34.3000
34.2500
34.2000
34.1500
34.1000
34.0500
34.0000
33.9500
33.9000
33.8500
33.8000
trans2
press dbar
latitude
salincor
psu
(b)

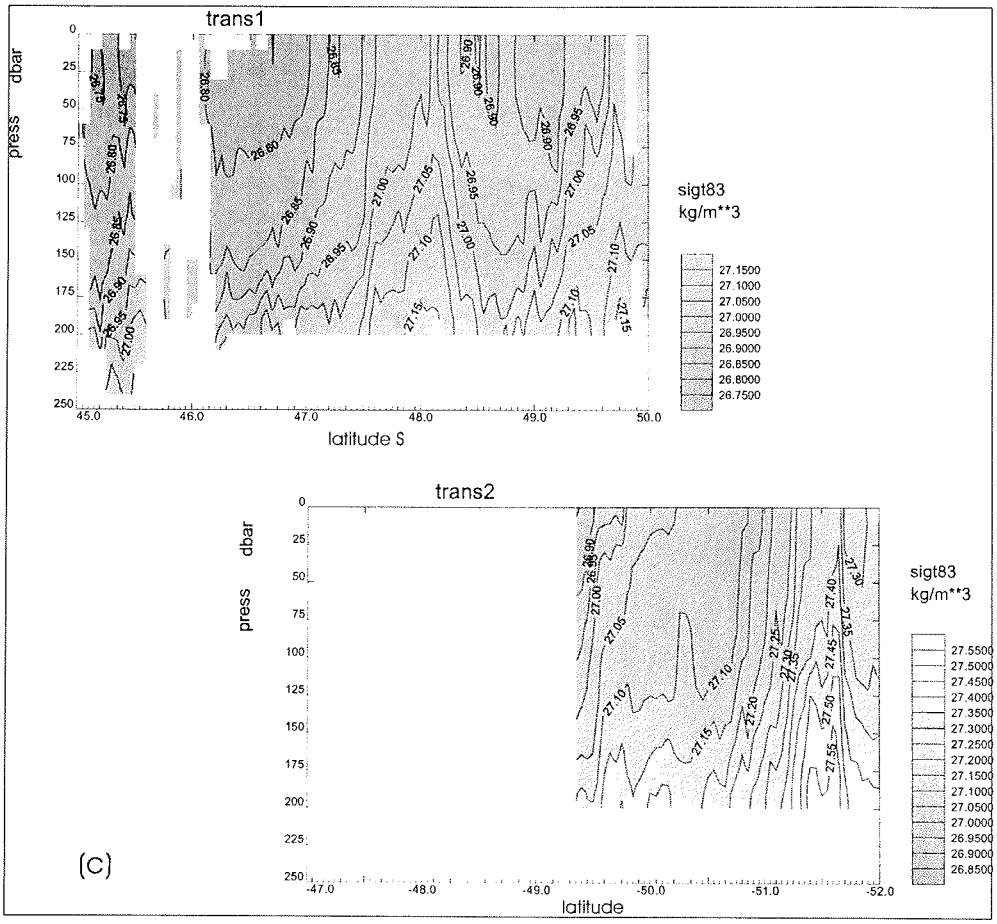
trans1
press dbar
latitude S
sigt83
kg/m**3
27.1500
27.1000
27.0500
27.0000
26.9500
26.9000
26.8500
26.8000
26.7500
trans2
press dbar
latitude
sigt83
kg/m**3
(c)

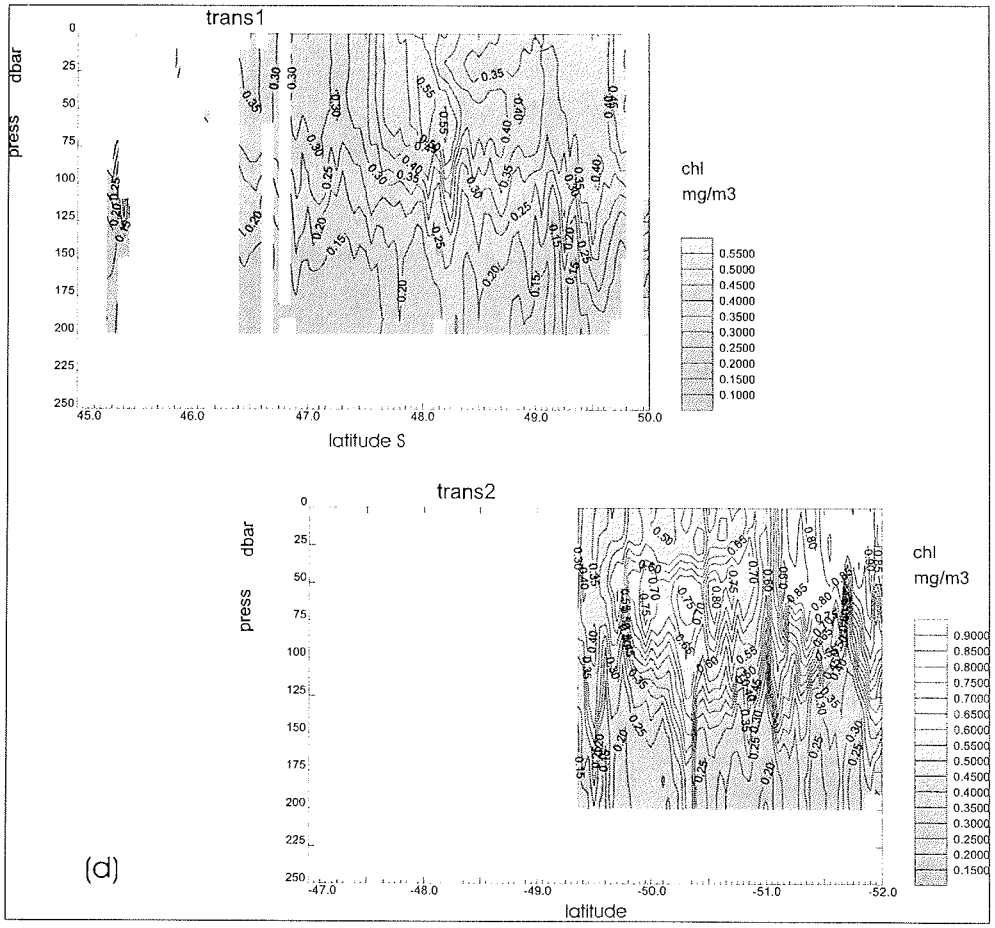

Fig. 10.2.1: Vertical distributions of potential temperature (a), salinity (b), density variable _ (c) and the chlorophyll concentration (d) between 45° S and 52° S along 20° E, measured during Scanfish transects 1 and 2. The cold and dense water mass anomaly centered around 48° S marks the western edge of the cyclonic eddy selected for the subsequent fertilisation experiment. The temperature (colder than 2° C at depths below 100 m), salinity and density in the eddy indicate that it originates from the Antarctic Polar Front which is centered around 49° 30' S. The chlorophyll concentrations in the top 100 m of the eddy prior to fertilisation vary between 0.3 and 0.6 mg m^{-3}.

10.3 Hydrographic Station Work with CTD and Water Bottle Sampling

V. Strass (AWI), H. Leach (Univ. Liverpool), S. Gonzalez (NIOZ), V. da Silva Duarte (FURG), F. Trumm (IfMH), J. Post (Hydromod) and B. Cisewski (AWI),

The CTD used for conventional deployments at hydrographic stations was, as the one in the Scanfish, also type Sea-Bird Electronics SBE 911*plus*. The CTD was supplemented by a transmissometer (Wet Labs, 660 nm wavelength) and a chlorophyll-sensitive fluorometer (Dr. Haardt BackScat). From cast 13 onwards, the Scanfish oxygen and PAR sensors were also attached to the CTD; the ogygen sensor, however, functioned only for a few casts, as did another oxygen sensor used during cast 8 – 12 before.

The CTD and peripheral instruments were attached to a multi-bottle water sampler type Sea-Bird SBE 32 Carousel holding 24 12-liter bottles. The performance of the water sampler was controlled by use of SIS reversing thermometers and pressure gauges attached to 8 of the water bottles. Salinity derived from the CTD measurements was calibrated to a final accuracy of better than 0.002 by comparison to salinity samples, taken from the water bottles, which were analysed by use of the Guildline-Autosal-8400A salinometer.

Alltogether, 151 CTD casts were made at a total of 101 hydrographic stations. Most casts were limited to only intermediate depths of 250 or 500 m, to yield high vertical resolution within and just below the photic zone. Only 9 casts extended to full ocean depth, made to support the analysis of the mesoscale flow field in the area. Many CTD stations were organised in 3 fine-meshed two-dimensional horizontal grids covering the fertilised patch of water. These CTD grids were worked in a Lagrangian manner with the ship navigating relative to the buoy which was drifting with the patch. In an attempt to achieve synoptic mapping of the patch these CTD surveys were conducted as fast as possible, i.e. without longer interruption by other work.

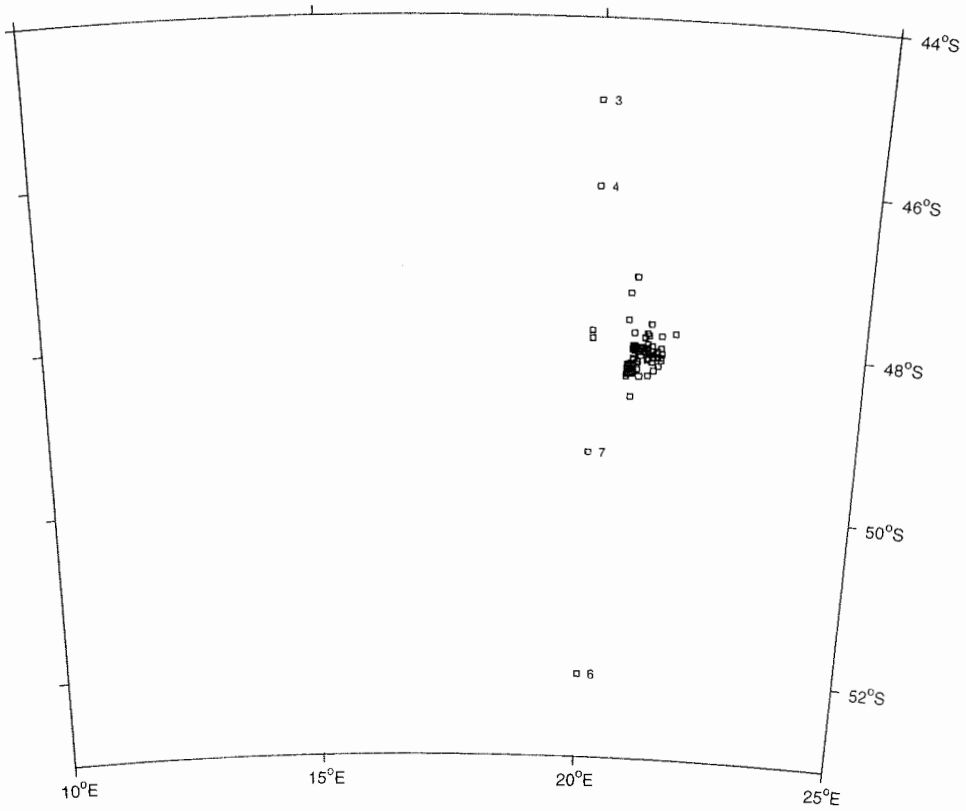

Fig. 10.3.1: Overview of all CTD station positions occupied during the cruise. Station positions within the narrower latitude/longitude range indicated by the inner frame are shown at enhanced resolution in Fig. i.3.2.

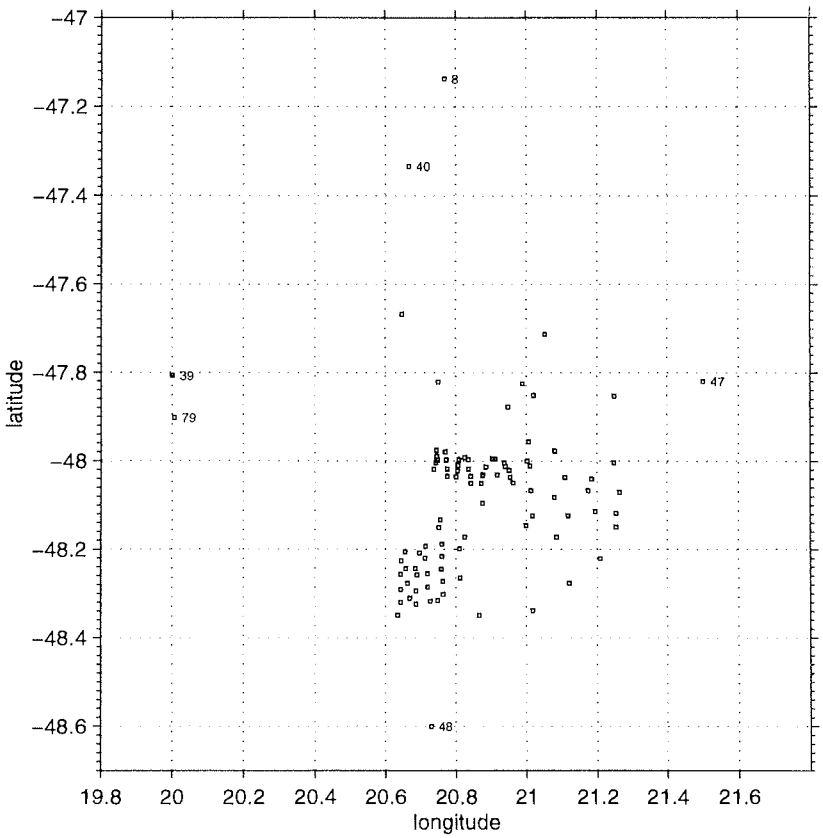

Fig. 10.3.2: Positions of CTD stations in the latitude/longitude range 47 – 48.7° S and 19.8 – 21.8 °E. Station positions within the narrower latitude/longitude range indicated by the inner frame are shown at enhanced resolution in Fig. i.3.3.

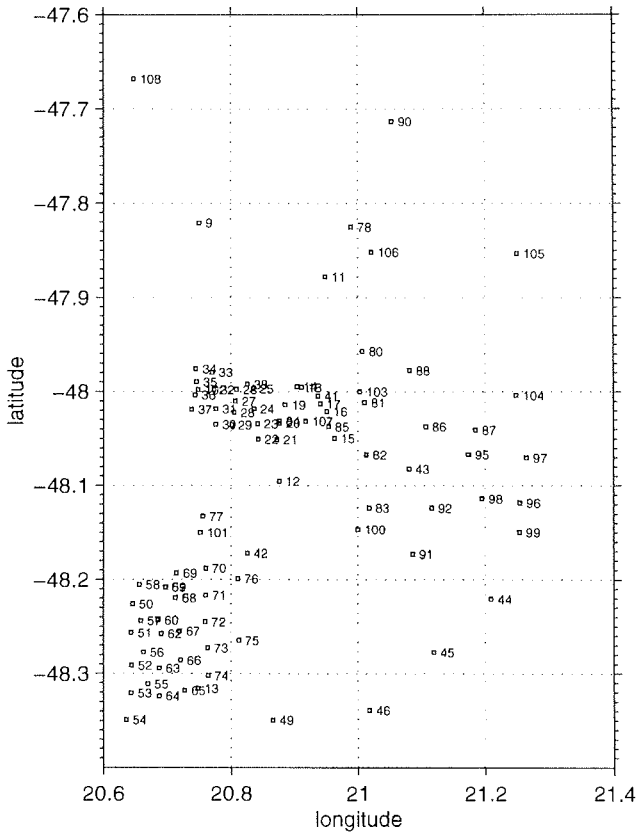

Fig. 10.3.3: Positions of CTD stations in the latitude/longitude range 47.6 – 48.4° S and 20.6 – 21.4 °E, within the core of the eddy.

Tab. i.3.1: ANTXVIII/2 CTD Casts

Lfd Nr	Stn/Cast	Date	DepthTime UTC	Lat degS	Lat minS	Long degE	Long minE	Depth m	Water Depth m	Altimeter	Fluorom.	Transm.	O2 sensor	PAR	Comments
1	e00301	28.10.00	18:00	45	0,19	19	59,99	500	4028	yes?	8060 -BS	CST-403DR	no	no	
2	e00303	28.10.00	21:36	45	0,44	20	1,27	3955	3997	yes?	BackScat	WetLab	no	no	
3	e00401	29.10.00	13:07	46	3,02	20	1,80		5093	yes?	BackScat	WetLab	no	no	
4	e00601	31.10.00	11:59	52	0,04	19	59,81	505	3446	yes	BackScat	WetLab	no	no	
5	e00603	31.10.00	15:03	52	0,97	19	59,96	3450	3445	yes	BackScat	WetLab	no	no	
6	e00701	01.11.00	end 19:43	49	17,65	20	0,75		4428	yes	BackScat	WetLab	no	no	all at the end
7	e00705	01.11.00	23:41	49	17,64	20	1,75	4470	4429	yes	BackScat	WetLab	no	no	
8	E00801	06.11.00	06:23	47	8,23	20	46,12	500	end - 4836	yes	BackScat	WetLab	290802	no	
9	E00902	06.11.00	23:25	47	49,26	20	45,00	269	4852	yes	BackScat	WetLab	290802	no	
10	E00904	07.11.00	03:12	47	48,99	20	46,98	4982	4925	yes	BackScat	WetLab	290802	no	
11	E00906	07.11.00	06:37	47	49,17	20	47,56	203	4929	yes	BackScat	WetLab	290802	no	
12	E00908	07.11.00	08:55	47	49,21	20	49,32	80	4598	yes	BackScat	WetLab	290802	no	all at the end
13	e01103	08.11.00	20:55	47	52,68	20	56,92	502	4498	no	BackScat	WetLab	scanfish	yes	
14	e01106	09.11.00	00:04	47	53,44	20	59,17	500	4356	no	BackScat	WetLab	scanfish	yes	
14a	e01201	09.11.00	09:15	48	5,72	20	52,57	500	4756	no	BackScat	WetLab	scanfish	yes	
15	e01204	09.11.00	11:21	48	6,02	20	51,93	500	4642		BackScat	WetLab	scanfish	yes	
16	e01205	09.11.00	13:01	48	6,29	20	51,74	500	4570		BackScat	WetLab	scanfish	yes	
17	e01301	09.11.00	16:31	48	18,95	20	44,88	4261	4246		BackScat	WetLab	scanfish	yes	
18	e01404	10.11.00	03:43	47	59,69	20	54,23	500	4470		BackScat	WetLab	scanfish	yes	
19	e01406	10.11.00	05:46	47	59,64	20	53,44	502	4562		BackScat	WetLab	scanfish	yes	
20	e01408	10.11.00	07:29	48	0,62	20	53,57	501	4329		BackScat	WetLab	scanfish	yes	
21	e01501	10.11.00	09:53	48	2,96	20	57,80	250	4639		BackScat	WetLab	scanfish	yes	F4
22	e01601	10.11.00	11:04	48	1,25	20	57,09	250	4279		BackScat	WetLab	scanfish	yes	F3
23	e01701	10.11.00	12:18	48	0,76	20	56,46	250	4250		BackScat	WetLab	scanfish	yes	F2
24	e01801	10.11.00	13:21	47	59,73	20	54,67	250	4459		BackScat	WetLab	scanfish	yes	E1
25	e01901	10.11.00	15:08	48	0,83	20	53,14	251	4325		BackScat	WetLab	scanfish	yes	E2
26	e02001	10.11.00	15:56	48	2,00	20	52,60	250	4934		BackScat	WetLab	scanfish	yes	E3
27	e02101	10.11.00	17:04	48	3,04	20	52,36	250	4914		BackScat	WetLab	scanfish	yes	E4

28	e02201	10.11.00	17:48	48	3,02	20	50,58	251	4907		BackScat	WetLab	scanfish	yes	D4
29	e02301	10.11.00	18:33	48	2,05	20	50,53	250	4947		BackScat	WetLab	scanfish	yes	D3
30	e02401	10.11.00	19:42	48	1,09	20	50,18	253	4849		BackScat	WetLab	scanfish	yes	D2
31	e02501	10.11.00	20:37	47	59,82	20	50,13	250	4602		BackScat	WetLab	scanfish	yes	D1
32	e02601	10.11.00	21:31	47	59,86	20	48,53	250	4666		BackScat	WetLab	scanfish	yes	C1
33	e02701	10.11.00	22:29	48	0,60	20	48,42	250	4699		BackScat	WetLab	scanfish	yes	C2
34	e02801	10.11.00	23:30	48	1,32	20	48,31	250	4907		BackScat	WetLab	scanfish	yes	C3
35	e02901	11.11.00	00:39	48	2,12	20	48,07	250	4910		BackScat	WetLab	scanfish	yes	C4
36	e03001	11.11.00	01:25	48	2,09	20	46,56	250	4894		BackScat	WetLab	scanfish	yes	B4
37	e03101	11.11.00	02:13	48	1,09	20	46,58	250	4902		BackScat	WetLab	scanfish	yes	B3
38	e03201	11.11.00	03:16	47	59,87	20	46,39	250	4790		BackScat	WetLab	scanfish	yes	B2
39	e03301	11.11.00	04:07	47	58,77	20	46,23	251	4866		BackScat	WetLab	scanfish	yes	B1
40	e03401	11.11.00	04:51	47	58,56	20	44,70	252	4879		BackScat	WetLab	scanfish	yes	A1
41	e03501	11.11.00	05:33	47	59,39	20	44,76	250	4881		BackScat	WetLab	scanfish	yes	A2
42	e03601	11.11.00	06:21	48	0,22	20	44,63	262	4757		BackScat	WetLab	scanfish	yes	A3
43	e03701	11.11.00	07:07	48	1,13	20	44,29	252	4898		BackScat	WetLab	scanfish	yes	A4
44	e03801	11.11.00	08:40	47	59,53	20	49,56	500	4715		BackScat	WetLab	scanfish	yes	
45	e03803	11.11.00	09:49	47	59,42	20	49,93	500	4711		BackScat	WetLab	scanfish	yes	
46	e03805	11.11.00	11:45	47	59,08	20	50,65	500	4660		BackScat	WetLab	scanfish	yes	
47	e03807	11.11.00	13:08	47	59,27	20	51,39	500	4676		BackScat	WetLab	scanfish	yes	
48	e03901	11.11.00	21:47	47	48,43	20	0,02	4763	4646		BackScat	WetLab	scanfish	yes	
49	e04001	12.11.00	05:05	47	20,03	20	40,03	4712	4675		BackScat	WetLab	scanfish	yes	
50	e04101	12.11.00	12:11	48	0,26	20	56,25	500	4242		BackScat	WetLab	scanfish	yes	
51	e04102	12.11.00	13:14	47	59,76	20	56,27	501	4441		BackScat	WetLab	scanfish	yes	
52	e04105	12.11.00	15:25	48	0,22	20	57,01	500	4284		BackScat	WetLab	scanfish	yes	
53	e04201	13.11.00	06:23	48	10,33	20	49,55	503	(?)4377		BackScat	WetLab	scanfish	yes	
54	e04202	13.11.00	07:38	48	10,57	20	49,48	502	4364		BackScat	WetLab	scanfish	yes	
55	e04205	13.11.00	09:50	48	10,95	20	49,39	(?)500	4340		BackScat	WetLab	scanfish	yes	
56	e04206	13.11.00	11:39	48	10,56	20	48,92	500	4366		BackScat	WetLab	scanfish	yes	
57	e04302	13.11.00	15:43	48	4,93	21	4,85	500	4839		BackScat	WetLab	scanfish	yes	
58	e04304	13.11.00	17:14	48	5,87	21	3,57	498	5003		BackScat	WetLab	scanfish	yes	
59	e04401	14.01.00	19:12	48	13,25	21	12,54	251	4793		BackScat	WetLab	scanfish	yes	
60	e04501	15.11.00	08:16	48	16,64	21	7,2	500	5017		BackScat	WetLab	scanfish	yes	

61	e04502	15.11.00	09:14	48	16,87	21	7,59	500	5015		BackScat	WetLab	scanfish	yes	
62	e04505	15.11.00	11:50	48	17,14	21	7,72	500	5020		BackScat	WetLab	scanfish	yes	
63	e04507	15.11.00	14:05	48	17,54	21	0,27	500	5022		BackScat	WetLab	scanfish	yes	
64	e04509	15.11.00	15:23	48	18,05	21	7,1	500	5026		BackScat	WetLab	scanfish	yes	
65	e04601	16.11.00	13:37	48	20,34	21	1,1	500	4731		BackScat	WetLab	no	yes	
66	e04603	16.11.00	14:40	48	20,35	21	0,97	500	4689		BackScat	WetLab	no	yes	
67	e04605	16.11.00	16:27	48	20,45	21	0,48	502	4633		BackScat	WetLab	no	yes	
68	e04701	17.11.00	03:19	47	49,2	21	30,12	5239	5179		BackScat	WetLab	no	yes	
69	e04801	17.11.00	12:03	48	36,01	20	43,77	500	4705		BackScat	WetLab	no	yes	
70	e04803	17.11.00	13:19	48	35,58	20	43,05	500	4742		BackScat	WetLab	no	yes	
71	e04805	17.11.00	15:08	48	35,08	20	41,92	500	4785		BackScat	WetLab	no	yes	
72	e04808	17.11.00	17:39	48	34,7	20	39,39	503	4918		BackScat	WetLab	no	yes	
73	e04901	18.11.00	11:03	48	20,97	20	51,97	500	4387		BackScat	WetLab	no	yes	
74	e04903	18.11.00	12:50	48	20,69	20	53,29	500	4345		BackScat	WetLab	no	yes	
75	e04905	18.11.00	15:27	48	20,65	20	52,83	250	4353		BackScat	WetLab	no	yes	
76	e05001	19.11.00	11:43	48	13,57	20	38,74	250	4540		BackScat	WetLab	no	yes	A1
77	e05101	19.11.00	12:46	48	15,4	20	38,59	250	4597		BackScat	WetLab	no	yes	A2
78	e05201	19.11.00	13:46	48	17,48	20	38,63	250	4657		BackScat	WetLab	no	yes	A3
79	e05301	19.11.00	14:39	48	19,24	20	38,59	250	4672		BackScat	WetLab	no	yes	A4
80	e05401	19.11.00	15:39	48	20,96	20	38,12	500	4683		BackScat	WetLab	no	yes	A5
81	e05501	19.11.00	17:11	48	18,67	20	40,16	251	4715		BackScat	WetLab	no	yes	B4
82	e05601	19.11.00	18:24	48	16,64	20	39,76	250	4549		BackScat	WetLab	no	yes	B3
83	e05701	19.11.00	19:17	48	14,64	20	39,5	251	4461		BackScat	WetLab	no	yes	B2
84	e05801	19.11.00	20:15	48	12,34	20	39,36	250	4466		BackScat	WetLab	no	yes	B1
85	e05901	19.11.00	21:14	48	12,49	20	41,84	250	4306		BackScat	WetLab	no	yes	C1
86	e06001	19.11.00	22:29	48	14,6	20	41,13	250	4354		BackScat	WetLab	no	yes	C2
87	e06101	19.11.00	23:36	48	12,48	20	41,79	250	4311		BackScat	WetLab	no	yes	C1
88	e06103	20.11.00	00:53	48	12,1	20	41,5	251	4318		BackScat	WetLab	no	yes	C1
89	e06105	20.11.00	01:55	48	12,09	20	41,21	101	4328		BackScat	WetLab	no	yes	C1
90	e06201	20.11.00	02:54	48	15,47	20	41,43	250	4366		BackScat	WetLab	no	yes	C3
91	e06301	20.11.00	03:50	48	17,66	20	41,25	250	4427		BackScat	WetLab	no	yes	C4
92	e06401	20.11.00	04:45	48	19,43	20	41,25	251	4687		BackScat	WetLab	no	yes	C5
93	e06501	20.11.00	05:39	48	19,08	20	43,65	252	4303		BackScat	WetLab	no	yes	D5

94	e06601	20.11.00	06:25	48	17,15	20	43,23	250	4359		BackScat	WetLab	no	yes	D4
95	e06701	20.11.00	07:18	48	15,3	20	43,17	257	4320		BackScat	WetLab	no	yes	D3
96	e06801	20.11.00	08:21	48	13,17	20	42,77	250	4282		BackScat	WetLab	no	yes	D2
97	e06901	20.11.00	09:16	48	11,6	20	42,87	250	4287		BackScat	WetLab	no	yes	D1
98	e07001	20.11.00	10:08	48	11,29	20	45,63	250	4335		BackScat	WetLab	no	yes	E1
99	e07101	20.11.00	11:02	48	13	20	45,61	250	4248		BackScat	WetLab	no	yes	E2
100	e07201	20.11.00	11:56	48	14,71	20	45,57	250	4150		BackScat	WetLab	no	yes	E3
101	e07301	20.11.00	12:48	48	16,37	20	45,8	250	4298		BackScat	WetLab	no	yes	E4
102	e07401	20.11.00	13:40	48	18,13	20	45,85	250	4316		BackScat	WetLab	no	yes	E5
103	e07501	20.11.00	14:27	48	15,89	20	48,73	250	4146		BackScat	WetLab	no	yes	F4
104	e07601	20.11.00	15:20	48	11,96	20	48,65	250	4210		BackScat	WetLab	no	yes	F2
105	e07701	20.11.00	16:31	48	7,96	20	45,35	251	4399		BackScat	WetLab	no	yes	E0
106	e07801	23.11.00	06:58	47	49,51	20	59,36	250	4082		BackScat	WetLab	no	yes	V1
107	e07902	23.11.00	08:38	47	54,18	20	0,4	250	4602		BackScat	WetLab	no	yes	V2
108	e08001	23.11.00	09:50	47	57,43	21	0,44	250	4686		BackScat	WetLab	no	yes	V3
109	e08101	23.11.00	11:00	48	0,68	21	0,64	250	4219		BackScat	WetLab	no	yes	V4
110	e08201	23.11.00	12:28	48	4,02	21	0,8	500	4876		BackScat	WetLab	no	yes	V5
111	e08301	23.11.00	14:43	48	7,43	21	1,06	250	5111		BackScat	WetLab	no	yes	V6
112	e08401	23.11.00	16:46	48	1,87	20	52,6	251	4915		BackScat	WetLab	no	yes	H1-pos't end
113	e08501	23.11.00	18:52	48	2,21	20	57,25	252	4296		BackScat	WetLab	no	yes	H2
114	e08601	23.11.00	20:46	48	2,23	21	6,46	250	4916		BackScat	WetLab	no	yes	H4
115	e08701	23.11.00	22:12	48	2,44	21	11,08	250	5134		BackScat	WetLab	no	yes	H5
116	e08802	24.11.00	02:02	47	58,65	21	4,92	500	5176		BackScat	WetLab	no	yes	
117	e08804	24.11.00	03:18	47	59,01	21	4,99	500	5184		BackScat	WetLab	no	yes	
118	e08807	24.11.00	04:52	47	59,52	21	5,2	501	4995		BackScat	WetLab	no	yes	
119	e08809	24.11.00	06:21	48	0,54	21	5,73	500	4557		BackScat	WetLab	no	yes	
120	e09001	25.11.00	01:28	47	42,79	21	3,22	500	4358		BackScat	WetLab	no	yes	
121	e09002	25.11.00	02:18	47	42,72	21	3,79	500	4351		BackScat	WetLab	no	yes	
122	e09003	25.11.00	03:31	47	42,72	21	4,67	500	4354		BackScat	WetLab	no	yes	
123	e09004	25.11.00	04:28	47	42,76	21	5,36	501	4390		BackScat	WetLab	no	yes	
124	e09101	25.11.00	13:04	48	10,38	21	5,19	500	4959		BackScat	WetLab	no	yes	
125	e09103	25.11.00	15:39	48	11,04	21	5,85	500	4919		BackScat	WetLab	no	yes	
126	e09104	25.11.00	17:52	48	12,56	21	3,11	500	4735		BackScat	WetLab	no	yes	

127	e09201	27.11.00	11:30	48	7,44	21	07:48	500	5169		BackScat	WetLab	no	yes	
128	e09203	27.11.00	13:28	48	6,82	21	10,12	500	5185		BackScat	WetLab	no	yes	
129	e09205	27.11.00	15:37	48	6,83	21	13,7	501	4901		BackScat	WetLab	no	yes	
130	e09206	27.11.00	16:36	48	6,91	21	13,76	500	4922		BackScat	WetLab	no	yes	
131	e09501	28.11.00	02:43	48	4,02	21	10,46	250	5293		BackScat	WetLab	no	yes	
132	e09601	28.11.00	03:49	48	7,11	21	15,21	250	4853		BackScat	WetLab	no	yes	
133	e09701	28.11.00	05:01	48	4,22	21	15,86	251	5293		BackScat	WetLab	no	yes	
134	e09801	28.11.00	06:00	48	6,85	21	11,7	250	5152		BackScat	WetLab	no	yes	
135	e09901	28.11.00	07:47	48	8,98	21	15,2	250	4680		BackScat	WetLab	no	yes	C3
136	e10001	28.11.00	09:35	48	8,8	21	0,01	250	4701		BackScat	WetLab	no	yes	B3
137	e10101	28.11.00	11:34	48	9,01	20	45,11	250	4405		BackScat	WetLab	no	yes	A3
138	e10201	28.11.00	13:10	47	59,88	20	44,92	250	4799		BackScat	WetLab	no	yes	A2
139	e10301	28.11.00	14:46	48	0	21	0,19	500	4327		BackScat	WetLab	no	yes	B2
140	e10401	28.11.00	16:39	48	0,24	21	14,9	249	5102		BackScat	WetLab	no	yes	C2
141	e10501	28.11.00	18:07	47	51,22	21	14,98	250	5130		BackScat	WetLab	no	yes	C1
142	e10601	28.11.00	19:49	47	51,12	21	1,27	251	4350		BackScat	WetLab	no	yes	B1
143	e10703	29.11.00	02:30	48	1,88	20	55,07	500	4560		BackScat	WetLab	no	yes	A1
144	e10704	29.11.00	04:09	47	57,19	21	1,95	501	4755		BackScat	WetLab	no	yes	
145	e10705	29.11.00	05:10	47	58,15	21	2,44	499	4965		BackScat	WetLab	no	yes	
146	e10706	29.11.00	06:52	47	57,52	21	2,11	500	4895		BackScat	WetLab	no	yes	
147	e10707	29.11.00	08:12	47	58,29	21	3,78	500	4891		BackScat	WetLab	no	yes	
148	e10709	29.11.00	10:48	47	59,33	21	6,22	5126	5126		BackScat	WetLab	no	yes	
149	e10801	29.11.00	15:33	47	40,09	20	38,84	500	4150		BackScat	WetLab	no	yes	
150	e10803	29.11.00	16:52	47	40,14	20	39,09	500	4166		BackScat	WetLab	no	yes	
151	e10807	29.11.00	20:00	47	40,44	20	40,37	501	4372		BackScat	WetLab	no	yes	

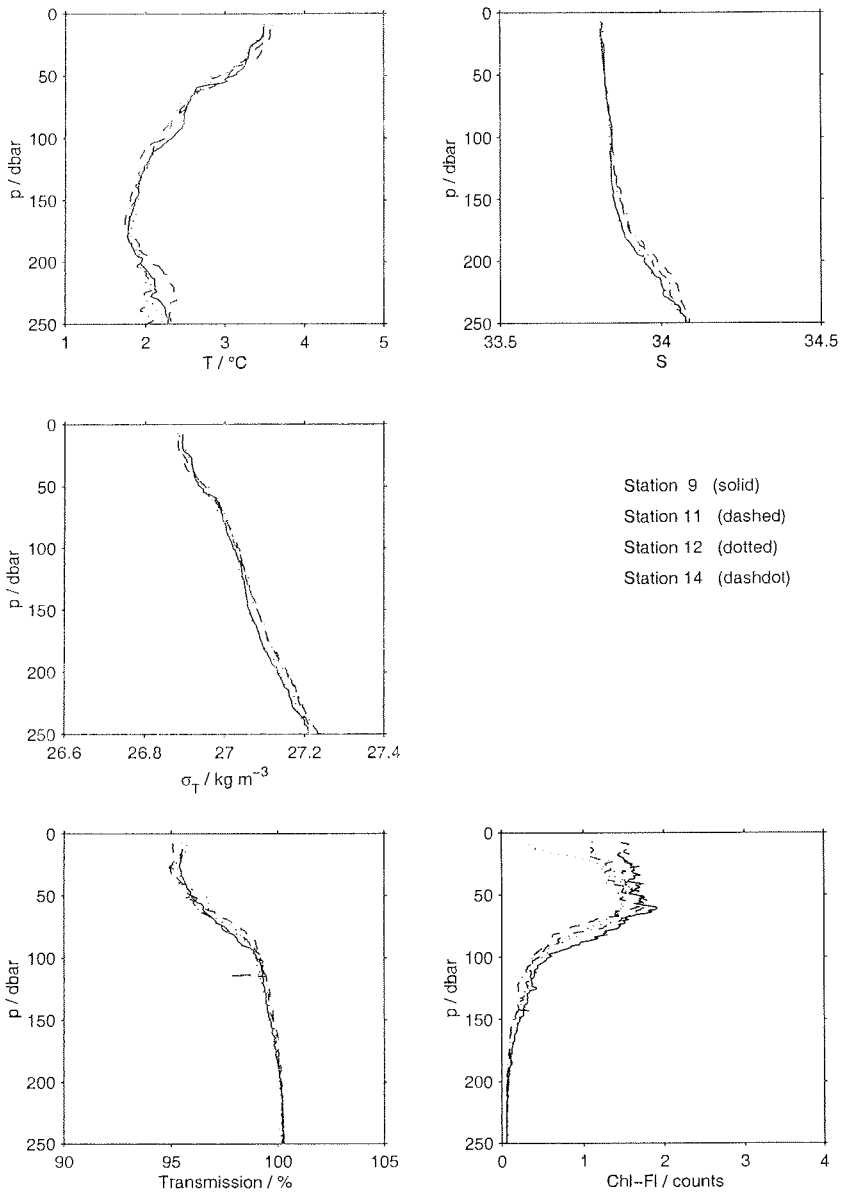

Fig. 10.3.4: Vertical profiles of temperature T, salinity S, density σ_T, light transmission and chlorophyll fluorescence obtained with the CTD at stations 9 – 14, occupied in the eddy centre before iron injection. Thanks to the prevailing calm weather which we enjoyed during the frist two weeks of the cruise, the water column is stably stratified close to the surface, with a mixed layer extending to not more than 20 m depth at the stations depicted.

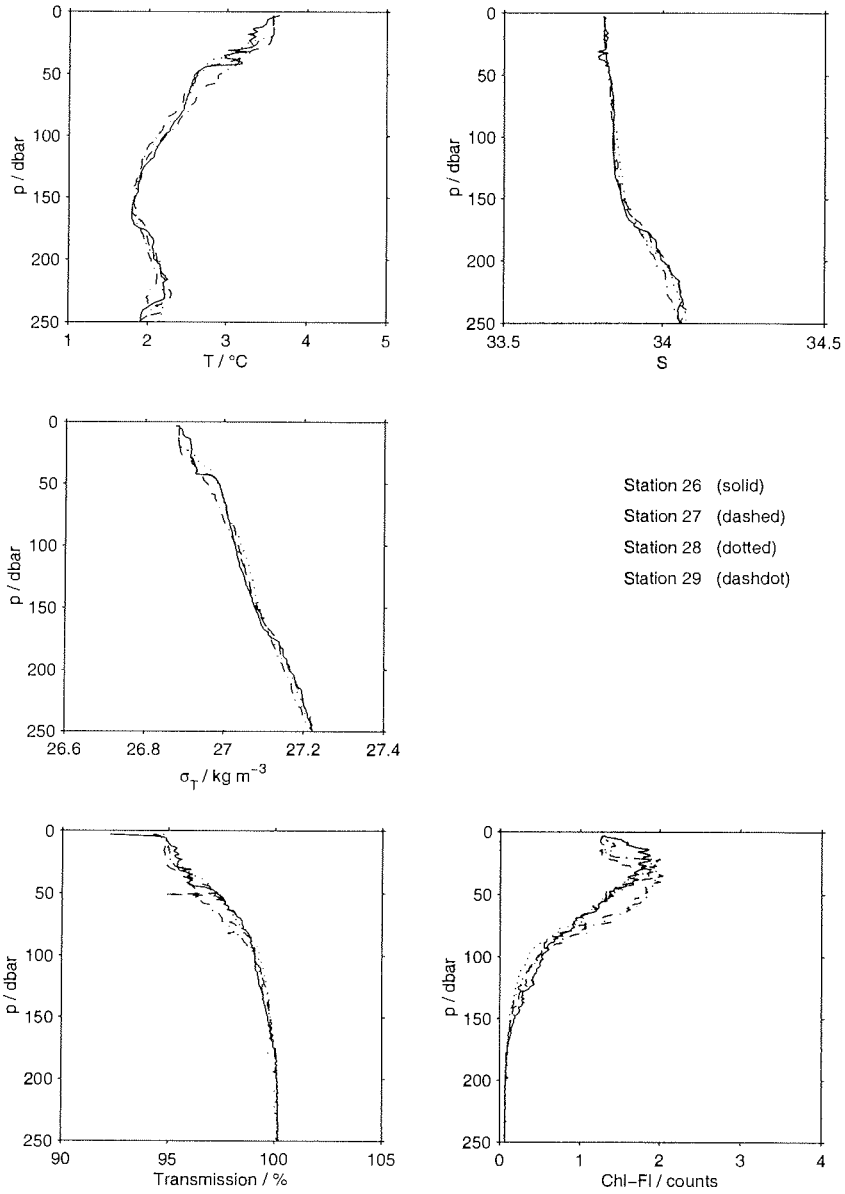

Fig. 10.3.5: Vertical profiles of temperature T, salinity S, density $_{T}$, light transmission and chlorophyll fluorescence obtained with the CTD at stations 26 – 29, part of the first CTD grid and located within the fertilised patch of water.

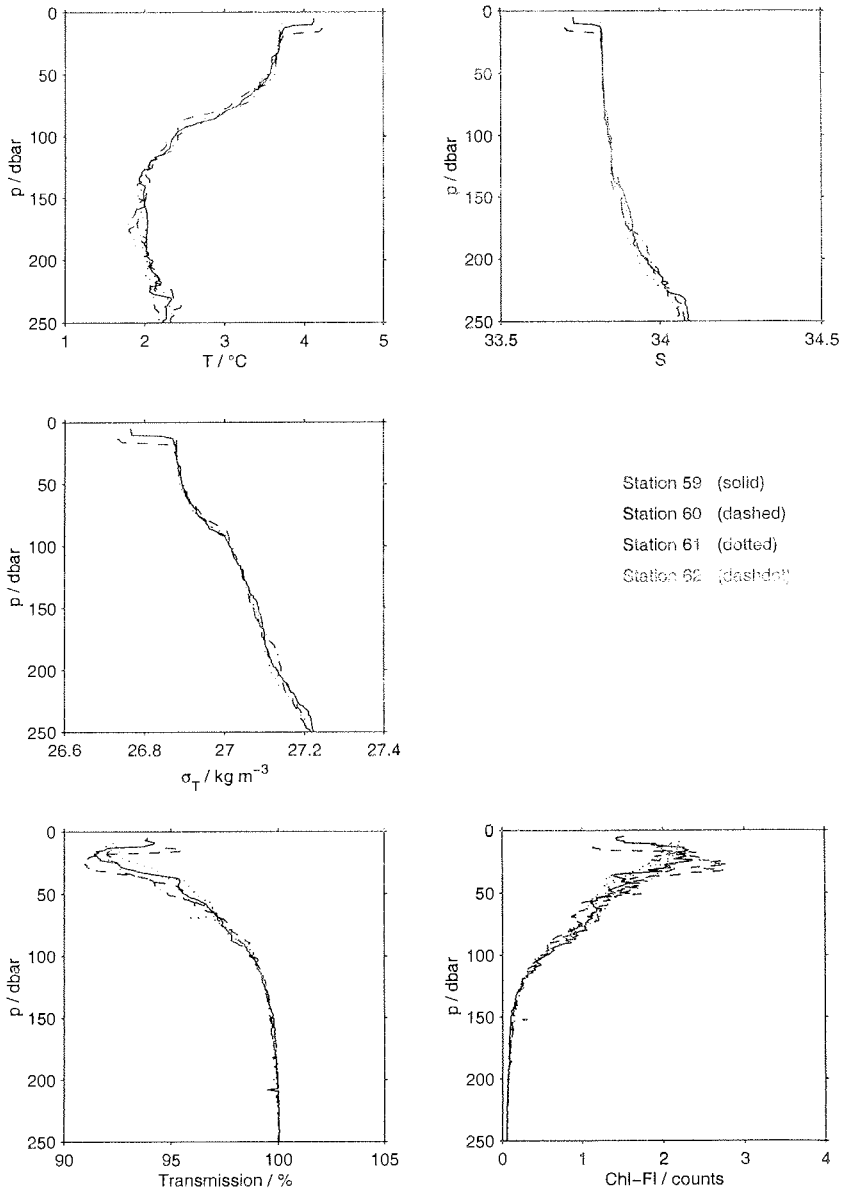

Fig. 10.3.6: Vertical profiles of temperature T, salinity S, density $_T$, light transmission and chlorophyll fluorescence obtained with the CTD at stations 59 – 62, located within the fertilised patch and performed as part of the second CTD grid.

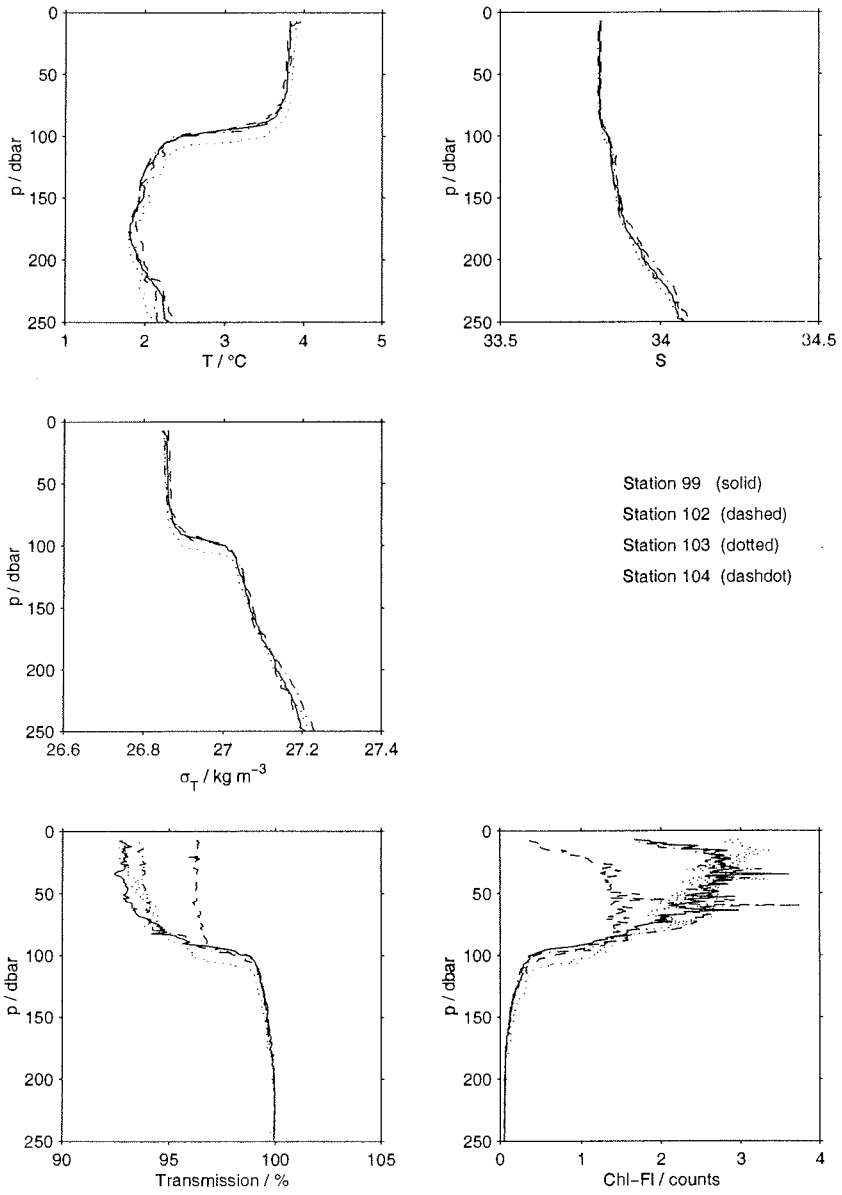

Fig. 10.3.7: Vertical profiles of temperature T, salinity S, density $_T$, light transmission and chlorophyll fluorescence obtained with the CTD at stations 99 – 104, forming part of the third CTD grid. Station 102 was located outside the fertilised patch while the other three stations were inside. The differences between the light transmission as well as fluorescence profiles taken at stations in and outside the patch, and the difference to the profiles taken prior to fertilisation (Fig. 10.3.5) are indicative of the pronounced biological response to iron fertilisation.

10.4 Drift Buoys

V.Strass, B. Cisewski (AWI) and A. Davidov (IfM Kiel)

Essential for conducting a Lagrangian experiment like EISENEX was to monitor continuously the motion of the fertilised patch. For that purpose surface buoys, drogued at roughly mid-depth of the mixed layer, were used.

The spherically shaped surface floats (manufactured by FLOTEC) of 360 kg buoyancy were equipped with GPS receivers giving their geographic position. That position was transmitted by radio (GPS/Radio module manufactured by Hydrosphere UK Ltd) as well as via satellite using ARGOS (GPS/ARGOS module manufactured by Sellmann&Kruse, Bremerhaven). While the radio-transmitted position was sent and received at 10 minute intervals by the ship-borne receiver station (also from Hydrosphere UK Ltd) when within a radius of about 15 km around the ship, ARGOS was used to get the buoy positions at irregular intervals of a few hours when outside the radio range.

The drogues, of basically cylindrical shape, 10 m long and 1.2 m wide, were made from heavy duty net garment according to our design by Engel-Netze, Bremerhaven. The line connecting top buoy and drogue was fitted with shock absorbers made from rubber, in order to damp tension peaks and to allow the buoy to follow the motion of the surface waves in high seas. However, the Kevlar line used was quickly worn by the sliding motion of the shock absorbers, and a second bypass line had to be used to avoid drogue losses. At its deepest point the buoy rig was ballasted so that the top floatation was half above and half below the water surface, when the surface was calm and flat.

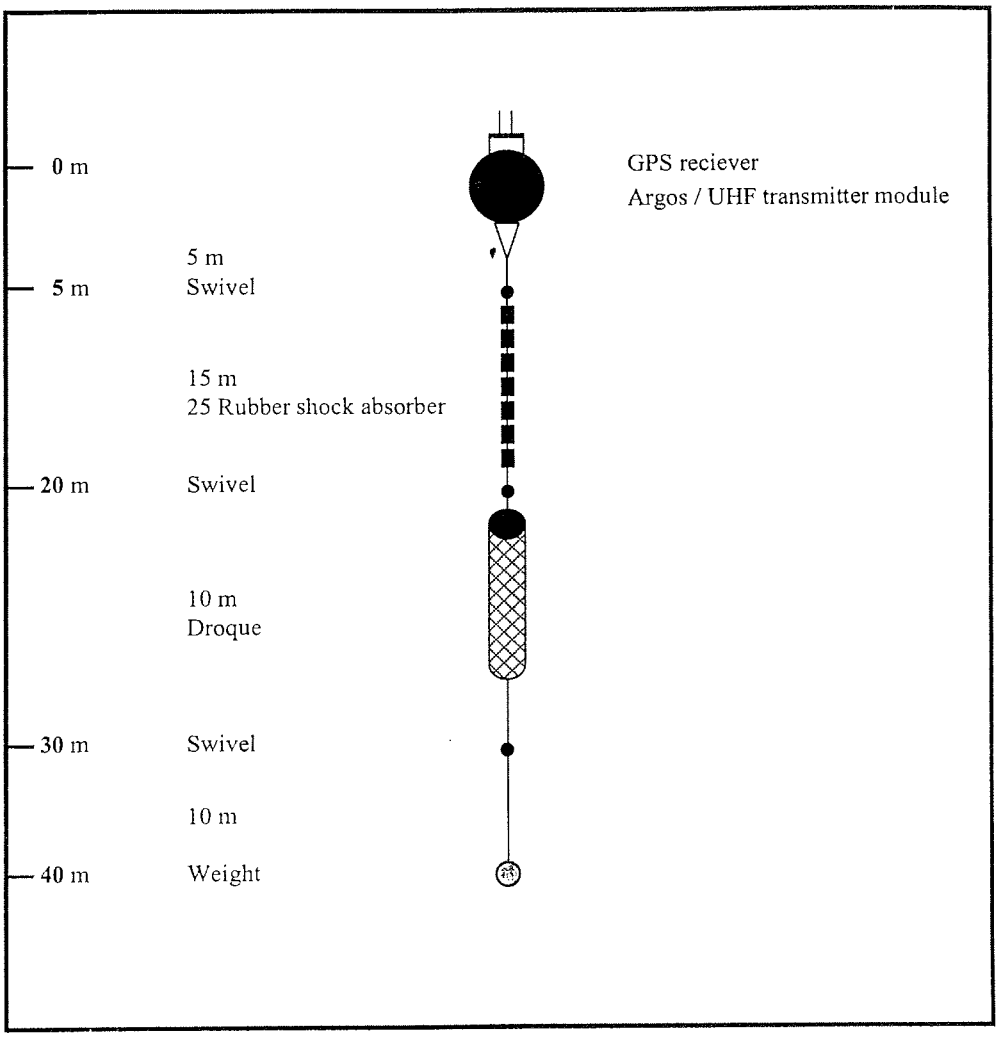

Fig.10i.4.1: Schematic drawing of a drift buoy rig.

Two buoy rigs were in use during the experiment, but, except of one day close to the end of EISENEX, only one at a time. At first instance a buoy was deployed in the centre of the identified eddy, directly prior to iron injection, to provide a navigation aid in order to produce a fertilised patch as homogeneous as possible. This was done with the ship steaming slowly along a widening spiral-shaped track around the drifting buoy while pumping the iron solution, mixed with the SF_6 tracer, into the sea. After iron injection the drift of the buoy, as monitored via radio and ARGOS, provided the primary source of information about the movement of the fertilised patch of water. Despite some losses of equipment and damage to parts of the buoy rigs, the buoys worked very well as trackers of the fertilised patch, given the passage of several storms and the rough seas.

Tab. 104.1: Buoy Deployments

Tracks	Buoy ID	Deployment		Recovery		Comments
	ARGOS 9355	47° 49.11'S, 20° 45.04'E	06.11.2000 22:47	47° 50.55'S, 20° 51.34'E	07.11.2000 13:40	relocation
	ARGOS 9355	47° 50.71'S, 20° 45.01'E	07.11.2000 15:04	47° 51.54'S, 20° 57.00'E	08.11.2000 09:05	loss of droque, SCADCP,CO_2 sensor
1	ARGOS 9355	47° 51.83'S, 20° 55.82'E	08.11.2000 19:15	48° 16.65'S, 21° 16.21'E	14.11.2000 13:45	broken radio antenna
2	ARGOS 9354	48° 13.86'S, 21° 11.10'E	14.11.2000 23:23	48° 21.57'S, 21° 12.18'E	15.11.2000 20:34	relocation
3	ARGOS 9354	48° 17.99'S, 21° 04.03'E	15.11.2000 22:27	48° 04.7 'S, 21° 09.9 'E	25.11.2000 11:11	relocation
4	ARGOS 9355	48° 00.23'S, 21° 05.07'E	24.11.2000 07:28	48° 07.1 'S, 21° 04.2 'E	25.11.2000 09:16	relocation
5	ARGOS 9354	48° 04.86'S, 21° 05.67'E	25.11.2000 11:56	48° 08.6 'S, 21° 16.3 'E	27.11.2000 21:15	loss of droque
	ARGOS 9354	48° 04.7 'S, 21° 11.5 'E	28.11.2000 00:14	48° 05.6 'S, 21° 14.4 'E	28.11.2000 06:30	recovered because of failure of radio transmitter

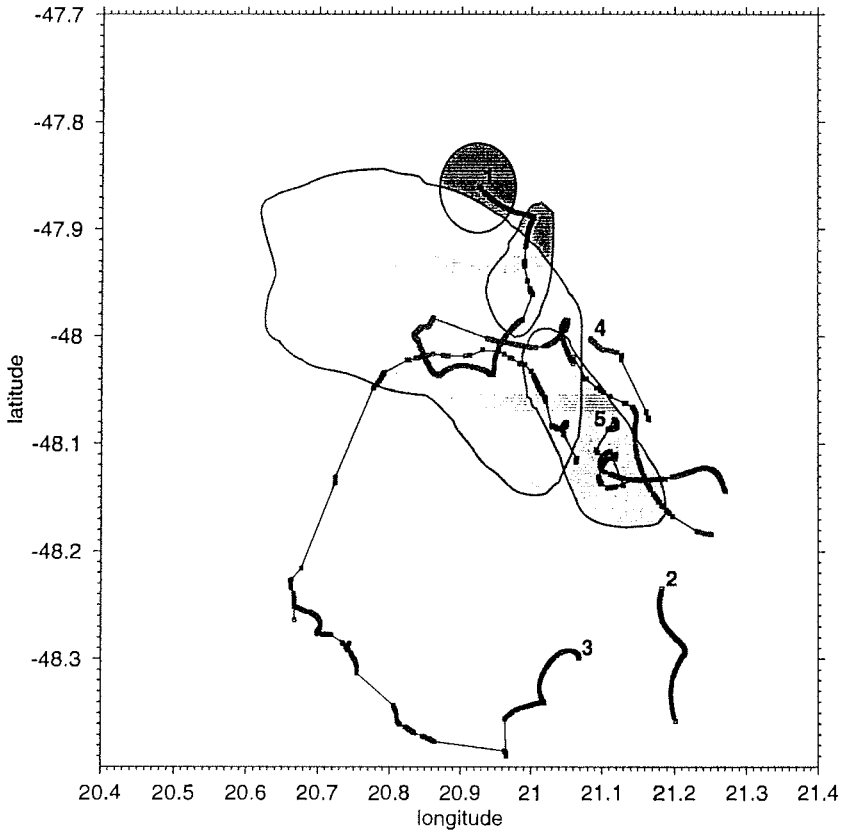

Fig. 10.4.2: Movement of the buoys and of the fertilised patch. The different buoy tracks are numbered, as given in Tab. i.4.1, at their start positions. The tracks of longest individual duration, 1 and 3, are indicative of the closed eddy circulation which, however, is superimposed by tidal motions and inertial oscillations which account for the cusp-like

distortions; that tracks 1 and 3 are not concentric reveals a slight shift of the eddy centre, consistent with repeated ADCP current vector mappings. The patch locations and sizes are drawn on the basis of SF_6 surveys (contribution of A. Watson and co-workers); the different grey shades of the patches indicate the decrease of SF_6 concentrations during the experiment, dark grey for the high concentrations at the beginning and light grey for the low concentrations at the end. Not shown is the patch mapped during the final SF_6 survey as it would almost cover the entire area of the shown four patch mappings. No SF_6 survey was performed when the patch moved more southerly, as is indicated by the southern part of buoy track 3.

10.5 Micro Structure Turbulence Profiling with the MST- Probe

J. Post (Hydromod), F. Trumm (IfMH), V.Strass (AWI)

The MST Profiler

The MST Profiler (also called MICSOS-Profiler) is a free sinking or rising multi-parameter probe equipped with high resolution microstructure (temperature) and turbulence (current shear) sensors and precision CTD sensors. To compensate for disturbing vibrations of the profiler itself, an internal vibration sensor is incorporated. The turbulence is measured by an aerofoil-shaped shear probe with a time constant of 4 ms. The high resolution temperature probe works with an NTC (negative temperature coefficient) which has a time constant of about 10 ms. Data resolution of all sensors is 16 bits. The sampling rate of the profiler is 1 kHz. The data are transmitted via a fast link to a computer on board ship. The descent rate of the profiler can be adjusted by removable weights.

The MST-System consists of a profiler, a special neutrally-buoyant cable, a data and power supply interface and a logger. The system is completed by a data evaluation software package.

Field Work

During the POLARSTERN Cruise ANTXVIII/2 the MST profiler was used to collect data on the micro scale, specifically, water stratification and turbulence characteristics in the upper 200 metres of the water column and especially in the surface mixed layer. The MST-profiler was adjusted to descend with a sinking velocity of about 80 to 90 cm/sec.

The measurements were carried out from the working deck. Downcasts were made by paying out the cable by hand whereas the instrument was recovered by heaving the cable over a block with a capstan on the working deck. To make sure that the probe would not endamage the ships propeller the probe

was lowered from the forward end of the working deck and carefully watching its sinking path.
In general a maximum measuring depth of about 200 metres was reached. Due to time restrictions on the one hand and the deep profiling depth on the other only five casts per station could be carried out. Between 2nd and 29th of November a total number of 19 measurements, i.e. 90 individual casts, were carried out. In total these measurements brought about 650 Mbytes recorded data. The MST station list is provided below.

First Results
Despite the first ten days of the cruise having calm weather and sea conditions most of the MST-profiling was done during more or less rough weather and sea conditions. These rough conditions caused a pronounced mixed layer which in the maximum reached about 100 metres. This layer clearly can be seen from the vertical profiles of both of the profiler's temperature sensors.
The raw data from the shear probe during stormy conditions reveal high shear values for the entire mixed layer and low shear values beneath the mixed layer. However, already a few hours after the wind has decreased a slight decrease of mixing in the deeper mixed layer could be observed from the shear probe data. Two profiler graphs are shown below as examples.
A thorough processing and evaluation of the MST-data will be carried out after the cruise in the home laboratories.

Tab. 10.5.1: Protocol – List for MST - Profiling

Event No.:	Cast No.:	Date	Time [UTC]	Position *LAT. S*	*LONG. E*	File-name	*MAX. DEPTH [M]*
007	001	02.11.00	02:50			E007c001	not recorded
„	002	„	03:12	49° 17.20'	20° 02.91'	E007c002	„
„	003	„	03:21	49° 17.18'	20° 02.98'	E007c003	„
„	004	„	03:32	49° 17.14'	20° 03.06'	E007c004	„
„	005	„	03:46	49° 17.12'	20° 03.17'	E007c005	„
009	001	07.11.00	09:20	47° 49.29'	20° 49.47'	E009c001	not recorded
„	002	„	09:35	47° 49.59'	20° 49.82'	E009c002	„
„	003	„	09:46	47° 49.73'	20° 49.99'	E009c003	max.140m
„	004	„	09:56	47° 49.83'	20° 50.21'	E009c004	not recorded
„	005	„	10:09	47° 49.88'	20° 50.23'	E009c005	ca. 200m
„	006	„	10:21	47° 49.91'	20° 50.24'	E009c006	not recorded
011	001	08.11.00	19:25	47° 51.32'	20° 55.35'	E011c001	not recorded
„	002	„	19:37	47° 51.98'	20° 56.02'	E011c002	„
„	003	„	19:52	47° 52.10'	20° 56.16'	E011c003	„
„	004	„	20:00	47° 52.23'	20° 56.35'	E011c004	„
„	005	„	20:17	47° 52.31'	20° 56.44'	E011c005	„
014	001	10.11.00	04:12	47° 59.67'	20° 54.67'	E014c001	not recorded
„	002	„	04:26	47° 59.70'	20° 54.01'	E014c002	„
„	003	„	04:39	47° 59.70'	20° 53.94'	E014c003	„
„	004	„	04:51	47° 59.70'	20° 53.79'	E014c004	„
„	005	„	05:03	47° 59.70'	20° 53.73'	E014c005	„
„	006	„	05:14	47° 59.70'	20° 53.59'	E014c006	„
018	001	10.11.00	13:44	47° 59.73'	20° 54.60'	E018c001	193m
„	002	„	13:53	47° 59.74'	20° 54.60'	E018c002	208m
„	003	„	14:04	47° 59.74'	20° 54.58'	E018c003	203m
„	004	„	14:13	47° 59.74'	20° 54.56'	E018c004	193m
„	005	„	14:25	47° 59.75'	20° 54.51'	E018c005	204m
038	001	11.11.00	13:35	47° 59.41'	20° 51.71'	E038c001	200m

„	002	„	13:48	47° 59.44'	20° 51.84'	E038c002	201m
„	003	„	13:59	47° 59.43'	20° 51.95'	E038c003	203m
„	004	„	14:09	47° 59.37'	20° 51.95'	E038c004	191m
„	005	„	14:19	47° 59.30'	20° 51.98'	E038c005	196m
„	006	„	14:30	47° 59.22'	20° 52.06'	E038c006	196m
041	001	12.11.00	14:12	47° 59.88'	20° 56.41'	E041c001	191m
„	002	„	14:25	47° 59.91'	20° 56.59'	E041c002	162m
„	003	„	14:35	47° 59.98'	20° 56.66'	E041c003	174m
„	004	„	14:46	48° 00.02'	20° 56.76'	E041c004	185m
„	005	„	14:56	48° 00.13'	20° 56.98'	E041c005	182m
043	001	13.11.00	14:14	48° 04.38'	21° 05.22'	E043c001	198m
„	002	„	14:33	48° 04.51'	21° 05.14'	E043c002	197m
„	003	„	14:45	48° 04.59'	21° 05.06'	E043c003	204m
„	004	„	14:58	48° 04.73'	21° 05.01'	E043c004	190m
„	005	„	15:07	48° 04.86'	21° 04.98'	E043c005	187m
045	001	15.11.00	09:56	48° 17.09'	21° 07.66'	E045c001	193m
„	002	„	10:09	48° 17.11'	21° 07.69'	E045c002	192m
„	003	„	10:22	48° 17.14'	21° 07.73'	E045c003	199m
„	004	„	10:32	48° 17.13'	21° 07.77'	E045c004	175m
„	005	„	10:45	48° 17.11'	21° 07.78'	E045c005	203m
„	006	„	10:56	48° 17.08'	21° 07.81'	E045c006	192m
046	001	16.11.00	15:08	48° 20.37'	21° 00.87'	E046c001	212m
„	002	„	15:21	48° 20.35'	21° 00.85'	E046c002	205m
„	003	„	15:32	48° 20.32'	21° 00.80'	E046c003	212m
„	004	„	15:46	48° 20.43'	21° 00.70'	E046c004	211m
„	005	„	15:58	48° 20.42'	21° 00.64'	E046c005	211m
048	001	17.11.00	13:50	48° 35.38'	20° 42.78'	E048c001	207m
„	002	„	14:01	48° 35.32'	20° 42.67'	E048c002	204m
„	003	„	14:13	48° 35.29'	20° 42.57'	E048c003	205m
„	004	„	14:23	48° 35.23'	20° 42.47'	E048c004	204m
„	005	„	14:34	48° 35.22'	20° 42.37'	E048c005	206m
049	001	18.11.00	11:24	48° 20.99'	20° 51.92'	E049c001	205m

„	002	„	11:36	48° 21.02'	20° 51.89'	E049c002	209m
„	003	„	11:46	48° 21.04'	20° 51.87'	E049c003	206m
„	004	„	11:57	48° 21.07'	20° 51.84'	E049c004	210m
„	005	„	12:07	48° 21.10'	20° 51.84'	E049c005	203m
078	001	29.11.00	06:02	47° 49.43'	20° 59.13'	E078c001	191m
„	002	„	06:23	47° 49.45'	20° 49.45'	E078c002	206m
(1)							
082	001	23.11.00	12:50	48° 04.03'	21° 00.81'	E082c001	205m
„	002	„	13:01	48° 04.09'	21° 00.84'	E082c002	195m
„	003	„	13:14	48° 04.20'	21° 00.82'	E082c003	191m
„	004	„	13:28	48° 04.30'	21° 00.80'	E082c004	201m
„	005	„	13:40	48° 04.38'	21° 00.75'	E082c005	200 m
084	001	23.11.00	17:05	48° 01.91'	20° 52.64'	E084c001	195m
„	002	„	17:16	48° 01.92'	20° 52.70'	E084c002	198m
„	003	„	17:27	48° 01.95'	20° 52.78'	E084c003	201m
„	004	„	17:43	48° 01.97'	20° 52.85'	E084c004	198m
„	005	„	17:52	48° 01.98'	20° 52.91'	E084c005	209m
087	001	23.11.00	22:36	48° 02.58'	21° 11.32'	E087c001	195m
„	002	„	22:47	48° 02.62'	21° 11.43'	E087c002	197m
„	003	„	23:01	48° 02.65'	21° 11.62'	E087c003	172m
„	004	„	23:11	48° 02.63'	21° 11.75'	E087c004	192m
„	005	„	23:18	48° 02.66	21° 11.85'	E087c005	187m
092	001	27.11.00	14:13	48° 06.85'	21° 12.69'	E092c001	204m
„	002	„	14:24	48° 06.84'	21° 12.77'	E092c002	200m
„	003	„	14:35	48° 06.81'	21° 12.85'	E092c003	200m
„	004	„	14:50	48° 06.82'	21° 12.89'	E092c004	201m
„	005	„	15:00	48° 06.82'	21° 12.91'	E092c005	200m
108	001	29.11.00	17:13	47° 40.15'	20° 39.28'	E108c001	209m
„	002	„	17:25	47° 40.18'	20° 39.34'	E108c002	210m
„	003	„	17:36	47° 40.21'	20° 39.40'	E108c003	207m
„	004	„	17:50	47° 40.25'	20° 39.47'	E108c004	204m
„	005	„	18:00	47° 40.26'	20° 39.56'	E108c005	201m

Tab. 10.5.2: List of Remarks

Event No.:	Cast No.:	Date	Remarks
007	001	02.11.00	NTC (fast temperature sensor) failed
009	003	07.11.00	Measuring depth max.140m ; strong drift of the ship
011	004	08.11.00	Recorded from 60m
038	004	11.11.00	not recorded
041	001 - 005	12.11.00	Wind force 8-9 Bft (19 m/s) , increasing to 21 m/s ; strong propeller activities
043	001 -005	13.11.00	Wind force 7-8 Bft.
045	001-006	15.11.00	strong thruster activities
078	003	29.11.00	After the 2nd cast failure of pressure sensor
092	001-005	27.11.00	Stormy weather conditions, high wind waves

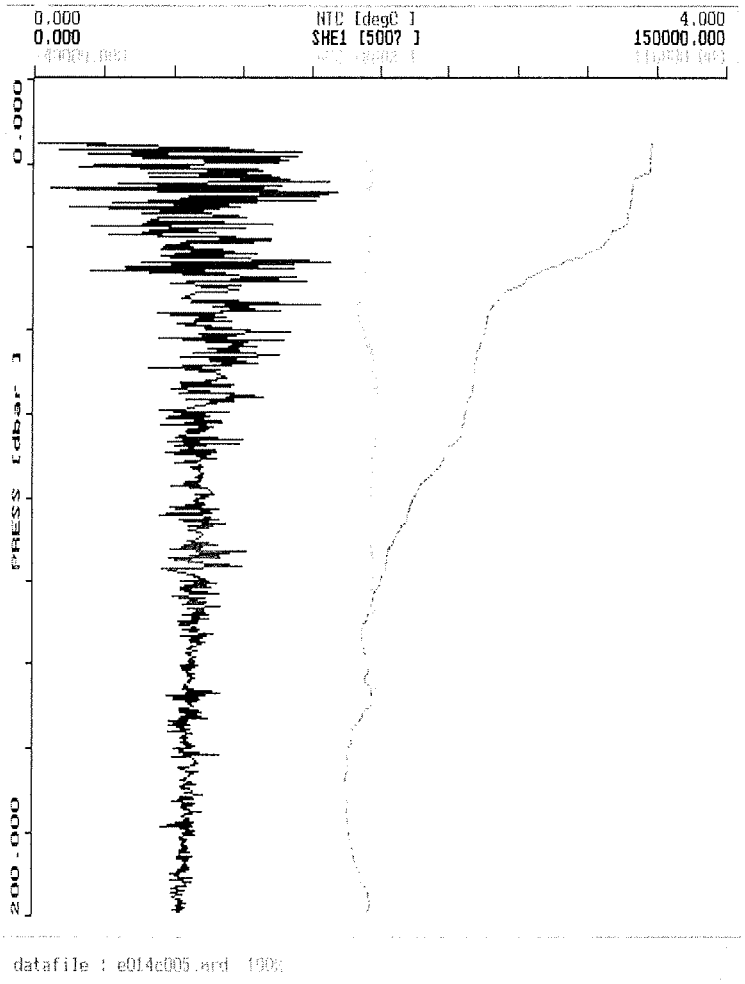

Fig. 10.5.1: Vertical profiles of temperature T (NTC), acceleration (ACC) and shear (SHE1) recorded with the MST-Probe at station 14.

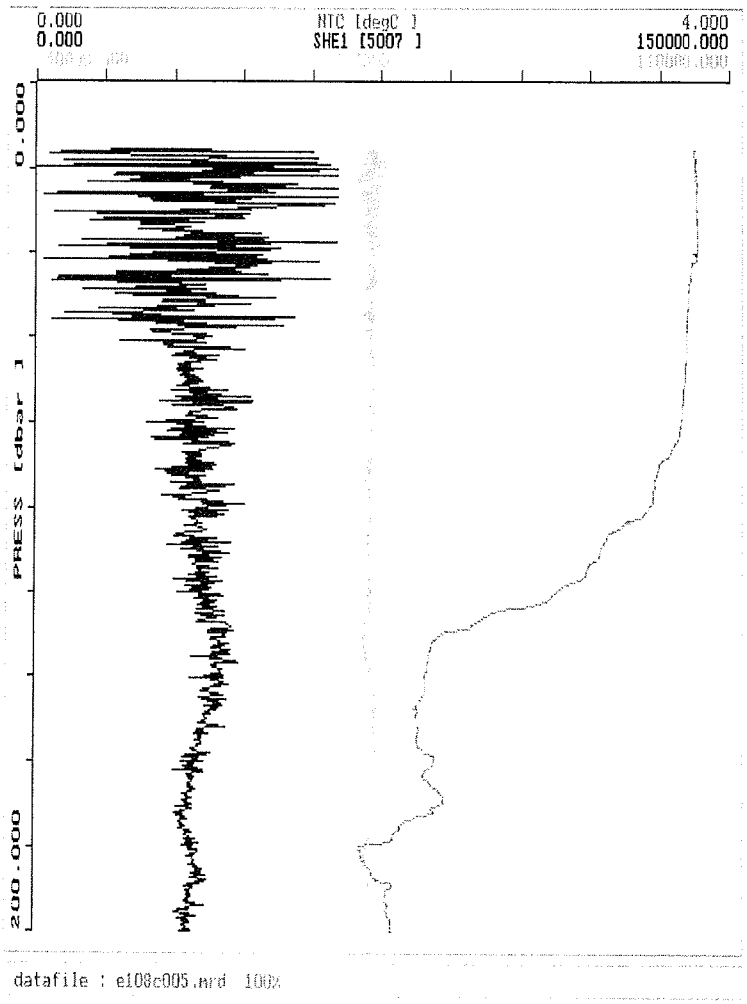

Fig. 10.5.2: Vertical profiles of temperature T (NTC), acceleration (ACC) and shear (SHE1) recorded with the MST-Probe at station 108.

11. SCANFISH: UNDERWAY MEASUREMENTS OF HYDROGRAPHIC AND BIOLOGICAL VARIABLES

S. Gonzalez, H. de Baar (NIOZ), V. Strass, H. Leach, J. Post, V. Duarte (AWI)

The Scanfish (GMI MKII 1250-15 DK.) is a streamlined, wing-shaped body towed behind the steaming ship. Two flaps at its rear end allow the Scanfish to made vertically undulations throughout the upper water column according to the parameter setting entered at the control unit deck. The deck range was enhanced by use of an active winch holding an unfaired Coax towing cable, cable which was paid out during dive of the Scanfish and retrieve during climb. A depth range of 4 to 220 m was achieved at ship's speed of 6.5 to 7.5 knots. The dive/climb rate was 0.4 m/s. Scanfish attitude while being towed, as well the scientific data were monitored and recorded in real-time on deck.

Scanfish components

-*Surface component*, means Scanfish MKII presentation, logging software, PowCom-Power and communication unit for vehicle interface. The navigational data from DGPS is incorporated in the data stream using the NMEA-interface of the Seabird deckunit.

-*Underwater vehicle and sensors*: inboard control unit, cables, depth sensor, altimeter, Seabird 911 interface, Seapoint Turbidity Meter, PAR sensor, Oxigen sensor and Chelsea fluorometer.

-*Winch type Cormac 1500*, equipped with ca. 2300 m cable ∅8.3 mm, type 32-OHM COAX2-20. Weight: 2000 kg.

- *Scanfish measures*
Cord: 800 mm
Span: 1560 mm
Area: 1250 m2
System weight: 110 kg

ANT XVIII / 2: Measurements with the instrument were made in a transect along the 20° E (Trans 1-2a) and during a mesoscale survey (Grid 1a-1f) as indicated in Table 11.1.

	Start Date	Start time	Start Latitude S	Start Longitude E	End Latitude S	End Longitude E	Tow Time hours	End Date	End time	Distance covered kms.	Minimun depth m	Maximun depth m
Trans1	28-Oct	23:44	45 00.64	20 00.59	46 00.32	19 59.58	9.4	29-Oct	08:40	112	1.4	244.4
Trans1b	29-Oct	14:13	46 06.83	20 00.47	47 40.84	20 00.01	13.5	30-Oct	03:43	138	1	218.8
Trans1c	30-Oct	03:50	47 41.78	20 00.03	49 54.39	20 00.11	19.1	30-Oct	22:56	158	1.0	196.10
Trans1d	30-Oct	23:36	49 56.47	19 59.29	50 01.68	20 00.08	0.8	31-Oct	08:36	9	2.7	195.10
Trans2a	31-Oct	19:44	52 02.04	19 59.02	49 19.51	20 00.22	22.6	01-Nov	18:52	209	3	196.3
Grid 1a	03-Nov	01:48	47 21.49	22 00.00	49 09.16	22 00.00	14.4	03-Nov	16:12	201	1.6	195.1
Grid 1b	03-Nov	16:18	49 09.88	21 48.04	49 09.47	21 59.26	1.1	03-Nov	17:24	2	1	186.2
Grid 1c	03-Nov	17:47	49 09.94	21 48.40	47 09.93	21 48.08	19.3	04-Nov	13:05	224	1.2	238.5
Grid 1d	04-Nov	13:13	47 10.11	21 27.14	47 09.60	21 27.24	1.6	04-Nov	14:49	19	1.5	213.8
Grid 1e	04-Nov	18:31	47 10.22	21 01.34	49 09.60	20 48.31	17.4	05-Nov	11:53	224	1	224.7
Grid 1f	05-Nov	12:01	49 09.97	20 47.53	47 09.48	20 47.12	17.6	06-Nov	05:37	224	2.1	227.4
									Total kms.	**1520**		

12. IRON FERTILISATION IN THE ATLANTIC SECTOR OF THE SOUTHERN OCEAN

P. Croot, M. Boye, J. Nishioka, A. Fischer, M Rijkenberg, K. Kroon, P. Laan, Y. Bozec, H. de Baar, K. Timmermans, T. van Oijen, Marcel Veldhuis, S. Gonzalez, M. Weinbauer, T. Arrieta (NIOZ)

Research conducted during the iron enrichment experiment by the Netherlands scientific team of the Netherlands Institute for Sea Research (NIOZ), Rijksuniversiteit Groningen (RUG) and Interfacultair Reactor Instituut Technische Universiteit Delft (IRI/TUD), and one guest investigator from CRIEPI (Japan). The Netherlands participation is supported by the EU program CARUSO, the bilateral Netherlands-Bremen Oceanography (NEBROC) program, and three grants of the Netherlands Antarctic Programme on (i) Biological Availability of trace metals for Antarctic phytoplankton, (ii) Positive feedback of UV-B via iron chemistry of seawater on phytoplankton growth and CO2 fixation, and (iii) In situ iron enrichment experiment in the Southern Ocean.

12.1 Size fractionation and chemistry of Fe during Fe fertilization experiment

J. Nishioka[1,2], M. Boye[2], P. Croot[2], P. Laan[2], K. R. Timmermans[2] and H.J.W de Baar[2]
1: Central Research Instituite of Electric Power Industry (CRIEPI)
2: Netherlands Institute for sea research (NIOZ)

Introduction

The relationship between Fe dynamics and phytoplankton growth is important for study Fe biogeochemistry after Fe fertilization. Size-fractionated Fe analysis will be one of useful approach for study the Fe dynamics.
Previous laboratory studies suggested that Fe in small colloidal particle form in traditionally dissolved fraction (< 0.2 _ m) might be one of available Fe form for oceanic phytoplankton with some mechanisms such as cell-surface reduction (Wells and Mayer, 1991; Wells et al., 1991; Kuma and Matsunaga, 1995; Nishioka and Takeda, 2000). Therefore, we investigated change of size-fractionated Fe during ambient phytoplankton growth by using trace metal clean filtration method, which using a 0.2 _ m pore size membrane filter and a 200 kDa nominal molecular weight polyethylene hollow-fiber ultrafilter (Nshioka and Takeda, 2000), after Fe fertilization.

We also compared size-fractionated Fe concentration with size-fractionated organic ligands concentration (with Boye) for study Fe chemistry in the seawater.

Method

Sample collection and size-fractionated Fe analysis

The samples were collected at every in patch station and several out patch station (Table 1). To characterize vertical profiles of size-fractionated Fe, seawater samples were collected using 10-L Go-Flo bottles suspended on Kevlar line and take samples from 5 ~ 10 depth at each station.

The 0.2 μm filtrate samples collected in 500-ml Polycarbonate bottles were immediately size-fractionated by a clean filtration method, which used a 200 kDa polyethylene hollow-fiber ultrafilter unit (filter area 70 cm^2, STERAPORE, Mitsubishi-rayon Co., Ltd.) attached to the end of a Teflon tube submerged in the seawater sample. All filtrates and unfiltered samples were then buffered at pH 3.2 with 10 M formic acid-2.4 M ammonium formate buffer solution (0.6 ml buffer solution per 125-ml of sample solution). In-line filtration and sample treatments were performed in a laminar flow clean air. Concentrations of Fe (III) in the buffered samples were determined with an automatic Fe (III) analyzer (Kimoto Electric Co. Ltd.) using chelating resin concentration and chemiluminescence detection (Obata et al., 1993,1997).

The determined Fe is a chemically labile species, which is in unfiltered and filtered seawater and strong reacts with 8-hydroxyquinoline resin at pH 3.2. Measured total acid-labile Fe (unfiltered, detected at pH 3.2) concentrations were divided into three size fractions: large labile particulate Fe (> 0.2 μm), small colloidal Fe (200 kDa–0.2 μm) and soluble Fe (< 200 kDa). Also we define dissolved Fe as Fe which passed through 0.2 μm and detectable at pH 3.2 (Nishioka et al., Submitted).

Table 12.1.1 Sampling station number for vertical distribution for size-fractionated Fe

Date	Station number	In or out of patch
7 Nov.	St.009	Before Fe release
9 Nov.	St.011	In patch station
9 Nov.	St.012	Out patch station
10 Nov	St.014	In patch station
11 Nov.	St.038	In patch station
12 Nov.	St.041	In patch station
15 Nov.	St.045	In patch station
16 Nov.	St.046	In patch station
17 Nov.	St.048	Out patch station
18 Nov.	St.049	In patch station
20 Nov.	St.061	In patch station
23 Nov.	St.081	In patch station
24 Nov.	St.088	In patch station
25 Nov.	St.090	In patch station
27 Nov.	St.092	In patch station
28 Nov.	St.103	In patch station
29 Nov.	St.107	In patch station
29 Nov.	St.108	Out patch station

Preliminary Results

Size-fractionated Fe in the patch

Before Fe release, ambient dissolved Fe (< 0.2 μm) concentration in surface mixed layer of experiment site was less than 0.1 nM. After the $FeSO_4$ solution was released to the surface seawater, dissolved Fe concentration increased significantly. With regard of size fraction, small colloidal Fe comprised more than 60 ~80 % of dissolved Fe just after Fe release. Fe concentration in the surface mixed layer decreased gradually during 6 days, however percentage of colloidal Fe in the dissolved phase was not so changeable. After the phytoplankton increased in the patch (21 days after the Fe release), the portion of Fe concentration in the large labile particle fraction (>0.2 μm, detectable at pH 3.2) was higher than initial of experiment (1 or 2 days after Fe release) (Fig 12.1.1 and 12.1.2). It may reflect that some of small colloidal Fe adsorbed on the organic particle during experiment and kept in the surface mixed layer in the patch.

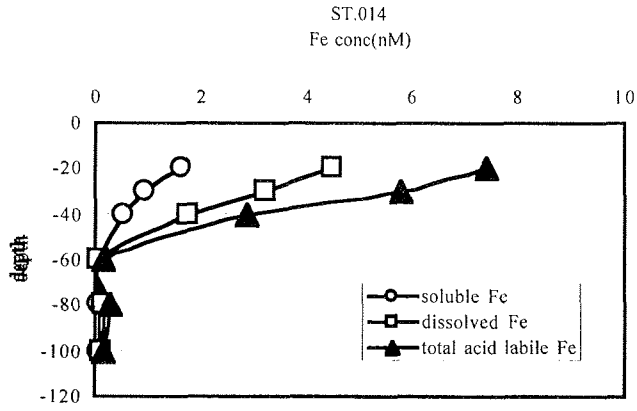

Fig. 12.1.1 Vertical distribution of size fractionated Fe concentrations in the patch (2 days after Fe release)

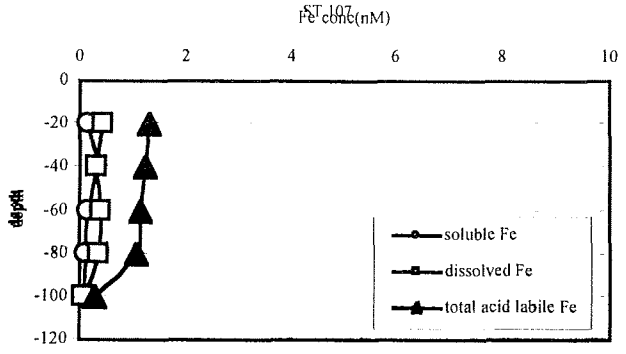

Fig. 12.1.2 Vertical distribution of size fractionated Fe concentration in the patch (21 days after Fe release)

Reference

Kuma, K. and K. Matsunaga. 1995. Availability of colloidal ferric oxides to coastal marine phytoplankton. Mar. Biol. **122**: 1-11.

Nishioka, J. and Takeda, S. 2000. Change in the concentrations of iron in different size fractions during growth of the Oceanic diatom *Chaetoceros* sp. : importance of small colloidal iron. Mar. Biol.

Nishioka, J. and Takeda, C. S. Wong[2], W. K. Johnson Submitted. Size-fractionated iron concentrations in the northeast Pacific Ocean: Distribution of soluble and small colloidal iron
Obata, H., H. Karatani and E. Nakayama. 1993. Automated determination of Iron in seawater by chelating resin concentration and chemiluminescence detection. Anal. Chem. **65**: 1524-1528.
Obata, H., H. Karatani, M. Matsui and E. Nakayama. 1997. Fundamental studies for chemical speciation of iron in seawater with an improved analytical method. Mar. Chem. **56**: 97-106.
Wells, M. L. and L. M. Mayer. 1991. The photoconversion of colloidal iron oxyhydroxides in seawater. Deep-Sea Res. I **38**: 1379-1395.
Wells, M. L. and L. M. Mayer, O. F. X. Donard, M. M. de Souza Sierra and S. G. Ackelson. 1991. The photolysis of colloidal iron in the oceans. Nature **353**: 248-250.

12.2 Organic complexation of dissolved iron

M. Boye[1,2], J. Nishioka[3,2], P. Croot[2], P. Laan[2], K.R. Timmermans[2] and H.J.W de Baar[2]
1: University of Groningen, The Netherlands.
2: Netherlands Institute for sea research (NIOZ)
3: Central Research Instituite of Electric Power Industry (CRIEPI)

A synopsis is presented here of measurement, by Cathodic Stripping Voltammetry (CSV), of the organic complexation of Fe in filtered seawater and in size-fractionated fraction (<200 kDa). Samples were taken within the course of the Fe-fertilization experiment in the patch as compared to out-patch stations.

1. Introduction

The organic complexation of Fe is described by the concentration of the organic Fe-binding ligand and by the complex stability of these ligands with Fe(III). These terms are of a particular importance for understanding the hidden processes of Fe limitation of the primary productivity, since the organic complexation would act to keep Fe longer in solution rather than allowing it to precipitate. The residence time of iron in sea-surface can thus be considerably enhanced by the organic complexation, providing a long term availability of Fe to micro-organisms. An increase of the iron-binding ligand concentration was previously observed during the course of iron-fertilization experiments (IronEx-II [Rue and Bruland, 97] and SOIREE [Croot et al., in prep.]), and this was investigated here.

Moreover, the organic ligand of Fe have been previously detected either in 0.45 _m or 0.2 _m filtered waters. But it is not known whether these ligands are trully soluble (as defined as <200 kDa) or are small organic colloides (200 kDa–0.2 μm) [see Nishioka et al. Report]. This was investigated here in natural seawater as well as in some Fe-fertilized waters.

2. Method

The sampling procedure is described in Croot et al. and in Nishioka et al. reports. The organic complexation of Fe was determined in filtered (0.2 _m) samples taken at depth at three out-patch stations (St.007, 009 and 048) and at 12 in-patch stations (St.011, 014, 038, 041, 045, 046, 049, 061, 088, 090, 092, 107). This was also determined in discrete size-fractionated samples (<200 kDa) of natural seawater samples (taken at St.007, 009, 048) and taken from in-patch stations (St.011,014, 061, 088 and 090).

To describe the CSV method briefly, a synthetic ligand (2-(2-thiazolylazo)p-cresol, e.g. TAC) is added in large amount to the seawater sample to bind iron, after which voltammetric analysis is carried out [adapted from Croot and Johansson, 2000]. The Fe-binding capacity in the seawater tank was estimated by titration of the free Fe-binding ligand against competition with TAC. The method is described in detail in Boye et al. (2001), whilst TAC was used here instead of NN in the previous study.

Voltammetric measurement was carried out at pH 8.1 using borate buffer (final concentration 5 mM), with 10 mM of TAC (giving a detection window of $10^{11.4}$ to $10^{13.4}$), and the Fe-step additions used to titrate the ligand were on the order of 0.25 nM to 1 nM Fe ranging from 0 to 8 nM Fe additions. The voltammetric procedure was carried out using the fast linear sweep waveform (10.1 $V.s^{-1}$, step potential 1.98 mV), with a deposition potential of –0.4 V.

3. Results

The cruise was devoted to the collection and analyses of the samples on board. Due to the relatively high number of samples taken for the organic complexation of Fe, the data processing was postponed until after the cruise and will be achieved in the next coming months.

References:
Boye M., C.M.G. van den Berg, J.T.M. de Jong, H. Leach, Peter Croot and Hein J.W. de Baar (2001). Organic complexation of iron in the Southern Ocean. *Deep-Sea Research I*, in press.
Croot P.L. and Johansson M. (2000).Determination of iron speciation by cathodic stripping voltammetry in seawater using the competing ligand 2-(2-thiazolylazo)-p-cresol (TAC). *Electroanalysis*, **12**, 565-576.
Rue E.L. and Bruland K.W. (1997). The role of organic complexation on ambient iron chemistry in the equatorial Pacific Ocean and the response of a mesoscale iron addition experiment. *Limnology and Oceanography*, **42**, vol.5, 901-910.

12.3 Effects of UV radiation on iron speciation and its availability for phytoplankton

M. Rijkenberg & A. Fischer, H. de Baar (NIOZ), L. Gerringa, K. Kroon (TU Delft), A. Buma, K. Timmermans (NIOZ), B. Wolterbeek (TU Delft), M. Veldhuis (NIOZ), H. van Elteren (TU Delft), P. Croot, P. Laan, M. Boye (NIOZ)

Introduction

The iron chemistry in the Southern Ocean receives currently considerable attention, but is still poorly understood. Therefore more research is needed. On board of R.V. Polarstern, during cruise ANTXVIII/2, a large scale iron enrichment experiment was carried out, In order to gain more information on the effect of iron on the phytoplankton community. In this iron enrichment experiment the focus of our research was on: firstly the effect of UV on the iron chemistry and, secondly the bioavailability of the different forms of Fe for phytoplankton growth.

Our research is based on the following hypotheses:

1. Most dissolved iron in the ocean is kept in solution by organic ligands.
2. The photo reduction of iron (III) to iron (II) is for an important part driven by UV radiation.
3. The bioavailability of iron is expected to depend on the kinetics between the different chemical forms of iron.

Special bottles were made for deckincubations on the helideck. These bottles were made from PMMA(polymethylmetacrylate) and are transparent for the total solar spectrum including UVA and UVB. Additional light regimes were 80% reduction of the total spectrum, 50% reduction of the total spectrum, UVA filter, UVA&B filter. With these different filters it was possible to investigate the

influence of the different wavelengths of light on iron chemistry and phytoplankton. Dark bottles were also included in this research as a blank. The deck incubations included filtered seawater (for the understanding of the iron chemistry in seawater) and phytoplankton experiments (both uni-algal Antarctic cultures and natural population samples). The iron chemistry of the water was followed during a day-night cycle and during the time of the daily maximum in UV irradiance. Three chemical forms of iron were measured during these experiments, total dissolved iron, Fe(II) and labile Fe(III). The labile Fe(III) fraction presents the fraction of iron not bound or weakly bound to organic ligands. It is a fraction defined by the procedure used in this investigation: the fraction that is adsorbed on a 1-nitroso-2-naphtol preloaded SepPak column (Gledhill & van den Berg 1994).
For the phytoplankton experiments the influence of light conditions on the growth of the natural population and uni-algal cultures were studied and daily uptake experiments of iron were performed. We used the radiotracers ^{55}Fe and ^{59}Fe for these experiments.

Methods
Day-night cycle of iron chemistry and kinetics of iron reduction.
Bottles were incubated with 1.25 nM $^{59}Fe(III)$ on a sunny day to have the largest differences between light regimes. For the daily cycle experiment bottles were incubated under 4 different light conditions : UVB+UVA+PAR (PAR is Photosynthetic Active Radiation), UVA+PAR, PAR and a dark bottle. Samples were taken to measure Fe(II), labile Fe(III) and total dissolved iron 5 times during 24 hours.
For the kinetics of iron reduction, samples were taken during a 2-hour period at the time of day when there was a maximum in the UV irradiance. Samples were taken for Fe(II) and labile Fe(III) measurements. At the start and at the end of the experiment samples for total dissolved iron were taken. For these experiments an amount of approximately 0.5 nM radiotracer ^{55}Fe or 2.5 nM radiotracer ^{59}Fe was added as inorganic Fe(III) species. The Fe(II) fraction was determined using a SepPak column preloaded with ferrozine (Whitney King et al. 1991) and labile Fe(III) using a SepPak column preloaded with 1-nitroso-2-naphtol (Gledhill & van den Berg 1994). These SepPak preconcentration columns were eluted with methanol to obtain the desired Fe fraction and afterwards eluted with hydrochloric acid to remove any unspecifically bound Fe from the column. Then the different isotopic fractions

were counted. The analytical error in the Fe(II) measurement is 2%, a similar or lower analytical error is expected in the labile Fe(III) measurement.

Daily iron uptake experiments.
Bottles were incubated with either seawater containing a natural phytoplankton population or uni-algal Antarctic cultures in filtered seawater. The natural population bottles were also incubated under different light regimes (50% total spectrum, 50% total spectrum minus UVB and 50% PAR. Adsorption of iron versus actual uptake was studied by Ti(III)citrate EDTA wash (Hudson & Morel 1989). For these experiments an amount of approximately 0.5 nM radiotracer ^{59}Fe was added as inorganic Fe(III) species.

Preliminary results
Kinetics of iron photoreduction.
An experiment to measure the kinetics of iron photoreduction was carried out on 2 November. A concentration of 2.5 nM ^{59}Fe was added to a PMMA bottle (no filter, total spectrum). The Fe species were followed during 4 hours, figure 12.3.1.

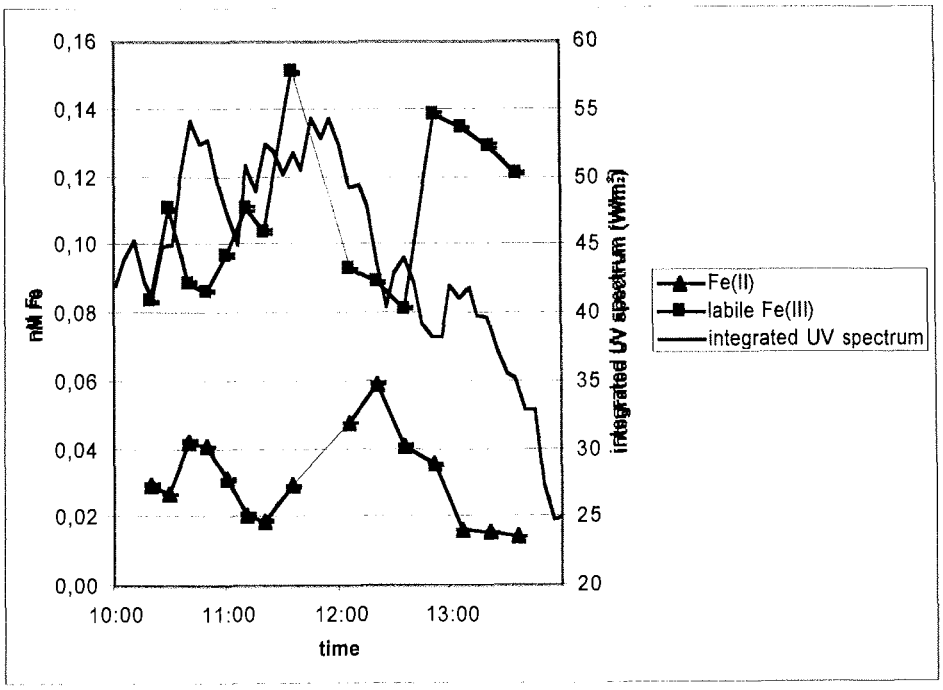

Figure 12.3.1 Kinetics of iron photoreduction.

In figure 12.3.1 the Fe(II) data is plotted together with the integrated UV spectrum. The UV light, as an input of energy, is one of the main causes for the photoreduction of Fe(III). The Fe(II) concentration seems to follow the solar spectrum. A negative correlation between labile Fe(III) and Fe(II) was observed. Since there should be an equilibrium between the Fe(II) and Fe(III) fraction this correlation was expected.

The daily cycle of Fe(II) under influence of solar radiation.
It is not yet fully understood what the bio-available form of iron is. One hypothesis is that Fe(II) is available for phytoplankton. Solar radiation and especially the UV part of the solar spectrum plays an important role in the photoreduction of Fe(III) to Fe(II).
In an experiment using the radioactive ^{59}Fe the influence of the UV part of the spectrum on the photoreduction of Fe(III) to Fe(II) was examined. Filtered seawater with an addition of $^{59}Fe(III)$ was incubated in PMMA bottles. We used four different light conditions, one bottle with the total solar spectrum, one bottle with UVA and PAR, one bottle with only PAR and a dark bottle. These bottles were incubated and the concentration of the Fe(II) was determined 5 times over the day.

The results are shown in figure 12.3.2 and 12.3.3. There is a clear trend between the intensity of the UV part of the spectrum and the presence of Fe(II). The UVB part is most important for the photoreduction followed by UVA and PAR.

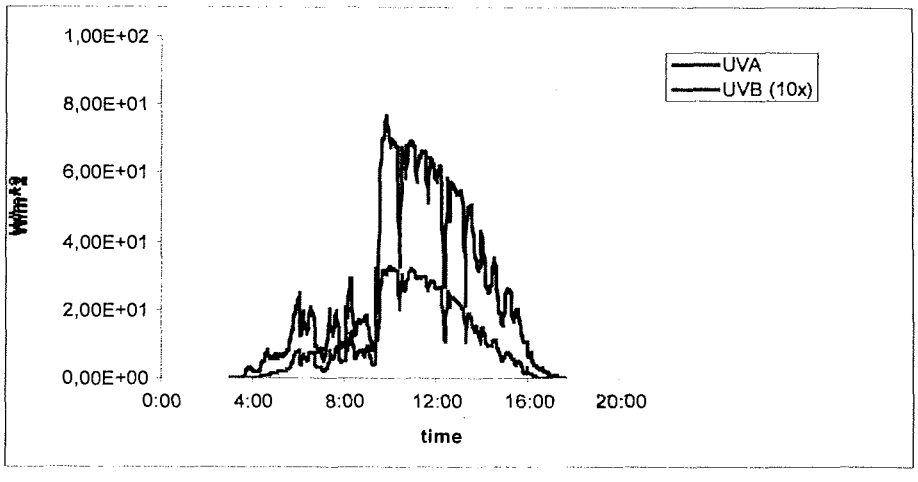

Figure 12.3.2. Photoreduction to Fe(II), a daily cycle.

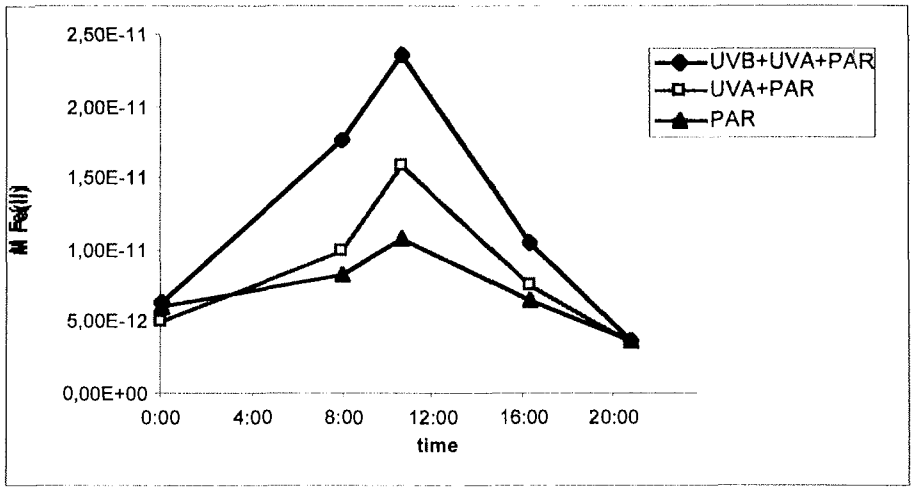

Figure 12.3.3 The UVB and UVA irradiation during the day.

Daily iron uptake experiments.

Figure 12.3.4 shows the daily uptake of iron for two size fractions (bigger than 10 µm, and between 0.2-10 µm) of the natural phytoplankton population after Tiwash, so actual Fe uptake. This experiment was performed under two different light conditions. We found that the size fraction of 0.2-10 µm did not change its iron uptake in time, but the fraction bigger than 10 µm increased its iron uptake in time. This was as expected since the smaller species should not be iron limited. Also a negative effect of UV light was observed.

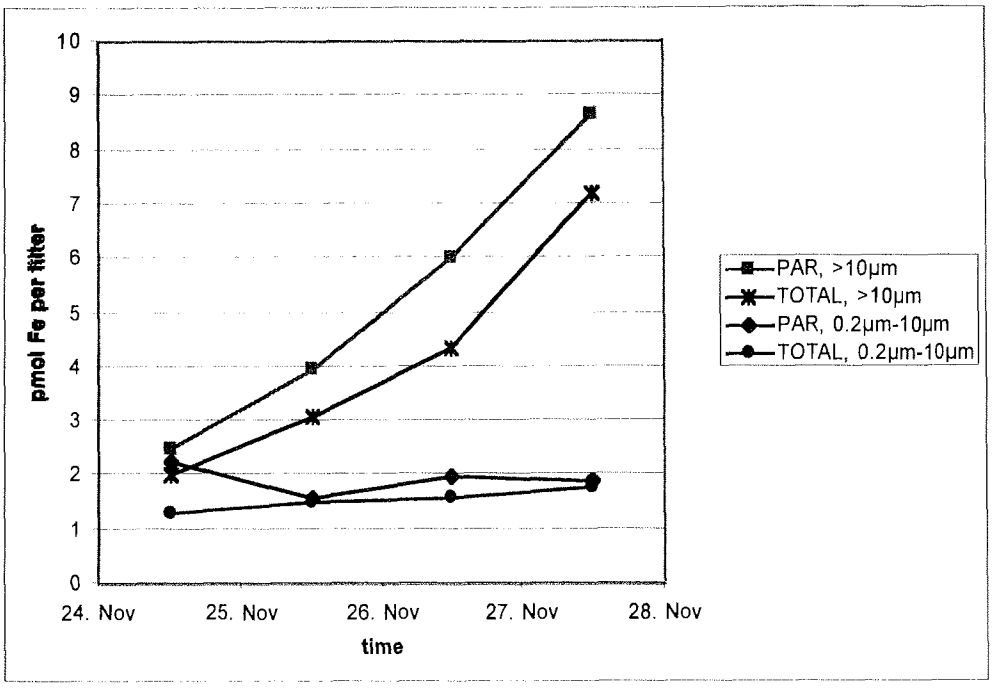

Figure 12.3.4: daily iron uptake by the natural phytoplankton population.

Literature

Gledhill, M, C.M.G. Van den Berg (1994) Determination of complexation of iron (III) with natural organic complexing ligands in sea water using cathodic stripping voltammetry. *Mar. Chem.*, 47, 41-54.

Hudson, R.J.M., and Morel, F.M.M. (1989) Distinghuising between extra- and intracellular iron in marine phytoplankton. *Limnol. Oceanogr.* 34, 1113-1120

King, D.W., Lin, J., and Kester, D.R. (1991) Spectrophotometric determination of iron(II) in seawater at nanomolar concentrations. *Anal.Chim.Acta* 247, 125-132

Acknowledgements

We want to thank W. Boot (IMAU), dr. F. Kuik (KNMI), Dr. S. el Naggar (AWI), W. Willemsen and R. Tax (RIVM) for the equipment to collect the UV data. We further want to express our gratitude to captain Keil and crew of R.V.Polarstern for support during the cruise, and to Victor Smetacek (AWI), the chief scientist. This research is funded by Netherlands Society for Scientific Research (NWO) and by the CARUSO project.

12.4 Production of iron fertilizer batches in seawater

Shipboard scientific party (rapporteur H. de Baar)

The production of iron-batches in seawater was designed jointly by AWI-NIOZ-UEA with the objective of safe and enclosed delivery of both the iron-sulphate powder and hydrochloric acid. None of the fine powder should be allowed in open air as to avoid it to enter the two nearby positioned clean air analytical laboratory containers for Fe measurements. Production of new tanks of iron in seawater solution should also be possible in heavy seas at foul weather conditions, such that any decision on a new iron release should not be hampered by inability of production of new batches. The iron-sulphate is not toxic but the fine powder upon excessive inhalation would affect the respiratory system. Hydrochloric acid was purchased in the non fuming 50 % diluted 6N HCl concentration, any inadvertent spills would easily be diluted with seawater, the very dilute acid is safe for both personal health and the environment.

Two large plastic tanks with 215 cm diameter and 217 cm height were constructed according to AWI directions and placed on the working deck within a strong steel scaffolding structure. The stirring motors and propellors were provided and installed by the UEA. For delivery a closed system was deisgned at NIOZ (dr. Timmermans). One NIOZ container van had been placed on the upper helicopter deck. Inside the van was a large funnel of about one square metre, connected by about 10 metres length of 13 cm diameter steel-reinforced transparent pvc tubing feeding into one of the tanks at the working deck. Delivery teams of three scientists were working inside the container van, dressed in protective pvc overalls, rubber gloves and rubber boots and wearing integral face masks with air filters as to avoid inhaling any fine dust. One more scientist adjacent to the door of the container was supervising while in contact by talkie-walkie with a fifth scientist serving as tank inspector at the below working deck. The fire hose of the helicopter deck with running seawater supply was used. The complete procedure was verified jointly with the ships medical doctor as to ensure there were no risks of health and safety.

First one 25 litre jerrycan of 6N HCl was placed inside the funnel, opened, the contents delivered and washed down with seawater. This was followed by the contents of 31 bags of iron sulphate powder also washed down with seawater

and one final jerrycan of another 25 litres 6N HCl. The tanks had a capacity of 8000 litres but were topped up to only the 6000 litres level, as to avoid any spillage of tank contents over some openings in the top due to ships movements. Upon 90 minutes stirring the pH was verified with pH paper and always found to be well below 2. Within the tanks the liquid was green due to the high abundance of Fe(II) ions, and turbid due to the amount of about 0.5 percent ground rock within the salt powder, an addition commonly used in commercial salt powders to ensure proper flow of fine salt grains. One sample bottle of 100 ml would become clear green upon about two days storage, with visible powder deposit on the bottom.

Overall fifteen tanks of the iron in acidified seawater solution had been prepared for three consecutive releases of five tanks each. During each release the net weight of released pure Fe was 780 kg. One release would take about fifteen hours, for delivering five tanks of 6000 litres each at a flow rate of about 2000 litres per hour. During the initial release this flow was mixed with a flow of about 200 litres per hour from the two SF_6 enriched seawater tanks.

The tank contents were in accordance with the SOIREE recipe which had been verified by the below rationale. In each 6000 liters tank 31 bags of 25 kg each dry $FeSO_4.7H_2O$ powder was added. Given the approximate atomic weights (Fe = 56, S = 32, O = 16, H_2O = 18) one derives that 1 mole dry $FeSO_4.7H_2O$ equals 278 grammes. Therefore an amount of (31 x 25 x 1000)/278 = 2788 moles per tank was added. For the 600 litres volume per tank this leads to a final concentration of 2788 moles / 6000 litres = 0.4644 moles/L. Upon dilution with a factor 100 million in ambient seawater this would yield $0.4644 \times 10^{-8} = 4.644$ nanomoles/L in central patch. This is about 100-fold higher than the 'typical' ambient dissolved Fe concentration of 0.05 nM. When using 5 tanks for one release to be distributed uniformly over an assumed 30 metres deep wind mixed layer in an area of 10 km by 10 km one would closely approach the assumed 100 million-fold dilution. For an assumed 60 metres deep layer the corresponding area would be 7 km by 7 km square.

Acidification to pH at about 2 is required to maintain the Fe in its dissolved Fe (II) state. At higher pH levels the Fe will become oxidized to Fe(III) which is highly insoluble, i.e. leading to colloidal and larger particulate Fe-oxides in the tanks.

Titration to endpoint at pH 3 of the typical Alkalinity of about 2300 µmoles L-1 of seawater would require 6000 x 2300 µmoles L-1 = 13.8 moles acid. Moreover at the very low pH 2 some of the 2788 moles sulphuric anion from the added $FeSO_4.7H_2O$ powder will associate with a proton

$$SO_4^{2-} + H^+ \rightarrow HSO_4^-$$

For this reaction the conditional stability constant

$$K_s^* = [H+][SO_4^{2-}] / [HSO_4^-]$$

in ambient Antarctic seawater (S=35, T=2 °C) is about $K_s^*=0.25$ such that at final pH=2 the ratio $[SO_4^{2-}] / [HSO_4^-]$ is about 25. Because of the very large amounts of both the dissolved $FeSO_4.7H_2O$ salt and the added HCl the ionic strength I of the tank solution will be much higher at about I=4.5 as compared to already quite high I=0.73 in seawater at S=35 salinity. This leads to major changes in the activity coefficients hence the conditional stability constants as used above would still need to be readjusted for the calculations of both Alkalinity titration and sulphate. Exact calculations will be done afterwards following our procedures for Mediterranean brines (Schijf et al., 1995). For the time being we reckon that the sulphate requires about 107 moles acid such that we end up with (2788-107)=2681 moles SO_4^{2-} and about 107 moles HSO_4^- per tank with the prescribed ratio of about 2681/107=25.
Finally one needs acid to bring pH to the required pH 2 value:

$pH = -\log [H^+]$ thus $[H^+] = 10^{-2}$ moles per liter

Therefore 6000 liters x 10^{-2} moles per liter = 60 moles acid is required. Summation of all acid requirements yields 13.8 + 107 + 60 = 123.8 = 180.8 moles acid per tank. Two 25 L jerrycans of 6N HCl = 2x25 x 6 = 300 moles would be in excess, by choice as to compensate for uncertainty due to incorrect activity coeffcients in above calculations. The free protons or excess acid of (300-13.8-107)= 180 moles acid in 6000 litres would yield a proton concentration of 0.03 moles L^{-1} corresponding to pH 1.5 which is in good agreement with the actual readings of the pH test papers.

Upon release the above mentioned 100 million fold dilution would add 10^{-10} moles acid to each liter ambient seawater. This is 10^{-4} µmoles per liter but will be mostly buffered by the natural CO_2 system buffer capacity. Even for a

tenfold higher acid addition of 10^{-3} µmoles per liter (corresponding to extreme limit of pH at 1 in each tank) the impact on the CO_2 system in ambient seawater will be negligible. Using CO_2 in seawater calculation models we reckon the pH change due to additions of 10^{-4} µmoles or even 10^{-3} µmoles per liter is much less than 0.0001 pH unit and therefore not detectable with the underway pH sensor with reproducibility of 0.001 pH unit. More importantly one may conclude that the addition in itself of the very dilute acid does not give rise to artefacts in either the dissolved CO_2 system or the viability of the plankton organisms.

The complete shipboard scientific party is most grateful to the officers and crew for their assistance in setting up and operating the delivery of iron. Special thanks are to the chief engineer for his advice and support.

Schijf, J. H.J.W. de Baar and F.J.Millero. (1995) Vertical distributions and speciation of dissolved rare earth elements in the anoxic brines of Bannock Basin, eastern Mediterranean. Geochim et Cosmochim. Acta, 59: 3285-3299.

12.5 Depletion of essential metals Zn, Mn, Co and Cd

P. Croot, P. Laan, J. Nishioka, H. de Baar (NIOZ)

In order to verify for ambient changes of essential trace metals Zn, Mn, Co and Cd in seawater both within and outside the Fe-enriched patch samples were collected to be analyzed afterwards at the NIOZ home laboratory. We collected both filtered and unfiltered seawater, in both small 250 ml bottles as well as large 1000 ml bottles. Overall 105 filtered samples and 78 unfiltered samples were collected into the small 250 ml bottles. Another 81 filtered sameples and 155 unfiltered samples were collected in the larger 1000 ml bottles.

13. FERROUS WHEELS IN THE OCEAN: THE SOUTHERN OCEAN FAIRGROUND

P.L. Croot and P Laan (NIOZ)

Introduction and Overview

The role of iron in limiting primary production in the oceans is now well established. Yet the processes by which iron is retained and recycled in the water column are still poorly understood. In an iron enrichment experiment such as has been carried out during ANTXVIII-2, there arises an opportunity to examine several of the key processes concerning iron biogechemistry on a larger scale. During this cruise, we undertook over 1500 analyses for dissolved and total iron in order to examine some of the processes that effected the bioavailability and absolute concentrations of Fe in the enriched patch. It is hoped that from this data we will be better able to understand the processes involved.

The role of Fe(II) in the Southern Ocean was studied during this experiment in greater detail than on any previous iron enrichment, thanks to some newly developed analysis systems designed specifically for that task. In the Southern Ocean, the low seawater temperatures and low H_2O_2 concentrations leads to slow oxidation of Fe(II) (half-life typically 1 hour at 4° C), allowing appreciable concentrations to exist for some time. This is in contrast to warmer regions, where Fe(II) is very much a short lived transient species (half-life typically 15 seconds at 25° C). For the iron enrichments, the added iron was as Fe(II) sulphate, this experiment allows us a unique opportunity to examine the processes that control Fe(II) concentrations in the Southern Ocean.

Methods

During cruise ANT XVIII/2 the fate of the iron added to the SF_6 labelled patch was studied. The work was characterized by high density sampling and profiling both inside and outside the patch. This was accomplished by using a towed sampling fish for underway-surface measurements and GO-FLO samplers on a Kevlar wire for the vertical distribution of iron at each station.

Spatial distribution of iron:

Measurement of iron

To prevent sample contamination, trace metal clean techniques were applied. All samples for total metal analysis were acidified to pH < 2 with ultraclean quartz distilled concentrated hydrochloric acid.

Total dissolved iron (0.2 μm) were measured on-board using a flow injection technique with in-line pre-concentration on a chelating resin followed by chemiluminescence detection (FIA-CL) ((de Jong et al., 1998; Landing et al., 1986; Obata et al., 1993). Iron from an acidified sample is buffered on line and preconcentrated onto a column of immobilizied 8-hydroxyquinoline. After a loading time of 1 to 4 minutes, the column is washed with deionised water and the iron is eluted with dilute hydrochloric acid. The iron mixes with luminol, hydrogen peroxide and ammonium hydroxide to produce chemiluminescence in the flow cell of a photomultiplier tube connected to a photon counter. The chemiluminescence occurs as a result of the iron catalyzed oxidation of luminol (3-aminophtalhydrazide) by hydrogen peroxide, producing blue light (424 nm). The accuracy of the method was checked and confirmed using NASS-5 reference sea water. Throughout the cruise, the blank and detection limit (3x standard deviation of blank) remained constant at 0.021 and 0.004 nM respectively. Reproducibility was typically 2% at the 0.3 nM concentration and better than 10% at the 0.06 nM level.

Fe(II) measurements

Fe(II) was measured continuously during underway sampling using a modification of the luminol flow injection method described above with the peroxide omitted and the reactions conditions altered to optimize the signal for Fe(II). The rapid reaction between Fe(II) and luminol was utilized to make rapid (90-112s per measurement) analyses of the Fe(II) concentration in the seawater. Vertical profiles for Fe(II) and H_2O_2 were also obtained were possible, in order to examine the redox kinetics of Fe during the experiment.

Preliminary results and discussion

During ANTXVIII-2, 11 separate underway sampling surveys were performed and these are summarised in Table 1. In addition 32 vertical stations were occupied (Table 2) during the cruise. All data presented in this report are considered preliminary and are subject to modification after further analysis post cruise.

Underway mapping was used extensively to map the surface expression of the infused patch. Initially after the first infusion the patch was quite small (figure 1) and not well mixed, subsequent storms mixed the iron and spread the patch, leading to a decrease in the dissolved iron concentrations throughout the patch. Suprisingly there was no rapid removal of the iron during this time from precipitation with subsequent sedimentation. When dissolved iron concentrations returned to close to pre infusion condition, a further iron infusion was made. This second reinfusion was more quickly mixed into the patch, thanks to the stormy conditions. Figure 2, shows the good agreement between the discrete underway iron measurements and the continuous Fe(II) sampling. Interestingly the oxidation of the added Fe(II) was slower than predicted by the O_2 and H_2O_2 concentrations, suggesting some complexation of the Fe(II). A further infusion into the central part of the patch was also carried out and this is just visible in Figure 3, as the surface iron values have been significantly lowered by the increasing patch dimensions and the deeper mixed layer. The south eastern corner of this grid was effected by a strong rain event which led to elevated concentrations of dissolved Fe(II) into the seawater.

Vertical profiles for Fe(II) (figure 4) showed a distribution perhaps consistent with Fe(II) production from photo-processes, though more work is required to model the kinetics of these processes. Dissolved iron profiles from out of the patch were consistent with earlier data collected during ANTXVI-3, in patch stations showed elevated concentrations of dissolved iron in the mixed layer as expected. Figure 5 shows the 2nd lagrangian grid survey and 2 out stations and one in station.

A intercollaboration exercise for iron was also conducted during this cruise in conjunction with Jun Nishoka (CRIEPI) and Marie Boye (RuG).

Acknowledgments

The authors would like to show their deep thanks and appreciation to the crew of the R.V. Polarstern, for all their efforts in helping us throughout ANTXVIII-2. The help of the other members of the GO-FLO team, Jun Nishoka and Klaas Timmermans is very appreciated. Special thanks must go to the deck crew for their efforts with deploying the iron-fish and the GO-FLOs. Thanks also to the Chief Scientist, Dr Victor Smetacek and to the AWI for making this cruise possible.

References

de Jong, J.T.M. et al., 1998. Dissolved iron at subnanomolar levels in the Southern Ocean as determined by ship-board analysis. Analytica Chimica Acta, 377: 113-124.

Landing, W.M., Haraldsson, C. and Paxeus, N., 1986. Vinyl Polymer Agglomerate Based Transition Metal Cation Chelating Ion-Exchange Resin Containing the 8-Hydroxyquinoline Functional Group. Analytical Chemistry, 58: 3031-3035.

Obata, H., Karatani, H. and Nakayama, E., 1993. Automated Determination of Iron in Seawater by Chelating Resin Concentration and Chemiluminescence Detection. Analytical Chemistry, 65: 1524-1528.

Table 13.1: Summary of underway sampling deployments during ANTXVIII/2. Samples numbers collected during each deployment of the 'Iron-Fish'.

Transect #	Comment	Timespan (UTC)
1	Pre-infusion survey along 20° E	00:00 29/10 – 11:00 31/10
2	Pre-infusion sampling grid	02:30 03/11 – 09:30 06/11
3	Post-infusion finding the patch	10:00 08/11 –18:20 08/11
4	Post-infusion finding the patch	02:03 09/11 – 08:47 09/11
5	Finding two patches?	09:33 14/11 - 13:10 14/11
6	Propellor	16:06 15/11 – 19:56 15/11
7	Post infusion 2 – dash across the patch	07:10 17/11 – 09:20 17/11
8	Propellor	06:50 18/11 – 10:00 18/11
9	Propellor	08:25 19/11 – 11:20 19/11
10	Past the buoys check on new patch	05:43 25/11 – 08:45 25/11
11	Large grid	19:02 25/11 – 17:50 26/11

Summary of stations sampled for iron during ANTXVIII-2

Station #	Depths	Comment
007	25, 50, 75, 100, 200, 250, 500, 750 and 1000m	Deep Station
009	20, 40, 60, 80, 150, 200, 250, 300 and 400m	Survey

011	20, 40, 60, 80 and 100m	IN Station
012	20, 40, 60, 80 and 100m	OUT Station
014	20, 30, 40, 60, 80 and 100m	IN Station
016	20, 40, 60, 80 and 100m	Lagrangian Grid
021	20, 40, 60, 80 and 100m	Lagrangian Grid
023	20, 40, 60, 80 and 100m	Lagrangian Grid
028	20, 40, 60, 80 and 100m	Lagrangian Grid
031	20, 40, 60, 80 and 100m	Lagrangian Grid
038	20, 40, 60, 80 and 100m	IN Station
041	20, 30, 40, 50, 60, 80 and 100m	IN Station
045	20, 40, 60, 80 and 100m	IN Station
046	20, 30, 40, 50, 60, 80 and 100m	IN Station
048	20, 30, 40, 60 and 80m	OUT Station
049	20, 30, 40, 50, 60, 80 and 100m	IN Station
054	20, 30, 40, 60 and 80m	Lagrangian Grid 2
055	20, 30, 40, 60 and 80m	Lagrangian Grid 2
061	20, 30, 40, 50, 60, 80 and 100m	IN Station
079	20, 30, 40, 60 and 80m	Cross
081	20, 30, 40, 60 and 80m	Cross
083	20, 30, 40, 60 and 80m	Cross
085	20, 30, 40, 60 and 80m	Cross
086	20, 30, 40, 60 and 80m	Cross
088	20, 30, 40, 60 and 80m	IN Station
091	50, 200, 300, 400, 500, 600, 800 and 1000m	IN Station
092	20, 40, 60, 80, 100, 150, 200 and 250m	IN Station
100	20, 40, 60, 80 and 100m	Small Grid
103	20, 40, 60, 80 and 100m	Small Grid
106	20, 40, 60, 80 and 100m	Small Grid
107	**20, 40, 60, 80 and 100m**	IN Station
108	20, 40, 60, 100, 150, 200 and 250m	OUT Station

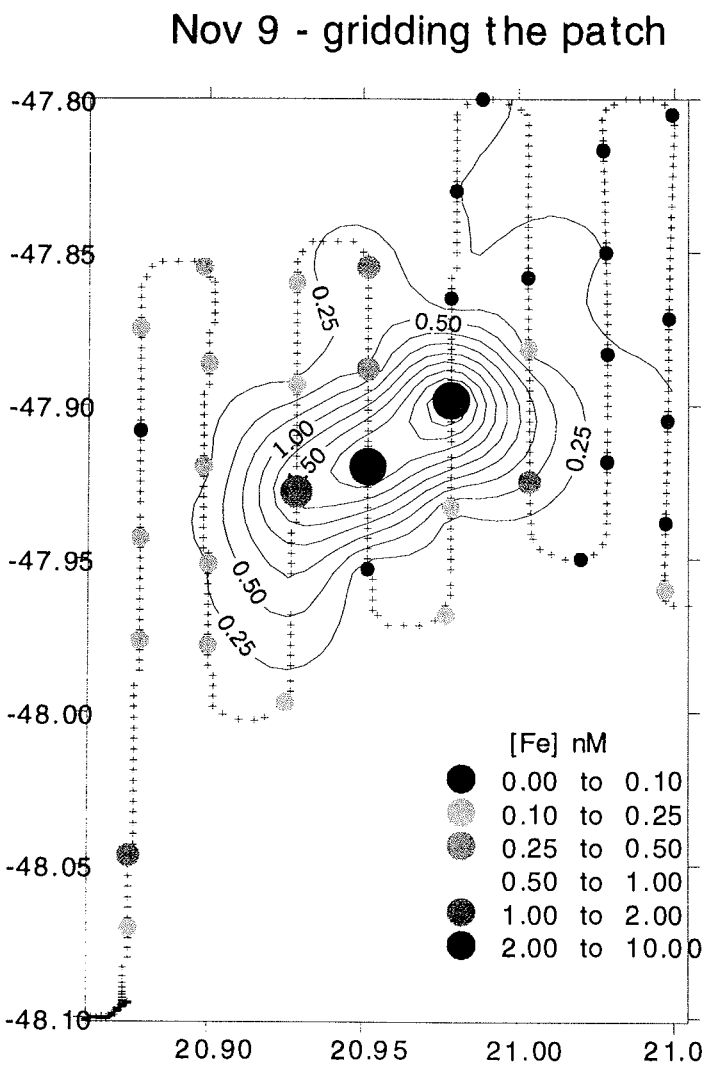
Nov 9 - gridding the patch
-47.80
-47.85
-47.90
-47.95
-48.00
-48.05
-48.10
20.90
20.95
21.00
21.0
0.25
0.50
1.00
0.50
0.25
0.50
0.25
[Fe] nM
0.00 to 0.10
0.10 to 0.25
0.25 to 0.50
0.50 to 1.00
1.00 to 2.00
2.00 to 10.00

Figure 13.1:

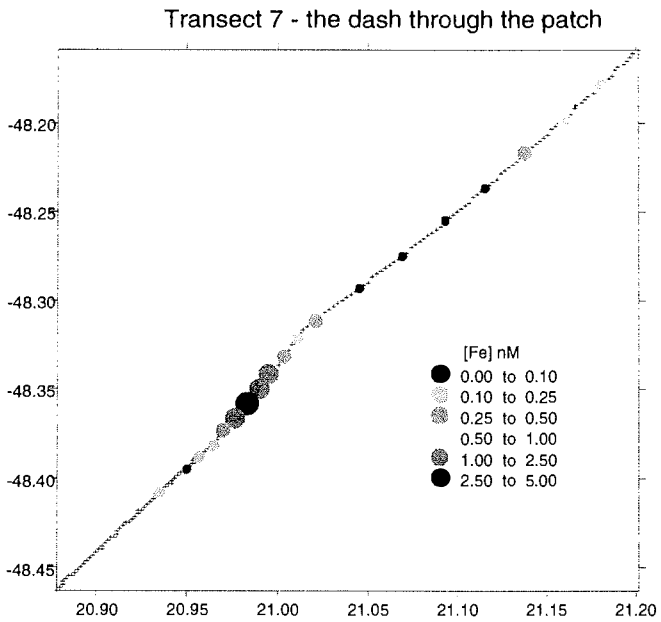

Figure 13.2(a): Surface dissolved iron concentrations across the patch Nov 17, 2000.

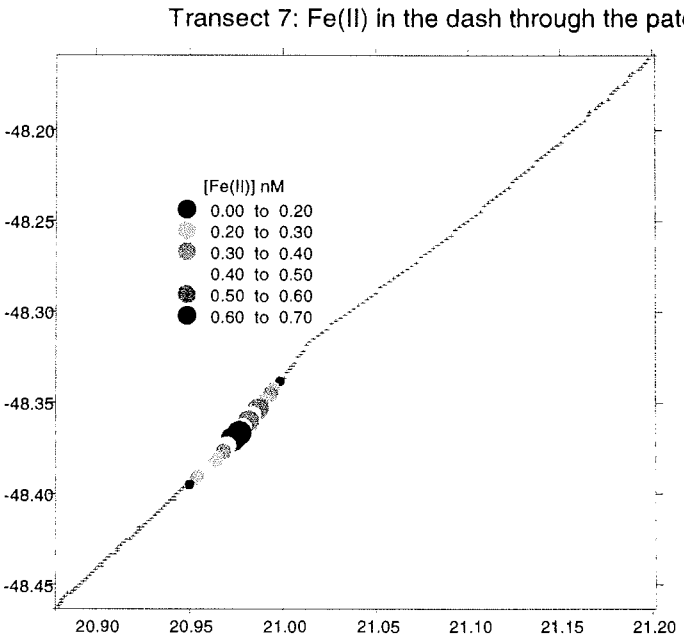

Figure 13.2(b): Surface concentrations of dissolved Fe(II) across the patch on Nov 17, 2000. The Fe(II) signal originates from the 2nd infusion which had taken place the previous day.

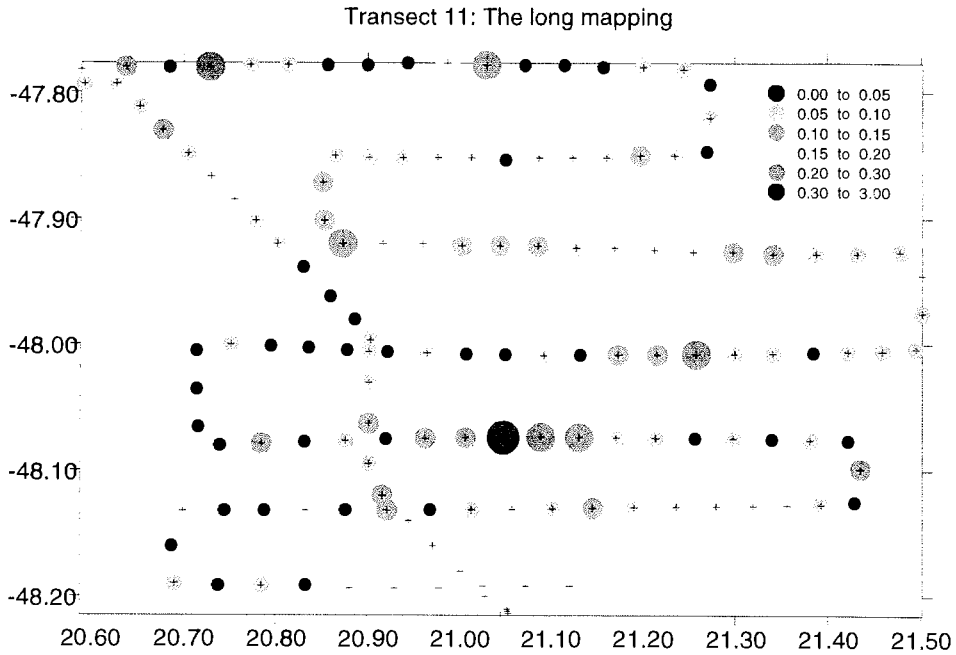

Figure 13.3: Large grid survey for dissolved iron of the patch on Nov 25-26, 2000.

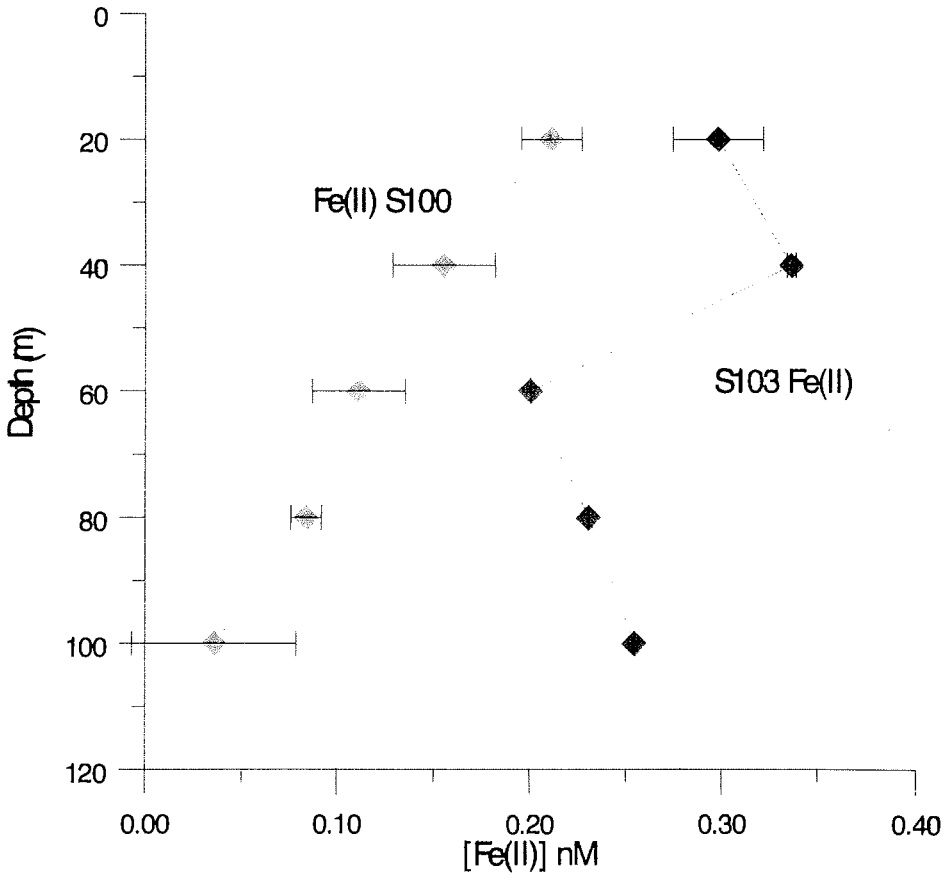

Figure 13.4: Vertical distribution of Fe(II) at IN patch stations S100 and S103.

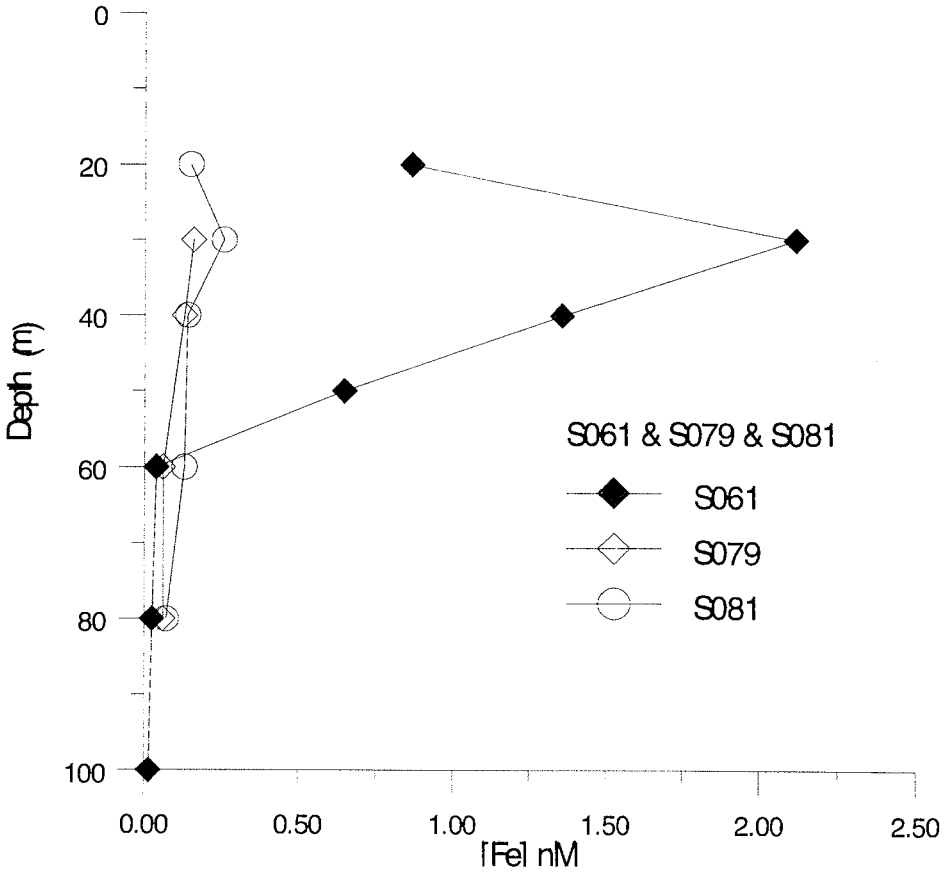

Figure 13.5: Vertical distribution of dissolved iron at stations occupied during the2nd Lagrangian Grid.

14. PHYTOPLANKTON RESPONSES TO IRON ADDITION.

Netherlands personnel involved (NIOZ or otherwise indicated):
K. Timmermans, M. Veldhuis, H. de Baar, T. van Ooijen (RUG)

14.1 Message in a bottle.

K. Timmermans, M. Veldhuis, M. Rijkenberg, P. Croot, P. Laan (NIOZ),
A. Fischer, K. Kroon (IRI, Delft).

We want to express our gratitude to the master and crew of F.S. Polarstern for the competent support throughout the cruise, and to Victor Smetacek (AWI), the chief-scientist.

Emphasis during the expedition has been on incubations of phytoplankton. These incubations have been performed with the natural phytoplankton assemblages inside ("IN") and outside ("OUT") the Fe-enriched patch, as well as with single diatom species cultures brought from the home laboratory. The incubations were done in the clean, temperature controlled (3 degrees Celsius) container NIOZ no. 25, or on deck, in the special full-spectrum transparent incubation site. Main parameters measured were: cell numbers, cell size and fluorescence, (flowcytometry, Marcel Veldhuis), microscopy, PAM fluorometry, nitrate reductase activity, ^{15}N nitrate and ammonium uptake, nutrient uptake (Carmen Hartmann, AWI), ^{14}C primary production (Frank Gervais), Fe speciation (Peter Croot, Patrick Laan), and Fe isotope uptake and kinetics (Astrid Fischer, Koos Kroon). Clean techniques (sample collection, sample handling) were applied throughout.

<u>Incubations with the natural phytoplankton inside and outside the Fe-enriched patch.</u>

10 liter samples from "IN" and "OUT" patch stations were incubated inside the clean container and the development of the phytoplankton was followed over a long period of time, that is 22 days. The results fitted well in the assumed size-class related response of the phytoplankton. The small phytoplankton seemed to be growing at relative high growth rates already before the iron addition. These small algae remained high growth rates and were kept low in numbers by the abundant micro-zooplankton grazers, present in the incubation bottles. The larger phytoplankton species (mainly large - >10 µm - diatoms), increased upon Fe addition their growth rates and increased significantly in numbers and biomass during the experimental period. In time,

the larger cells increased in the "IN" culture. These results confirm the previous experiments with large and small diatoms from the Southern Ocean (Timmermans et al, in press L&O). The F_v/F_m measurements showed distinct differences between the "IN" and "OUT" cultures. F_v/F_m values were always higher in the "IN" cultures. Silicate and nitrate depletion were more rapid in the "IN" than in the "OUT" culture. In fact, 6 _M nitrate was left in the "OUT" culture at the end of the experiment, indicative of a higher silicate to nitrate uptake in this culture.

Incubations with the single species Antarctic diatom species.
The algae were grown in filtered seawater from inside and outside the Fe-enriched patch. When grown in "IN" patch seawater, the F_v/F_m values in C. brevis showed no difference with outside Fe-patch seawater. Obviously, this species was not Fe-limited at the low dissolved Fe concentrations as measured in this water (0.03 nM). In contrast, F_v/F_m values increased substantially in cultures of both C. dichaeta and F. kerguelensis, when grown in inside patch seawater. These species were clearly Fe-limited at the ambient Fe concentrations.
Kinetics of Fe bound by ligands were studied in an experiment with C. brevis, in which four ligands (desferrioxamine B, protoporphyrine, enterobactine and oxine) were pre-loaded with ^{59}Fe. Subsequently, the fate of the ^{59}Fe was followed in the particulate fraction (= C. brevis) , the dissolved fraction and the fraction containing the ligands. These experiments showed that, with the exception of Fe bound by desferrioxamine B, all other ligands still left Fe available for C. brevis. Obviously, the conditional stability constant of these ligands do not explain bioavailability of these ligands.

Timmermans, Klaas R., Loes J.A. Gerringa, Hein J.W. de Baar, Bas van der Wagt, Marcel J.W.Veldhuis, M. Boye, Jeroen T.M. de Jong, Peter L. Croot. Growth rates of large and small Southern Ocean diatoms in relation to availability of iron in natural seawater. Limnol. Oceanogr. (in press)

14.2 Phytoplankton abundance and cellular properties during an iron fertilisation experiment in the Southern Ocean.

M. J.W. Veldhuis & K. R. Timmermans (NIOZ)

Introduction

The main hypothesis to be tested during this cruise was the role of iron as the growth limiting factor for marine phytoplankton in the Southern Ocean during the austral spring season. For this purpose a large area (several square miles) was fertilised with iron and a tracer gas SF6 in order to track the patch over a longer period. The phytoplankton composition, distribution, size and pigmentation was studied prior and during the whole time span of this mesoscale outdoor experiment (ca. 3 weeks).

The general objective can be separated in the flowing topics:

1) determination of the phytoplankton abundance and succession. This includes the separation in different size classes/species applying flow cytometry. In addition, changes in the cell size and pigmention (chlorophyll) was traced.
2) Effect of iron on the species specific cell viability and gross growth rate. This was examined in the field as well as in a number of culture experiments.

Ad 1) spatial and temporal abundance was determined using discrete water samples, which were collected with a CTD-rosette water sampling system. Samples were stored on melting ice and analysis by hand to avoid heating up of the sample. Sampling was carried out for a period of close to 4 weeks outside as well as inside the iron-fertilised patch. At three different periods cells size distribution was examined using filters with a different pore size (10, 5, 3, 2, 1, and 0.6 µm). Additional samples were taken for microscopic measurements (P. Verity), photosynthetic activity (M. Gorbunov) and plant pigments (I. Peeken).

Ad 2) the viability of the phytoplankton community was examined at two different levels. The first one was based on a recently developed method testing the membrane integrity of the individual phytoplankton cell. This method examined the general physiological status of the cell. Phytoplankton cells with a compromised cell membrane are in a process of dying. The second method tests more specifically the photosynthetic activity of the phytoplankton cells (Fv/Fm).

Material and methods

Analysis of the individual phytoplankton cells was done with a bench top flow cytometer (Coulter XL-MCL). This instrument is equipped with a 15mW laser. Excitation wavelength 488 nm and emission bands in the green (FL1: 525 ±20nm) orange (FL2: 575 ± 20nm) and red (FL3: > 630 nm) region.

Practical considerations

Due to the low numerical abundance of phytoplankton cells relative large volumes are needed to be analysis to meet proper statistics. On the other hand the low ambient water temperature (ca. 2 – 5 ºC) prohibits long exposure of the live samples to room temperature. Therefore, the samples were analysed using the manual mode of the flow cytometer and measuring time was limited to 5 min.

Chains of diatoms (*Pseudonitszchia*) and colonies of *Phaeocystis* could be identified as bursts of cells. These multicellular phytoplankton species were observed ca. 10 days after fertilisation.

Data files of the phytoplankton samples were post-analysed on a work station and up to 5 distinguishable clusters of cells could be assigned. This included a PE-containing *Synechococcus*, a ca. 1 µm large pico-eukaryote and 3 larger groups.

Results

In general phytoplankton cell numbers ranged between 10,000 and 16,000 cells per ml for the surface waters (upper 60 m). Cell densities were 4 to 8 fold higher than observed in the autumn season of 1999 in the same area. A comparison of the chlorophyll fluorescence based biomass indicated that ca. 55% of the phytoplankton population was smaller than 5 µm (Fig. 14.2.1) prior to and outside the iron fertilised area. This fraction corresponded with 80% of the cell total cell counts. After fertilisation the <5 µm biomass fraction dropped slightly to ca. 40% (day 22).

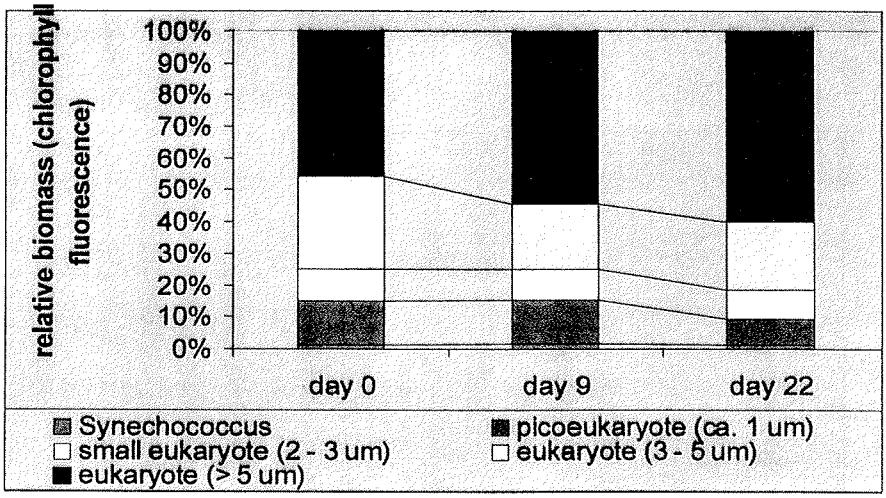

Fig. 14.2.1 relative chlorophyll fluorescence of different size classes of phytoplankton. Samples taken inside the iron enriched patch at different sampling days (stations 9, 46 and 107). Average values of 20 to 40 m depth range.

This was caused by two factors. Firstly, by a proportional increase in the relative abundance of the larger fraction of cell sizes. Secondly, by an increase in pigment concentration per cell as observed in the whole phytoplankton population (Fig.14.2. 2).
This increase in pigmentation per cell was not equal for all size classes. For the smaller cells the increase was in the order of a factor two steadily increasing to a factor 4 for the large cell sizes (fig. 14.2.2). This observation suggests that the iron enrichment stimulated pigmentation in all phytoplankton cells but in particular the large cells. In terms of total phytoplankton biomass a doubling of the pigment concentration per cell implies changes in the Carbon to Chlorophyll a ratio as well. Based on the present data ca. 30% of the observed increase in chlorophyll biomass in the iron enriched are was due to changes in C:chlor. rather than true increase in biomass.

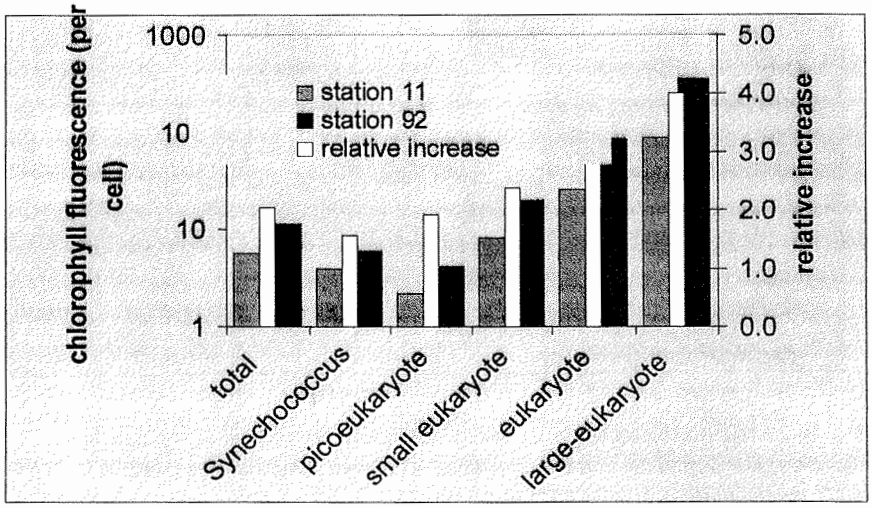

Fig. 14.2.2 relative chlorophyll fluorescence per cell of the different groups of phytoplankton present (left axis) and relative increase prior and after iron fertilisation (right axis).

15. CARBOHYDRATE METABOLISM OF PHYTOPLANKTON DURING AN *IN SITU* IRON ENRICHMENT

T. van Oijen (RUG)

Introduction

Iron limitation has been identified as a major factor controlling phytoplankton growth in the Southern ocean. At limiting iron concentrations, the functioning of the photosynthetic apparatus and several metabolic processes is affected. During the ANT18/2 cruise, we studied the effect of *in situ* iron enrichment on the particulate carbohydrate concentration and several other physiological parameters. Based on literature and results of iron enrichment experiments in bottles, performed during the ANT16/3 cruise and at the home laboratory, we hypothesize that the diurnal production and nocturnal consumption of intracellular storage carbohydrates by phytoplankton both increase in response to iron addition. Also, the average volume and chlorophyll content of phytoplankton cells are expected to increase. A differential response to iron enrichment by different algal species might lead to a shift in species composition, which might alter the general monosaccharide composition of the phytoplankton-derived carbohydrates.

Objectives:

-to compare the diel variation in particulate carbohydrate concentration inside and outside the iron-fertilised patch (experiment A).
-to determine the relation between light intensity and polysaccharide production by phytoplankon sampled inside the patch (experiment B).
-to determine changes in carbohydrate composition inside the patch and relate it to changes in phytoplankton species composition (CTD rosette samples).

Material and methods

-Experiment A:

24h deck incubations were carried out at 60% of the ambient light intensity with natural phytoplankton populations sampled inside and outside the patch. This experiment was carried out three times during the cruise. Seawater was taken from the iron fish (see Croot et al.). Before the start of the experiment, samples were taken for total unfiltered iron concentration, chlorophyll *a* concentration and species composition. Phytoplankton was incubated in polycarbonate bottles in a deck incubator and kept at ambient temperature using running surface seawater. PAR and water temperature data were

logged continuously (five minute average). Samples for flow cytometry, fluorometry, POC analysis and dissolved and particulate carbohydrate analysis were taken at dawn (t=0), dusk (t=1) and the next morning (t=2). Flow cytometric and fluorometric measurements were done on board, the other samples will be processed at the home laboratory.

-Experiment B:
24h deck incubations were carried out at three light intensities (60%, 30% and 10%) with phytoplankton populations sampled inside the patch. This experiment was carried out four times during the iron fertilisation experiment. Seawater was taken from either the iron fish or the CTD rosette. The sampling parameters and scheme were the same as for experiment A.

-*in situ* measurements:
Besides deck incubations, samples for carbohydrate concentration and composition (GC-analysis) were collected with the CTD rosette (0, 10, 20, 40, 60, 80 and 100m) at all the 'big' in-patch and out-patch stations.

Preliminary results
Results of flow cytometry and fluorometry are presented for one representative experiment of each type.

-Experiment A (exp.nr. 5, 13 November, five days after iron fertilisation):
The flow cytometric data on cellular fluorescence (a rough measure for chlorophyll *a* content) and cell size were processed for one specific cluster of cells smaller than one micrometer. These cells showed a clear diel change in average cell volume (fig. 1A) and fluorescence (fig. 1B). Both parameters increased during the day and decreased at night. The cells from the iron enriched patch had higher initial values (at t=0) and showed a bigger diel change in both parameters. Thus, five days after fertilisation a physiological response to iron was clearly visible for this cluster of cells.
The outside-patch algal community had a lower Fv/Fm and a higher sigma PSII, showing that the cells were not 'healthy'. Fv was lower for outside patch samples, indicating a lower chlorophyll concentration. This low chlorophyll concentration is not only the result of lower cell numbers but also of a lower chlorophyll content per cell, as indicated by the relatively low fluorescence of iron-limited cells measured by the flow cytometer.

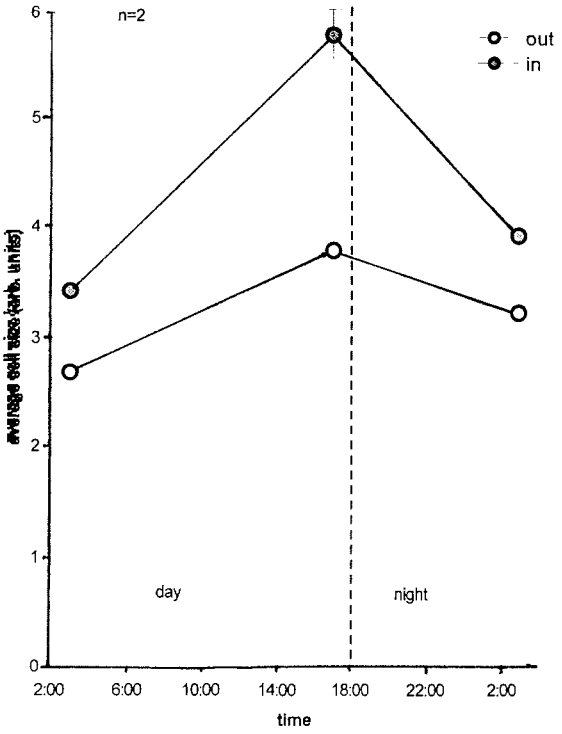
n=2
out
in
6
5
4
3
2
1
0
day
night
2:00
6:00
10:00
14:00
18:00
22:00
2:00
time

Figure 15.1.A

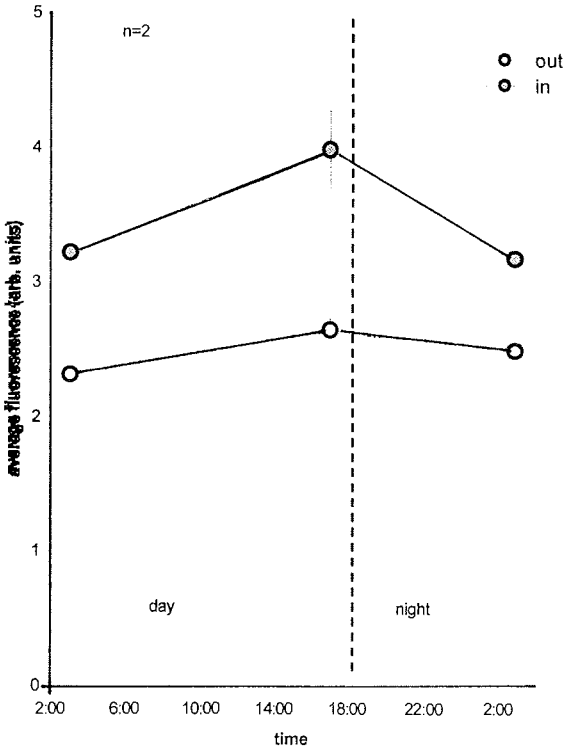
n=2
out
in
5
4
3
2
1
0
day
night
2:00
6:00
10:00
14:00
18:00
22:00
2:00
time

Figure 15.1.B

-Experiment B (exp.nr. 4, 10 November):
The flow cytometric data were processed for the same cluster of cells as described above. The cells showed a clear light dependent diel variation in average cell volume (fig. 2A) and fluorescence (fig. 2B). The diurnal increase in cell volume was highest for the high light insities, whereas the fluorescence was highest for the 10% light intensity. This indicates that at the 10% light intensity, the cells were light limited and required specific adaptations to low light.

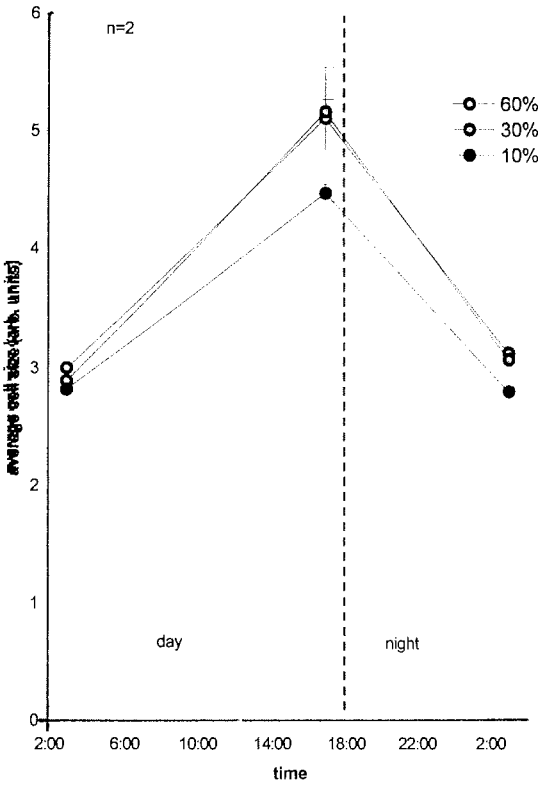

Figure 15.2.A

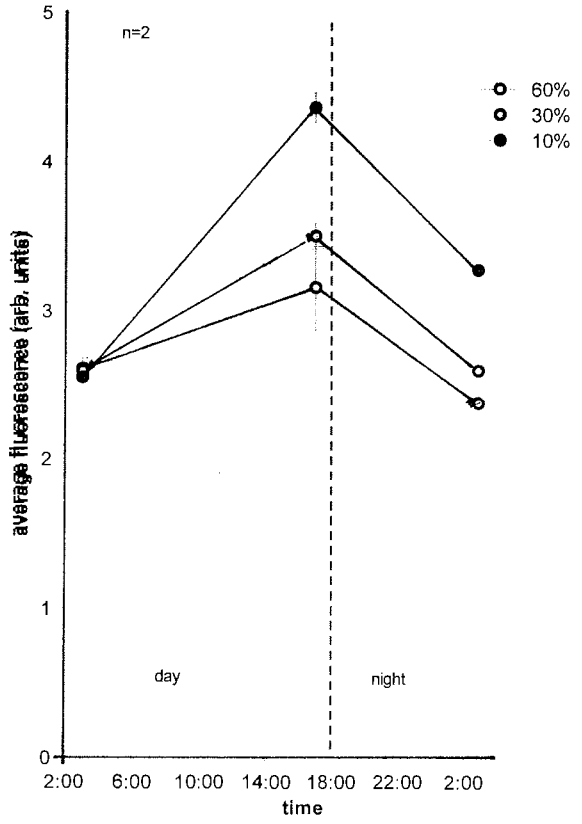

Figure 15.2.B

This work was supported by: J. Nishioka (analysis of iron concentrations); M. Gorbunov (fluorometry); M. Veldhuis (flow cytometry); C. Hartmann et al. (nutrient analysis); U. Riebesell et al. (chlorophyll *a* analysis); and P. Croot, P. Laan and K. Timmermans (general assistance).

16. PHYTOPLANKTON COMPOSITION AND SPECIES ABUNDANCE DURING EISENEX

P. Assmy, U. Freier, J. Henjes, C. Klaas, V. Smetacek

Introduction

In iron enrichment experiments, in order to assess the impact on the pelagic community and the biogeochemical processes driven by changes in plankton distribution, an aolean dust input into the surface water of the open ocean is simulated by an artificial iron infusion. HNLC (**H**igh **N**utrients **L**ow **C**hlorophyll) regions like the equatorial Pacific Ocean and the Southern Ocean have demonstrated increased phytoplankton growth rates as well as biomass in response to iron enrichment (Coale *et al.* 1996; Boyd *et al.* 2000). This seems to be especially the case for large-celled diatoms like *Fragilariopsis. kerguelensis, Pseudonitzischia spp.*, large *Cheatoceros* of the Phaeoceros group, *Thalassiothrix spp., Corethron criophilum* and *C. inerme.*

Changes in phytoplankton assemblages are central to the iron hypothesis. A combination of two different effects of iron enrichment might be responsible for the observed changes in atmospheric CO_2 draw-down from interglacial to glacial periods (Archer *et al.* 2000): an increase in diatom production and sedimentation (biological pump) combined with a decrease in $CaCO_3$ production by coccolithophorids (alkalinity pump).

Our study during ANT XVIII/2 followed two purposes:

- To provide a rapid assessment of the diatom distribution and assemblage composition as a means to determine natural variability in the field prior to fertilisation site selection.
- Describe the community succession subsequent to iron fertilisation.

Material and Methods

Before fertilisation, a survey was conducted along two transects southward from 45°11'S to 49°59'S and northward from 52°08'S to 49°22'S at 20°00'E. In order to investigate the variability of plankton assemblages in the area surrounding the fertilisation site a grid survey was carried out between 47°23'S and 48°59'S, 22°00'E and 20°45'E. During both surveys, 10 l of surface water were collected, by bucket, at hourly intervals (about every 7' of degree). Samples were immediately concentrated down to ~50 ml by pouring the water gently through a 10 µm mesh net. Samples were then fixed with 1%

Lugol's iodine and 0.5% hexamine buffered formaline and transferred into Hydrobios sedimentation chambers.
Each chamber was thoroughly checked to ensure that cells had settled and were evenly distributed. Density estimates were given for entire chambers and organisms larger than 10 µm were counted in one mid transect with an inverted microscope (Axiovert 25, Axiovert 135 and IM 35).

After iron fertilisation the same procedure was followed using water samples taken at discrete depths from a CTD (**C**onductivity **T**emperature **D**epth) sampling rosette. For each depth, the total contents of a Niskin bottle (~ 12 l) was concentrated to a volume of approximately 50 ml and later fixed and counted as described above. Non-concentrated water samples were taken systematically and fixed with 2% buffered formaline. These samples were stored at 4°C in the dark for subsequent counting of heterotrophic protists and in order to calibrate the counts of the concentrated samples back in the home laboratory.

Preliminary results and discussion
During the transect of the Antarctic Circumpolar Current (ACC), starting at the Subantarctic Front and throughout the Polar Frontal Zone (PFZ), diatom abundance was low with a small peak at around 48°S dominated by *F. kerguelensis* and *Ch. dichaeta.* In contrast, in the Antarctic Zone (south of 51°S) higher diatom abundance was observed, dominated by *F. kerguelensis*, *Pseudonitzschia spp., Chaetoceros neglectum* and *Ch. curvisetus* (Fig. 16.1A).

In both transects surveyed a few diatom species generally accounted for about 70% of total diatom abundance:
- *Chaetoceros neglectum* and *Ch. curvisetus*
- *F. kerguelensis*
- *Pseudonitzschia spp.*

A high degree of variability was nevertheless observed in the assemblage composition due primarily to changes in the relative contributions of the main diatom species present. Some exceptions were observed with higher relative abundance of *Rhizosolenia cylindrus, R. chunii* and discoid diatoms, *Thalassiosira spp.* (Fig. 16.1B).

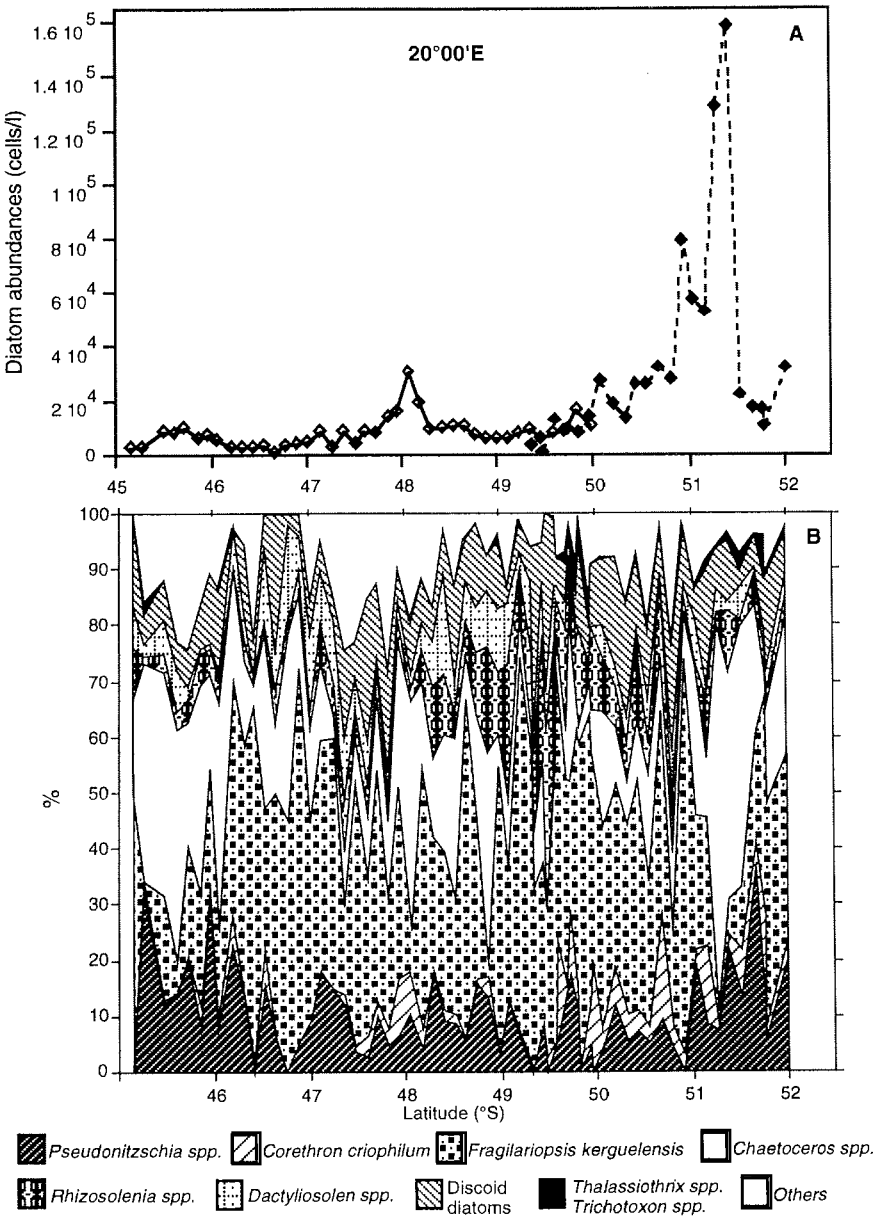

Fig. 1. (A) Diatom abundances and (B) assemblage composition during the North-South (solid line) and South-North (dashed line) transects.

Fig. 16.1 A and 16.1 B

Results from the grid survey in the Polar Frontal Zone revealed a similar situation. Variable but low diatom abundance was found (max. 30000 cells l^{-1}) and assemblages were generally dominated by *Ch. neglectum, Ch. curvisetus, F. kerguelensis* and *Pseudonitzschia spp.* In addition to the dominant species, discoid diatoms (mainly *Thalassiosira spp.*) and *Rhizosolenia* species (mainly *R. chunii* and *R. cylindrus*) were relatively high in abundance (Fig. 16.2).

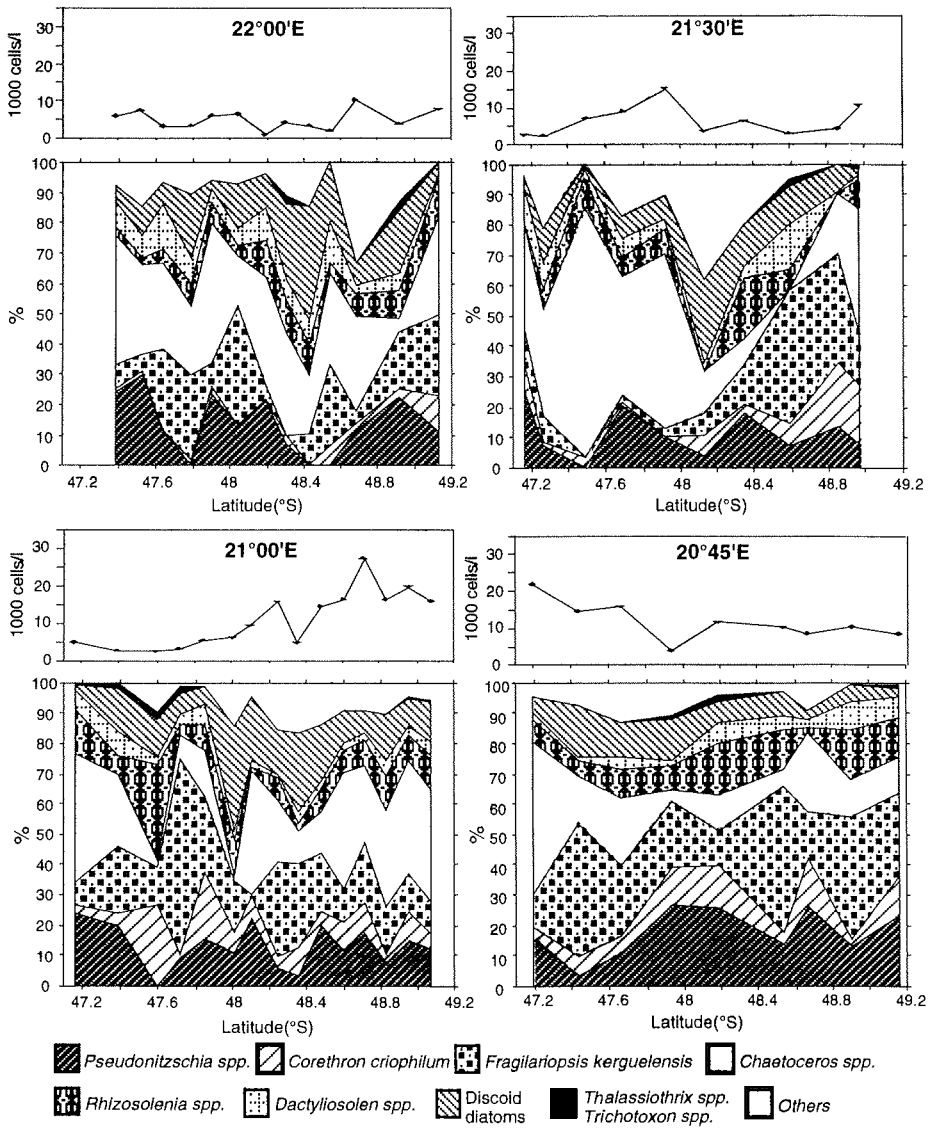

Fig. 2. Diatom abundances (in 1000 cells/l) and assemblage composition (in %) during the grid survey. The survey consisted of 4 meridionaly orlented transects at 22°00'E, 21°30'E, 21°00'E and 20°45'E.

Fig. 16.2

Prior to and shortly after fertilisation diatom abundance was generally low throughout the water column inside (T_{-2}: station 9 and T_1: station 11) and outside (T_1: station 12) the patch with somewhat higher values observed at depth than at the surface (Fig 3: T_{-2} - T_1). At T_2 (station 14) an increase in cell

numbers was detected with maximum values generally around 40-60 m water depth. However, assemblage composition did not differ markedly from that observed in the surface surveys. During the week following fertilisation no clear increase in diatom abundance occurred compared to T_2 (station 14). Instead a shift towards higher surface values could be observed (Fig. 16.3: T_4 -T_5).

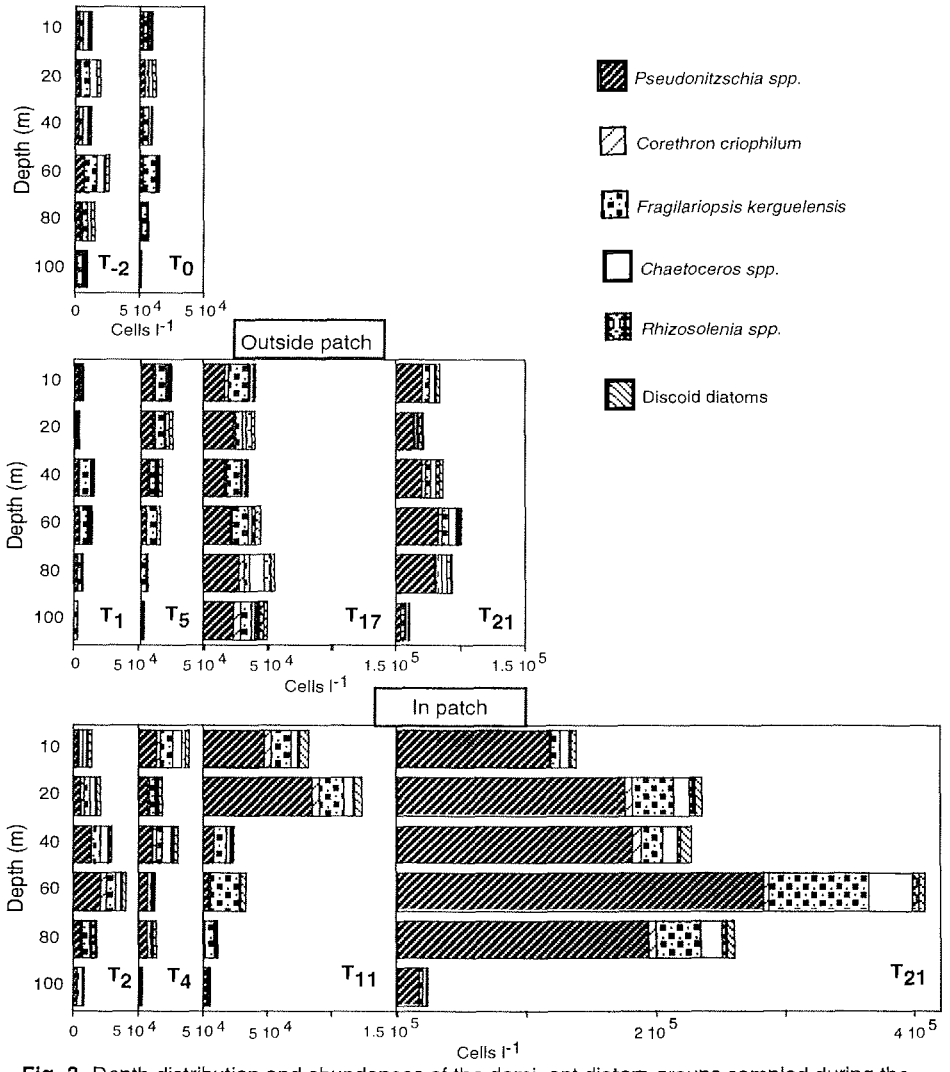

Fig. 3. Depth distribution and abundances of the dominant diatom groups sampled during the days before (T_{-2}) and during the fertilisation experiment (T_0-T_{21}). Corresponding station numbers are: (T_{-2}) Station 9; (T_0) Station 11. Outside patch: (T_1) Station 12; (T_5) Station 42;(T_{17}) Station 90; (T_{21}) Station 108. Inside patch: (T_2) Station 14; (T_4) Station 41;(T_{11}) Station 60; (T_{21}) Station 107.

Fig. 16.3.

Higher abundances were found above 40 m depth within the patch at T_4 and T_7 than at the out patch station on T_5. The variability of diatom abundance and assemblages in the fertilised patch until T_7 may well be due to the general conditions in the whole Polar Frontal Zone during that period. Therefore our results for the first week after iron enrichment indicate no significant effect of iron on diatom growth rates.

On T_{11}, however, a clear increase in diatom abundance was found at 'in' station 61 in the upper 20 m of the water column. Comparison of integrated values between 'in' patch T_{11} and 'out' patch T_{17} (station 90) shows a similar increase in diatom standing stocks at both sites of 4.16 x 10^9 cells m^{-2} and 4.37 x 10^9 cells m^{-2}, respectively. Estimates of doubling time were also not markedly different between sites (7 days for the 'in' patch station and 8 days for the 'out' patch station). Similar changes in assemblage composition were also observed.

At $T_{11/17}$ the increase in diatom abundance as compared to the situation 5 days post-fertilisation was marked by a doubling in *F. kerguelensis* number, reaching 1.17 x 10^9cells m^{-2} 'in' patch and 0.82 x 10^9 cells m^{-2} 'out' patch and about a 3-fold increase in *Pseudonitzschia spp.* abundance, reaching 1.81 x 10^9 cells m^{-2} 'in' patch and 2.01 10^9 cells m^{-2} 'out' patch. Bearing in mind that T_{11} and T_{17} were 6 days apart, the integrated values indicate that cell numbers inside the fertilised patch had reached similar values at T_{11} to those outside the patch at T_{17}. Results of size fractionated Chl a analysis (ref. Riebesell *et al.*) suggest that significant increases in diatom abundance occurred after 13 days inside the fertilised patch compared to the outside situation. A significant increase in diatom abundance can be observed within the patch by the end of the experiment at T_{21} (station 107) compared to the 'out' station (108) on the same day. Integrated values of 23.63 x 10^9 cells m^{-2} at 'in' station T_{21} are about 6.5-fold higher than the integrated values (3.59 x 10^9 cells m^{-2}) for the 'out' station T_{21}. A slight decrease in diatom standing stocks from 3.59 x 10^9 cells m^{-2} at T_{21} (station 108) to 4.37 x 10^9 cells m^{-2} at T_{17} (station 90) can be noted outside the patch. This is in sharp contrast with the strong increase from 4.16 x 10^9 cells m^{-2} at T_{11} (station 61) to 23.63 x 10^9 cells m^{-2} at T_{21} (station 107) within the fertilised patch. Both inside and outside the patch, the diatom standing stock was mainly dominated by *Pseudonitzschia spp.* by the end of the experiment with integrated values of 16.87 x 10^9 cells m^{-2} and 2.05 x 10^9 cells m^{-2}, respectively. Abundance of the thick shelled diatom, *F. kerguelensis,* increased almost 9 fold, 21 days after fertilisation to 3.16 x 10^9 cells m^{-2} inside the patch compared to 0.36 10^9 cells m^{-2} outside the patch.

These results clearly show that diatom growth in the Polar Frontal Zone (PFZ) of the Southern Ocean is limited by iron availability and that addition of iron can lead to a strong increase in diatom standing stocks, despite heavy grazing pressure and poor light conditions characteristic of the austral spring.

It should be noted that the >10 µm fraction of the phytoplankton is not accounted for with our "rapid assessment" procedure and therefore counts of non-concentrated water samples require analysis to get a more complete picture of the plankton community. Similarly, the nets might not retain quantitatively large but thin diatoms. As a consequence our results might not give a accurate view of the total >10 µm diatom fraction. Therefore, counts of non-concentrated water samples will also determine the precision of our "rapid assessment" procedure.

References

Archer, D., A. Winguth, D. Lea and N. Mahowald (2000): What caused the glacial/interglacial atmospheric pCO_2 cycles? Review of Geophysics, Vol. 38, pp. 159-189.

Boyd, P. W. *et al.* (2000): A mesoscale phytoplankton bloom in the polar Southern Ocean stimulated by iron fertilisation. Nature, Vol. 407, pp. 695-702

Coale, K. H. *et al.* (1996): A massive phytoplankton bloom induced by an ecosystem-scale iron fertilization experiment Pacific Ocean. Nature, Vol. 383, pp. 495-501

17. PHYTOPLANKTON DISTRIBUTION AND TAXON-SPECIFIC GROWTH RATES DURING AN IRON FERTILIZATION EXPERIMENT IN THE REGION OF THE ANTARCTIC POLAR FRONTAL ZONE

I. Peeken (IfM, Kiel)

Approach:

Previous studies have shown that the determination of marker pigments is a valuable tool to determine phytoplankton distribution and biomass in the southern Ocean (Peeken 1997; Veth et al. 1997). The main goals of the present study were:

1. To follow the development of biomass and composition of phytoplankton including their physiological state by means of pigment finger prints during the iron fertilization experiment.

2. Monitor the growth rates of taxon specific phytoplankton groups inside and outside the iron patch.

Pigment Analyses

Materials and Methods

Seawater samples were filtered onto 25 mm Whatman GF/F filters and stored in 1,5 ml cryo tubes at -80 °C until analysis. In total 678 samples from 72 CTD sampling cast and 100 samples from surface transects have been performed. On 4 stations additional samples for size fractionation (< 10 µ, < 5 µ, < 3 µ, < 1 µ) were taken from the chlorophyll maximum.

For analytical preparation, 50 µl internal standard (canthaxanthin) and 2 ml acetone were added to each filter sample and then homogenized for 5 minutes in a cell mill. After centrifugation, the supernatant liquid was prefiltered and transferred in auto sampler vials. Just prior to analysis 100µl of the sample was premixed with water (HPLC-grade) in the ratio 1:1 (v/v) and 150 µl injected onto the high performance liquid chromatography (HPLC)-system. The pigments were analyzed using the method described in Barlow *et al.* (1997). Eluting pigments were detected by absorbance (440 nm) and fluorescence (Ex: 410 nm, Em: > 600 nm).

Pigments were identified by comparing their retention times with those of pure standards and algal extracts. Additional confirmation for each pigment was done using on-line diode array absorbance spectra between 390-750 nm. Pigment concentrations were quantified based on peak areas of external standards, which were spectrophotometrically calibrated using extinction coefficients published by Bidigare (1991). For correction of experimental losses and volume changes, the concentrations of the pigments were normalized to the internal standard canthaxanthin.

Preliminary results

Fucoxanthin and 19´-hexanoyloxyfucoxanthin were the most prominent pigments during the course of the experiment (fig. 17.1). Fucoxanthin is used as a marker of diatoms and shows a clear increase inside the iron patch, particular during the last week of the experiment, suggesting a clear preferential growth for these organisms due to the iron fertilization. A slight

increase of the diatom marker was also found outside the patch, suggesting also a succession towards a diatom-dominated phytoplankton community outside the iron-patch. In opposite, the marker of prymnesiophytes, 19´-hexanoyloxyfucoxanthin (19-hex), decreases inside and less pronounced outside the patch.

Peridinin and chlorophyll b, the markers of autotroph dinoflagellates and chlorophytes were less effected by the iron addition with slightly higher concentrations inside the patch (fig. 17.2). Additional to the presented markers, 19´-butanoyloxyfucoxanthin, alloxanthin and zeaxanthin, the markers of pelagophytes, cryptophytes and cyanophytes were present during the investigation.

After evaluation of the whole data set, the CHEMTAX program of Mackey *et al.* (1996) will be used to calculate the contributions of different algae groups to the phytoplankton community.

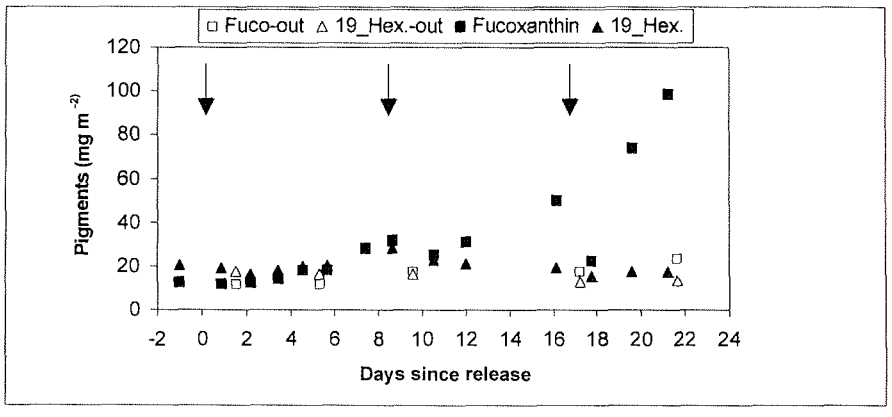

Figure 17.1: Depth integrated (100 m) concentrations of fucoxanthin (fuco) and 19´-hexanoyloxyfucoxanthin (19-hex) inside (filled symbols) and outside (open symbols) the iron fertilised patch. Arrows present iron release.

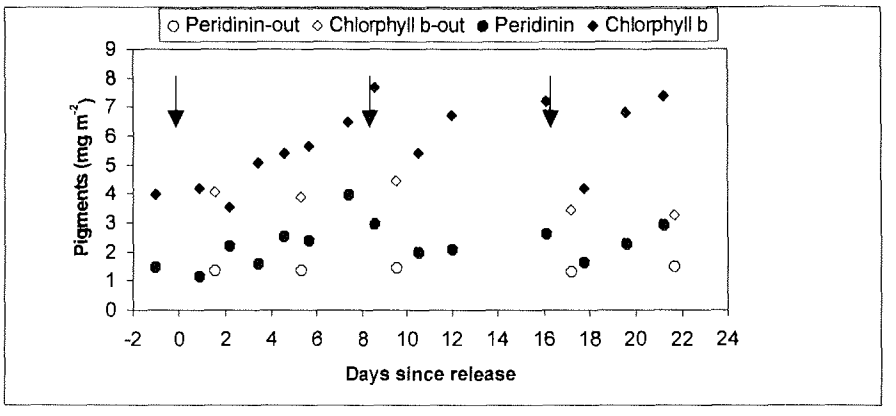

Figure 17.2: Depth integrated (100 m) concentrations of peridinin and chlorophyll b inside (filled symbols) and outside (open symbols) the iron fertilized patch. Arrows present iron release.

Taxon specific growth rates

Materials and methods

Experiments to determine the growth rates of taxon specific phytoplankton groups were performed 10 times inside and 6 times outside the iron patch. 1.8-2.2 l of seawater was sampled from the chlorophyll maximum using GOFLO-bottles. $H^{14}CO_3^-$ was transferred into the 2.3 l bottles and incubated for 24 h in decks incubators with 50% ambient light level. To determine ^{14}C incorporation into Chl a and taxon specific carotenoids samples were filtered on GF/F-filters at the end of the incubation and frozen at -80°C until analyses. Phytoplankton growth rates are determined from the specific ^{14}C-activity of Chl a or taxon-specific carotenoids using functions which relate pigment specific activity to growth rates. Thus estimates of phytoplankton growth rate are unaffected by the recycling of carbon in the incubation bottles (e.g. algae respiration, zooplankton grazing) because specific ^{14}C-activity of a pigment a ratio is not affected when zooplankton remove and destroy pigments over the course of an incubation. The isolation of Chl a and the marker carotenoids will be performed according to Goericke and Welschmeyer (1993; 1993)in the isotopic lab in Kiel.

References

Barlow, R. G., D. G. Cummings, et al. (1997). "Improved resolution of mono- and divinyl chlorophylls *a* and *b* and zeaxanthin and lutein in phytoplankton extracts using reverse phase C-8 HPLC." Marine Ecology Progress Series 161: 303-307.

Bidigare, R. R. (1991). Analysis of algal chlorophylls and carotenoids. Marine particles: Analysis and Characterisation. D. C. Hurd and D. W. Spencer, American Geophysical Union. Geophysical Monograph: 119-123.

Goericke, R. and N. A. Welschmeyer (1993). "The carotenoid-labeling method: Measuring specific rates of carotenoid synthesis in natural phytoplankton communities." Marine Ecology Progress Series 98: 157-171.

Goericke, R. and N. A. Welschmeyer (1993). "The chlorophyll-labeling method: Measuring specific rates of chlorophyll *a* synthesis in cultures and in the open ocean." Limnology and Oceanography 38(1): 80-95.

Mackey, M. D., D. J. Mackey, et al. (1996). "'CHEMTAX'- a program for estimating class abundances from chemical markers: application to HPLC measurements of phytoplankton." Marine Ecology Progress Series 144: 265-283.

Peeken, I. (1997). "Photosynthetic pigment fingerprints as indicators of phytoplankton biomass and development in different water masses of the Southern Ocean during austral spring." Deep-Sea Research II 44(1/2): 261-282.

Veth, K., I. Peeken, et al. (1997). "Physical anatomy of fronts and surface waters in the ACC near the 6°W meridian during austral spring 1992." Deep-Sea Research Part II 44(1/2): 23-50.

18. MOLECULAR ASSESSMENT OF IRON-LIMITATION USING FLAVODOXIN/FERRODOXIN ASSAYS

J. La Roche and I. Peeken, (IfM, Kiel)

Approach:

It has been previously demonstrated that flavodoxin replaces ferredoxin in iron-limited diatoms and that it is possible to use the presence of flavodoxin as an indicator of iron limitation in this group of algae. Immunological probes allow the presence or absence and the relative abundance of proteins to be measured using small amounts of material. Western blots of total protein extracts will allow the simultaneous measurements of relative abundances of a number of proteins including flavodoxin, ferredoxin on the same samples.

Methods

Sample collection: Samples for proteins from bulk particulate matter were collected either with a surface pumping system or with Niskin bottles from CTD-casts. Each sample required between 20-40 L of water depending on the ambient chlorophyll concentration. Samples were collected at 12 stations inside the patch and at 6 stations outside the patch. At selected stations, samples were collected along a vertical profile to the bottom of the euphotic zone to characterize the relationship between phytoplankton Fe-status and light. Seawater was filtered on 3 µm pore, 142 mm diameter polycarbonate filters. Approximately 100 µg of total proteins corresponding to about 5 µg of chl a was preferred for determining flavodoxin, ferredoxin and other photosynthetic proteins in total protein extracts. The filters containing the phytoplankton were rinsed into 2 x 15 ml conical centrifuge tubes and the samples pelleted in a bench top centrifuge. The supernatant was discarded and the pellet transferred to a 1.5 ml conical cryo vial , pelleted in a micro centrifuge, the supernatant discarded, and the pellet stored –80 °C until analysis. Sample processing using the method describe here (i.e. with bench top and micro centrifuge) has been used successfully at sea both in the sub arctic Pacific (La Roche et al. 1996) and in the Southern Ocean (Boyd et al. 2000). Samples frozen at -80 °C are stable for longer then 1 year.

Western blotting will be conducted using total protein extracts to determine flavodoxin, ferredoxin, Rubisco, fucoxanthin-chlorophyll complex, and nitrate reductase. The liquid N_2 frozen pellet will be disrupted by sonicating in SDS carbonate protein extraction buffer as described in La Roche et al. (1996).

Protein concentrations will be measured using the bicinchoninic acid method and equal amounts of proteins for each sample will be separated by sodium dedocyl sulfate polyacrylamide electrophoresis (SDS-PAGE), followed by transfer to nitrocelullose membrane as described (La Roche et al., 1995). Samples on western blots are therefore loaded on an equal amount of protein basis and flavodoxin variations are thus normalized to microgram of proteins. Abundance of specific proteins will be determined from immunoassays using the ECL (enchanced chemiluminescence) technique (Amersham).

References

Boyd, P., A. Watson, et al. (2000). "A mesoscale phytoplankton bloom in the polar Southern Ocean stimulated by iron fertilization." Nature **407**: 695-702.

La Roche, J., P. W. Boyd, et al. (1996). "Flavodoxin as an *in situ* marker for iron stress in phytoplankton." Nature **382**: 802-805.

La Roche, J., H. Murray, et al. (1995). "Flavodoxin expression as an indicator of iron limitation in marine diatoms." Journal of Phycology **31**: 520-530.

19) BACTERIAL RESPONSES TO IRON ADDITION

M. Weinbauer, T. Arrieta (NIOZ)

Bacterioplankton represent the largest living surface and biomass in the ocean, exhibiting abundances in the range 10^5-10^6 ml^{-1} in the photic zone of the open ocean. Because of their high metabolic activity, bacteria play an essential role in the carbon and energy flux through marine food webs by converting dissolved organic carbon (DOC) into living biomass and CO_2. Bacterioplankton are basically the only consumers of DOC and their activity is intimately linked to phytoplankton activity. In HNLC areas bacteria might be iron-limited in a similar fashion as phytoplankton are and probably also carbon limited as the production of labile dissolved carbon by phytoplankton is low.

Bacterial abundance and production (measured as ^{3}H-thymidine and ^{3}H-leucine incorporation) increased rapidly inside the patch over the first few days after iron fertilization while the abundance and production of the outside-the-patch community remained comparatively stable.

Bacterial hydrolysis of macromolecules is the rate-limiting step in bacterial processing of DOM, as bacteria can only take up small molecules not bigger than about 600 Da. Bacterial protein hydrolysis increased inside of the patch together with the increase in bacterial numbers, while the hydrolysis of both __ and __linked carbohydrates increased from almost undetectable levels outside the patch to up to a few hundreds pmol l^{-1} h^{-1} inside the patch.

The rapid increase in bacterial abundance, production and activity suggests that bacteria reacted to iron addition faster than could be expected by increased carbon availability (due to the production of labile dissolved carbon by phytoplankton) only.

The iron addition itself as well as the subsequent increase in primary production might have favoured a change in the bacterial species composition. Since less than 1% of marine bacterioplankton can be cultured, we collected and concentrated bacteria in order to track these potential changes in the lab by means of DNA fingerprinting techniques.

Additionally we collected samples for estimating the iron-induced changes in viral diversity, viral mortality of bacteria, lysogeny and _-glucosidase diversity. Bacterial communities of selected stations were fractionated alive by means of capillary electrophoresis in order to estimate the metabolic activities of different subpopulations, to circumvent the cultivation problems mentioned above.

As D-amino acids in seawater are produced only at significant rates by bacteria, the role of bacteria in the release of DOM and its consumption by bacteria during iron fertilization will be estimated in selected samples by analyzing the concentrations of D- and L-amino acids and bacterial uptake of D-and L-aspartic acid.

Overall, our aim was to investigate, whether iron has an effect on the abundance, performance and diversity of bacteria and viruses in the Southern Ocean.

20. DISTRIBUTION OF NUTRIENTS DURING THE IRON EXPERIMENT (AWI)

C. Hartmann, K.-U. Richter, C. Harms (AWI)

Distribution and dynamics of the major nutrients were determined in the Polar Frontal Zone during the iron experiment. The interaction between nutrients and phytoplankton development was the major topic.
Underway measurements were conducted along the 20° meridian from 45° to 52°S to get an overview of the positions of the fronts. Nutrient levels generally increase from north to south in the Southern Ocean.
To support the search for iron deployment we also monitored continously the nutrient concentrations of surface water at short intervals along a 350 km diagonal transect through the suspected eddy area found by ADCP profiles. Additionally we measured nutrients in a grid consisting of 4 north-south-transects.
The result of iron supply was an enhanced algal stock associated with nutrient uptake. The influence of the iron fertilization on the concentrations of nutrients with depth were determined at selected in-patch stations and were compared with out-patch stations.

Sampling and analysis methods
Nutrients were determined from underway samples, CTD bottles and Goflo bottles. CTD samples were taken from so-called "CTD 1" according biological request. Underway samples were taken from about 8 m depth by the on-board water supply system. The sampling intervals were 30 min during the north-south-transect, near the fronts 15 min and 30 min during grids. The determination of silicate, phosphate, nitrate, nitrite and ammonium essentially followed the routinely used methods for seawater analysis and was performed with a Technicon Autoanalyser II system.

Preliminary data and results
Along the north-south-transect the nutrient concentrations were closely related to the frontal systems. Their concentrations were generally high and not limiting phytoplankton growth. North of the Polar Front silicate was low in contrast to nitrate and phosphate concentrations which were always high. In the Polar Front region surface silicate values slightly increased and towards

the south the concentrations reached values about 55 µM at the southern Polar Front at 51°S (Fig. 20.1). The Polar Front was encountered at 49.7°S. Nitrate concentrations were always high and varied between 22 and 25 µM at the Polar Front. Further south nitrate increased to about 30 µM (Fig. 20.2). Phosphate closely followed the pattern of nitrate. The concentrations ranged between 1.2 and 1.7 µM and reached maximum values of 2.2 µM at about 52°S (Fig. 20.3).

Within the area selected for the iron-fertilization silicate measurements clearly showed the eddy structure found by ADCP. The local maximum of silicate at 47.8°S 21°E coincides with the center of the eddy (Fig. 20.4).

Significant uptake of nutrients could be observed due to iron-increased primary production. Between the first in-patch station no. 11 after iron-supply and the last in-patch station no. 107 after 21 days we found a clear decrease of nutrient concentrations in the mixed surface layer: silicate decreased by about 4 µM, nitrate by about 2 µM and phosphate by about 0.2 µM (Fig. 20.5).

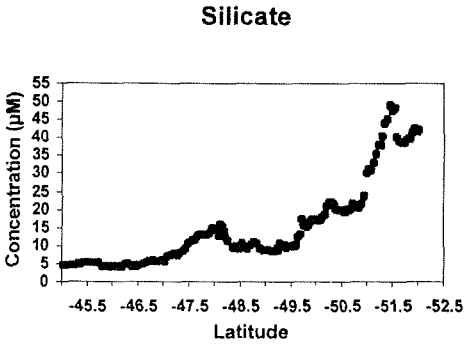

Fig. 1 Silicate concentrations during the north-south transect

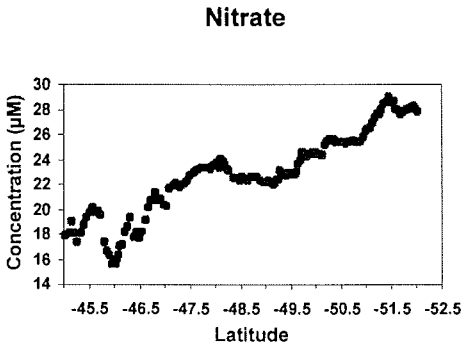

Fig. 2 Nitrate concentrations during the north-south transect

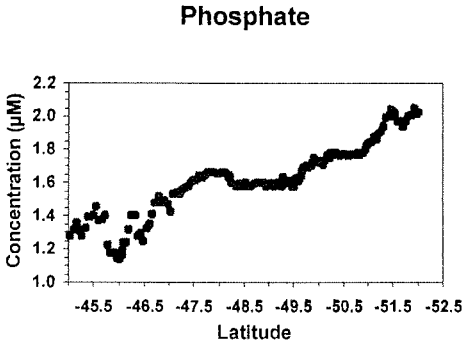

Fig. 3 Phosphate concentrations during the north-south transect

Fig.4 Silicate surface data (μM) in the iron supply area

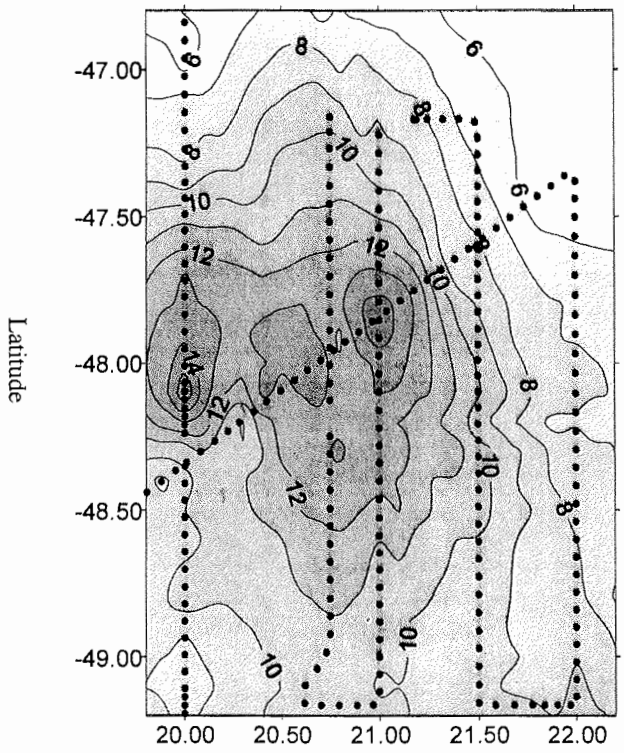

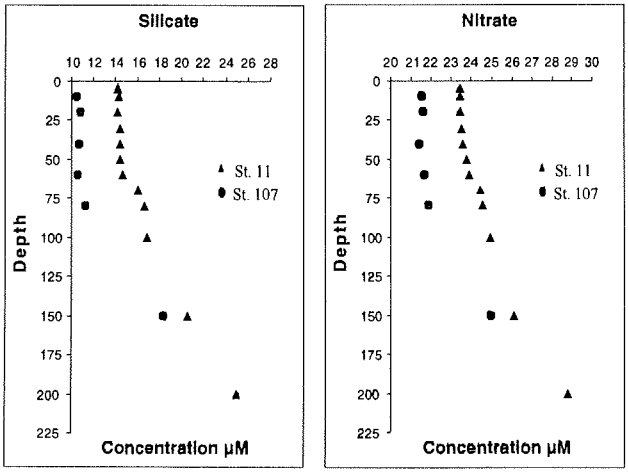

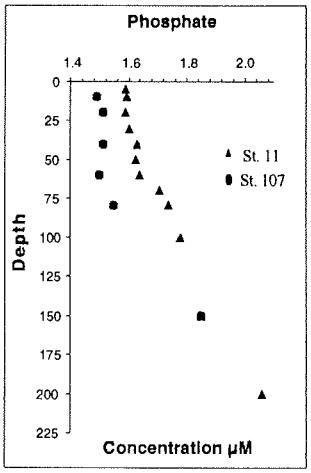

Fig.5 Silicate, nitrate, phosphate concentrations at Station 11 (first in-patch station) and Station 107 (last in-patch station)

21. CHLOROPHYLL-*A*, PARTICULATE AND DISSOLVED ORGANIC MATTER, PRIMARY PRODUCTION AND STABLE ISOTOPE COMPOSITION OF POM AND PHYTOPLANKTON OVER THE COURSE OF THE IRON FERTILISATION EXPERIMENT

U. Riebesell, F. Gervais, A. Benthien, A. Terbrüggen, U. Schneider (AWI),
B. Luz and E. Barkan (Hebrew University Jerusalem)
M. Altabet (University of Massachusetts)
R. Saunders (Southampton Oceanographic Center; DON, DOP)

1 Introduction

The objectives of our work were

- the monitoring of the spatial and temporal distribution of the chlorophyll-*a* concentration during Eisenex I.
- to determine the development of particulate organic matter and dissolved organic matter over the course of the induced phytoplankton bloom.
- to monitor changes in the stable carbon and nitrogen isotopic compositions ($\Delta^{13}C$, $\Delta^{15}N$) of particulate organic matter, phytoplankton biomarkers, nitrate and dissolved inorganic carbon in and outside of the iron fertilised patch.
- to measure ^{14}C primary production in different phytoplankton size fractions and to quantify gross primary production within and outside of iron-enriched waters.

2 Chlorophyll-*a* concentration

2.1 Introduction: The monitoring of chlorophyll-*a* concentration (as an indicator of phytoplankton biomass) was necessary during Eisenex I to find a suitable ocean region and to describe the temporal and spatial dynamics of phytoplankton biomass within and outside of the Fe-fertilised patch.

2.2 Methods: Water samples were filtered on GF/F filters, immediately extracted in 90 % acetone and subsequently analysed fluorometrically (before and after acidification of the extract) with a Turner Design Model 10-AU digital fluorometer. Results were available approximately 3-6 h after sampling. In total we performed 653 chlorophyll-*a* and phaeopigment analyses from surface transects and 1160 analyses from 88 CTD sampling casts. Most of the samples taken from different sampling depths were analysed in size fractions (<2 µm, 2-20 µm, >20 µm). The use of chlorophyll fluorescence to

determine algal biomass proved to be unreliable during Eisenex I due to light quenching of fluorescence during the day and due to different and varying chlorophyll-specific fluorescence of Fe-limited and Fe-replete algae.

2.3 Preliminary results:

The areal amount of chlorophyll-*a* was about 50 mg m^{-2} outside of the iron fertilised patch throughout the experiment (Fig. 21.1). In the centre of the iron fertilised water body, the chlorophyll-*a* amount increased to a maximum of 230 mg m^{-2} in the 3 weeks after the first iron infusion (Fig. 21.1). The percentage of the chlorophyll-*a* size fraction >20 µm increased inside as well as outside of the patch (Fig. 21.2). Compared to the situation outside the patch, this percentage was higher inside the patch in the second half of the experiment (Fig. 21.2). On day 18 of the experiment, the patch of elevated chlorophyll-*a* concentration covered an area of roughly 1000 km^2 (Fig. 21.3). In the third week of the experiment, the increase of the chlorophyll-*a* concentration was evident in the upper 80 m of the water column (example in Fig. 21.4).

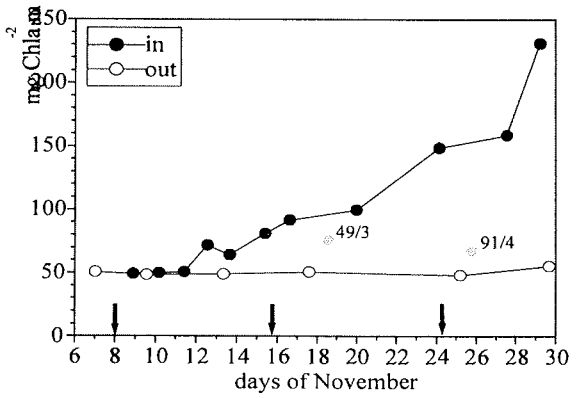

Fig. 21.1: Areal amount of chlorophyll-*a* in the centre and outside of the iron fertilised patch (0-100 m, 6-11 samples). Sampling casts 49/3 and 91/4 were situated at the edge of the patch. Arrows mark the iron infusions.

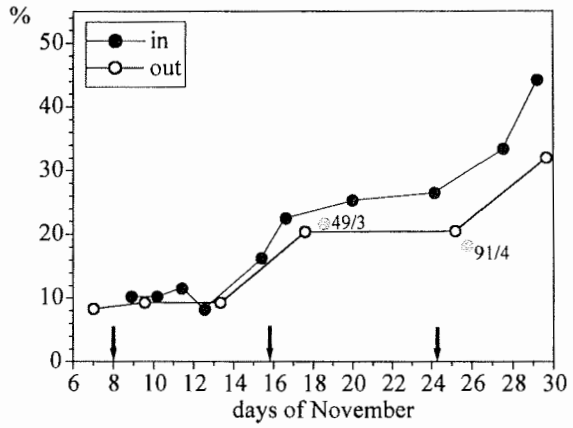

Fig. 21.2: Percentage of the chlorophyll-*a* size fraction >20µm in the subsurface samples (mostly taken from 20 m depth) in the centre and outside of the iron fertilised patch. Sampling casts 49/3 and 91/4 were situated at the edge of the patch. Arrows mark the iron infusions.

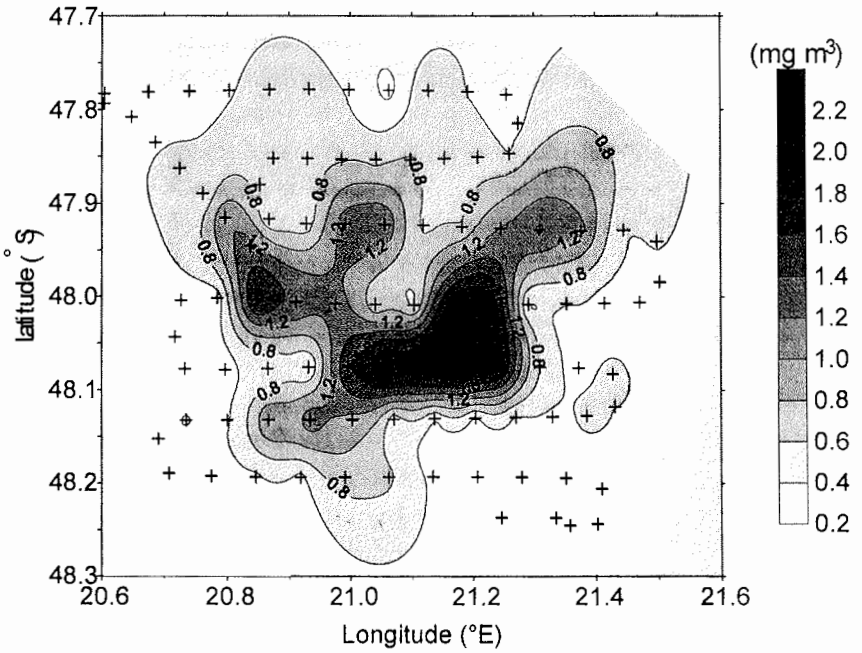

Fig. 21.3: Horizontal distribution of the surface chlorophyll-*a* concentration in the region of the iron fertilised patch. Samples were taken from 8 m depth through the ship's uncontaminated seawater system from 25.11.00 20:30 GMT to 26.11.00 20:00 GMT. Crosses mark the sampling positions.

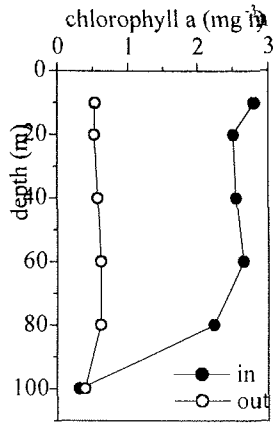

$\delta^{13}C$ Fig. 21.4: Vertical distribution of the chlorophyll-*a* concentration in the centre and outside of the iron fertilised patch on November 29th 2000.

3 Particulate and dissolved organic matter

3.1 Introduction: The analyses of POC and PON will provide estimates of changes in bulk organic matter and phytoplankton biomass and – in combination with other measurements – will help to determine the response of the plankton community to iron enrichment. DOC, DON and DOP measurements will contribute in assessing the fate of organic matter produced in response to Fe fertilisation.

3.2 Methods: Water samples were collected from CTD sampling casts (238 samples) and horizontal surface transects (35 samples) and filtered on GF/F filters. POC and PON filter samples are kept frozen until mass spectrometric analysis. In 187 samples, the concentrations of DOC, DON and DOP will be measured.

4 Stable isotope composition of particulate organic matter and phytoplankton biomarkers

4.1 Introduction: The stable carbon and nitrogen isotopic compositions of marine organic matter ($\delta^{13}C$, $\delta^{15}N$) provide important insights into the environmental conditions under which the organic matter was formed. The isotopic signals incorporated in phytoplankton organic matter are known to be affected by the availability of inorganic carbon and nitrogen, by the form of

carbon (CO_2 or HCO_3^-) and nitrogen (NO_3^- or NH_4^+) taken up by the cells, by the rate of growth, and by the growth-limiting resource (among other factors). Significant differences in the isotopic compositions are therefore expected in Fe-fertilised relative to Fe-deplete phytoplankton. Such differences may help to determine changes in iron availability and related changes in primary production over the geological past from the isotopic compositions of sedimentary organic matter. To account for possible interference from non-phytoplankton organic matter, stable isotopes will be measured in both bulk organic matter and individual biomarkers of marine autotrophic origin (phytol, sterols, alkenones).

4.2 Methods: The determination of bulk organic matter $\delta^{13}C$ and $\delta^{15}N$ will be performed on the filters prepared for POM analysis (see x.3.2). To be able to calculate the carbon isotope fractionation, additional samples were taken to analyse the $\delta^{13}C$ of dissolved inorganic carbon. 213 filtrate samples from CTD sampling casts and transects were preserved for the analysis of nitrate-$\delta^{15}N$. At most of the CTD sampling stations, water from the vessel's uncontaminated seawater system was filtered on GF 55 filters for $\delta^{13}C$ measurements of individual biomarkers (152 samples). All filter samples are stored frozen until mass spectrometric analysis.

5 Carbon uptake

5.1 Introduction: One of the basic questions of Eisenex I was to what extent the primary production of phytoplankton would change in response to the iron addition. Based on previous iron enrichment experiments it was expected that the response differed between phytoplankton size classes. Therefore size fractionated ^{14}C uptake was quantified.

5.2 Methods: ^{14}C primary production was measured in simulated *in situ* (SIS) incubations in a laboratory incubator according to Babin et al. (L&O 39: 694-702, 1994). Samples were taken from 18 CTD sampling casts inside and outside of the Fe-fertilised patch. For each cast, 10 samples from different depths were incubated at the light intensity they would have seen at a surface photon flux density of 450 µmol m^{-2} s^{-1} at ambient temperature for 4 h. Additionally, a subsurface sample (usually from 20 m depth) was incubated at 12 different light intensities (from 1400 to 1 µmol m^{-2} s^{-1}) in the Babin incubator for an analysis of the relationship between productivity and irradiance (P vs. E) at a representative depth.

^{14}C uptake in the >0.45 µm fraction of the SIS samples was measured in three parallels. In the P vs. E incubation, ^{14}C uptake in each sample was analysed in three different size fractions (>0.45, >0.2 and >20 µm). ^{14}C was analyzed by liquid scintillation counting (Tricarb 1900 TR). The relationship between algal photosynthesis and irradiance (P vs. E curves) will be analysed. By combining the results with measurements of global radiation and the vertical light attenuation coefficient, areal daily primary production will be calculated.

5.3 Preliminary results:

The results of the simulated *in situ* incubations indicate a clear increase in the primary production potential of the phytoplankton inside the iron fertilised patch compared to the algae in the unfertilised region (Fig. 21.5). The percentage of the primary production in the phytoplankton size fraction >20 µm increased inside as well as outside of the patch and was higher inside the patch in the second half of the experiment (Fig. 21.6). Inside the patch, between 35 and 65 % of the primary production was performed by phytoplankton smaller than 2 µm.

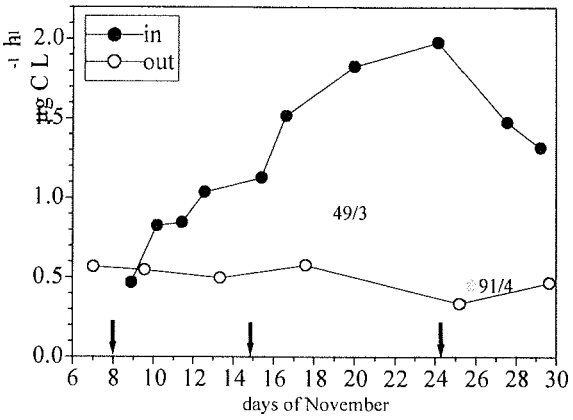

Fig. 21.5: Carbon uptake in the simulated *in situ* incubations of subsurface samples (10 m) in the centre and outside of the iron fertilised patch. The incubation assumed a surface irradiance of 450 µmol m^{-2} s^{-1}. Sampling casts 49/3 and 91/4 were situated at the edge of the patch. Arrows mark the iron infusions.

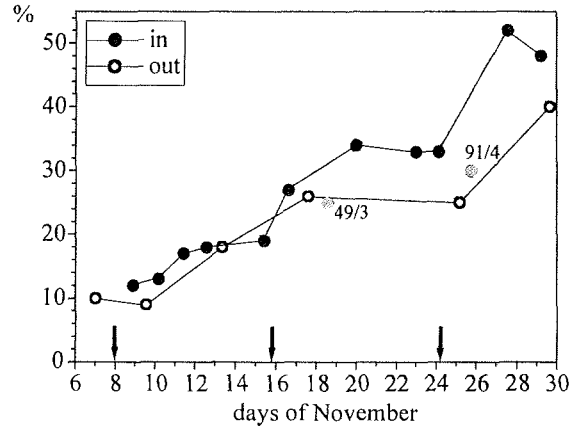

Fig. 21.6: Percentage of the primary production in the phytoplankton size fraction >20µm in the subsurface samples (mostly taken from 20 m depth) in the centre and outside of the iron fertilised patch. Sampling casts 49/3 and 91/4 were situated at the edge of the patch. Arrows mark the iron infusions.

6 Gross primary production

6.1 Introduction: Estimates of primary production (bottle incubations, changes in O_2 concentration, calculations from P vs. E curves etc.) all have their advantages and shortcomings. An independent and potentially powerful method to determine *in situ* gross and net community primary production is through measurements of the triple isotope composition of dissolved oxygen and the ratio of O_2/Ar (see Luz et al., Nature 400, 547-550, 1999; Luz & Barkan, Science 288: 2028-2031, 2000). The advantage of this method is that it will provide temporally integrated estimates of gross and net primary production in response to iron fertilisation.

6.2 Methods: 198 seawater samples were taken from 17 CTD sampling casts inside and outside the iron-fertilised patch. Additionally, 40 reference samples were taken below 3000 m depth and from surface transects. Measurements of oxygen isotopes and determination of O_2/Ar will be performed according to Luz et al. (Nature 400, 547-550, 1999; Luz & Barkan, Science 288: 2028-2031, 2000).

22. PRIMARY PRODUCTIVITY AND PHOTOSYNTHETIC RESPONSE OF PHYTOPLANKTON TO IRON ENRICHMENT IN THE SOUTHERN OCEAN

M. Y. Gorbunov, P. G. Falkowski and Z. S. Kolber
Environmental Biophysics and Molecular Ecology Program
Institute of Marine and Coastal Sciences
Rutgers, The State University of New Jersey
71 Dudley Road, New Brunswick, New Jersey 08901, U.S.A.
gorbunov@imcs.rutgers.edu; falko@imcs.rutgers.edu; zkolber@imcs.rutgers.edu

Introduction

Because of its sensitivity and convenience, chlorophyll fluorescence is routinely used to estimate phytoplankton biomass and photosynthetic activity (e.g., Falkowski and Kolber 1995). Fluorescence-based measurements have been successfully employed during the previous iron enrichment experiments in the equatorial Pacific (IronEx-I and IronEx-II, Kolber et al. 1994, Behrenfeld et al. 1996) and the polar Southern Ocean (SOIREE, Boyd et al. 2000) and unequivocally established physiological limitation of phytoplankton by iron in these High Nutrient Low Chlorophyll (HNLC) regions of the ocean. The data from the three previous *in situ* experiments revealed that iron enrichment stimulated all taxa and cell size fractions of phytoplankton, however, big diatoms exhibited higher accumulation rates and, as a consequence, became dominant in the iron-mediated blooms. Whether big diatoms are more responsive, photosynthetically and physiologically, to iron enrichment or more resistant to grazing pressure, or both, remains unclear.

In the EISENEX-1 experiment, we evaluated the photosynthetic response of phytoplankton to iron enrichment by using the Fast Repetition Rate (FRR) fluorometry (Kolber et al. 1998). Our goals have been:

to quantify dynamics of the iron-mediated phytoplankton bloom and modifications in the photosynthetic apparatus of phytoplankton;

to identify unique photosynthetic signatures of different cell size groups of phytoplankton and the species dominating the iron-stimulated bloom with the overarching goal to understand the cause of the iron-mediated change in the phytoplankton community structure;
to assess the effect of environmental conditions (such as irradiance level, vertical mixing and horizontal dispersal) on the bloom development.
Also, we performed underway surveys of the region before and during the iron release experiment and provided FRR fluorescent and photosynthetic parameters of phytoplankton in the on-deck incubation experiments conducted by scientists from AWI and NIOZ.

Methods and Sampling Procedures

The Fast Repetition Rate (FRR) Fluorometry provides a comprehensive suite of fluorescence yields and photosynthetic parameters in phytoplankton (Falkowski and Kolber 1995; Kolber et al, 1998). These parameters include the quantum efficiency of photochemical energy conversion in PSII (F_v/F_m), the functional absorption cross section of PSII ($\_{PSII}$), the kinetics of electron transport on the acceptor side of PSII (i.e. the rate of re-oxidation of the first quinone acceptor Q_a), the kinetics of electron transport between PSII and PSI (i.e. re-oxidation of the plastoquinone pool), and the parameters of photosynthesis versus irradiance (P-I) curves (Kolber et al. 1998). These measurements permit rapid assessment of photosynthetic performance (i.e. of *how 'healthy'* are phytoplankton) and identification of the environmental factors controlling photosynthetic rates (i.e. *why* phytoplankton are not healthy).
In the EISENEX-1 we employed two instruments: the bench-top FRR fluorometer and the Single Cell FRR fluorometer. The first instrument was used for continuous measurements in a flow-through cuvette during the underway survey of near-surface phytoplankton and for analysis of water samples collected at various depths. In this instrument, fluorescence is measured on bulk water samples and, thus, represents the average photosynthetic performance of the ensemble of the myriad phytoplankton taxa that comprise the assemblage. In an effort to examine phytoplankton photosynthetic processes on a taxonomic level, we extended the basic FRR fluorometry approach to retrieve photosynthetic parameters for individual algal cells (Gorbunov et al. 1999).

Results and Discussion

FRR fluorescence survey of phytoplankton prior to iron fertilization - With the aim to choose a place for the iron release experiment, we started an underway survey of near-surface phytoplankton on October 26. The horizontal distribution of phytoplankton abundance and photosynthetic efficiency along the southward transect 1700 km on the ca. 20°E meridian is shown in Fig. 22.1. On the northern part of the transect (by station 3 (S3), 45°S), the phytoplankton distribution was "patchy" with chlorophyll concentration varying from 0.4 to 3.1 mg/m^3, which is typical for spring phytoplankton blooms. F_v/F_m values varied from ~0.35 to 0.45 (i.e. 50% to 70% of its maximum) at night and declined down to 0.2 under bright ambient light due to photoinhibition (Fig. 22.1). The high night values of F_v/F_m are indicative for high growth rates of phytoplankton, suggesting high nutrient availability in that region.

On the southern part of the transect (45°S to 52°S, between the Subantarctic Front (SAF) and the Polar Front), the phytoplankton distribution was characterized by low spatial variability and lower fluorescence corresponding to chlorophyll concentrations from 0.3 to 0.5 mg/m^3. The night values of F_v/F_m were also lower and averaged 0.30, the value typical for nutrient (in this region - iron) limited phytoplankton.

The underway FRRf survey 5 weeks later (on the way back to Cape Town) showed the similar pattern of F_v/F_m (~ 0.26 to 0.30 - south of the SAF and 0.37 to 0.42 – north of the SAF), suggesting that the pattern of nutrient availability remained the same.

On Nov. 2 – Nov. 6, a grid across the mesoscale eddy with the center at ca. 48°S, 19°E has been made (data not shown), which confirmed little variability in phytoplankton photosynthetic efficiency ($F_v/F_m = 0.32 \pm 0.03$) over the region. Chlorophyll concentration in the central part of the eddy also varied in a narrow range (~20%). Thus, together with physical and chemical conditions, the quasi-uniform spatial distribution of phytoplankton made the eddy center a good spot for the iron fertilization experiment.

Interplay between iron and light limitation of phytoplankton photosynthesis in the euphotic zone -

Although low iron availability is thought to be the main factor limiting phytoplankton growth in the Southern Ocean, low irradiance may also become a limiting or co-liming factor, especially in winter, when the water is deeply mixed (e.g., Mitchell et al. 1991). Theoretically, the interplay between the effects of low iron and low irradiance on phytoplankton is complex. At low

light, algae exhibit high cellular Fe requirements for growth, because photoacclimation to low light involves an increase in the concentration of light-harvesting complexes and the abundance of Fe-containing components of the photosynthetic apparatus. On the other hand, the required flux of nutrients, including iron, into the cell is significantly lowered at low light because of low growth rates. During EISENEX-1, we inferred the effect of low light and iron limitation from the biophysical essay of photosynthetic performance over the water column (Fig.22.2). The main results are:

At out-patch stations, F_v/F_m was low (~0.3) in the upper layers, but increased to 0.4- 0.45 (and even 0.5 by the end of the experiment) at depths below 50m (Fig. 22.2B), suggesting that phytoplankton growth was limited by iron only in the upper portion of the euphotic zone.

Stratification of the water column under low wind conditions tended to increase the extent of iron limitation in the near-surface layers, as evidended from a related decrease in F_v/F_m (e.g., profile for St.12 in Fig.22.2B).

$\_{PSII}$ was constant throughout the mixed layer, but increased significantly below the mixed layer due to photoacclimation to low light, a pattern indicative to light limitation of phytoplankton growth.

As the mixed layer deepened, $\_{PSII}$ throughout the layer increased significantly (e.g., profile for St. 48 in Fig. 22.2C). A sign of photoacclimation to low light, this increase in $\_{PSII}$ suggests that phytoplankton became severely light limited in the whole water column.

The oscillations in subsurface $\_{PSII}$, both outside and inside the patch, driven by the changes in the mixed layer depth, indicate that the phytoplankton ability to photoacclimate was not affected by low iron concentrations. The high values of $\_{PSII}$ in the low light environment imply that ambient iron concentrations were still high enough to maintain high cellular Fe requirements.

The rate of photosynthetic electron transport between PSII and PSI decreased significantly with depth (Fig. 22.2D). At depths > 60m, the diurnal values of $(\_{PQ})^{-1}$ decreased down to the values measured at surface after the extended exposure to darkness (e.g., the profile for S9 in Fig. 22.2D, sampled at 1:00 a.m.). The low values of $(\_{PQ})^{-1}$ indicate that the photosynthetic electron transport became deactivated at low light, a sign of severe light limitation.

Evolution of the iron-mediated bloom –

The first indication of a phytoplankton response to iron enrichment was a slight, but detectable increase in F_v/F_m, recorded during the underway survey 24 hours following the iron release (Fig. 22.3, Fig. 22.4A). The temporal

pattern of F_v/F_m was characterized by a half time of ca. 48 h. (Fig. 22.3), which is as twice as lower than that during IronEx I and II, but apparently faster than during SOIREE. The increase in F_v/F_m was accompanied by a proportional increase in the rate of electron transport on the acceptor side of PSII (i.e. re-oxidation of Q_a acceptor, $(\tau_{Qa})^{-1}$), in consistence with the previous laboratory studies of nutrient limitation. In contrast to $(\tau_{Qa})^{-1}$, the values of $(\tau_{PQ})^{-1}$ remained the same, implying that the maximum rates of electron transport, measured at saturating light, were not affected by iron enrichment. This conclusion appears to be consistent with C^{14}-based measurements of P^{max}.
τ_{PSII} decreased in the patch (not shown), however, in contrast to F_v/F_m, the change in τ_{PSII} was much slower and paralleled an increase in chlorophyll concentration. Preliminary analysis suggests that the observed decrease in τ_{PSII} was a consequence of the shift in species composition and cellular pigment density, rather than of the iron-mediated modifications of photosynthetic apparatus. This pattern suggests that the iron limitation of phytoplankton in the region was not so severe as in the equatorial Pacific (data from both IronEx experiments), presumably due to low light being a co-limiting factor.
Although the slow development of the bloom in the Southern Ocean has been previously attributed to low temperature (Boyd et al., 2000; Boyd and Abraham, in press), our data clearly suggest that the primary reason is light limitation. Another reason may be rapid decline in the iron concentration several days following each of the iron releases and, thus, below optimal iron concentrations during significant periods of the experiment. A virtual absence of the chlorophyll build-up during the first 4-5 days could be also caused, at least in part, by rapid dispersal of the fertilized patch of a small initial size. Further examination is required for the contributions of each factor to be evaluated.
The FRRf data acquired both at stations and during underway surveys provide background for further modeling of the budget of phytoplankton stock and production during EISENEX-1.

Cell size and taxa specific photosynthetic response of phytoplankton to iron enrichment -
We evaluated the cell size specific response of phytoplankton to iron enrichment using the Single Cell FRR fluorometry. While data analysis, the fluorescence signals from individual cells were integrated over 4 groups of cell sizes (Fig. 22.5), allowing both photosynthetic efficiency and chlorophyll to be calculated for each group.

These measurements revealed that prior to iron enrichment, small cells (pico- and nanoplankton) dominated the phytoplankton community (Fig. 22.5, left), contributing ca. 80% to total biomass. F_v/F_m averaged 0.3 with lower values in biggest cells (Fig. 22.5, left), suggesting that big cells were more susceptible to iron deficiency than small ones. Following the iron fertilization, F_v/F_m increased in all cell size groups (Fig. 22.5, right), indicating that iron enrichment stimulated photosynthetic activity in all groups of phytoplankton. However, the relative increase in F_v/F_m was much higher in big cells (mainly diatoms), suggesting stronger stimulation of photosynthetic activity by iron (Fig.22.5). As a result of the enhanced growth of big diatoms, the structure of phytoplankton community changed towards big cells being dominant (data of V.Smetacek's group), the pattern typical for phytoplankton blooms in the Southern Ocean. Furthermore, by the end of the experiment, the long-chain forming diatom *Pseudo-Nitzschia* became dominant in the bloom. Why has this species become dominant in the phytoplankton community?
Preliminary analysis of the single cell FRRf data indicates that *Pseudo-Nitzschia* is characterized by a very large functional absorption cross section of PSII. The measured values of λ_{PSII} have been found to be as high as in small cells and as twice as higher than the values typically observed in cells of the same effective size. The primary reason appears to be very low self-shading effect in these cells due to low optical thickness. Since λ_{PSII} is the key photosynthetic parameter which determines the photosynthetic electron transport at low light, i.e., the initial slope of photosynthesis-versus-irradiance curves (e.g. Falkowski and Kolber 1995), the low values of λ_{PSII} in *Pseudo-Nitzschia* suggest that the photosynthetic performance of this species has advantages in the low light environment.

References

Behrenfeld, M. J., Bale, A. J., Kolber, Z. S., Aiken, J., Falkowski, P. G. (1996) Confirmation of iron limitation of phytoplankton photosynthesis in the Equatorial Pacific Ocean. - *Nature*, **383**: 508-511.
Boyd P.W. et al. (2000) A mesoscale phytoplankton bloom in the polar Southern Ocean stimulated by iron fertilization. - *Nature*, **407**: 695-702.
Falkowski P.G. and Kolber Z. 1995. Variations in chlorophyll fluorescence yields in phytoplankton in the world oceans. - *Austr. J. Plant Physiol.* **22**:341-355.
Gorbunov M.Y., Kolber Z., and Falkowski P.G. 1999. Measuring photosynthetic parameters of individual algal cells by Fast Repetition Rate Fluorometry - *Photosynth. Res.*, **62**(2-3): 141-153.

Kolber, Z. S., Barber, R. T., Coale, K. H., Fitzwater, S. E., Greene, R. M., Johnson, K. S., Lindley, S., and Falkowski, P. G. (1994) Iron limitation of phytoplankton photosynthesis in the equatorial Pacific Ocean. - *Nature* **371**:145-149.

Kolber Z., Prasil O. and Falkowski P.G. 1998. Measurements of variable chlorophyll fluorescence using fast repetition rate technique. I. Defining methodology and experimental protocols. - *Biochem. Biophys. Acta*, **1367**:88-106.

Mitchell B.G., Brody E.A., Holm-Hansen O., McClain C. and Bishop J. 1991. Light limitation of phytoplankton biomass and macronutrient utilization in the Southern Ocean. – Limnol. Oceanogr., **36**: 1662-1677.

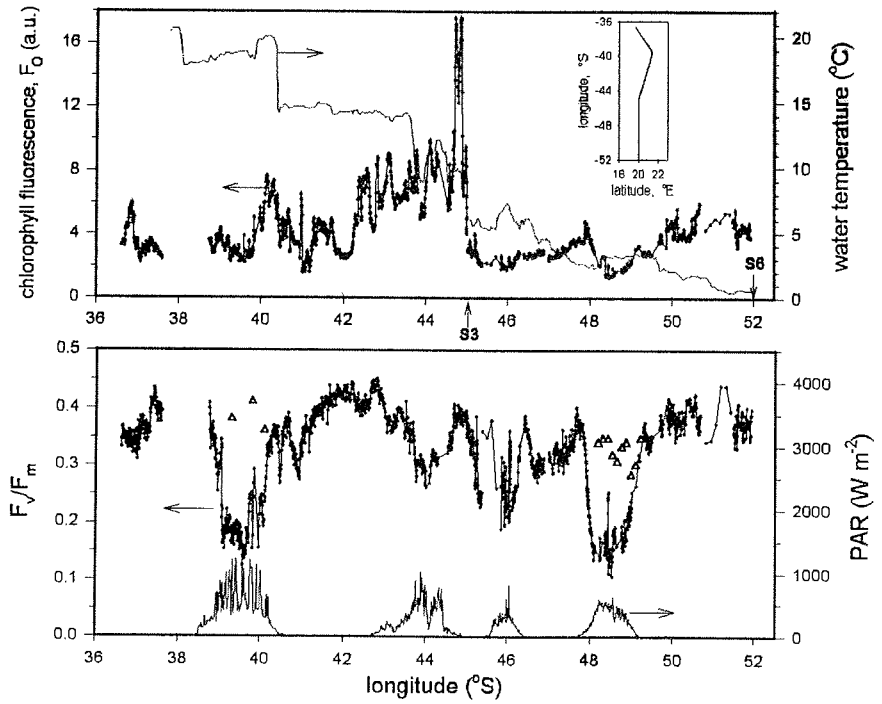

Figure 22.1. The horizontal distributions of near-surface phytoplankton, measured along 1700 km southward transect on the 20°E meridian (Oct. 26 – Nov. 01, 2000). The ship track is shown on the insert. The minimum chlorophyll fluorescence, F_o, is an estimate of phytoplankton abundance, while F_v/F_m is their photosynthetic efficiency. The lower panel includes profiles of PAR irradiance. The decline in F_v/F_m under high PAR (> 200 W m^{-2}) is due to photoinhibition of photosynthesis. Adaptation of phytoplankton samples at low light (~2 W m^{-2}) for an hour led to the recovery of damaged PSII reaction centers and an increase in F_v/F_m (triangles) to the values typical for night measurements.

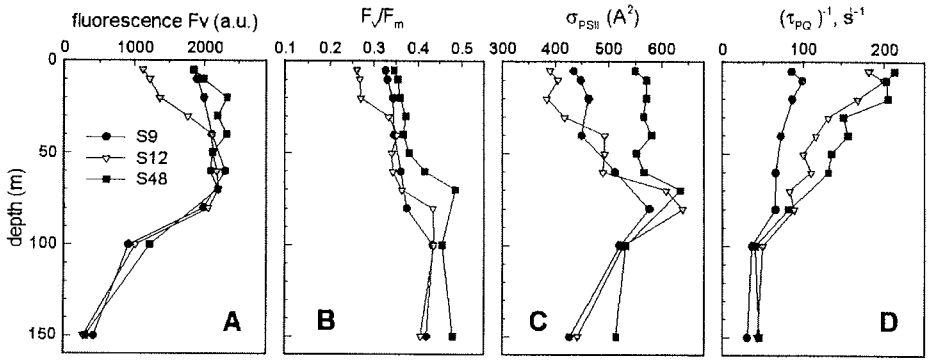

Figure 22.2. Vertical profiles of fluorescence and photosynthetic parameters measured prior to iron fertilization (Station 9) and at out-patch stations (S12 and S48). (**A**) "variable" component of chlorophyll fluorescence (F_v), which is the best fluorescent estimate of chlorophyll concentration; (**B**) the maximum quantum efficiency of photochemical energy conversion in PSII (F_v/F_m); (**C**) the functional absorption cross section of PSII (λ_{PSII}); and (**D**) the rate of photosynthetic electron transport between PSII and PSI, i.e. the reciprocal time constant (λ_{PQ}) for the plastoquinone (PQ) pool re-oxidation. The samples collected at depth <30m during a day were measured after adaptation at low light for the effects of photoinhibition and non-photochemical quenching of fluorescence to be alleviated.

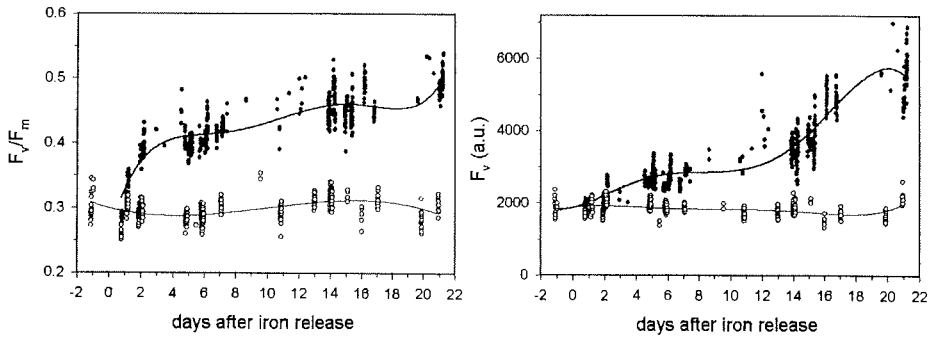

Figure 22.3. Temporal evolution of the photosynthetic efficiency (F_v/F_m) and the "variable component" of chlorophyll fluorescence (F_v, which is an estimate of chlorophyll concentration) of subsurface phytoplankton during EISENEX-1. Open and filled cycles show measurements outside and inside iron fertilized waters, respectively.

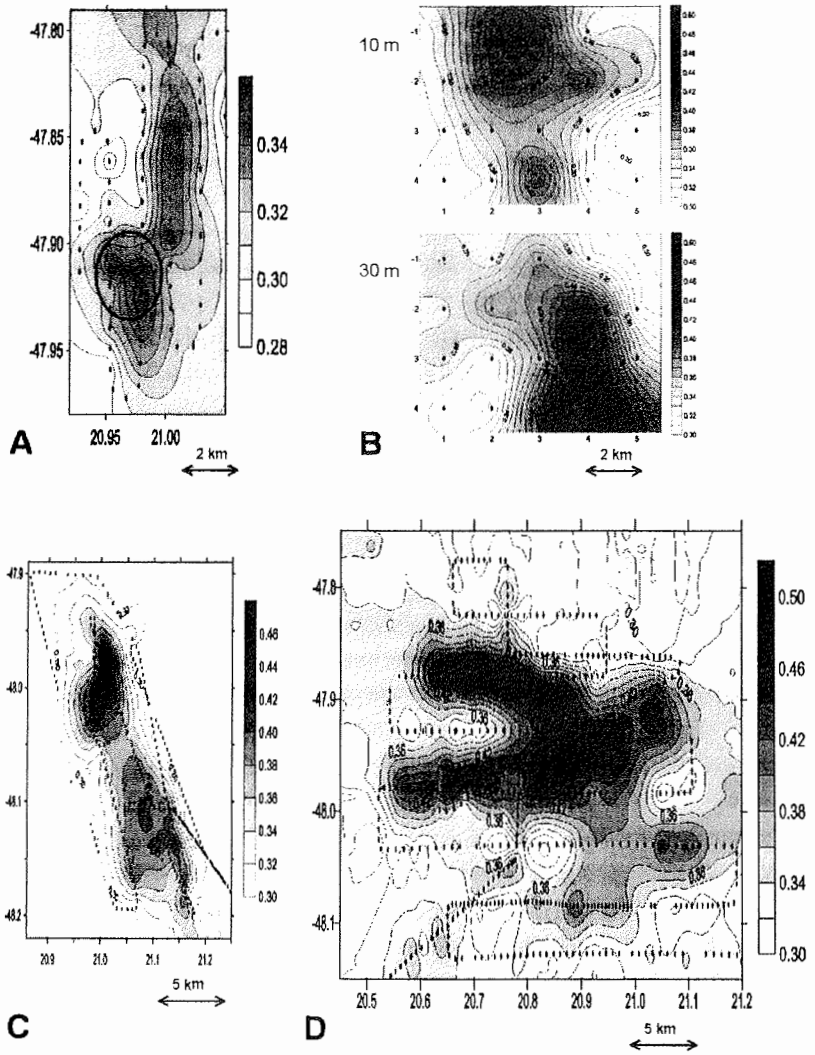

Figure 22.4. Temporal evolution of the iron-stimulated patch of phytoplankton during EISENEX-1. The figures show maps of subsurface F_v/F_m measured during underway surveys (X-axis – latitude, °E; Y-axis – longitude, °S):

(A) 1 day after iron release (Nov. 8-9). The cycle indicates location of the main portion of the SF_6 patch, as determined by A.Watson's group.

(B) 3 days after iron release - data from the grid on Nov. 10-11. Note that the upper layer (10 m depth – upper sub-panel) of the stratified water column has been shifted west-northward relative to the deeper layers (map for 30m depth - lower sub-panel);

(C) 6 days after iron release (Nov. 13-14);

(D) 14 days after iron release (Nov. 21-22).

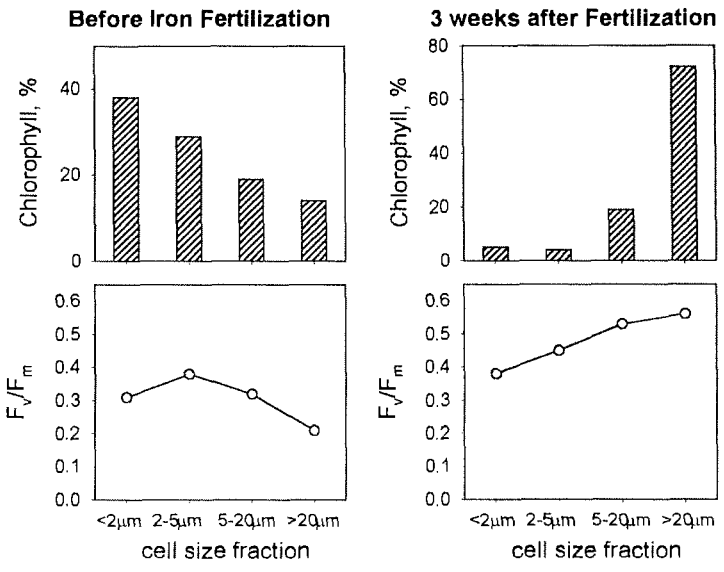

Figure 22.5. The effect of iron enrichment on the structure of phytoplankton community and photosynthetic performance of different cell groups. Cell size specific chlorophyll (in percent of total chlorophyll) and photosynthetic efficiency (F_v/F_m) have been determined for four groups of phytoplankton using the Single Cell FRR fluorometer.

23. THE CONTRIBUTION OF GRAZING BY MICROZOOPLANKTON DURING ECOSYSTEM RESPONSE TO IRON ENRICHMENT IN THE SOUTHERN OCEAN IN AUSTRAL SPRING

P. G. Verity

Introduction

The major focus of this study was the potential role of small zooplankton in the processing of primary production during system response to Fe fertilization. Despite their acknowledged role as usually the dominant grazers of primary (and bacterial) production, microzooplankton have hitherto been largely ignored during prior Fe experiments. We conducted dilution experiments measuring their grazing of <200 um primary production using the dilution method (Landry and Hassett, 1982). The dilution technique yields estimates of both microzooplankton community grazing and phytoplankton community biomass growth. These were done using natural communities in

the enrichment patch and also in non-enriched waters. Samples were also collected at regular intervals from vertical profiles inside and outside the iron-fertilized patch, and from surface samples along the transect along 20 E from 45 S to 52 S, to determine the abundance and biomass of auto- and heterotrophic nano- and microplankton (Verity and Sieracki, 1993). Samples were analyzed back in the lab using quasi-automated image analyzed fluorescence microscopy, providing taxonomic and functional group specific growth and grazing rates. Separate experiments could be conducted in conjunction with metazooplankton scientists to quantify community or species-specific predation by larger zooplankton upon microzooplankton, but these data are reported elsewhere.

Methods

Dilution protocol: Surface water was apportioned into two carboys for use as dilution water and experimental water. All equipment which came in contact with seawater (e.g. carboys, tubing, filtration equipment, and meshes) was stored in dilute hydrochloric acid between uses and rinsed with deionized water immediately prior to use. Dilution water was prepared by gravity filtration directly from carboys through sequential 3.0 m and 0.2 um Gelman capsule filters into 25 liter polyethylene carboys. This process removed all phytoplankton including the smallest picoplankton, which has been shown previously (Verity et al., 1996) and was confirmed here by pigment fluorometry. Most bacteria were also retained except very small vibrios. The capsule filters were soaked in 10 % HCl for one day before initial use and in-between uses. Prior to each use, ca. 10 liters of seawater were passed through them to remove any traces of acid. Post-cruise nutrient analyses showed that the concentrations of ammonium, nitrate+nitrite, silicate, and phosphate were the same in seawater before and after capsule filtration, as previously shown in more oligotrophic waters (Verity et al. 1996). Cartridges were changed after every three experiments.

Concurrently, experimental water was gently sieved through 200 um Nitex mesh into a separate acid-cleaned polyethylene carboy. Two liter Teflon bottles served as incubation vessels. Experimental water was gently added to dilution water to create five duplicated dilution treatments in 20 % increments. Bottles were incubated in flowing seawater in deck incubators covered with one layer of neutral density screening to match near-surface irradiance. Incubations began at various times of the day, but always during daylight; at T_0 and T_{24} hours, samples were collected to measure chlorophyll *a*

from all dilutions. Samples for chlorophyll *a* were collected in duplicate on Gelman GF/F filters, stored frozen in the dark, and measured fluorometrically after dark extraction into cold 90 % acetone using a Turner-Designs fluorometer (Strickland & Parsons 1972). Calibration factors were determined and checked at regular intervals using pigments derived from phytoplankton cultures and measured using HPLC. The range in coefficient of variation for chlorophyll *a* was 3 to 5 %.

Phytoplankton growth rates and grazing by microzooplankton were estimated as described by Landry & Hassett (1982) and Landry (1993). Deviations from linearity in the relationship between apparent growth rate and dilution (Gifford 1988, Gallegos 1989) were not apparent in these experiments, similar to observations in other polar waters (Verity & Vernet 1992).

Abundance and biomass of microzooplankton and their prey: Numerically abundant auto- and heterotrophic protozoa, including ciliates, aplastidic flagellates and dinoflagellates (the microzooplankton) were enumerated in samples from typically eight depths in the upper 200m. Subsamples were preserved in glutaraldehyde (final concentration = 0.3 %) and then stained with 3-6-diaminoacridine hemisulfate (proflavin) for 1 minute (5 ug ml^{-1} final concentration) and 4'6-diamindino-2-phenylindole (DAPI) for 4 minutes (5 ug ml^{-1} final concentration). Separate volumes were then filtered onto 0.2 and 0.8 um black Nuclepore filters: bacteria were measured on the smaller pore-size filters, and microzooplankton on the larger filters. To achieve an even distribution for counting and measurement purposes, black filters were placed on top of pre-wetted Whatman GF/F backing filters. After filtration, the damp filter was placed on a slide. A drop of low fluorescence immersion oil was placed on top of the filter, which was covered with a cover slip and frozen at - 20 C. Samples were analyzed upon return to the laboratory.

An Olympus BX-60 microscope equipped with 100-watt epifluorescence illuminators was employed, with appropriate exciter/barrier filter sets for UV (335-365 nm), blue (435-490 nm), and green (510-560 nm) excitation. Dinoflagellates were distinguished from other flagellates based upon cell morphology and structure of the nucleus, especially the unique condensed chromosomes visible by DAPI staining. Heterotrophic and autotrophic cells were discriminated by the absence and presence of

autofluorescent chloroplasts, respectively. The autotrophic category also includes mixotrophic cells. Cell abundance, dimensions, and biovolumes were determined via quasi-automated color image analysis (Verity & Sieracki 1993) equipped with a Photonics Science cooled integrating 3-chip color CCD with variable frame rates from 1/10,000 sec to 4 minutes, and an electronic shutter mounted in-line in the microscope lightpath so that the sample was exposed to excitation for only as long as the camera shutter was open. The computer could automatically select random locations on the slide and return to each location +/- 1um. The commercial driver software (Image Pro Plus v3.0) was customized so that the entire process (moving to a given location, focusing, opening an electronic shutter, grabbing an image, closing the shutter, and moving to a new location) was automated and computer-controlled.

A minimum of 200 plankton cells of each type was measured. The average coefficient of variation of triplicate counts of nanoplankton was 11 %. Data were automatically dumped into spreadsheets, and every cell in an image was uniquely identified for post-measurement visual confirmation. Cell biovolume measurements were converted to carbon biomass using conversion factors based on literature values of carbon density of microplankton (Verity et al. 1992 and references therein).

Results and Discussion

Only preliminary data are available at this time. Perhaps surprisingly so early in the growth season, auto- and heterotrophic nano- and microplankton were very abundant over the entire study area. Changes occurred in the dominant taxa over the transect, particularly at frontal boundaries but also at mesoscale features, e.g. eddy edges. Important small phytoplankton groups included prymnesiophytes, coccolithophorids, cryptophytes, and especially small naviculoid pennate diatoms. The heterotrophic nanoplankton was also salient and included important contributions by choanoflagellates and various small monads. Ciliates were regularly but not always abundant. Phagotrophic taxa included several species of Laboea, Strobilidium, and Strombidium, and the average cell size was large relative to communities from temperate waters. Typically 30-40% of the ciliates contained plastids. The obligatory photosynthetic ciliate, Mesodinium, was commonly present and occasionally quite abundant. Heterotrophic dinoflagellates were also commonly abundant, especially (but not exclusively) in waters containing abundant medium and large diatoms.

The dilution experiments indicated clear responses to iron enrichment by both auto- and heterotrophic nano- and microplankton. Initially, the control and fertilized sites showed statistically similar phytoplankton (chlorophyll a-based) growth rates and grazing losses to microzooplankton. Much of the small phytoplankton daily production was ingested, leaving little for consumption by metazooplankton or for vertical export. In general, this pattern continued at the nonfertilized sites throughout the study period. In contrast, within one week of enrichment, growth rates of nano- and microphytoplankton increased significantly, especially small naviculoid diatoms. Grazing by small protozooplankton lagged this response by ca. one week, which resulted in increased phytoplankton abundance. Microzooplankton grazing then ramped up, however, so that further increases in biomass of nano- (especially) and microalgae were reduced. The abundance and biomass of nano- and (especially) microzooplankton in situ did not increase markedly, suggesting control by larger metazooplankton. Other incubation experiments appeared to support this tentative conclusion.

In summary, this region of the Southern Ocean in austral spring supported an abundant microbial food web, sporadically superimposed with larger diatoms. This scenario is thought to be common (Verity and Smetacek, 1996). Iron fertilization quickly stimulated microalgal productivity and biomass accumulation, but microzooplankton soon responded. Accordingly, long term increases in small phytoplankton were prevented by grazing; in fact, overgrazing of the iron-stimulated response by small phytoplankton apparently was prevented only by predation of microzooplankton by larger metazooplankton. Thus, the accumulation of biomass of small phytoplankton in this region during austral spring is best considered to be grazer-limited rather than iron-limited.

References

Gallegos CL (1989) Microzooplankton grazing on phytoplankton in the Rhode River, Maryland: nonlinear feeding kinetics. Mar Ecol Prog Ser 57: 23-33.

Gifford DJ (1988) Impact of grazing by microzooplankton in the Northwest Arm of Halifax Harbour, Nova Scotia. Mar Ecol Prog Ser 47: 249-258.

Landry MR, Hassett RP (1982) Estimating the grazing impact of marine microzooplankton. Mar Biol 67: 283-288.

Landry MR (1993) Estimating rates of growth and grazing mortality of phytoplankton by the dilution method. In: Kemp PF, Sherr BF, Sherr EB, Cole JJ (eds) Handbook of methods in aquatic microbial ecology. Lewis, New York, p. 715-722.

Strickland JDH, Parsons TR (1972) A practical handbook of seawater analysis. Bull Fish Res Bd Can 167: 1-310.

Verity PG, Vernet M (1992) Microzooplankton grazing, pigments and composition of plankton communities during the late spring in two Norwegian fjords. Sarsia 77: 263-274.

Verity PG, Sieracki ME (1993) Use of color image analysis and epifluorescence microscopy to measure plankton biomass. In: Kemp PF, Sherr BF, Sherr EB, Cole JJ (eds) Handbook of methods in aquatic microbial ecology. Lewis, New York, p. 327-338.

Verity PG, Smetacek V (1996) Organism life cycle, predation and the structure of marine pelagic ecosystems. Mar Ecol Prog Ser 130: 277-293.

Verity PG, Robertson CY, Tronzo CR, Andrews MG, Nelson JR, Sieracki ME (1992) Relationship between cell volume and the carbon and nitrogen content of marine photosynthetic nanoplankton. Limnol Oceanogr 37: 1434-1446.

Verity PG, Stoecker DK, Sieracki ME, Nelson JR (1996) Microzooplankton grazing of primary production at 140W in the equatorial Pacific. Deep Sea Res 43: 1227-1255.

24. ZOOPLANKTON WORK DURING "EISENEX"

U. Bathmann, S. Schultes, S. Krägefsky

Previous studies of the zooplankton community in the Southern Ocean have shown a particular importance of small copepods(e.g. *Oithona* sp.; Dubischar et al. in press) and salps (Dubischar and Bathmann 1997) in controlling phytoplankton development. Feeding selectivity of small and large copepod species can possibly influence the phytoplankton community composition (Atkinson 1995). Heavily silicified algal species (e.g. *Fragilariopsis kerguelensis*) that are commonly observed in the waters of the Southern Ocean and that have been shown to form monoalgal blooms might be avoided by grazers (Verity and Smetacek 1996) and contribute strongly to export of silica and carbon.

Aim of the study

Three major objectives guided zooplankton work during EISENEX. First, zooplankton biomass distribution inside and outside the iron-fertilized patch and the dominance in species composition contributing to this biomass were to be determined. Secondly, emphasis was put on the influence of herbivorous zooplankton grazing on the turnover of phytoplankton carbon built-up following the fertilization. Thirdly, selective grazing on specific groups of the existing (non-fertilized) and developing (fertilized) phytoplankton assemblage was studied in order to estimate the impact of zooplankton feeding on the biogeochemical cycling of carbon and silica.

Abundance, spatial distribution and migration of zooplankton

A Simrad EK 60 multifrequency scientific echo sounder with operating frequencies of 38, 70, 120 and 200 kHz was used to investigate abundance as well as patterns of distribution and migration of zooplankton inside and outside the fertilized patch. The processed acoustic data show vertical migrations that occur on a diurnal basis but also on time scales of several days (Fig. 24.1).

The water column was sampled with carefully directed hauls of a multi net (100µm mesh size), bongo net (300µm mesh size) and ring net (Ø 110cm, mesh size 1000µm). Towing speed varied between 0.3, 0.5 and 1.0 ms^{-1} and maximum sampling depth was 750m. For later identification and a detailed count of zooplankton community composition in the home laboratory, samples

were fixed with buffered formaldehyde up to a final concentration of 4%. At a first glance, salps only were caught in unfertilized waters with low chl *a* concentrations (i.e. before the iron addition and outside the patch). Whether, as seems to be the case, migration behavior and composition of the zooplankton community inside the fertilized patch changed in comparison to the unfertilized waters, remains to be verified by further processing of the acoustic data, analysis of zooplankton samples and comparison with other data sets. Furthermore, it will be attempted to estimate the export of particulate material through vertical migration of zooplankton grazers.

In one net haul with the 1000µm ring net, towed vertically at 1.0 ms^{-1}, a rare specimen belonging to group of the drift fishes was caught. These fishes move rather passively with ocean currents and lack escape muscles, the latter being probably the reason for the fish being caught by our net. The specimen was dissected and photographed for documentation.

Zooplankton grazing impact on the plankton community
Already at the beginning of the fertilization experiment, the very diverse plankton community appeared to be heavily grazed by the well developed zooplankton assemblage.
Zooplankton for experiments were collected inside and outside the patch, during day and night, with a 300µm Bongo net towed vertically from maximum 300m depth to the surface at a speed of 0.3 ms^{-1}. The contents of the cod-end were diluted immediately after capture in 0.2 µm filtered seawater.

For determination of the *in situ* gut fluorescence and gut clearance rates subsamples from the diluted animals were collected on a piece of mesh no later then 3 to 5 min after the net was on deck (t0) and at t2, t5, t10, t15, t25, t40 and t70 min. The mesh was immediately frozen in liquid nitrogen and animals sorted as well as pigments extracted and measured later in the day. Ingestion rates derived with the gut fluorescence method, mainly for small copepods (< 2mm), *C.acutus*, *R. gigas*, krill larvae and salps, indicate an especially high, herbivorous grazing impact for the very abundant small copepods (Fig. 24.2).

Grazing selectivity was studied in additional experiments where one of the above mentioned zooplankton species was selectively enriched in 1 or 2 liter bottles with CTD-water from the chl *a* maximum. Bottles were incubated on a plankton wheel for 24 to 36h, at ambient temperature (4°C) and dim light. At

the beginning and end of these incubations, subsamples were taken for a detailed count of phyto-, mircozoo- and nanoplankton as well as for determination of chl *a*, phaeopigments and nutrients. First results from the chl *a* measurements indicate a clear herbivory grazing response only for *C. acutus* (Fig. 24.3). A 10 to 20% reduction in chl *a* concentration in the control bottles (without added grazers) was frequently observed (Fig. 24.4). We speculate that microzooplankton and copepods <500µm, the latter being present at an *in situ* abundance of approx. 30 ind. l^{-1}, grazed heavily on small phytoplankton. Larger copepods like *R. gigas* and *C.acutus* might also have grazed on microzooplankton. This, however, remains to be confirmed by a profound microscopic analysis. Cellcounts will be done with an Utermöhl microscope and by quasi-automated image analyzed fluorescence microscopy (collaboration by P. Verity). Moreover, samples will be studied with scanning electron microscopy (SEM) in order to detect grazing marks and signs of silica dissolution through ingestion of diatoms by zooplankton.

Respiration (O_2) and NH_4-excretion rates for the dominant zooplankton groups have also been determined on a regular basis. However, the results from these experiments still need to be analyzed as is the case for possible differences in grazing activity inside and outside the iron-fertilized patch.

References

Atkinson, A. 1995, Omnivory and feeding selectivity in five copepod species during spring in the Bellingshausen Sea, Antarctica. ICES J Mar Sci 52:385-396

Dubischar, C.D. and U.V. Bathmann. 1997. Grazing impact of copepods and salps on phytoplankton in the Atlantic sector of the Southern Ocean. Deep Sea Res II 44: 415-433

Dubischar C.D., Lopes, R.M. and U.V. Bathmann. in press. High summer abundances of small pelagic copepods at the Antarctic Polar Front and implications for ecosystem dynamics. Deep Sea Res II "Mesoscale physics and biogeochemistry at the Antarctic Polar Front, Atlantic Sector"

Verity, P.G. and V. Smetacek. 1996. Organism life cycles, predation, and the structure of marine pelagic ecosystems. Mar Ecol Prog Ser 130: 277-293

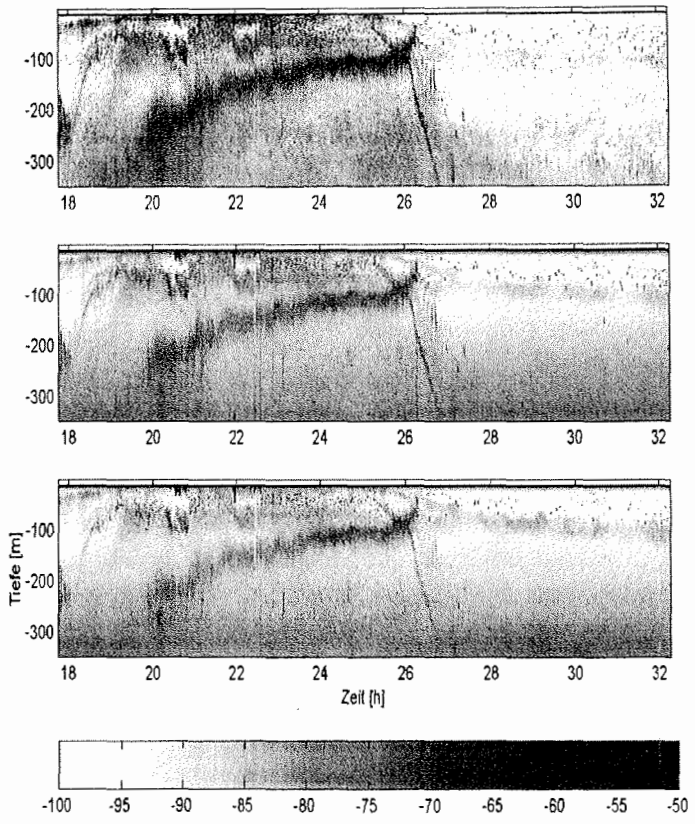

Fig. 24.1

Visualization of the mean volume backscattering strength [dB] as a vertical section down to – 350 m from 15-11-00 18:00 GMT until 16-11-00 8:00 GMT. The three panels show the frequencies 38, 70 and 120 kHz. Different scattering layers can easily be distinguished.

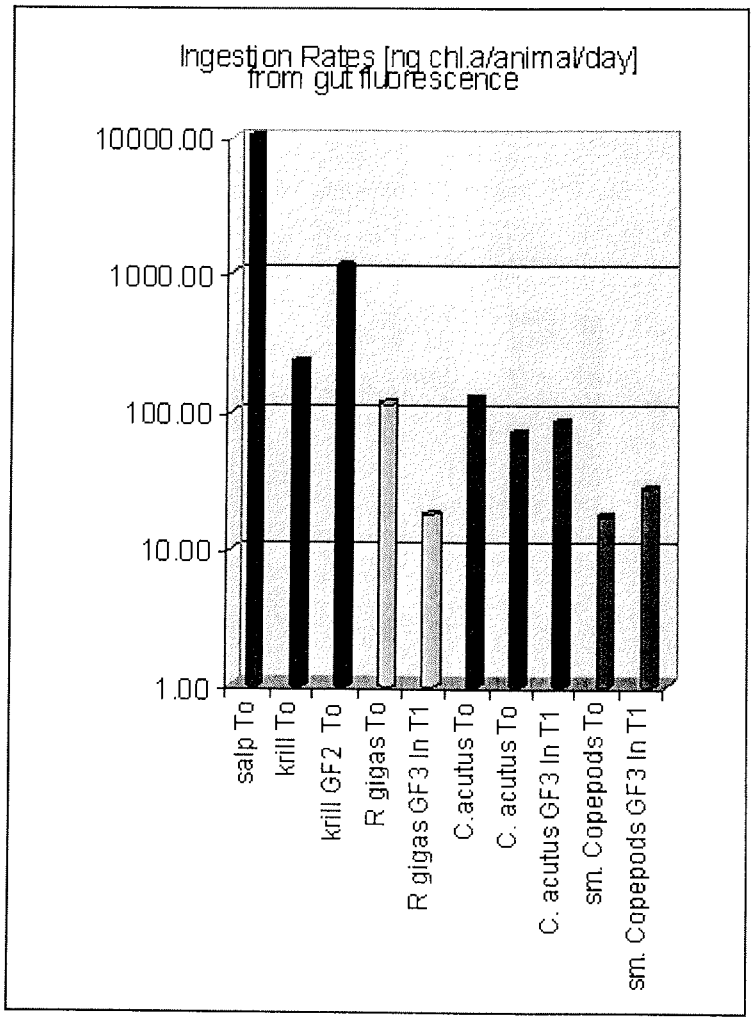

Fig. 24.2
Ingestion rates of dominant meta- and macrozooplankton organisms derived from *in situ* gut fluorescence.

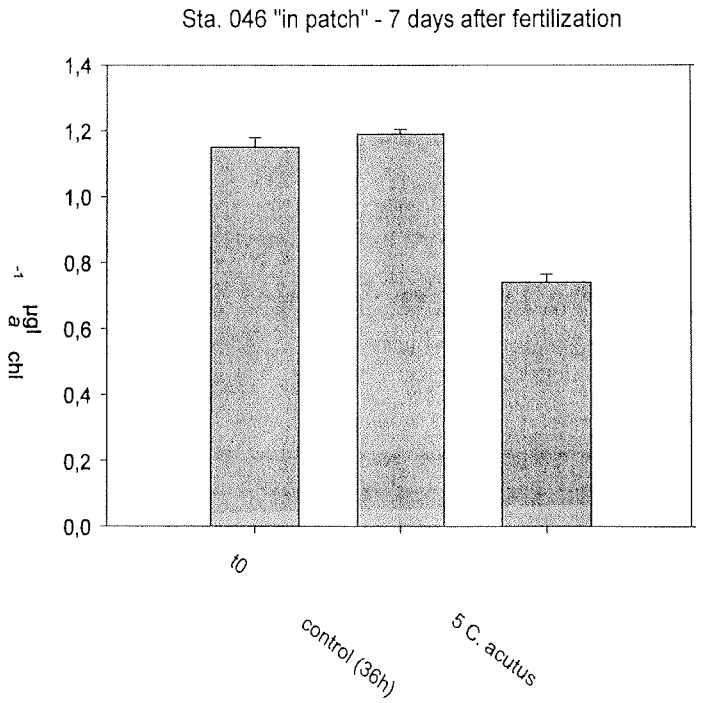

Fig. 24.3
Chl *a* concentration at time 0h and after 36h of incubation in control and grazing (5 adult *Calanoides acutus*) bottles. Error bars indicate std for duplicate (control) or triplicate (grazing) bottles.

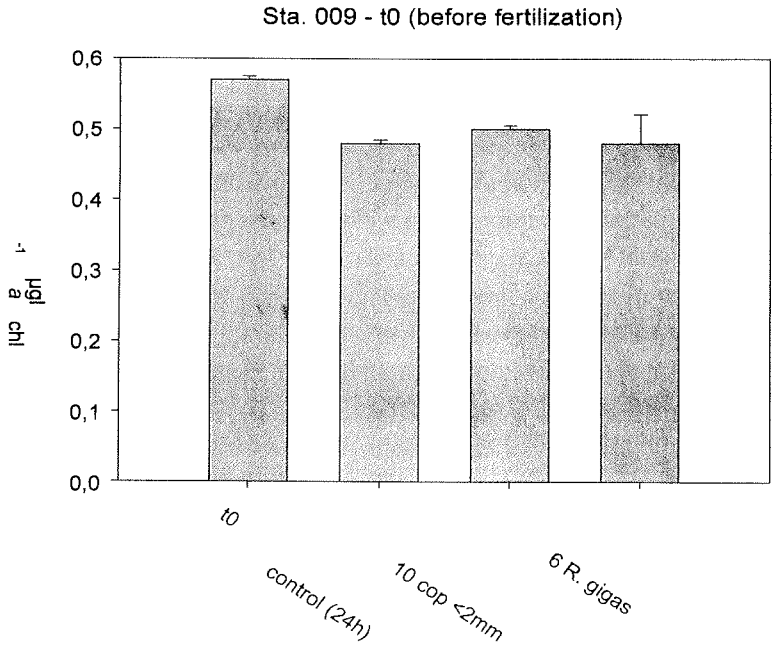

Fig.24. 4
Chl *a* concentration at time 0h and after 24h of incubation in control and grazing bottles (10 copepods <2mm and 6 adult *Rhincalanus gigas*). Error bars indicate std for duplicate (control) or triplicate (grazing) bottles.

25. DOES FE FERTILISATION ENHANCE THE EXPORT PRODUCTION AS MEASURED THROUGH THE $^{234}TH/^{238}U$ DISEQUILIBRIUM IN SURFACE WATER?

M. Rutgers van der Loeff & I. Vöge.

Introduction

The radioisotope ^{234}Th is produced at a well-known rate from decay of uranium in seawater. As thorium is a highly particle-reactive element, the downward flux of particles through the water column causes a depletion of ^{234}Th in surface waters relative to its parent ^{238}U. This depletion can be used to quantify the export flux on a timescale of the half-life of ^{234}Th (24 days).
In previous expeditions we observed the adsorption of ^{234}Th to particles during the development of a bloom, and the subsequent removal of ^{234}Th from the surface water as proof of the export of particles.
The previous iron enrichment experiment in the Southern Ocean, SOIREE, started in summer, and a strong depletion of ^{234}Th relative to ^{238}U at the onset of the experiment showed that there had been a bloom and export previously. During the 13 days of the experiment, total ^{234}Th activity grew in to equilibrium, implying that no export was observed.
One of the questions addressed in the Eisenex experiment was whether a longer experiment would allow us to observe whether an iron-induced bloom would lead to additional export from the euphotic zone.

Export production before the fertilization

On the transect from Cape Town to the Polar Front we have measured particulate and total ^{234}Th /^{238}U ratio in surface water collected with the ship's seawater supply. The brandnew teflon seawater tubing had become contaminated in dock as observed by blackish particles on the filters. On October 28 (approx. 44 °S) the system was rinsed with maximum flowrate, thus removing sand sized metalliferous particles. The data collected before this rinsing operation should be considered questionable.
South of 43°S ^{234}Th was in equilibrium with ^{238}U within analytical precision. This means that export of particles out of the photic zone had not yet started (Fig. 25.1).

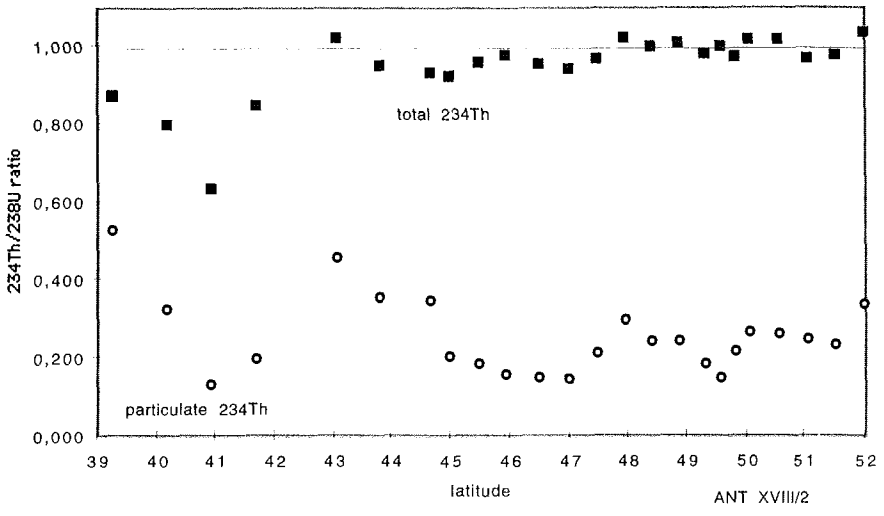

Fig. 25.1: particulate (open symbols) and total (closed symbols) ^{234}Th /^{238}U ratio in surface water on the southward transect from Cape Town to the Polar Front showing that no export had occurred in the PFZ in the weeks before the start of the experiment.

Development of $^{234}Th/^{238}U$ disequilibrium after the iron enrichment

After the enrichment with iron we followed the distribution of the $^{234}Th/^{238}U$ disequilibrium inside and outside the enriched patch. The vertical distribution of ^{234}Th was measured on 20-Liter samples collected with the Rosette sampler. A modified method requiring only 5 L samples gave a small offset at the higher particle loads in surface water and was abandoned. ^{238}U is calculated from salinity. From the beginning (day 0, station 9), there was a depletion in the upper 100 m. Inside, not outside, the patch, a subsurface maximum developed in particulate ^{234}Th (Fig. 25.2) that was not correlated with chloropyll. This may have resulted from scavenging by ironoxides formed after the enrichment.

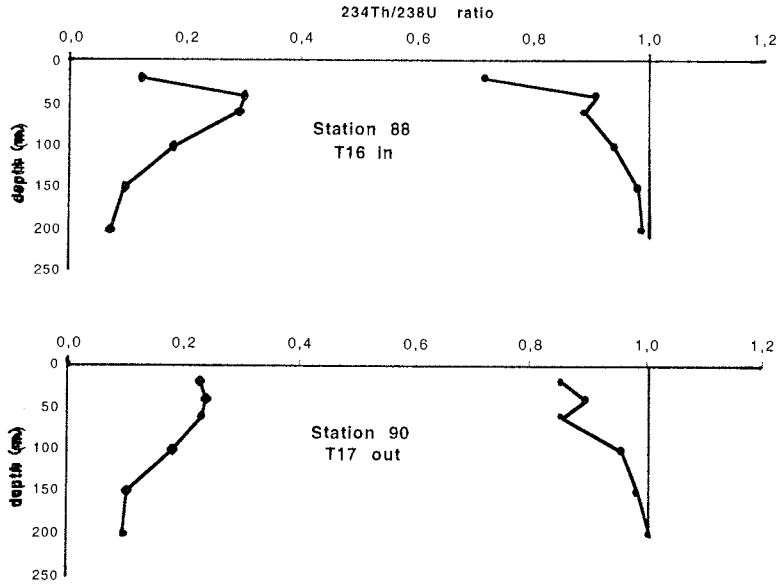

Fig. 25.2. Profiles of particulate (left) and total (right curves) ^{234}Th /^{238}U ratio on day 16 inpatch (above) and on day 17 outpatch (below) showing inpatch a subsurface maximum of particulate ^{234}Th.

The integrated depletion in the upper 150m (Fig. 25.3) is a measure of the amount of ^{234}Th removed from the surface layer to deeper waters. The most important feature is that a similar amount of ^{234}Th was removed inside and outside the patch. We have no explanation for the absence of a depletion at station 48 (day 9). At this station, the samples at 20 and 40m depth had a ^{234}Th excess of 26 and 10%, respectively.

The relatively constant depletion of 600 Bq m^{-2} corresponds at steady state with an export rate of 1030 dpm m^{-2} d^{-1}. In order to be able to convert this to fluxes of organic carbon and opal, POC and BSi were sampled in parallel by the group of Riebesell. As it has been argued that the export flux is primarily due to larger particles, we have also collected the fraction >20µ for analysis of ^{234}Th, POC and BSi.

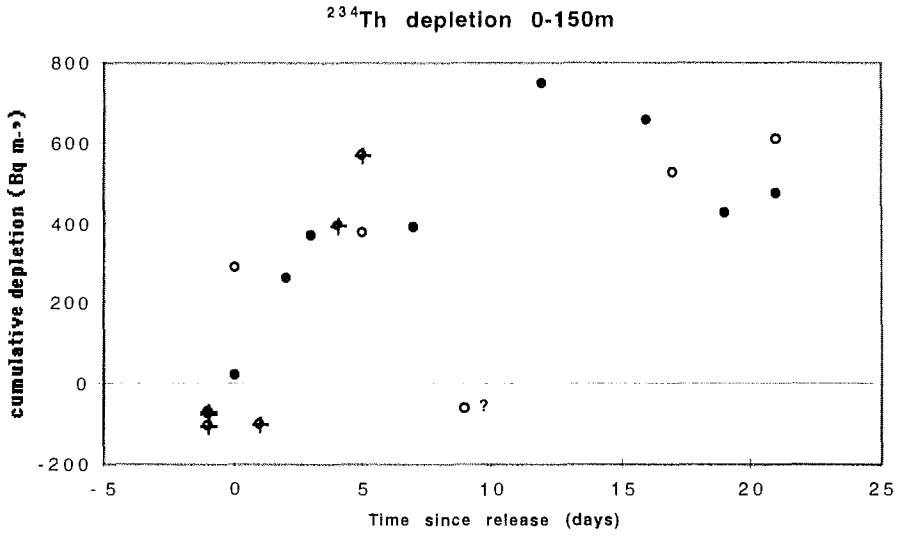

Fig. 25.3. Development of the cumulative depletion of ^{234}Th in the upper 150m inside (closed symbols) and outside (open symbols) the iron-enriched patch showing that iron supply did not enhance the export rates in the three weeks following the enrichment. Analyses using the 5-L method marked with + .

26. BETEILIGTE INSTITUTIONEN/ PARTICIPATING INSTITUTIONS ANT XVIII/2

1. Arrieta, J.M.	NIOZ
2. Assmy, P.	AWI
3. Bakker, D.	NIOZ
4. Bathmann, U.	AWI
5. Benthien; A.	AWI
6. Boye, M.	NIOZ
7. Bozec, Yann	NIOZ
8. Chuck, A.	UEA
9. Cisewski, B.	AWI
10. Croot, I.	NIOZ
11. Davidov, A.	IfM, Kiel
12. De Baar, H.	NIOZ
13. Dentler, F.-U.	DWD
14. Duarte Vagner	FURG
15. Fischer, A.C.	RUG
16. Freier, U.	AWI
17. Gervais, F.	AWI
18. Goldson, I.	UEA
19. Gonzales, S.	NIOZ
20. Gorbunov, M.	USA
21. Guttau, S.	TU, Hamburg
22. Harms, C.	AWI
23. Hartmann, C.	AWI
24. Henjes, J.	AWI
25. Huhn, O.	Uni HB
26. Klaas, C.	AWI
27. Krägefsky, S.	AWI
28. Kringstad, S.	PML
29. Kroon, P.	NIOZ
30. Laan, P.	NIOZ
31. Leach, H.	Uni. Liverpool
32. Liddicoat, M.	UEA
33. Loeff, M.R.v.d.	AWI
34. Messias, M.-J.	UEA
35. Nightingale, P.	UEA
36. Nishioka, J.	NIOZ

37. Peeken, I.	MLRG
38. Post, J.	Uni HH
39. Richter, K.-U.	AWI
40. Riebesell, U.	AWI
41. Rijkenberg, M.	NIOZ
42. Schneider, U.	AWI
43. Schultes, S.	AWI
44. Skjelvan, I.	UEA
45. Smetacek, V.	AWI
46. Sonnabend, H.	DWD
47. Strass, V.	AWI
48. Terbrüggen, A.	AWI
49. Timmermans, K.	NIOZ
50. Trumm, F.	Uni HH
51. Turner, Susan	UEA
52. Van Oijen, Tim	NIOZ
53. Veldhuis, M.	NIOZ
54. Verity, P.	Skidaway
55. Viergutz, Thomas	WERUM
56. Vöge, I.	AWI
57. Watson, A.	UEA
58. Weinbauer, M.	NIOZ

27. PARTICIPANTING INSTITUTES / BETEILIGTE INSTITUTE

England
UEA
School of Environmental Sciences
University of East Anglia
Norwich NR4 7TJ

PML Plymouth Marine Laboratory
Citadel Hill
Plymouth PL1 2PB

Dept. of Oceanography
The University
Liverpool, L69 3BX

Germany
Alfred-Wegener-Institut für
Polar- und Meeresforschung
Columbusstrasse
27515 Bremerhaven

DWD Deutscher Wetterdienst
Geschäftsfeld Seeschiffahrt
z.Hd. Herren U.Dentler/Sonnabend
Jenfelder Allee 70 A
D-22043 Hamburg

Reederei F. Laeisz
Barkhausenstr. 37
27568 Bremerhaven

Institut für Meereskunde
an der Universität Kiel (IFM)
Düsternbrooker Weg 20
24105 Kiel

Institut für Meereskunde
der Universität Hamburg
Troplowitz Str. 7
22529 Hamburg

Universität Bremen
Postfach 33 04 40
28334 Bremen

Netherlands
RuG University of Groningen
Department of Marine Biology
P.O. Box 14
Kerklaan 30
9750 AA Haren (Gn)

NIOZ Dept. Biol. Oceanog.
Postbox 59
NL-1790 AB Den Burg/Texel
THE NETHERLANDS

Interfacultair Reactor Instituut
Technische Universiteit Delft
(IRI/TUD)

USA
Skidaway Institute of Oceanography
10 Ocean Science Circle
Savannah, GA, 31411

Environmental Biophysics and Molecular Ecology Program
Institute of Marine and Coastal Sciences
71 Dudley Road
New Brunswick, NJ 08901-8521

University of California, San Diego
Scripps Institution of Oceanography
Marine Life Research Group
University of California, San Diego,
9500 Gilman Dr. MC: 0218
La Jolla, CA 92093-0218

Norway
Global Environmental change in
Oceanographic Systems (GEOS)
Geophysical Institute
University of Bergen
Allégt. 70
N-5007 Bergen

Brasil
Fundação Universidade de Rio Grande (FURG)
Departamento de Fisica
Caixa Postal 474 - Rio Grande - RS - Brasil
96201-900

28. SHIP'S CREW / SCHIFFSBESATZUNG ANT XVIII/2

Master	Keil, Jürgen
1. Offc,	Grundmann, Uwe
1. Offc.	Rodewald, Martin
2. Offc.	Peine, Lutz
2. Offc.	Thieme, Wolfgang
R. Offc.	Hecht, Andreas
Doctor	Kohlberg, Eberhard
1. Eng	Delff, Wolfgang
2. Eng.	Folta, Henryk
2. Eng.	Simon, Wofgang
Electr.	Holtz, Hartmut
Electron.	Piskorzynski, Andreas
Electron.	Fröb, Martin
Electron.	Baier, Ulrich
Electron.	Dimmler, Werner
Boatsw.	Loidl, Reiner
Carpenter	Neisner, Winfried
A.B.	Bäcker, Andreas
A.B.	Hagemann, Manfred
A.B.	Schmidt, Uwe
A.B.	Winkler, Michael
A.B.	Moser, Siegfried
A.B.	Bindernagel, Knuth
A.B.	Bohne, Jens
A.B.	Bastigkeit, Kai
Storekeep.	Beth, Detlef
Mot-man	Arias Iglesias, Bnr.
Mot-man	Schubert, Holger
Mot-man	Fritz, Günter
Mot-man	Krösche, Eckard
Mot-man	Dinse, Horst
Cook	Fischer, Matthias
Cooksmate	Tupy, Mario
Cooksmate	Martens, Michael

1. Stwdess	Dinse, Petra
Stwdss/KS	Brendel, Christina
2. Stwdess	Streit, Christina
2. Stwdess	Schmidt, Maria
2. Stwdess	Deuß, Stefanie
2. Stwdess	Tu, Jlan Min
2. Stwdess	Wu, Chi Lung
Laundrym.	Yu, Chung Leung
Trainee	Buchner, Bernd

Folgende Hefte der Reihe „Berichte zur Polarforschung“ sind bisher erschienen:

- **Sonderheft Nr. 1/1981** – „Die Antarktis und ihr Lebensraum“
  Eine Einführung für Besucher – Herausgegeben im Auftrag von SCAR
- **Heft Nr. 1/1982** – „Die Filchner-Schelfeis-Expedition 1980/81“
  zusammengestellt von Heinz Kohnen
- **Heft Nr. 2/1982** – „Deutsche Antarktis-Expedition 1980/81 mit FS „Meteor“
  First International BIOMASS Experiment (FIBEX) – Liste der Zooplankton- und Mikronektonnetzfänge
  zusammengestellt von Norbert Klages
- **Heft Nr. 3/1982** – „Digitale und analoge Krill-Echolot-Rohdatenerfassung an Bord des Forschungsschiffes ‚Meteor‘“ (im Rahmen von FIBEX 1980/81, Fahrtabschnitt ANT III), von Bodo Morgenstern

  Heft Nr. 4/1982 – „Filchner-Schelfeis-Expedition 1980/81“
  Liste der Planktonfänge und Lichtstärkemessungen
  zusammengestellt von Gerd Hubold und H. Eberhard Drescher
- **Heft Nr. 5/1982** – “Joint Biological Expedition on RRS ‘John Biscoe’, February 1982“
  by G. Hempel and R. B. Heywood
- **Heft Nr. 6/1982** – „Antarktis-Expedition 1981/82 (Unternehmen ‚Eiswarte‘)“
  zusammengestellt von Gode Gravenhorst

  Heft Nr. 7/1982 – „Marin-Biologisches Begleitprogramm zur Standorterkundung 1979/80 mit MS ‚Polarsirkel‘ (Pre-Site Survey)“ – Stationslisten der Mikronekton- und Zooplanktonfänge sowie der Bodenfischerei
  zusammengestellt von R. Schneppenheim

  Heft Nr. 8/1983 – “The Post-Fibex Data Interpretation Workshop“
  by D. L. Cram and J.-C. Freytag with the collaboration of J. W. Schmidt, M. Mall, R. Kresse, T. Schwinghammer
- **Heft Nr. 9/1983** – “Distribution of some groups of zooplankton in the inner Weddell Sea in summer 1979/80“
  by I. Hempel, G. Hubold, B. Kaczmaruk, R. Keller, R. Weigmann-Haass

  Heft Nr. 10/1983 – „Fluor im antarktischen Ökosystem“ – DFG-Symposium November 1982
  zusammengestellt von Dieter Adelung

  Heft Nr. 11/1983 – “Joint Biological Expedition on RRS ‘John Biscoe’, February 1982 (II)“
  Data of micronecton and zooplankton hauls, by Uwe Piatkowski

  Heft Nr. 12/1983 – „Das biologische Programm der ANTARKTIS-I-Expedition 1983 mit FS ‚Polarstern‘“
  Stationslisten der Plankton-, Benthos- und Grundschleppnetzfänge und Liste der Probennahme an Robben und Vögeln, von H. E. Drescher, G. Hubold, U. Piatkowski, J. Plötz und J. Voß
- **Heft Nr. 13/1983** – „Die Antarktis-Expedition von MS ‚Polarbjörn‘ 1982/83“ (Sommerkampagne zur Atka-Bucht und zu den Kraul-Bergen), zusammengestellt von Heinz Kohnen
- **Sonderheft Nr. 2/1983** – „Die erste Antarktis-Expedition von FS ‚Polarstern‘ (Kapstadt, 20. Januar 1983 – Rio de Janeiro, 25. März 1983)“, Bericht des Fahrtleiters Prof. Dr. Gotthilf Hempel

  Sonderheft Nr. 3/1983 – „Sicherheit und Überleben bei Polarexpeditionen“
  zusammengestellt von Heinz Kohnen
- **Heft Nr. 14/1983** – „Die erste Antarktis-Expedition (ANTARKTIS I) von FS ‚Polarstern‘ 1982/83“
  herausgegeben von Gotthilf Hempel

  Sonderheft Nr. 4/1983 – “On the Biology of Krill *Euphausia superba*“ – Proceedings of the Seminar and Report of the Krill Ecology Group, Bremerhaven 12. - 16. May 1983, edited by S. B. Schnack

  Heft Nr. 15/1983 – “German Antarctic Expedition 1980/81 with FRV ‘Walther Herwig’ and RV ‘Meteor’“ – First International BIOMASS Experiment (FIBEX) – Data of micronekton and zooplankton hauls
  by Uwe Piatkowski and Norbert Klages

  Sonderheft Nr. 5/1984 – “The observatories of the Georg von Neumayer Station“, by Ernst Augstein

  Heft Nr. 16/1984 – “FIBEX cruise zooplankton data“
  by U. Piatkowski, I. Hempel and S. Rakusa-Suszczewski
- **Heft Nr. 17/1984** – Fahrtbericht (cruise report) der ‚Polarstern‘-Reise ARKTIS I, 1983“
  von E. Augstein, G. Hempel und J. Thiede

  Heft Nr. 18/1984 – „Die Expedition ANTARKTIS II mit FS ‚Polarstern‘ 1983/84“,
  Bericht von den Fahrtabschnitten 1, 2 und 3, herausgegeben von D. Fütterer

  Heft Nr. 19/1984 – „Die Expedition ANTARKTIS II mit FS ‚Polarstern‘ 1983/84“,
  Bericht vom Fahrtabschnitt 4, Punta Arenas-Kapstadt (Ant-II/4), herausgegeben von H. Kohnen

  Heft Nr. 20/1984 – „Die Expedition ARKTIS II des FS ‚Polarstern‘ 1984, mit Beiträgen des FS ‚Valdivia‘ und des Forschungsflugzeuges ‚Falcon 20‘ zum Marginal Ice Zone Experiment 1984 (MIZEX)“
  von E. Augstein, G. Hempel, J. Schwarz, J. Thiede und W. Weigel

  Heft Nr. 21/1985 – “Euphausiid larvae in plankton from the vicinity of the Antarctic Penisula, February 1982“ by Sigrid Marschall and Elke Mizdalski

  Heft Nr. 22/1985 – “Maps of the geographical distribution of macrozooplankton in the Atlantic sector of the Southern Ocean“ by Uwe Piatkowski

  Heft Nr. 23/1985 – „Untersuchungen zur Funktionsmorphologie und Nahrungsaufnahme der Larven des Antarktischen Krills *Euphausia superba* Dana“ von Hans-Peter Marschall

Heft Nr. 24/1985 – „Untersuchungen zum Periglazial auf der König-Georg-Insel Südshetlandinseln/ Antarktika. Deutsche physiogeographische Forschungen in der Antarktis. – Bericht über die Kampagne 1983/84" von Dietrich Barsch, Wolf-Dieter Blümel, Wolfgang Flügel, Roland Mäusbacher, Gerhard Stäblein, Wolfgang Zick

- **Heft Nr. 25/1985** – „Die Expedition ANTARKTIS III mit FS ‚Polarstern' 1984/1985" herausgegeben von Gotthilf Hempel.
- **Heft Nr. 26/1985** – "The Southern Ocean"; A survey of oceanographic and marine meteorological research work by Hellmer et al.
- **Heft Nr. 27/1986** – „Spätpleistozäne Sedimentationsprozesse am antarktischen Kontinentalhang vor Kapp Norvegia, östliche Weddell-See" von Hannes Grobe

Heft Nr. 28/1986 – „Die Expedition ARKTIS III mit ‚Polarstern' 1985 mit Beiträgen der Fahrtteilnehmer, herausgegeben von Rainer Gersonde

- **Heft Nr. 29/1986** – „5 Jahre Schwerpunktprogramm ‚Antarktisforschung' der Deutschen Forschungsgemeisnchaft." Rückblick und Ausblick. Zusammengestellt von Gotthilf Hempel, Sprecher des Schwerpunktprogramms

Heft Nr. 30/1986 – "The Meteorological Data of the Georg-von-Neumayer-Station for 1981 and 1982" by Marianne Gube and Friedrich Obleitner

- **Heft Nr. 31/1986** – „Zur Biologie der Jugendstadien der Notothenioidei (Pisces) an der Antarktischen Halbinsel" von A. Kellermann
- **Heft Nr. 32/1986** – „Die Expedition ANTARKTIS IV mit FS ‚Polarstern' 1985/86" mit Beiträgen der Fahrtteilnehmer, herausgegeben von Dieter Fütterer

Heft Nr. 33/1987 – „Die Expedition ANTARKTIS-IV mit FS ‚Polarstern' 1985/86 – Bericht zu den Fahrtabschnitten ANT-IV/3-4" von Dieter Karl Fütterer

Heft Nr. 34/1987 – „Zoogeographische Untersuchungen und Gemeinschaftsanalysen an antarktischen Makroplankton" von U. Piatkowski

Heft Nr. 35/1987 – „Zur Verbreitung des Meso- und Makrozooplanktons in Oberflächenwasser der Weddell See (Antarktis)" von E. Boysen-Ennen

Heft Nr. 36/1987 – „Zur Nahrungs- und Bewegungsphysiologie von *Salpa thompsoni* und *Salpa fusiformis*" von M. Reinke

Heft Nr. 37/1987 – "The Eastern Weddell Sea Drifting Buoy Data Set of the Winter Weddell Sea Project (WWSP)" 1986 by Heinrich Hoeber und Marianne Gube-Lehnhardt

Heft Nr. 38/1987 – "The Meteorological Data of the Georg von Neumayer Station for 1983 and 1984" by M. Gube-Lenhardt

Heft Nr. 39/1987 – „Die Winter-Expedition mit FS ‚Polarstern' in die Antarktis (ANT V/1-3)" herausgegeben von Sigrid Schnack-Schiel

Heft Nr. 40/1987 – "Weather and Synoptic Situation during Winter Weddell Sea Project 1986 (ANT V/2) July 16 - September 10, 1986" by Werner Rabe

Heft Nr. 41/1988 – „Zur Verbreitung und Ökologie der Seegurken im Weddellmeer (Antarktis)" von Julian Gutt

Heft Nr. 42/1988 – "The zooplankton community in the deep bathyal and abyssal zones of the eastern North Atlantic" by Werner Beckmann

- **Heft Nr. 43/1988** – "Scientific cruise report of Arctic Expedition ARK IV/3" Wissenschaftlicher Fahrtbericht der Arktis-Expedition ARK IV/3, compiled by Jörn Thiede
- **Heft Nr. 44/1988** – "Data Report for FV 'Polarstern' Cruise ARK IV/1, 1987 to the Arctic and Polar Fronts" by Hans-Jürgen Hirche

Heft Nr. 45/1988 – „Zoogeographie und Gemeinschaftsanalyse des Makrozoobenthos des Weddellmeeres (Antarktis)" von Joachim Voß

Heft Nr. 46/1988 – "Meteorological and Oceanographic Data of the Winter-Weddell-Sea Project 1986 (ANT V/3)" by Eberhard Fahrbach

Heft Nr. 47/1988 – „Verteilung und Herkunft glazial-mariner Gerölle am Antarktischen Kontinentalrand des östlichen Weddellmeeres" von Wolfgang Oskierski

Heft Nr. 48/1988 – „Variationen des Erdmagnetfeldes an der GvN-Station" von Arnold Brodscholl

- **Heft Nr. 49/1988** – „Zur Bedeutung der Lipide im antarktischen Zooplankton" von Wilhelm Hagen
- **Heft Nr. 50/1988** – „Die gezeitenbedingte Dynamik des Ekström-Schelfeises, Antarktis" von Wolfgang Kobarg

Heft Nr. 51/1988 – „Ökomorphologie nototheniider Fische aus dem Weddellmeer, Antarktis" von Werner Ekau

Heft Nr. 52/1988 – „Zusammensetzung der Bodenfauna in der westlichen Fram-Straße" von Dieter Piepenburg

- **Heft Nr. 53/1988** – „Untersuchungen zur Ökologie des Phytoplanktons im südöstlichen Weddellmeer (Antarktis) im Jan./Febr. 1985" von Eva-Maria Nöthig

Heft Nr. 54/1988 – „Die Fischfauna des östlichen und südlichen Weddellmeeres: geographische Verbreitung, Nahrung und trophische Stellung der Fischarten" von Wiebke Schwarzbach

Heft Nr. 55/1988 – "Weight and length data of zooplankton in the Weddell Sea in austral spring 1986 (Ant. V/3)" by Elke Mizdalski

Heft Nr. 56/1989 – "Scientific cruise report of Arctic expeditions ARK IV/1, 2 & 3" by G. Krause, J. Meinke und J. Thiede

Heft Nr. 57/1989 – „Die Expedition ANTARKTIS V mit FS ‚Polarstern' 1986/87"
Bericht von den Fahrtabschnitten ANT V/4-5 von H. Miller und H. Oerter

* **Heft Nr. 58/1989** – „Die Expedition ANTARKTIS VI mit FS ‚Polarstern' 1987/88"
von D. K. Fütterer

Heft Nr. 59/1989 – „Die Expedition ARKTIS V/1a, 1b und 2 mit FS ‚Polarstern' 1988"
von M. Spindler

Heft Nr. 60/1989 – „Ein zweidimensionales Modell zur thermohalinen Zirkulation unter dem Schelfeis"
von H. H. Hellmer

Heft Nr. 61/1989 – "Die Vulkanite im westlichen und mittleren Neuschwabenland,
Vestfjella und Ahlmannryggen, Antarktika" von M. Peters

* **Heft Nr. 62/1989** – "The Expedition ANTARKTIS VII/1 and 2 (EPOS I) of RV 'Polarstern'
in 1988/89", by I. Hempel

Heft Nr. 63/1989 – „Die Eisalgenflora des Weddellmeeres (Antarktis): Artenzusammensetzung und Biomasse
sowie Ökophysiologie ausgewählter Arten" von Annette Bartsch

Heft Nr. 64/1989 – "Meteorological Data of the G.-v.-Neumayer-Station (Antarctica)" by L. Helmes

Heft Nr. 65/1989 – "Expedition Antarktis VII/3 in 1988/89" by I. Hempel, P. H. Schalk, V. Smetacek

Heft Nr. 66/1989 – „Geomorphologisch-glaziologische Detailkartierung
des arid-hochpolaren Borgmassivet, Neuschwabenland, Antarktika" von Karsten Brunk

Heft Nr. 67/1990 – "Identification key and catalogue of larval Antarctic fishes",
edited by Adolf Kellermann

Heft Nr. 68/1990 – "The Expedition Antarktis VII/4 (Epos leg 3) and VII/5 of RV 'Polarstern' in 1989",
edited by W. Arntz, W. Ernst, I. Hempel

Heft Nr. 69/1990 – „Abhängigkeiten elastischer und rheologischer Eigenschaften des Meereises vom
Eisgefüge", von Harald Hellmann

* **Heft Nr. 70/1990** – „Die beschalten benthischen Mollusken (Gastropoda und Bivalvia) des
Weddellmeeres, Antarktis", von Stefan Hain

Heft Nr. 71/1990 – „Sedimentologie und Paläomagnetik an Sedimenten der Maudkuppe (Nordöstliches
Weddellmeer)", von Dieter Cordes

Heft Nr. 72/1990 – "Distribution and abundance of planktonic copepods (Crustacea) in the Weddell Sea
in summer 1980/81", by F. Kurbjeweit and S. Ali-Khan

Heft Nr. 73/1990 – „Zur Frühdiagenese von organischem Kohlenstoff und Opal in Sedimenten des südlichen
und östlichen Weddellmeeres", von M. Schlüter

Heft Nr. 74/1990 – „Expeditionen ANTARKTIS-VIII/3 und VIII/4 mit FS ‚Polarstern' 1989"
von Rainer Gersonde und Gotthilf Hempel

Heft Nr. 75/1991 – „Quartäre Sedimentationsprozesse am Kontinentalhang des Süd-Orkey-Plateaus im
nordwestlichen Weddellmeer (Antarktis)", von Sigrun Grünig

Heft Nr. 76/1990 – „Ergebnisse der faunistischen Arbeiten im Benthal von King George Island
(Südshetlandinseln, Antarktis)", von Martin Rauschert

Heft Nr. 77/1990 – „Verteilung von Mikroplankton-Organismen nordwestlich der Antarktischen Halbinsel
unter dem Einfluß sich ändernder Umweltbedingungen im Herbst", von Heinz Klöser

Heft Nr. 78/1991 – „Hochauflösende Magnetostratigraphie spätquartärer Sedimente arktischer
Meeresgebiete", von Norbert R. Nowaczyk

Heft Nr. 79/1991 – „Ökophysiologische Untersuchungen zur Salinitäts- und Temperaturtoleranz
antarktischer Grünalgen unter besonderer Berücksichtigung des β-Dimethylsulfoniumpropionat
(DMSP) - Stoffwechsels", von Ulf Karsten

Heft Nr. 80/1991 – „Die Expedition ARKTIS VII/1 mit FS ‚Polarstern' 1990",
herausgegeben von Jörn Thiede und Gotthilf Hempel

Heft Nr. 81/1991 – „Paläoglaziologie und Paläozeanographie im Spätquartär am Kontinentalrand des
südlichen Weddellmeeres, Antarktis", von Martin Melles

Heft Nr. 82/1991 – „Quantifizierung von Meereseigenschaften: Automatische Bildanalyse von
Dünnschnitten und Parametisierung von Chlorophyll- und Salzgehaltsverteilungen", von Hajo Eicken

Heft Nr. 83/1991 – „Das Fließen von Schelfeisen - numerische Simulationen
mit der Metholde der finiten Differenzen", von Jürgen Determann

Heft Nr. 84/1991 – „Die Expedition ANTARKTIS-VIII/1-2, 1989 mit der Winter Weddell Gyre Study
der Forschungsschiffe ‚Polarstern' und ‚Akademik Fedorov'", von Ernst Augstein,
Nikolai Bagriantsev und Hans Werner Schenke

Heft Nr. 85/1991 – „Zur Entstehung von Unterwassereis und das Wachstum und die Energiebilanz
des Meereises in der Atka Bucht, Antarktis", von Josef Kipfstuhl

* **Heft Nr. 86/1991** – „Die Expedition ANTARKTIS-VIII mit FS ‚Polarstern' 1989/90. Bericht vom
Fahrtabschnitt ANT-VIII/5", von Heinz Miller und Hans Oerter

Heft Nr. 87/1991 – "Scientific cruise reports of Arctic expeditions ARK VI/1-4 of RV 'Polarstern'
in 1989", edited by G. Krause, J. Meincke & H. J. Schwarz

Heft Nr. 88/1991 – „Zur Lebensgeschichte dominanter Copepodenarten (*Calanus finmarchicus,
C. glacialis, C. hyperboreus, Metridia longa*) in der Framstraße", von Sabine Diel

Heft Nr. 89/1991 – „Detaillierte seismische Untersuchungen am östlichen Kontinentalrand des Weddell-Meeres vor Kapp Norvegia, Antarktis", von Norbert E. Kaul

Heft Nr. 90/1991 – „Die Expedition ANTARKTIS-VIII mit FS ‚Polarstern' 1989/90. Bericht von den Fahrtabschnitten ANT-VIII/6-7", herausgegeben von Dieter Karl Fütterer und Otto Schrems

Heft Nr. 91/1991 – "Blood physiology and ecological consequences in Weddell Sea fishes (Antarctica)", by Andreas Kunzmann

Heft Nr. 92/1991 – „Zur sommerlichen Verteilung des Mesozooplanktons im Nansen-Becken, Nordpolarmeer", von Nicolai Mumm

Heft Nr. 93/1991 – „Die Expedition ARKTIS VII mit FS ‚Polarstern', 1990. Bericht vom Fahrtabschnitt ARK VII/2", herausgegeben von Gunther Krause

Heft Nr. 94/1991 – „Die Entwicklung des Phytoplanktons im östlichen Weddellmeer (Antarktis) beim Übergang vom Spätwinter zum Frühjahr", von Renate Scharek

Heft Nr. 95/1991 – „Radioisotopenstratigraphie, Sedimentologie und Geochemie jungquartärer Sedimente des östlichen Arktischen Ozeans", von Horst Bohrmann

Heft Nr. 96/1991 – „Holozäne Sedimentationsentwicklung im Scoresby Sund, Ost-Grönland", von Peter Marienfeld

Heft Nr. 97/1991 – „Strukturelle Entwicklung und Abkühlungsgeschichte von Heimefrontfjella (Westliches Dronning Maud Land/Antarktika)", von Joachim Jacobs

Heft Nr. 98/1991 – „Zur Besiedlungsgeschichte des antarktischen Schelfes am Beispiel der Isopoda (Crustacea, Malacostraca)", von Angelika Brandt

* **Heft Nr. 99/1992** – "The Antarctic ice sheet and environmental change: a three-dimensional modelling study", by Philippe Huybrechts

* **Heft Nr. 100/1992** – „Die Expeditionen ANTARKTIS IX/1-4 des Forschungsschiffes ‚Polarstern' 1990/91" herausgegeben von Ulrich Bathmann, Meinhard Schulz-Baldes, Eberhard Fahrbach, Victor Smetacek und Hans-Wolfgang Hubberten

Heft Nr. 101/1992 – „Wechselbeziehungen zwischen Schwermetallkonzentrationen (Cd, Cu, Pb, Zn) im Meerwasser und in Zooplanktonorganismen (Copepoda) der Arktis und des Atlantiks", von Christa Pohl

Heft Nr. 102/1992 – „Physiologie und Ultrastruktur der antarktischen Grünalge *Prasiola crispa ssp. antarctica* unter osmotischem Streß und Austrocknung", von Andreas Jacob

* **Heft Nr. 103/1992** – „Zur Ökologie der Fische im Weddellmeer", von Gerd Hubold

Heft Nr. 104/1992 – „Mehrkanalige adaptive Filter für die Unterdrückung von multiplen Reflexionen in Verbindung mit der freien Oberfläche in marinen Seismogrammen", von Andreas Rosenberger

Heft Nr. 105/1992 – "Radiation and Eddy Flux Experiment 1991 *(REFLEX I)*", von Jörg Hartmann, Christoph Kottmeier und Christian Wamser

Heft Nr. 106/1992 – „Ostracoden im Epipelagial vor der Antarktischen Halbinsel - ein Beitrag zur Systematik sowie zur Verbreitung und Populationsstruktur unter Berücksichtigung der Saisonalität", von Rüdiger Kock

* **Heft Nr. 107/1992** – „ARCTIC '91: Die Expedition ARK-VIII/3 mit FS ‚Polarstern' 1991", von Dieter K. Fütterer

Heft Nr. 108/1992 – „Dehnungsbeben an einer Störungszone im Ekström-Schelfeis nördlich der Georg-von-Neumayer-Station, Antarktis. – Eine Untersuchung mit seismologischen und geodätischen Methoden", von Uwe Nixdorf.

* **Heft Nr. 109/1992** – „Spätquartäre Sedimentation am Kontinentalrand des südöstlichen Weddellmeeres, Antarktis", von Michael Weber.

* **Heft Nr. 110/1992** – „Sedimentfazies und Bodenwasserstrom am Kontinentalhang des nordwestlichen Weddellmeeres", von Isa Brehme.

Heft Nr. 111/1992 – „Die Lebensbedingungen in den Solekanälchen des antarktischen Meereises", von Jürgen Weissenberger.

Heft Nr. 112/1992 – „Zur Taxonomie von rezenten benthischen Foraminiferen aus dem Nansen Becken, Arktischer Ozean", von Jutta Wollenburg.

Heft Nr. 113/1992 – „Die Expedition ARKTIS VIII/1 mit FS ‚Polarstern' 1991", herausgegeben von Gerhard Kattner.

* **Heft Nr. 114/1992** – „Die Gründungsphase deutscher Polarforschung, 1865 - 1875", von Reinhard A. Krause.

Heft Nr. 115/1992 – "Scientific Cruise Report of the 1991 Arctic Expedition ARK VIII/2 of RV 'Polarstern' (EPOS II)", by Eike Rachor.

Heft Nr. 116/1992 – "The Meteorological Data of the Georg-von-Neumayer-Station (Antarctica) for 1988, 1989, 1990 and 1991", by Gert König-Langlo.

Heft Nr. 117/1992 – „Petrogenese des metamorphen Grundgebirges der zentralen Heimefrontfjella (westliches Dronning Maud Land / Antarktis)", von Peter Schulze.

Heft Nr. 118/1993 – „Die mafischen Gänge der Shackleton Range / Antarktika: Petrographie, Geochemie, Isotopengeochemie und Paläomagnetik", von Rüdiger Hotten.

* **Heft Nr. 119/1993** – „Gefrierschutz bei Fischen der Polarmeere", von Andreas P. A. Wöhrmann.

* **Heft Nr. 120/1993** – "East Siberian Arctic Region Expedition '92: The Laptev Sea - its Significance for Arctic Sea-Ice Formation and Transpolar Sediment Flux", by D. Dethleff, D. Nürnberg, E. Reimnitz, M. Saarso and Y. P. Sacchenko. – "Expedition to Novaja Zemlja and Franz Josef Land with RV. 'Dalnie Zelentsy'", by D. Nürnberg and E. Groth.

* **Heft Nr. 121/1993** – „Die Expedition ANTARKTIS X/3 mit FS ‚Polarstern' 1992", herausgegeben von Michael Spindler, Gerhard Dieckmann und David Thomas

Heft Nr. 122/1993 – „Die Beschreibung der Korngestalt mit Hilfe der Fourier-Analyse: Parametrisierung der morphologischen Eigenschaften von Sedimentpartikeln", von Michael Diepenbroek.

* **Heft Nr. 123/1993** – „Zerstörungsfreie hochauflösende Dichteuntersuchungen mariner Sedimente", von Sebastian Gerland.

Heft Nr. 124/1993 – „Umsatz und Verteilung von Lipiden in arktischen marinen Organismen unter besonderer Berücksichtigung unterer trophischer Stufen", von Martin Graeve.

Heft Nr. 125/1993 – „Ökologie und Respiration ausgewählter arktischer Bodenfischarten", von Christian F. von Dorrien.

Heft Nr. 126/1993 – „Quantitative Bestimmung von Paläoumweltparametern des Antarktischen Oberflächenwassers im Spätquartier anhand von Transferfunktionen mit Diatomeen", von Ulrich Zielinski

* **Heft Nr. 127/1993** – „Sedimenttransport durch das arktische Meereis: Die rezente lithogene und biogene Materialfracht", von Ingo Wollenburg.

Heft Nr. 128/1993 – "Cruise ANTARKTIS X/3 of RV 'Polarstern': CTD-Report", von Marek Zwierz.

Heft Nr. 129/1993 – „Reproduktion und Lebenszyklen dominanter Copepodenarten aus dem Weddellmeer, Antarktis", von Frank Kurbjeweit

Heft Nr. 130/1993 – „Untersuchungen zu Temperaturregime und Massenhaushalt des Filchner-Ronne-Schelfeises, Antarktis, unter besonderer Berücksichtigung von Anfrier- und Abschmelzprozessen", von Klaus Grosfeld

Heft Nr. 131/1993 – „Die Expedition ANTARKTIS X/5 mit FS ‚Polarstern' 1992", herausgegeben von Rainer Gersonde

Heft Nr. 132/1993 – „Bildung und Abgabe kurzkettiger halogenierter Kohlenwasserstoffe durch Makroalgen der Polarregionen", von Frank Laturnus

Heft Nr. 133/1994 – "Radiation and Eddy Flux Experiment 1993 *(REFLEX II)*", by Christoph Kottmeier, Jörg Hartmann, Christian Wamser, Axel Bochert, Christof Lüpkes, Dietmar Freese and Wolfgang Cohrs

* **Heft Nr. 134/1994** – "The Expedition ARKTIS-IX/1", edited by Hajo Eicken and Jens Meincke

Heft Nr. 135/1994 – „Die Expeditionen ANTARKTIS X/6-8", herausgegeben von Ulrich Bathmann, Victor Smetacek, Hein de Baar, Eberhard Fahrbach und Gunter Krause

Heft Nr. 136/1994 – „Untersuchungen zur Ernährungsökologie von Kaiserpinguinen *(Aptenodytes forsteri)* und Königspinguinen *(Aptenodytes patagonicus)*", von Klemens Pütz

* **Heft Nr. 137/1994** – „Die känozoische Vereisungsgeschichte der Antarktis", von Werner U. Ehrmann

Heft Nr. 138/1994 – „Untersuchungen stratosphärischer Aerosole vulkanischen Ursprungs und polarer stratosphärischer Wolken mit einem Mehrwellenlängen-Lidar auf Spitzbergen *(79° N, 12° E)*", von Georg Beyerle

Heft Nr. 139/1994 – „Charakterisierung der Isopodenfauna (Crustacea, Malacostraca) des Scotia-Bogens aus biogeographischer Sicht: Ein multivariater Ansatz", von Holger Winkler.

Heft Nr. 140/1994 – „Die Expedition ANTARKTIS X/4 mit FS ‚Polarstern' 1992", herausgegeben von Peter Lemke

Heft Nr. 141/1994 – „Satellitenaltimetrie über Eis – Anwendung des GEOSAT-Altimeters über dem Ekströmisen, Antarktis", von Clemens Heidland

Heft Nr. 142/1994 – "The 1993 Northeast Water Expedition. Scientific cruise report of RV 'Polartstern' Arctic cruises ARK IX/2 and 3, USCG 'Polar Bear' cruise NEWP and the NEWLand expedition", edited by Hans-Jürgen Hirche and Gerhard Kattner

Heft Nr. 143/1994 – „Detaillierte refraktionsseismische Untersuchungen im inneren Scoresby Sund Ost-Grönland", von Notker Fechner

Heft Nr. 144/1994 – "Russian-German Cooperation in the Siberian Shelf Seas: Geo-System Laptev Sea", edited by Heidemarie Kassens, Hans-Wolfgang Hubberten, Sergey M. Pryamikov and Rüdiger Stein

* **Heft Nr. 145/1994** – "The 1993 Northeast Water Expedition. Data Report of RV ‚Polarstern' Arctic Cruises IX/2 and 3", edited by Gerhard Kattner and Hans-Jürgen Hirche.

Heft Nr. 146/1994 – "Radiation Measurements at the German Antarctic Station Neumayer 1982 - 1992", by Torsten Schmidt and Gerd König-Langlo.

Heft Nr. 147/1994 – „Krustenstrukturen und Verlauf des Kontinentalrandes im Weddell-Meer / Antarktis", von Christian Hübscher.

* **Heft Nr. 148/1994** – "The expeditions NORILSK/TAYMYR 1993 and BUNGER OASIS 1993/94 of the AWI Research Unit Potsdam", edited by Martin Melles.

** **Heft Nr. 149/1994** – „Die Expedition ARCTIC '93. Der Fahrtabschnitt ARK-IX/4 mit FS ‚Polarstern' 1993", herausgegeben von Dieter K. Fütterer.

Heft Nr. 150/1994 – „Der Energiebedarf der Pygoscelis-Pinguine: eine Synopse", von Boris M. Culik.

Heft Nr. 151/1994 – "Russian-German Cooperation: The Transdrift I Expedition to the Laptev Sea", edited by Heidemarie Kassens and Valeriy Y. Karpiy.

Heft Nr. 152/1994 – „Die Expedition ANTARKTIS-X mit FS ‚Polarstern' 1992. Bericht von den Fahrtabschnitten / ANT-X / 1a und 2", herausgegeben von Heinz Miller.

Heft Nr. 153/1994 – „Aminosäuren und Huminstoffe im Stickstoffkreislauf polarer Meere", von Ulrike Hubberten.

Heft Nr. 154/1994 – "Regional and seasonal variability in the vertical distribution of mesozooplankton in the Greenland Sea", by Claudio Richter.

Heft Nr. 155/1995 – „Benthos in polaren Gewässern", herausgegeben von Christian Wiencke und Wolf Arntz.
Heft Nr. 156/1995 – "An adjoint model for the determination of the mean oceanic circulation, air-sea fluxes and mixing coefficients", by Reiner Schlitzer.
Heft Nr. 157/1995 – „Biochemische Untersuchungen zum Lipidstoffwechsel antarktischer Copepoden", von Kirsten Fahl.
** **Heft Nr. 158/1995** – „Die Deutsche Polarforschung seit der Jahrhundertwende und der Einfluß Erich von Drygalskis", von Cornelia Lüdecke.
* **Heft Nr. 159/1995** – "The distribution of $\delta^{18}O$ in the Arctic Ocean: Implications for the freshwater balance of the halocline and the sources of deep and bottom waters", by Dorothea Bauch.
* **Heft Nr. 160/1995** – „Rekonstruktion der spätquartären Tiefenwasserzirkulation und Produktivität im östlichen Südatlantik anhand von benthischen Foraminiferenvergesellschaftungen", von Gerhard Schmiedl.
Heft Nr. 161/1995 – „Der Einfluß von Salinität und Lichtintensität auf die Osmolytkonzentrationen, die Zellvolumina und die Wachstumsraten der antarktischen Eisdiatomeen *Chaetoceros sp.* und *Navicula sp.* unter besonderer Berücksichtigung der Aminosäure Prolin", von Jürgen Nothnagel.
Heft Nr. 162/1995 – „Meereistransportiertes lithogenes Feinmaterial in spätquartären Tiefseesedimenten des zentralen östlichen Arktischen Ozeans und der Framstraße", von Thomas Letzig.
Heft Nr. 163/1995 – „Die Expedition ANTARKTIS-XI/2 mit FS ‚Polarstern' 1993/94", herausgegeben von Rainer Gersonde.
Heft Nr. 164/1995 – „Regionale und altersabhängige Variation gesteinsmagnetischer Parameter in marinen Sedimenten der Arktis", von Thomas Frederichs.
Heft Nr. 165/1995 – „Vorkommen, Verteilung und Umsatz biogener organischer Spurenstoffe: Sterole in antarktischen Gewässern", von Georg Hanke.
Heft Nr. 166/1995 – „Vergleichende Untersuchungen eines optimierten dynamisch-thermodynamischen Meereismodells mit Beobachtungen im Weddellmeer", von Holger Fischer.
* **Heft Nr. 167/1995** – „Rekonstruktionen von Paläo-Umweltparametern anhand von stabilen Isotopen und Faunen-Vergesellschaftungen planktischer Foraminiferen im Südatlantik", von Hans-Stefan Niebler
Heft Nr. 168/1995 – „Die Expedition ANTARKTIS XII mit FS ‚Polarstern' 1993/94.
Bericht von den Fahrtabschnitten ANT XII/1 und 2", herausgegeben von Gerhard Kattner und Dieter Karl Fütterer
Heft Nr. 169/1995 – „Medizinische Untersuchung zur Circadianrhythmik und zum Verhalten bei Überwinterern auf einer antarktischen Forschungsstation", von Hans Wortmann
Heft-Nr. 170/1995 – DFG-Kolloquium: Terrestrische Geowissenschaften – Geologie und Geophysik der Antarktis.
Heft Nr. 171/1995 – „Strukturentwicklung und Petrogenese des metamorphen Grundgebirges der nördlichen Heimfrontfjella (westliches Dronning Maud Land/Antarktika)", von Wilfried Bauer.
Heft Nr. 172/1995 – „Die Struktur der Erdkruste im Bereich des Scoresby Sund, Ostgrönland: Ergebnisse refraktionsseismischer und gravimetrischer Untersuchungen", von Holger Mandler.
Heft Nr. 173/1995 – „Paläozoische Akkretion am paläopazifischen Kontinentalrand der Antarktis in Nordvictorialand – P-T-D-Geschichte und Deformationsmechanismen im Bowers Terrane", von Stefan Matzer.
Heft Nr. 174/1995 – "The Expedition ARKTIS-X/2 of RV 'Polarstern' in 1994", edited by Hans-W. Hubberten
Heft Nr. 175/1995 – "Russian-German Cooperation: The Expedition TAYMYR 1994", edited by Christine Siegert and Gmitry Bolshiyanov.
* **Heft Nr. 176/1995** – "Russian-German Cooperation: Laptev Sea System", edited by Heidemarie Kassens, Dieter Piepenburg, Jörn Thiede, Leonid Timokhov, Hans-Wolfgang Hubberten and Sergey M. Priamikov.
Heft Nr. 177/1995 – „Organischer Kohlenstoff in spätquartären Sedimenten des Arktischen Ozeans: Terrigener Eintrag und marine Produktivität", von Carsten J. Schubert
Heft Nr. 178/1995 – "Cruise ANTARKTIS XII/4 of RV 'Polarstern' in 1995: CTD-Report", by Jüri Sildam.
Heft Nr. 179/1995 – „Benthische Foraminiferenfaunen als Wassermassen-, Produktions- und Eisdriftanzeiger im Arktischen Ozean", von Jutta Wollenburg.
Heft Nr. 180/1995 – „Biogenopal und biogenes Barium als Indikatoren für spätquartäre Produktivitätsänderungen am antarktischen Kontinentalhang, atlantischer Sektor", von Wolfgang J. Bonn.
Heft Nr. 181/1995 – „Die Expedition ARKTIS X/1 des Forschungsschiffes ‚Polarstern' 1994", herausgegeben von Eberhard Fahrbach.
Heft Nr. 182/1995 – "Laptev Sea System: Expeditions in 1994", edited by Heidemarie Kassens.
Heft Nr. 183/1996 – „Interpretation digitaler Parasound Echolotaufzeichnungen im östlichen Arktischen Ozean auf der Grundlage physikalischer Sedimenteigenschaften", von Uwe Bergmann.
Heft Nr. 184/1996 – "Distribution and dynamics of inorganic nitrogen compounds in the troposphere of continental, coastal, marine and Arctic areas", by Maria Dolores Andrés Hernández.
Heft Nr. 185/1996 – "„Verbreitung und Lebensweise der Aphroditen und Polynoiden (Polychaeta) im östlichen Weddellmeer und im Lazarevmeer (Antarktis)", von Michael Stiller.
Heft Nr. 186/1996 – "Reconstruction of Late Quaternary environmental conditions applying the natural radionuclides ^{230}Th, ^{10}Be, ^{231}Pa and ^{230}U: A study of deep-sea sediments from the eastern sector of the Antarctic Circumpolar Current System", by Martin Frank.
Heft Nr. 187/1996 – "The Meteorological Data of the Neumayer Station (Antarctica) for 1992, 1993 and 1994", by Gert König-Langlo and Andreas Herber.
Heft Nr. 188/1996 – „Die Expedition ANTARKTIS-XI/3 mit FS ‚Polarstern' 1994", herausgegeben von Heinz Miller und Hannes Grobe.
Heft Nr. 189/1996 – „Die Expedition ARKTIS-VII/3 mit FS ‚Polarstern' 1990", herausgegeben von Heinz Miller und Hannes Grobe

Heft Nr. 190/1996 – "Cruise report of the Joint Chilean-German-Italian Magellan ‚Victor Hensen' Campaign in 1994", edited by Wolf Arntz and Matthias Gorny.

Heft Nr. 191/1996 – „Leitfähigkeits- und Dichtemessung an Eisbohrkernen", von Frank Wilhelms.

Heft Nr. 192/1996 – „Photosynthese-Charakteristika und Lebensstrategie antarktischer Makroalgen", von Gabriele Weykam.

Heft Nr. 193/1996 – „Heterogene Reaktionen von N_2O_5 und Hbr und ihr Einfluß auf den Ozonabbau in der polaren Stratosphäre", von Sabine Seisel.

Heft Nr. 194/1996 – „Ökologie und Populationsdynamik antarktischer Ophiuroiden (Echinodermata)", von Corinna Dahm.

Heft Nr. 195/1996 – „Die planktische Foraminifere *Neogloboquadrina pachyderma* (Ehrenberg) im Weddellmeer, Antarktis", von Doris Berberich.

Heft Nr. 196/1996 – „Untersuchungen zum Beitrag chemischer und dynamischer Prozesse zur Variabilität des stratosphärischen Ozons über der Arktis", von Birgit Heese

Heft Nr. 197/1996 – "The Expedition ARKTIS-XI/2 of 'Polarstern' in 1995", edited by Gunther Krause.

Heft Nr. 198/1996 – „Geodynamik des Westantarktischen Riftsystems basierend auf Apatit-Spaltspuranalysen", von Frank Lisker.

Heft Nr. 199/1996 – "The 1993 Northeast Water Expedition. Data Report on CTD Measurements of RV 'Polarstern' Cruises ARKTIS IX/2 and 3", by Gerion Budéus and Wolfgang Schneider.

Heft Nr. 200/1996 – "Stability of the Thermohaline Circulation in analytical and numerical models", by Gerrit Lohmann.

Heft Nr. 201/1996 – „Trophische Beziehungen zwischen Makroalgen und Herbivoren in der Potter Cove (King George-Insel, Antarktis)", von Katrin Iken.

Heft Nr. 202/1996 – „Zur Verbreitung und Respiration ökologisch wichtiger Bodentiere in den Gewässern um Svalbard (Arktis)", von Michael K. Schmid.

* **Heft Nr. 203/1996** – „Dynamik, Rauhigkeit und Alter des Meereises in der Arktis – Numerische Untersuchungen mit einem großskaligen Modell", von Markus Harder.

Heft Nr. 204/1996 – „Zur Parametrisierung der stabilen atmosphärischen Grenzschicht über einem antarktischen Schelfeis", von Dörthe Handorf.

Heft Nr. 205/1996 – "Textures and fabrics in the GRIP ice core, in relation to climate history and ice deformation", by Thorsteinn Thorsteinsson.

Heft Nr. 206/1996 – „Der Ozean als Teil des gekoppelten Klimasystems: Versuch der Rekonstruktion der glazialen Zirkulation mit verschieden komplexen Atmosphärenkomponenten", von Kerstin Fieg.

Heft Nr. 207/1996 – „Lebensstrategien dominanter antarktischer Oithonidae (Cyclopoida, Copepoda) und Oncaeidae (Poecilostomatoida, Copepoda) im Bellingshausenmeer", von Cornelia Metz.

Heft Nr. 208/1996 – „Atmosphäreneinfluß bei der Fernerkundung von Meereis mit passiven Mikrowellenradiometern", von Christoph Oelke.

Heft Nr. 209/1996 – „Klassifikation von Radarsatellitendaten zur Meereiserkennung mit Hilfe von Line-Scanner-Messungen", von Axel Bochert.

Heft Nr. 210/1996 – „Die mit ausgewählten Schwämmen (Hexactinellida und Demospongiae) aus dem Weddellmeer, Antarktis, vergesellschaftete Fauna", von Kathrin Kunzmann.

Heft Nr. 211/1996 – "Russian-German Cooperation: The Expedition TAYMYR 1995 and the Expedition KOLYMA 1995", by Dima Yu. Bolshiyanov and Hans-W. Hubberten.

Heft Nr. 212/1996 – "Surface-sediment composition and sedimentary processes in the central Arctic Ocean and along the Eurasian Continental Margin", by Ruediger Stein, Gennadij I. Ivanov, Michael A. Levitan, and Kirsten Fahl.

Heft Nr. 213/1996 – „Gonadenentwicklung und Eiproduktion dreier *Calanus*-Arten (Copepoda): Freilandbeobachtungen, Histologie und Experimente", von Barbara Niehoff

Heft Nr. 214/1996 – „Numerische Modellierung der Übergangszone zwischen Eisschild und Eisschelf", von Christoph Mayer.

Heft Nr. 215/1996 – „Arbeiten der AWI-Forschungsstelle Potsdam in Antarktika, 1994/95", herausgegeben von Ulrich Wand.

Heft Nr. 216/1996 – „Rekonstruktion quartärer Klimaänderungen im atlantischen Sektor des Südpolarmeeres anhand von Radiolarien", von Uta Brathauer.

Heft Nr. 217/1996 – „Adaptive Semi-Lagrange-Finite-Elemente-Methode zur Lösung der Flachwassergleichungen: Implementierung und Parallelisierung", von Jörn Behrens.

Heft Nr. 218/1997 – "Radiation and Eddy Flux Experiment 1995 (REFLEX III)", by Jörg Hartmann, Axel Bochert, Dietmar Freese, Christoph Kottmeier, Dagmar Nagel and Andreas Reuter.

Heft Nr. 219/1997 – „Die Expedition ANTARKTIS-XII mit FS ‚Polarstern' 1995. Bericht vom Fahrtabschnitt ANT-XII/3, herausgegeben von Wilfried Jokat und Hans Oerter.

Heft Nr. 220/1997 – „Ein Beitrag zum Schwerefeld im Bereich des Weddellmeeres, Antarktis. Nutzung von Altimetermessungen des GEOSAT und ERS-1", von Tilo Schöne.

Heft Nr. 221/1997 – „Die Expeditionen ANTARKTIS-XIII/1-2 des Forschungsschiffes ‚Polarstern' 1995/96", herausgegeben von Ulrich Bathmann, Mike Lukas und Victor Smetacek.

Heft Nr. 222/1997 – "Tectonic Structures and Glaciomarine Sedimentation in the South-Eastern Weddell Sea from Seismic Reflection Data", by László Oszkó.

Heft Nr. 223/1997 – „Bestimmung der Meereisdicke mit seismischen und elektromagnetisch-induktiven Verfahren", von Christian Haas.

Heft Nr. 224/1997 – „Troposphärische Ozonvariationen in Polarregionen", von Silke Wessel.

Heft Nr. 225/1997 – „Biologische und ökologische Untersuchungen zur kryopelagischen Amphipodenfauna des arktischen Meereises", von Michael Poltermann.

Heft Nr. 226/1997 – "Scientific Cruise Report of the Arctic Expedition ARK-XI/1 of RV 'Polarstern' in 1995", edited by Eike Rachor.

Heft Nr. 227/1997 – „Der Einfluß kompatibler Substanzen und Kryoprotektoren auf die Enzyme Malatdehydrogenase (MDH) und Glucose-6-phosphat-Dehydrogenase (G6P-DH) aus *Acrosiphonia arcta* (Chlorophyta) der Arktis", von Katharina Kück.

Heft Nr. 228/1997 – „Die Verbreitung epibenthischer Mollusken im chilenischen Beagle-Kanal", von Katrin Linse.

Heft Nr. 229/1997 – „Das Mesozooplankton im Laptevmeer und östlichen Nansen-Becken - Verteilung und Gemeinschaftsstrukturen im Spätsommer", von Hinrich Hanssen.

Heft Nr. 230/1997 – „Modell eines adaptierbaren, rechnergestützten, wissenschaftlichen Arbeitsplatzes am Alfred-Wegener-Institut für Polar- und Meeresforschung", von Lutz-Peter Kurdelski

Heft Nr. 231/1997 – „Zur Ökologie arktischer und antarktischer Fische: Aktivität, Sinnesleistungen und Verhalten", von Christopher Zimmermann

Heft Nr. 232/1997 – „Persistente chlororganische Verbindungen in hochantarktischen Fischen", von Stephan Zimmermann

Heft Nr. 233/1997 – „Zur Ökologie des Dimethylsulfoniumpropionat (DMSP)-Gehaltes temperierter und polarer Phytoplanktongemeinschaften im Vergleich mit Laborkulturen der Coccolithophoride *Emiliania huxleyi* und der antarktischen Diatomee *Nitzschia lecointei*", von Doris Meyerdierks.

Heft Nr. 234/1997 – „Die Expedition ARCTIC '96 des FS ‚Polarstern' (ARK XIII) mit der Arctic Climate System Study (ACSYS)", von Ernst Augstein und den Fahrtteilnehmern.

Heft Nr. 235/1997 – „Polonium-210 und Blei-219 im Südpolarmeer: Natürliche Tracer für biologische und hydrographische Prozesse im Oberflächenwasser des Antarktischen Zirkumpolarstroms und des Weddellmeeres", von Jana Friedrich

Heft Nr. 236/1997 – "Determination of atmospheric trace gas amounts and corresponding natural isotopic ratios by means of ground-based FTIR spectroscopy in the high Arctic", by Arndt Meier.

Heft Nr. 237/1997 – "Russian-German Cooperation: The Expedition TAYMYR/SEVERNAYA ZEMLYA 1996", edited by Martin Melles, Birgit Hagedorn and Dmitri Yu. Bolshiyanov

Heft Nr. 238/1997 – "Life strategy and ecophysiology of Antarctic macroalgae", by Iván M. Gómez.

Heft Nr. 239/1997 – „Die Expedition ANTARKTIS XIII/4-5 des Forschungsschiffes ‚Polarstern' 1996", herausgegeben von Eberhard Fahrbach und Dieter Gerdes.

Heft Nr. 240/1997 – „Untersuchungen zur Chrom-Speziation in Meerwasser, Meereis und Schnee aus ausgewählten Gebieten der Arktis", von Heide Giese.

Heft Nr. 241/1997 – "Late Quaternary glacial history and paleoceanographic reconstructions along the East Greenland continental margin: Evidence from high-resolution records of stable isotopes and ice-rafted debris", by Seung-Il Nam.

Heft Nr. 242/1997 – "Thermal, hydrological and geochemical dynamics of the active layer at a continuous permafrost site, Taymyr Peninsula, Siberia", by Julia Boike.

Heft Nr. 243/1997 – „Zur Paläoozeanographie hoher Breiten: Stellvertreterdaten aus Foraminiferen", von Andreas Mackensen.

Heft Nr. 244/1997 – "The Geophysical Observatory at Neumayer Station, Antarctica, Geomagnetic and seismological observations in 1995 and 1996", by Alfons Eckstaller, Thomas Schmidt, Viola Graw, Christian Müller and Johannes Rogenhagen.

Heft Nr. 245/1997 – „Temperaturbedarf und Biogeographie mariner Makroalgen - Anpassung mariner Makroalgen an tiefe Temperaturen, von Bettina Bischoff-Bäsmann.

Heft Nr. 246/1997 – „Ökologische Untersuchungen zur Fauna des arktischen Meereises", von Christine Friedrich.

Heft Nr. 247/1997 – „Entstehung und Modifizierung von marinen gelösten organischen Substanzen", von Berit Kirchhoff.

Heft Nr. 248/1997 – "Laptev Sea System: Expeditions in 1995", edited by Heidemarie Kassens.

Heft Nr. 249/1997 – "The Expedition ANTARKTIS XIII/3 (EASIZ I) of RV 'Polarstern' to the eastern Weddell Sea in 1996", edited by Wolf Arntz and Julian Gutt.

Heft Nr. 250/1997 – „Vergleichende Untersuchungen zur Ökologie und Biodiversität des Mega-Epibenthos der Arktis und Antarktis", von Adreas Starmans.

Heft Nr. 251/1997 – „Zeitliche und räumliche Verteilung von Mineralvergesellschaftungen in spätquartären Sedimenten des Arktischen Ozeans und ihre Nützlichkeit als Klimaindikatoren während der Glazial/Interglazial-Wechsel", von Christoph Vogt.

Heft Nr. 252/1997 – „Solitäre Ascidien in der Potter Cove (King George Island, Antarktis). Ihre ökologische Bedeutung und Populationsdynamik", von Stephan Kühne.

Heft Nr. 253/1997 – "Distribution and role of microprotozoa in the Southern Ocean", by Christine Klaas.

Heft Nr. 254/1997 – „Die spätquartäre Klima- und Umweltgeschichte der Bunger-Oase, Ostantarktis", von Thomas Kulbe

Heft Nr. 255/1997 – "Scientific Cruise Report of the Arctic Expedition ARK-XIII/2 of RV 'Polarstern' in 1997", edited by Ruediger Stein and Kirsten Fahl.

Heft Nr. 256/1998 – „Das Radionuklid Tritium im Ozean: Meßverfahren und Verteilung von Tritium im Südatlantik und im Weddellmeer", von Jürgen Sültenfuß.

Heft Nr. 257/1998 – „Untersuchungen der Saisonalität von atmosphärischem Dimethylsulfid in der Arktis und Antarktis", von Christoph Kleefeld.

Heft Nr. 258/1998 – „Bellingshausen- und Amundsenmeer: Entwicklung eines Sedimentationsmodells", von Frank-Oliver Nitsche.

Heft Nr. 259/1998 – "The Expedition ANTARKTIS-XIV/4 of RV 'Polarstern' in 1997", by Dieter K. Fütterer.

* **Heft Nr. 260/1998** – „Die Diatomeen der Laptevsee (Arktischer Ozean): Taxonomie und biogeographische Verbreitung", von Holger Cremer

Heft Nr. 261/1998 – „Die Krustenstruktur und Sedimentdecke des Eurasischen Beckens, Arktischer Ozean: Resultate aus seismischen und gravimetrischen Untersuchungen", von Estella Weigelt.

Heft Nr. 262/1998 – "The Expedition ARKTIS-XIII/3 of RV 'Polarstern' in 1997", by Gunther Krause.

Heft Nr. 263/1998 – „Thermo-tektonische Entwicklung von Oates Land und der Shackleton Range (Antarktis) basierend auf Spaltspuranalysen", von Thorsten Schäfer.

Heft Nr. 264/1998 – „Messungen der stratosphärischen Spurengase ClO, HCl, O_3, N_2O, H_2O und OH mittels flugzeuggetragener Submillimeterwellen-Radiometrie", von Joachim Urban.

Heft Nr. 265/1998 – „Untersuchungen zu Massenhaushalt und Dynamik des Ronne Ice Shelfs, Antarktis", von Astrid Lambrecht.

Heft Nr. 266/1998 – "Scientific Cruise Report of the Kara Sea Expedition of RV 'Akademic Boris Petrov' in 1997", edited by Jens Matthiessen and Oleg Stepanets.

Heft Nr. 267/1998 – „Die Expedition ANTARKTIS-XIV mit FS ‚Polarstern' 1997. Bericht vom Fahrtabschnitt ANT-XIV/3", herausgegeben von Wilfried Jokat und Hans Oerter.

Heft Nr. 268/1998 – „Numerische Modellierung der Wechselwirkung zwischen Atmosphäre und Meereis in der arktischen Eisrandzone", von Gerit Birnbaum.

Heft Nr. 269/1998 – "Katabatic wind and Boundary Layer Front Experiment around Greenland (KABEG '97)", by Günther Heinemann.

Heft Nr. 270/1998 – "Architecture and evolution of the continental crust of East Greenland from integrated geophysical studies", by Vera Schlindwein.

Heft Nr. 271/1998 – "Winter Expedition to the Southwestern Kara Sea - Investigations on Formation and Transport of Turbid Sea-Ice", by Dirk Dethleff, Per Loewe, Dominik Weiel, Hartmut Nies, Gesa Kuhlmann, Christian Bahe and Gennady Tarasov.

Heft Nr. 272/1998 – „FTIR-Emissionsspektroskopische Untersuchungen der arktischen Atmosphäre", von Edo Becker.

Heft Nr. 273/1998 – „Sedimentation und Tektonik im Gebiet des Agulhas Rückens und des Agulhas Plateaus (‚SETA-RAP')", von Gabriele Uenzelmann-Neben.

Heft Nr. 274/1998 – "The Expedition ANTARKTIS XIV/2", by Gerhard Kattner.

Heft Nr. 275/1998 – „Die Auswirkung der 'NorthEastWater'-Polynya auf die Sedimentation von NO-Grönland und Untersuchungen zur Paläo-Ozeanographie seit dem Mittelweichsel", von Hanne Notholt.

Heft Nr. 276/1998 – „Interpretation und Analyse von Potentialfelddaten im Weddellmeer, Antarktis: der Zerfall des Superkontinents Gondwana", von Michael Studinger.

Heft Nr. 277/1998 – „Koordiniertes Programm Antarktisforschung". Berichtskolloquium im Rahmen des Koordinierten Programms „Antarktisforschung mit vergleichenden Untersuchungen in arktischen Eisgebieten", herausgegeben von Hubert Miller.

Heft Nr. 278/1998 – „Messung stratosphärischer Spurengase über Ny-Ålesund, Spitzbergen, mit Hilfe eines bodengebundenen Mikrowellen-Radiometers", von Uwe Raffalski.

Heft Nr. 279/1998 – "Arctic Paleo-River Discharge (APARD). A New Research Programme of the Arctic Ocean Science Board (AOSB)", edited by Ruediger Stein.

Heft Nr. 280/1998 – „Fernerkundungs- und GIS-Studien in Nordostgrönland" von Friedrich Jung-Rothenhäusler.

Heft Nr. 281/1998 – „Rekonstruktion der Oberflächenwassermassen der östlichen Laptevsee im Holozän anhand von aquatischen Palynomorphen", von Martina Kunz-Pirrung.

Heft Nr. 282/1998 – "Scavenging of ^{231}Pa and ^{230}Th in the South Atlantic: Implications for the use of the ^{231}Pa/^{230}Th ratio as a paleoproductivity proxy", by Hans-Jürgen Walter.

Heft Nr. 283/1998 – „Sedimente im arktischen Meereis - Eintrag, Charakterisierung und Quantifizierung", von Frank Lindemann.

Heft Nr. 284/1998 – „Langzeitanalyse der antarktischen Meereisbedeckung aus passiven Mikrowellendaten", von Christian H. Thomas.

Heft Nr. 285/1998 – „Mechanismen und Grenzen der Temperaturanpassung beim Pierwurm *Arenicola marina* (L.)", von Angela Sommer.

Heft Nr. 286/1998 – „Energieumsätze benthischer Filtrierer der Potter Cove (King George Island, Antarktis)", von Jens Kowalke.

Heft Nr. 287/1998 – "Scientific Cooperation in the Russian Arctic: Research from the Barents Sea up to the Laptev Sea", edited by Eike Rachor.

Heft Nr. 288/1998 – „Alfred Wegener. Kommentiertes Verzeichnis der schriftlichen Dokumente seines Lebens und Wirkens", von Ulrich Wutzke.

Heft Nr. 289/1998 – "Retrieval of Atmospheric Water Vapor Content in Polar Regions Using Spaceborne Microwave Radiometry", by Jungang Miao.

Heft Nr. 290/1998 – „Strukturelle Entwicklung und Petrogenese des nördlichen Kristallingürtels der Shackleton Range, Antarktis: Proterozoische und Ross-orogene Krustendynamik am Rand des Ostantarktischen Kratons", von Axel Brommer.

Heft Nr. 291/1998 – „Dynamik des arktischen Meereises - Validierung verschiedener Rheologieansätze für die Anwendung in Klimamodellen", von Martin Kreyscher.

Heft Nr. 292/1998 – „Anthropogene organische Spurenstoffe im Arktischen Ozean, Untersuchungen chlorierter Biphenyle und Pestizide in der Laptevsee, technische und methodische Entwicklungen zur Probenahme in der Arktis und zur Spurenstoffanalyse", von Sven Utschakowski.

Heft Nr. 293/1998 – „Rekonstruktion der spätquartären Klima- und Umweltgeschichte der Schirmacher Oase und des Wohlthat Massivs (Ostantarktika)", von Markus Julius Schwab.

Heft Nr. 294/1998 – „Besiedlungsmuster der benthischen Makrofauna auf dem ostgrönländischen Kontinentalhang", von Klaus Schnack.

Heft Nr. 295/1998 – „Gehäuseuntersuchungen an planktischen Foraminiferen hoher Breiten: Hinweise auf Umweltveränderungen während der letzten 140.000 Jahre", von Harald Hommers.

Heft Nr. 296/1998 – "Scientific Cruise Report of the Arctic Expedition ARK-XIII/1 of RV 'Polarstern' in 1997", edited by Michael Spindler, Wilhelm Hagen and Dorothea Stübing.

Heft Nr. 297/1998 – „Radiometrische Messungen im arktischen Ozean - Vergleich von Theorie und Experiment", von Klaus-Peter Johnsen.

Heft Nr. 298//1998 – "Patterns and Controls of CO_2 Fluxes in Wet Tundra Types of the Taimyr Peninsula, Siberia - the Contribution of Soils and Mosses", by Martin Sommerkorn.

Heft Nr. 299/1998 – "The Potter Cove coastal ecosystem, Antarctica. Synopsis of research performed within the frame of the Argentinean-German Cooperation at the Dallmann Laboratory and Jubany Station (Kind George Island, Antarctica, 1991 - 1997)", by Christian Wiencke, Gustavo Ferreyra, Wolf Arntz & Carlos Rinaldi.

Heft Nr. 300/1999 – "The Kara Sea Expedition of RV 'Akademik Boris Petrov' 1997: First Results of a Joint Russian-German Pilot Study", edited by Jens Matthiessen, Oleg V. Stepanets, Ruediger Stein, Dieter K. Fütterer, and Eric M. Galimov.

Heft Nr. 301/1999 – "The Expedition ANTARKTIS XV/3 (EASIZ II)", edited by Wolf E. Arntz and Julian Gutt.

Heft Nr. 302/1999 – „Sterole im herbstlichen Weddellmeer (Antarktis): Großräumige Verteilung, Vorkommen und Umsatz", von Anneke Mühlebach.

Heft Nr. 303/1999 – „Polare stratosphärische Wolken: Lidar-Beobachtungen, Charakterisierung von Entstehung und Entwicklung", von Jens Biele.

Heft Nr. 304/1999 – „Spätquartäre Paläoumweltbedingungen am nördlichen Kontinentalrand der Barents- und Kara-See. Eine Multi-Parameter-Analyse", von Jochen Knies.

Heft Nr. 305/1999 – "Arctic Radiation and Turbulence Interaction Study (ARTIST)", by Jörg Hartmann, Frank Albers, Stefania Argentini, Axel Bochert, Ubaldo Bonafé, Wolfgang Cohrs, Alessandro Conidi, Dietmar Freese, Teodoro Georgiadis, Alessandro Ippoliti, Lars Kaleschke, Christof Lüpkes, Uwe Maixner, Giangiuseppe Mastrantonio, Fabrizio Ravegnani, Andreas Reuter, Giuliano Trivellone and Angelo Viola.

Heft Nr. 306/1999 – "German-Russian Cooperation: Biogeographic and biostratigraphic investigations on selected sediment cores from the Eurasian continental margin and marginal seas to analyze the Late Quaternary climatic variability", edited by Robert R. Spielhagen, Max S. Barash, Gennady I. Ivanov, and Jörn Thiede.

Heft Nr. 307/1999 – „Struktur und Kohlenstoffbedarf des Makrobenthos am Kontinentalhang Ostgrönlands", von Dan Seiler.

Heft Nr. 308/1999 – "ARCTIC '98: The Expedition ARK-XIV/1a of RV 'Polarstern' in 1998", edited by Wilfried Jokat.

Heft Nr. 309/1999 – „Variabilität der arktischen Ozonschicht: Analyse und Interpretation bodengebundener Millimeterwellenmessungen", von Björn-Martin Sinnhuber.

Heft Nr. 310/1999 – „Rekonstruktion von Meereisdrift und terrigenem Sedimenteintrag im Spätquartär: Schwermineralassoziationen in Sedimenten des Laptev-See-Kontinentalrandes und des zentralen Arktischen Ozeans", von Marion Behrends.

Heft Nr. 311/1999 – „Parameterisierung atmosphärischer Grenzschichtprozesse in einem regionalen Klimamodell der Arktis", von Christoph Abegg.

Heft Nr. 312/1999 – „Solare und terrestrische Strahlungswechselwirkung zwischen arktischen Eisflächen und Wolken", von Dietmar Freese.

Heft Nr. 313/1999 – "Snow accumulation on Ekströmisen, Antarctica", by Elisabeth Schlosser, Hans Oerter and Wolfgang Graf.

Heft Nr. 314/1999 – „Die Expedition ANTARKTIS XV/4 des Forschungsschiffes ‚Polarstern' 1998", herausgegeben von Eberhard Fahrbach.

Heft Nr. 315/1999 – "Expeditions in Siberia in 1998", edited by Volker Rachold.

Heft Nr. 316/1999 – „Die postglaziale Sedimentationsgeschichte der Laptewsee: schwermineralogische und sedimentpetrographische Untersuchungen", von Bernhard Peregovich.

Heft-Nr. 317/1999 – „Adaption an niedrige Temperaturen: Lipide in Eisdiatomeen", von Heidi Lehmal.

Heft-Nr. 318/1999 – „Effiziente parallele Lösungsverfahren für elliptische partielle Differentialgleichungen in der numerischen Ozeanmodellierung", von Natalja Rakowsky.

Heft-Nr. 319/1999 – „The Ecology of Arctic Deep-Sea Copepods (Euchaetidae and Aetideidae). Aspects of their Distribution, Trophodynamics and Effect on the Carbon Flux", by Holger Auel.

Heft-Nr. 320/1999 – „Modellstudien zur arktischen stratosphärischen Chemie im Vergleich mit Meßdaten", von Veronika Eyring.

Heft-Nr. 321/1999 – „Analyse der optischen Eigenschaften des arktischen Aerosols", von Dagmar Nagel.

Heft-Nr. 322/1999 – „Messungen des arktischen stratosphärischen Ozons: Vergleich der Ozonmessungen in Ny-Ålesund, Spitzbergen, 1997 und 1998", von Jens Langer

Heft-Nr. 323/1999 – „Untersuchung struktureller Elemente des südöstlichen Weddellmeeres / Antarktis auf der Basis mariner Potentialfelddaten", von Uwe F. Meyer.

Heft-Nr. 324/1999 – „Geochemische Verwitterungstrends eines basaltischen Ausgangsgesteins nach dem spätpleistozänen Gletscherrückzug auf der Taimyrhalbinsel (Zentralsibirien) - Rekonstruktion an einer sedimentären Abfolge des Lama Sees", von Stefanie K. Harwart.

Heft-Nr. 325/1999 – „Untersuchungen zur Hydrologie des arktischen Meereises - Konsequenzen für den kleinskaligen Stofftransport", von Johannes Freitag.

Heft-Nr. 326/1999 – „Die Expedition ANTARKTIS XIV/2 des Forschungsschiffes 'Polarstern' 1998", herausgegeben von Eberhard Fahrbach.

Heft-Nr. 327/1999 – „Gemeinschaftsanalytische Untersuchungen der Harpacticoidenfauna der Magellanregion, sowie erste similaritätsanalytische Vergleiche mit Assoziationen aus der Antarktis", von Kai Horst George.

Heft-Nr. 328/1999 – „Rekonstruktion der Paläo-Umweltbedingungen am Laptev-See-Kontinentalrand während der beiden letzten Glazial/Interglazial-Zyklen anhand sedimentologischer und mineralogischer Untersuchungen", von Claudia Müller.

Heft-Nr. 329/1999 – „Räumliche und zeitliche Variationen atmosphärischer Spurengase aus bodengebundenen Messungen mit Hilfe eines Michelson Interferometers", von Justus Notholt.

Heft-Nr. 330/1999 – „The 1998 Danish-German Excursion to Disko Island, West Greenland", edited by Angelika Brandt, Helge A. Thomsen, Henning Heide-Jørgensen, Reinhardt M. Kristensen and Hilke Ruhberg.

Heft-Nr. 331/1999 – „Poseidon" Cruise No. 243 (Reykjavik - Greenland - Reykjavik, 24 August - 11 September 1998): Climate change and the Viking-age fjord enviroment of the Eastern Settlement, sw Greenland", by Gerd Hoffmann, Antoon Kuijpers, and Jörn Thiede.

Heft-Nr. 332/1999 – „Modeling of marine biogeochemical cycles with an emphasis on vertical particle fluxes", by Regina Usbeck.

Heft-Nr. 333/1999 – „Die Tanaidaceenfauna des Beagle-Kanals und ihre Beziehungen zur Fauna des antarktischen Festlandsockels", von Anja Schmidt.

Heft-Nr. 334/1999 – „D-Aminosäuren als Tracer für biogeochemische Prozesse im Fluß-Schelf-Ozean-System der Arktis", von Hans Peter Fitznar.

Heft-Nr. 335/1999 – „Ökophysiologische Ursachen der limitierten Verbreitung reptanter decapoder Krebse in der Antarktis", von Markus Frederich.

Heft-Nr. 336/1999 – „Ergebnisse der Untersuchung des grönländischen Inlandeises mit dem elektromagnetischen Reflexionsverfahren in der Umgebung von NGRIP", von Fidan Göktas.

Heft-Nr. 337/1999 – „Paleozoic and mesozoic tectono-thermal history of central Dronning Maud Land, East Antarctica, – evidence from fission-track thermochronology", by Stefanie Meier.

Heft-Nr. 338/1999 – „Probleme hoher Stoffwechselraten bei Cephalopoden aus verschiedenen geographischen Breiten", von Susanne Zielinski.

Heft-Nr. 339/1999 – „The Expedition ARKTIS XV/1", edited by Gunther Krause.

Heft-Nr. 340/1999 – „Microbial Properties and Habitats of Permafrost Soils on Taimyr Peninsula, Central Siberia", by Nicolé Schmidt.

Heft-Nr. 341/1999 – „Photoacclimation of phytoplankton in different biogeochemical provinces of the Southern Ocean and its significance for estimating primary production", by Astrid Bracher.

Heft-Nr. 342/1999 – „Modern and Late Quaternary Depositional Environment of the St. Anna Trough Area, Northern Kara Sea", edited by Ruediger Stein, Kirsten Fahl, Gennadij I. Ivanov, Michael A. Levitan, and Gennady Tarasov.

Heft-Nr. 343/1999 – „ESF-IMPACT Workshop/Oceanic impacts: mechanisms and environmental perturbations, 15 - 17 April 1999 in Bremerhaven", edited by Rainer Gersonde and Alexander Deutsch.

Heft-Nr. 344/1999 – „Die Klimageschichte der hohen nördlichen Breiten seit dem mittleren Miozän: Hinweise aus sedimentologischen-tonmineralogischen Analysen (OPD Leg 151, zentrale Framstraße)", von Amelie Winkler.

Heft-Nr. 345/1999 – „Kurzfristige Klimaschwankungen im Scotiameer und Ergebnisse zur Kalbungsgeschichte der Antarktis während der letzten 200 000 Jahre", von Annette Hofmann.

Heft-Nr. 346/2000 – „Glazialmarine Sedimentationsentwicklung am westantarktischen Kontinentalrand im Amundsen- und Bellingshausenmeer - Hinweise auf Paläumweltveränderungen während der quartären Klimazyklen", von Claus-Dieter Hillenbrand

Heft-Nr. 347/2000 – „Zur Ökologie des Phytoplanktons im arktischen Laptevmeer - ein jahreszeitlicher Vergleich", von Kirsten Tuschling.

Heft-Nr. 348/2000 – „Untersuchungen zum Fettstoffwechsel des Südlichen See-Elefanten *(Mirounga leonina* L.) in der Antarktis", von Sven Ramdohr.

Heft-Nr. 349/2000 – „Licht- und Temperatureinfluß auf den enzymatischen Oxidationsschutz der antarktischen Eisdiatomee *Entomoneis kufferathii* Manguin", von Raimund Schriek.

Heft-Nr. 350/2000 – „Die Expedition ARKTIS XV/3 des Forschungsschiffes 'Polarstern' 1999"
herausgegeben von Ursula Schauer.

Heft-Nr. 351/2000 – „Dissolution kinetics of biogenic silica in marine enviroments", by Dirk Rickert.

Heft-Nr. 352/2000 – „Geometrie und Kinematik des tertiären Deckenbaus im West Spitzbergen Falten- und Überschiebungsgürtel, Brøggerhalvøya, Svalbard", von Kerstin Saalmann.

Heft-Nr. 353/2000 – „Zur Ökplogie der Benthos-Foraminiferen der Potter Cove (King George Island, Antarktis)",
von Michaela Mayer.

Heft-Nr. 354/2000 – „Expeditions in Siberia in 1999", edited by Volker Rachold.

Heft-Nr. 355/2000 – „Temperaturrekonstruktion im Tropischen Atlantik für das Letzte Glaziale Maximum:
CLIMAP neu betrachtet.", von Carsten Porthun.

Heft-Nr. 356/2000 – „Niederfrequente Variabilität großräumiger atmosphärischer Zirkulationsstrukturen in spektralen Modellen niederer Ordnung", von Antje Weisheimer.

Heft-Nr. 357/2000 – „Late Quaternary paleoclimatic reconstructions along the Eurasian continental margin",
by Hans Peter Kleiber.

Heft-Nr. 358/2000 – „Holocene environmental history of East Greenland - evidence from lake sediments",
by Bernd Wagner.

Heft-Nr. 359/2000 – „Scientific Cooperation in the Russian Arctic: Ecology of the White Sea with Emphasis on its Deep Basin", edited by Eike Rachor.

Heft-Nr. 360/2000 – „Scientific Cruise Report of the Joint Russian-German Kara-Sea Expedition of RV 'Akademik Boris Petrov' in 1999", edited by Ruediger Stein and Oleg Stepanets.

Heft-Nr. 361/2000 – „Planktic foraminifer ecology and stable isotope geochemistry in the Arctic Ocean: implications from water column and sediment surface studies for quantitative reconstructions of oceanic parameters" by Renate Volkmann.

Heft-Nr. 362/2000 – „Eisbohrkernuntersuchungen zur räumlichen und zeitlichen Variabilität von Temperatur und Niederschlagsrate im Spätholozän in Nordgrönland", von Matthias Schwager.

Heft-Nr. 363/2000 – „Benthische Peracarida (Crustacea, Malacostraca) des arktischen Mellemfjordes, West-Grönland",
von Anne-Nina Lörz.

Heft-Nr. 364/2000 – Die Expeditionen ANTARKTIS XVI / 3-4 des Forschungsschiffes „POLARSTERN" 1999,
herausgegeben von Ulrich Bathmann, Victor Smetacek und Manfred Reinke.

Heft-Nr. 365/2000 – „Organic carbon in Late Quaternary sediments: Responses to paleoenvironmental charges in the Laptev and Kara seas (Arctic Ocean)" by Bettina Boucsein.

Heft-Nr. 366/2000 – „Flugzeuggestützte Topographie- und Schweremessung: Meßsystem und Anwendung auf die Region Framstraße, Spitsbergen und Nordostgrönland", von Tobias Boebel.

Heft-Nr. 367/2000 – „Messung dielektrischer Eigenschaften polarer Eiskerne", von Frank Wilhelms.

Heft-Nr. 368/2000 – „The Expedition ARKTIS-XV/2 of RV 'Polarstern' in 1999", edited by Wilfried Jokat.

Heft-Nr. 369/2000 – „Interpretation seismischer und gravimetrischer Daten des Weddellmeeres, Antarktis",
von Johannes Rogenhagen.

Heft-Nr. 370/2000 – „Struktureigenschaften und Nahrungsbedarf der Zoobenthosgemeinschaften im Bereich des Lomonossowrückens im Arktischen Ozean", von Hendrik Deubel.

Heft-Nr. 371/2000 – „Die Rolle der Schneebedeckung für die Kryptogamen-Vegetation in der maritimen Antarktis (Potter-Halbinsel, King George Island)", von Jana Barbro Winkler.

Heft-Nr. 372/2000 – „Biodiversity of the Weddell Sea: macrozoobenthic species (demersal fish included) sampled during the expedition ANT XIII/3 (EASIZ I) with RV 'Polarstern'", edited by Julian Gutt, Boris I. Sirenko, Wolf E. Arntz, Igor S. Smirnov, and Claude De Broyer.

Heft-Nr. 373/2000 – „Benthische Foraminiferen im Boreas-Becken, Grönlandsee: Verbreitung und paläo-ozeanographische Rekonstruktionen für die letzten 450.000 Jahre", von Sabine Magnus.

Heft-Nr. 374/2000 – „Scherwellendoppelbrechungsanalyse von Registrierungen der Stationen des seismologischen Netzwerkes an der Neumayer Station, Antarktis: Seismische Anisotropie und die tektonische Entwicklung des Kontinentalrandes Queen Maud Lands", von Christian Müller.

Heft-Nr. 375/2000 – „Effects of enhanced UV-radiation on photosynthesis of Arctic/cold-temperate macroalgae",
by Kai Bischof.

Heft-Nr. 376/2000 – „Saisonalität und kurzperiodische Variabilität des Seesalz-Aerosols und des bodennahen Ozons in der Antarktis (Neumayer-Station) unter Berücksichtigung der Meereisbedeckung", von Jörg Hofmann.

Ab dem Heft-Nr. 377 erscheint die Reihe unter dem Namen: „Berichte zur Polar- und Meeresforschung"

Heft-Nr. 377/2000 – „Rekrutierungsmuster ausgewählter Wattfauna nach unterschiedlich strengen Wintern"
von Matthias Strasser

Heft-Nr. 378/2001 – „Der Transport von Wärme, Wasser und Salz in den Arktischen Ozean", von Boris Cisewski

Heft-Nr. 379/2001 – „Analyse hydrographischer Schnitte mit Satellitenaltimetrie", von Martin Losch

Heft-Nr. 380/2001 – „Die Expeditionen ANTARKTIS XI/1-2 des Forschungsschiffes POLARSTERN 1998/1999", herausgegeben von Eberhard Fahrbach und Saad El Naggar.

Heft-Nr. 381/2001 – „UV-Schutz- und Reparaturmechanismen bei antarktischen Diatomeen und *Phaeocystis antarctica*", von Lieselotte Riegger.

Heft-Nr. 382/2001 – „Age determination in polar Crustacea using the autofluorescent pigment lipofuscin", by Bodil Bluhm.

Heft-Nr. 383/2001 – „Zeitliche und räumliche Verteilung, Habitatspräferenzen und Populationsdynamik benthischer Copepoda Harpacticoida in der Potter Cove (King George Island, Antarktis)", von Gritta Veit-Köhler.

Heft-Nr. 384/2001 – „Beiträge aus geophysikalischen Messungen in Dronning Maud Land, Antarktis, zur Auffindung eines optimalen Bohrpunktes für eine Eiskerntiefbohrung", von Daniel Steinhage.

Heft-Nr. 385/2001 – „Actinium-227 als Tracer für Advektion und Mischung in der Tiefsee", von Walter Geibert.

Heft-Nr. 386/2001 – „Messung von optischen Eigenschaften troposphärischer Aerosole in der Arktis" von Rolf Schumacher.

Heft-Nr. 387/2001 – „Bestimmung des Ozonabbaus in der arktischen und subarktischen Stratosphäre", von Astrid Schulz.

Heft-Nr. 388/2001 – „Russian-German Cooperation SYSTEM LAPTEV SEA 2000: The Expedition LENA 2000", edited by Volker Rachold and Mikhail N. Grigoriev.

Heft-Nr. 389/2001 – „The Expeditions ARKTIS XVI/1 and ARKTIS XVI/2 of the Research Vessel 'Polarstern' in 2000", edited by Gunther Krause and Ursula Schauer.

Heft-Nr. 390/2001 – „Late Quaternary climate variations recorded in North Atlantic deep-sea ostracodes", by Claudia Didié.

Heft-Nr. 391/2001 – „The polar and subpolar North Atlantic during the last five glacial-interglacial cycles", by Jan. P. Helmke.

Heft-Nr. 392/2000 – „Geochemische Untersuchungen an hydrothermal beeinflußten Sedimenten der Bransfield Straße (Antarktis)", von Anke Dählmann.

Heft-Nr. 393/2001 – „The German-Russian Project on Siberian River Run-off (SIRRO): Scientific Cruise Report of the Kara-Sea Expedition 'SIRRO 2000' of RV 'Boris Petrov' and first results", edited by Ruediger Stein and Oleg Stepanets.

Heft-Nr. 394/2001 – „Untersuchung der Photooxidantien Wasserstoffperoxid, Methylhydroperoxid und Formaldehyd in der Troposphäre der Antarktis", von Katja Riedel.

Heft-Nr. 395/2001 – „Role of benthic cnidarians in the energy transfer processes in the Southern Ocean marine ecosystem (Antarctica)", by Covadonga Orejas Saco del Valle.

Heft-Nr. 396/2001 – „Biogeochemistry of Dissolved Carbohydrates in the Arctic", by Ralph Engbrodt.

Heft-Nr. 397/2001 – „Seasonality of marine algae and grazers of an Antarctic rocky intertidal, with emphasis on the role of the limpet *Nacilla concinna* Strebel (Gastropoda: Patellidae)", by Dohong Kim.

Heft-Nr. 398/2001 – „Polare Stratosphärenwolken und mesoskalige Dynamik am Polarwirbelrand", von Marion Müller.

Heft-Nr. 399/2001 – „North Atlantic Deep Water and Antarctic Bottom Water: Their Interaction and Influence on Modes of the Global Ocean Circulation", by Holger Brix.

Heft-Nr. 400/2001 – „The Expeditions ANTARKTIS XVIII/1-2 of the Research Vessel 'Polarstern' in 2000" edited by Victor Smetacek, Ulrich Bathmann, Saad El Naggar.

* vergriffen/out of print.
** nur noch beim Autor/only from the author.